UNCLASSIFIED

AD NUMBER

AD886794

LIMITATION CHANGES

TO:

Approved for public release; distribution is unlimited.

FROM:

Distribution authorized to U.S. Gov't. agencies only; Test and Evaluation; AUG 1971. Other requests shall be referred to Armament Development and Test Center, Attn: DLII, Eglin AFB, FL 32542.

AUTHORITY

AFATL ltr, 1 Apr 1976

THIS PAGE IS UNCLASSIFIED

3

AEDC-TR-71-162
AFATL-TR-71-99

ARCHIVE COPY
DO NOT LOAN

Cy1

LONGITUDINAL STATIC STABILITY AND DRAG CHARACTERISTICS OF F-4D AIRCRAFT WITH VARIOUS EXTERNAL STORE CONFIGURATIONS AT TRANSONIC SPEEDS

D. K. Smith

ARO, Inc.

This document has been approved for public release
its distribution is unlimited. per DyTe 7/6/71

August 1971

Distribution limited to U. S. Government agencies only; this report contains information on test and evaluation of military hardware; August 1971; other requests for this document must by referred to Armament Development and Test Center (DLII), Eglin AFB, FL 32542.

PROPULSION WIND TUNNEL FACILITY
ARNOLD ENGINEERING DEVELOPMENT CENTER
AIR FORCE SYSTEMS COMMAND
ARNOLD AIR FORCE STATION, TENNESSEE

PROPERTY OF U S AIR FORCE
AEDC LIBRARY
F40600-72-C-0003

AEDC TECHNICAL LIBRARY
5 0720 00033 2090

NOTICES

When U. S. Government drawings specifications, or other data are used for any purpose other than a definitely related Government procurement operation, the Government thereby incurs no responsibility nor any obligation whatsoever, and the fact that the Government may havc formulated, furnished, or in any way supplied the said drawings, specifications, or other data, is not to be regarded by implication or otherwise, or in any manner licensing the holder or any other person or corporation, or conveying any rights or permission to manufacture, use, or sell any patented invention that may in any way be related thereto.

Qualified users may obtain copies of this report from the Defense Documentation Center.

References to named commercial products in this report are not to be considered in any sense as an endorsement of the product by the United States Air Force or the Government.

LONGITUDINAL STATIC STABILITY AND DRAG CHARACTERISTICS OF F-4D AIRCRAFT WITH VARIOUS EXTERNAL STORE CONFIGURATIONS AT TRANSONIC SPEEDS

D. K. Smith
ARO, Inc.

Distribution limited to U. S. Government agencies only; this report contains information on test and evaluation of military hardware; August 1971; other requests for this document must by referred to Armament Development and Test Center (DLII), Eglin AFB, FL 32542.

FOREWORD

The work reported herein was sponsored by the Air Force Armament Laboratory (DLII/Capt V. E. Studwell), Air Force Armament Development and Test Center (ADTC). Air Force Systems Command (AFSC), under Program Element 62602F, Project 2567.

The test results presented were obtained by ARO, Inc. (a subsidiary of Sverdrup & Parcel and Associates, Inc.), contract operator of the Arnold Engineering Development Center (AEDC), AFSC, Arnold Air Force Station, Tennessee, under Contract F40600-72-C-0003. The test was conducted from April 22 to 27, 1971, under ARO Project No. PC0144. The manuscript was submitted for publication on June 11, 1971.

This technical report has been reviewed and is approved.

George F. Garey
Lt Colonel, USAF
AF Representative, PWT
Directorate of Test

Joseph R. Henry
Colonel, USAF
Director of Test

ABSTRACT

Force and moment data were obtained with a 0.05-scale model of the F-4D aircraft at Mach numbers from 0.75 to 1.30 to determine the effects of different store and rack configurations on the static stability and drag of the aircraft. Six proposed rack launchers and four proposed store shapes were tested for a total of 57 external loading configurations.

CONTENTS

APPENDIXES

I. ILLUSTRATIONS

Figure

Figure | Page

Figure | Page

NOMENCLATURE

A_b	Base area, 0.0747 ft^2
BL	Buttock line from plane of symmetry, in.
C_A	Measured axial-force coefficient, measured axial force/$q_\infty S$
$C_{A,b}$	Base axial-force coefficient, $(p_\infty - p_b) A_b/q_\infty S$
$C_{A,F}$	Forebody axial-force coefficient, $C_A - C_{A,b}$
C_D	Forebody drag coefficient, forebody drag/$q_\infty S$
C_m	Pitching-moment coefficient, pitching moment/$q_\infty S\bar{c}$, moment reference at FS 16.233 and WL 1.55
dC_m/dC_L	The derivative of the pitching-moment coefficient with respect to the lift coefficient at $C_L = 0.20$, in percentage of $\bar{c}$ from the moment reference
C_L	Forebody lift coefficient, forebody lift/$q_\infty S$
$\bar{c}$	Mean aerodynamic chord, 0.802 ft
FS	Fuselage station, in.
M_∞	Free-stream Mach number
p_∞	Free-stream static pressure, psfa
p_b	Model base pressure, psfa
q_∞	Free-stream dynamic pressure, psf
S	Wing reference area, 1.3250 ft^2
WL	Waterline from reference-horizontal plane, in.
α	Model angle of attack, angle between a model waterline and the free-stream velocity vector, deg

SECTION I
INTRODUCTION

At transonic and supersonic speeds, the external carriage of weapons on fighter-type aircraft can produce an added drag and sometimes a destabilizing pitching moment which may be detrimental to the aircraft mission. Therefore, at the request of the Air Force Armament Laboratory, Eglin Air Force Base, Florida, tests utilizing a 0.05-scale model of the F-4D aircraft were conducted in the Aerodynamic Wind Tunnel (4T) of the AEDC Propulsion Wind Tunnel Facility (PWT) to evaluate the effect of several new store configurations and rack launchers upon aircraft static stability and drag. Four Triple Rack Launchers (TRL1 through TRL4) and a Quadruple Rack Launcher (QRL1) configured with four weapon stores (M1 through M4) were tested, as well as an Advanced Tactical Rocket Launcher (ATRL 30 x 30). These weapons and launchers are proposed new systems of weapon carriage. Longitudinal static stability and drag data were obtained at Mach numbers of 0.75, 0.85, 0.95, 1.10, and 1.30 for 57 loading configurations of the above weapons and launchers.

Similar tests have been previously conducted in Tunnel 4T with different store configurations and rack launchers; the results are presented in Refs. 1 and 2.

SECTION II
APPARATUS

2.1 TEST FACILITY

Tunnel 4T is a closed-loop, continuous flow, variable density tunnel in which the Mach number can be varied from 0.2 to 1.3. At all Mach numbers, the stagnation pressure can be varied from 200 to 3400 psfa. The test section is 4 ft square and 12.5 ft long with perforated, variable porosity (0.5- to 10-percent open) walls. It is completely enclosed in a plenum chamber from which the air can be evacuated, allowing part of the tunnel airflow to be removed through the perforated walls of the test section. A more thorough description of the tunnel may be found in Ref. 3. A sketch of the test section wall details and the location of the test model in the test section is shown in Fig. 1, Appendix I.

2.2 TEST ARTICLES

The test articles were 0.05-scale models of the F-4D aircraft, 370-gal fuel tanks, and various new stores and rack launchers. The horizontal tail setting of the F-4D aircraft was at a positive 1.0-deg incidence angle with respect to the model waterline. The wing-root chord also had a 1.0-deg incidence angle with respect to the waterline. All tests were conducted with free boundary-layer transition on the model.

A sketch showing the basic dimensions of the F-4D aircraft model is presented in Fig. 2. The location of the forward end of the pylons, 370-gal tank, racks, and stores is also given in Fig. 2. Details and dimensions of the pylons are given in Fig. 3, and details and dimensions of the rack launchers are given in Fig. 4. Details and dimensions of the 370-gal fuel tank on the outboard pylon are shown in Fig. 5. Details and dimensions

of the weapon stores are shown in Fig. 6. The numbering sequence of the various rack launcher stations is shown in Fig. 7 along with the roll orientation of the store at each launcher station.

Photographs of seven configurations installed in the test section are shown in Fig. 8 and include each of the different stores and rack launchers tested. A list of all the configurations tested is presented in Table I, Appendix II.

2.3 INSTRUMENTATION

A six-component, moment-type, internal strain-gage balance was used to obtain the force and moment data. Three base pressure measurements were made with pressure transducers connected to three orifices located on the sting inside the base of the aircraft model.

SECTION III
TEST DESCRIPTION

3.1 TEST CONDITIONS AND PROCEDURES

Force and moment data were obtained on various store configurations of the F-4D aircraft. The Mach numbers at which the tests were conducted were 0.75, 0.85, 0.95, 1.10, and 1.30 at a free-stream dynamic pressure of 750, 820, 885, 955, and 900 psf, respectively. The Reynolds number per foot was held at 5.0×10^6 for all Mach numbers except $M_\infty = 1.30$. At Mach number 1.3 the Reynolds number was 4.4×10^6 ft^{-1}. The total temperature was varied from 100 to 120°F. The test section wall porosity was varied with free-stream Mach number in order to achieve the minimum lift interference while reducing blockage effects. The tunnel conditions were held constant at the prescribed Mach number and Reynolds number while the angle of attack was varied from -4 to 15 deg. Data were recorded at 0.5-deg increments for angles of attack from -4 to 4 deg and 1.0-deg increments from 4 to 15 deg.

3.2 CORRECTIONS

Balance and sting deflections caused by aerodynamic loads on the model were accounted for in the data reduction program to determine the angle of attack. Model weight tare corrections were made to calculate net aerodynamic forces on the model. A model base drag correction was made to obtain the forebody coefficients.

3.3 PRECISION OF MEASUREMENTS

The precision of the data which can be attributed to the inaccuracies in balance measurements and in setting tunnel conditions was determined for a confidence level of 95 percent and is presented below for the set of conditions that produces the largest errors.

C_D (C_L = 0.3)	C_L	C_m	dC_m/dC_L	q_∞
±0.0015	±0.006	±0.002	±0.2%	±10

The error in setting Mach number is within ±0.005. The Mach number variation in the portion of the test section occupied by the model is no greater than ±0.002 for Mach numbers up to 0.95 and ±0.01 for Mach numbers greater than 1.0. The error in setting angle of attack is ±0.1 deg.

SECTION IV
RESULTS AND DISCUSSION

The force and moment coefficients were machine plotted and faired with straight lines with the exception of the dC_m/dC_L and C_D versus M_∞ plots, which were hand plotted. The data are presented in the following format and order for each group of data: (1) C_L versus α, (2) C_m versus C_L, (3) C_D versus C_L, (4) dC_m/dC_L versus M_∞, and (5) C_D versus M_∞. The derivative of the pitching-moment coefficient with respect to the lift coefficient (dC_m/dC_L) was determined by curve fitting the C_m versus C_L curve with a quadratic equation over the range $0 \leqslant C_L \leqslant 0.4$ and evaluating the derivative of this equation at $C_L = 0.2$. The resulting value for dC_m/dC_L is the static margin for the aircraft, and negative values indicate a stable aircraft. Although the aircraft is not trimmed at this condition ($C_L \doteq 0.20$), with the horizontal stabilizer setting used during these tests, the values presented should closely approximate the true static margin for the power-off case. The drag coefficient versus Mach number is plotted at $C_L = 0.3$ and $C_L = 0.1$ for $M_\infty < 1.0$ and $M_\infty > 1.0$, respectively. For a comparison base the results from the clean F-4D aircraft are shown for each group of data. Only the results from selected configurations are presented for brevity.

The aerodynamic coefficients are presented in Figs. 9 through 52. Figures 9 through 12 present data for configurations which have combinations of the inboard pylon without racks and the outboard 370-gal fuel tank. The addition of the fuel tanks (configurations F402 and F404) produce a large increase in the drag coefficient and a large decrease in the static margin compared to the clean aircraft (see Fig. 12). Figures 13 through 16 and 17 through 20 present data for configurations which have M1 stores on the TRL1 rack and M2 stores on the TRL2 rack, respectively, all with the outboard fuel tanks. As shown in Fig. 16, the addition of M1 stores to the TRL1 rack (configuration F408) reduced the static margin to about zero at Mach numbers 0.75 and 0.85. As shown in Fig. 20, the addition of M2 stores to the TRL2 rack (configuration F412) reduced the static margin to about 1 percent at the lower Mach numbers.

Data are presented in Figs. 21 through 32 for configurations with fully loaded racks with and without the outboard 370-gal fuel tanks. As can be seen from the results, the addition of the fuel tanks with a full load of carriage weapons greatly reduced the static margin and increased the drag coefficient of the aircraft (see Figs. 24, 28, and 32).

Data are presented in Figs. 33 through 36 and 37 through 40 for configurations which have empty and fully loaded M2, M4, and M3 stores on racks TRL2 and QRL1, respectively, with the outboard fuel tanks. Figures 41 through 44 and 45 through 48 present data for essentially the same weapon configurations as above without the outboard fuel tanks. These results show that the different stores on a particular rack produced little change in the aerodynamic coefficients or the static margin for models either with or without the fuel tank (see Figs. 33 through 48).

Data are presented in Figs. 49 through 52 for configurations which have the outboard ATRL 30 x 30, the inboard ATRL 30 x 30, and the inboard ATRL 30 x 30 with the outboard fuel tanks. The aircraft was unstable at Mach numbers 0.75 and 0.85 with both the inboard ATRL 30 x 30 and the outboard 370-gal fuel tanks (configuration F456) as can be seen in Figs. 50a, 50b, and 52a.

SECTION V
CONCLUSIONS

Based on the results of the test to determine the longitudinal static stability and drag characteristics of the F-4D aircraft with various external store configurations, the following conclusions are made:

1. The addition of any of the various weapon racks and stores to the aircraft resulted in a significant decrease in the static margin of the aircraft and increase in the drag coefficient.

2. Using the inboard ATRL 30 x 30 in combination with the outboard 370-gal fuel tank resulted in an unstable aircraft at Mach numbers 0.75 and 0.85.

REFERENCES

1. Kukainis, Janis. "Aerodynamic Characteristics of the F-4E Aircraft with 35 External Load Configurations." AEDC-TR-70-171 (AD872694), August 1970.

2. Davis, Ronald E. "Longitudinal Static Stability and Drag Characteristics of A-7D and F-4E Aircraft with Various External Store Configurations at Transonic Speeds." AEDC-TR-71-54 (AD882624L), April 1971.

3. Test Facilities Handbook (Eighth Edition). "Propulsion Wind Tunnel Facility, Vol. 5." Arnold Engineering Development Center, December 1969 (AD863646).

APPENDIXES

I. ILLUSTRATIONS

II. TABLE

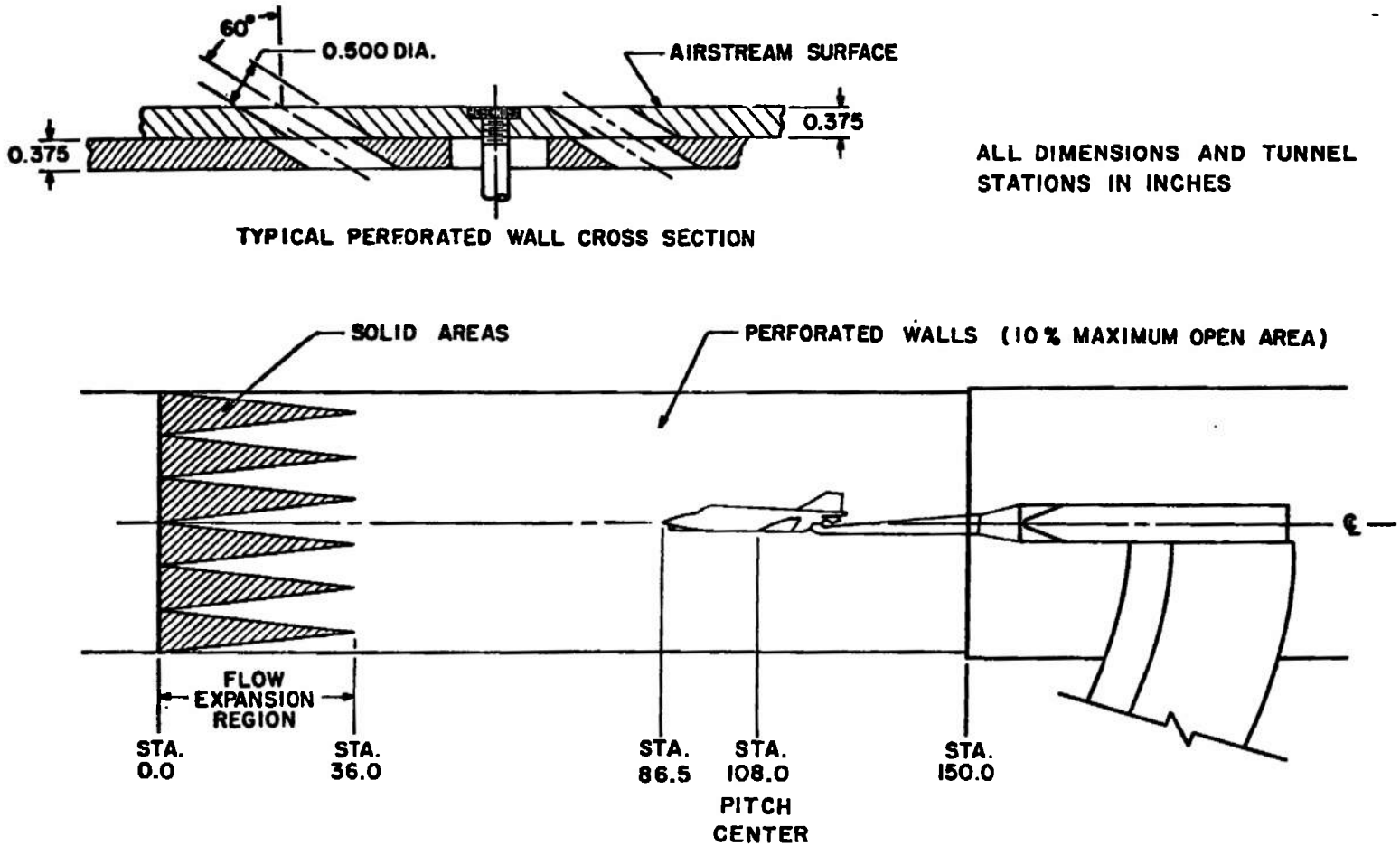

Fig. 1 Schematic of Tunnel Test Section Showing Model Location

AEDC-TR-71-162

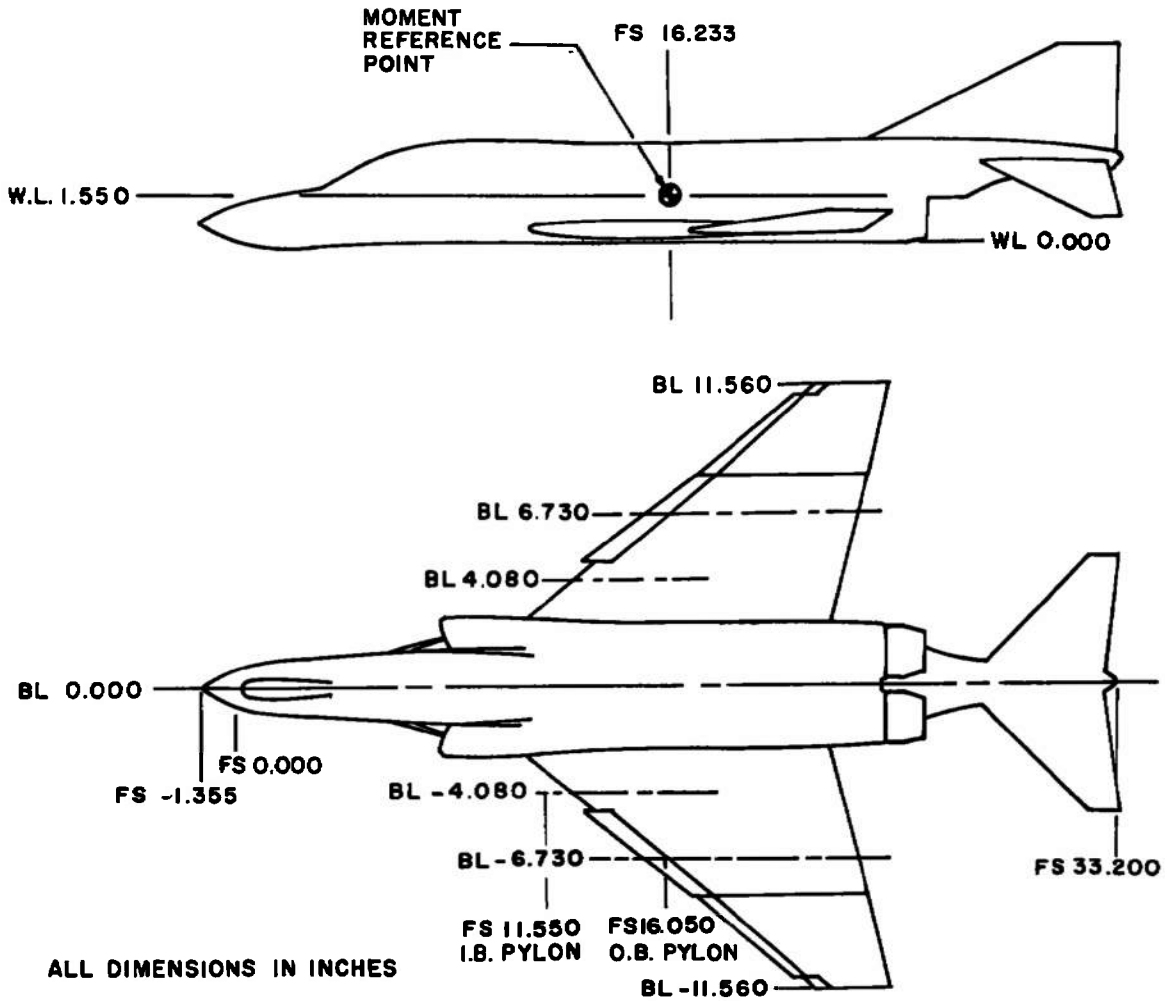

PART	UPSTREAM END OF STORES AND ASSOCIATED HARDWARE	
	I B. PYLON (F.S 11.55)	O B PYLON (F.S. 16 05)
TRL 1	F.S. 11.04	
TRL 2, TRL3, TRL 4 OR QRL 1	F.S. 11.68	
M1 ON TRL 1	F.S. 10.52	
M2 ON TRL2, TRL3, TRL4, OR QRL1	F.S. 10.87	
M3 ON TRL2, TRL3, TRL4, OR QRL1	F.S. 11.03	
M4 ON TRL2 OR QRL1	F.S. 10.87	
370-.GALLON FUEL TANK		F.S. 10.65
ATRL 30 X 30	F.S. 9.67	F.S. 14.36

Fig. 2 Sketch of the F-4D Aircraft Model

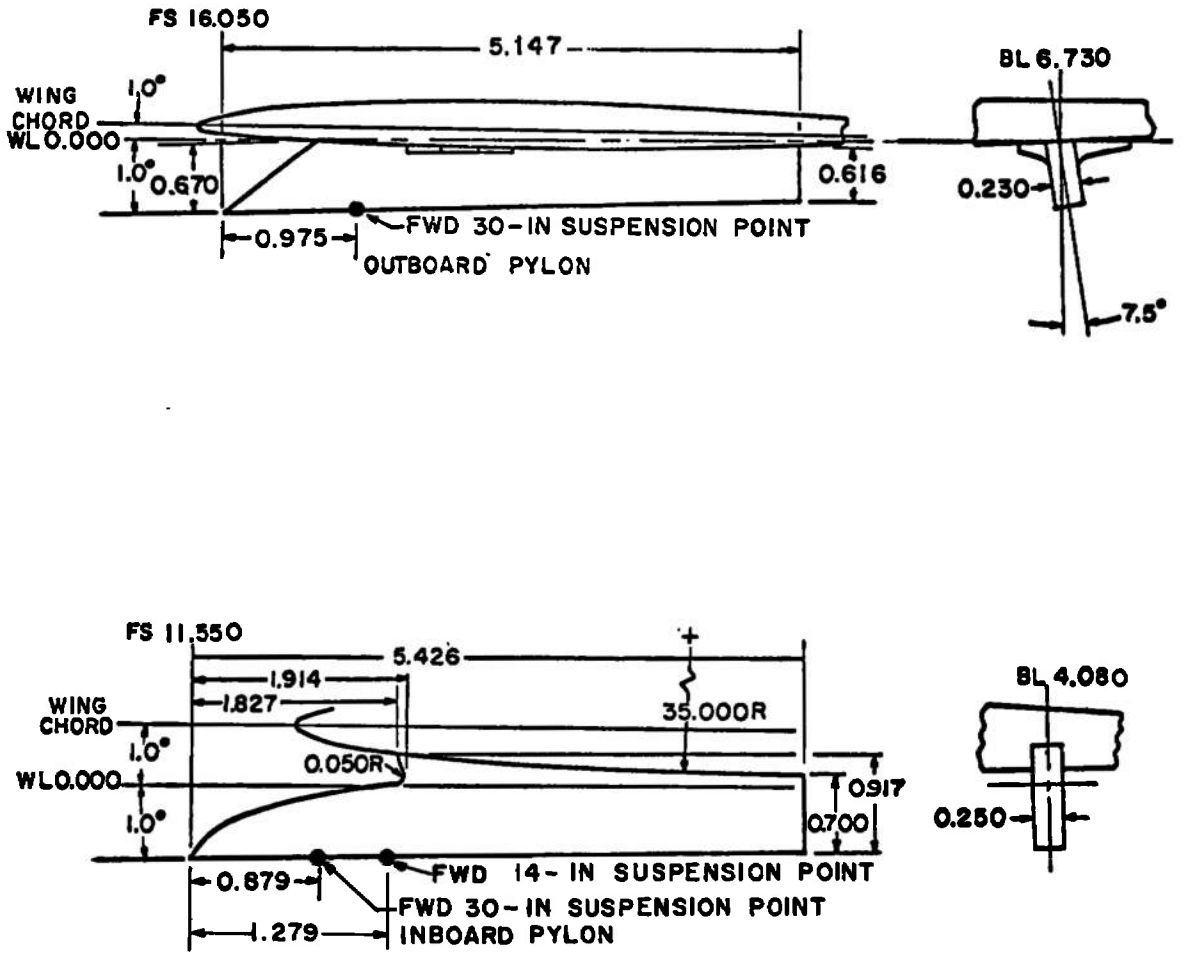

Fig. 3 Details and Dimensions of the Aircraft Model Pylons

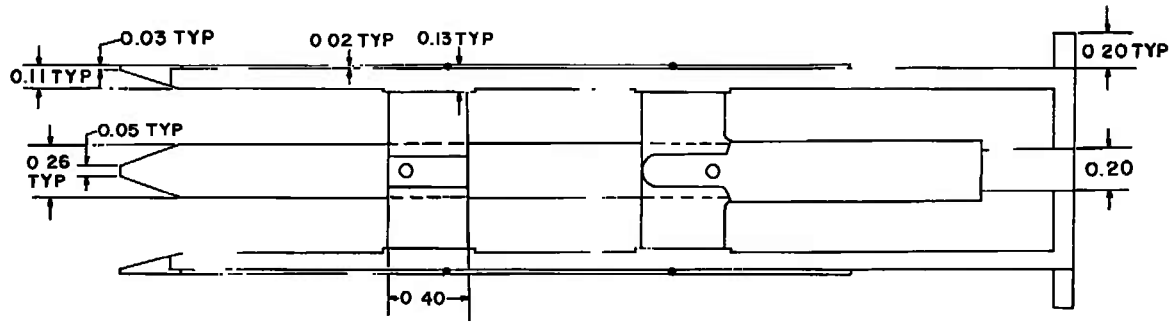

ALL DIMENSIONS IN INCHES

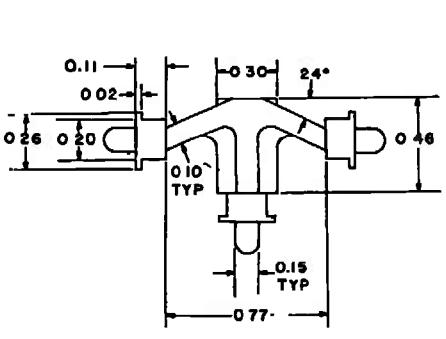

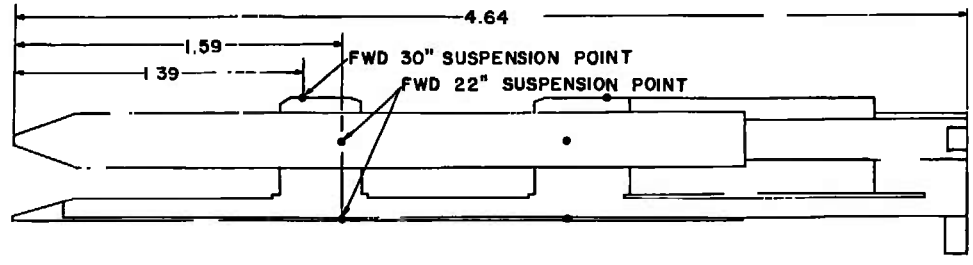

a. TRL 1

Fig. 4 Details and Dimensions of the Launcher Rack Models

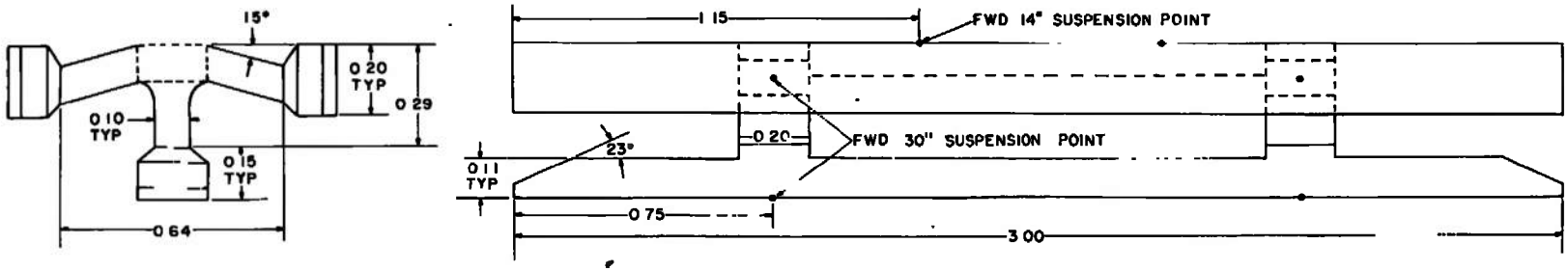

ALL DIMENSIONS IN INCHES

b. TRL 2
Fig. 4 Continued

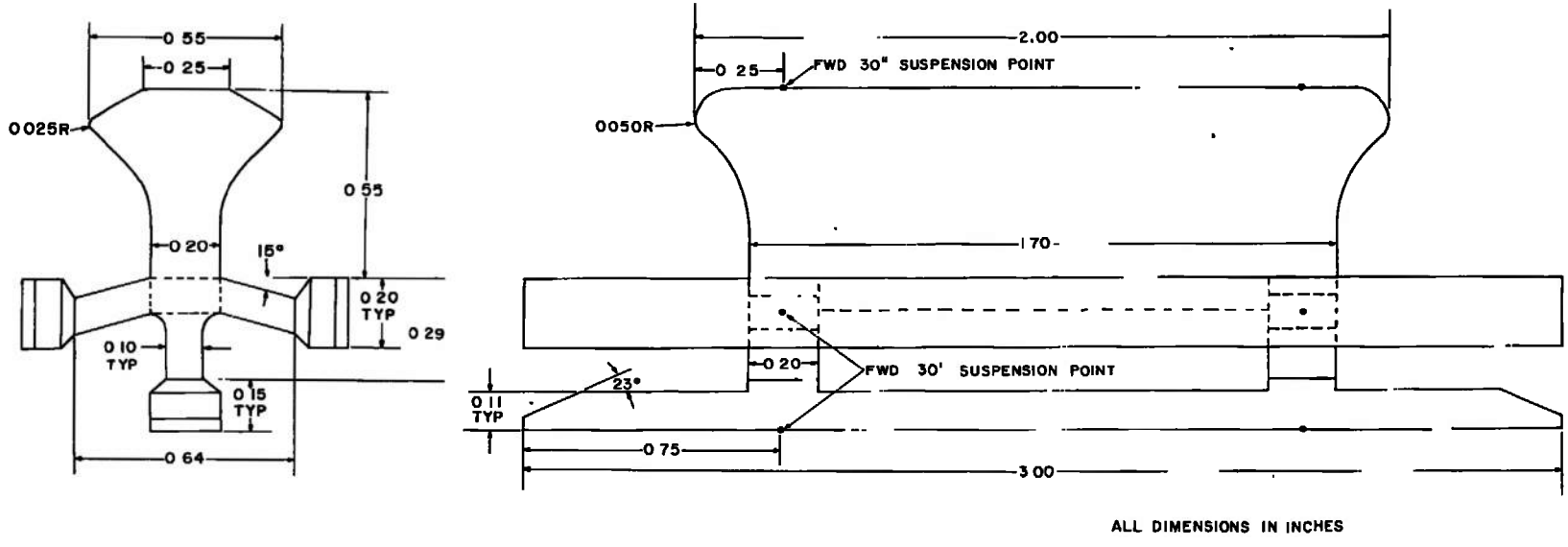

c. TRL 3
Fig. 4 Continued

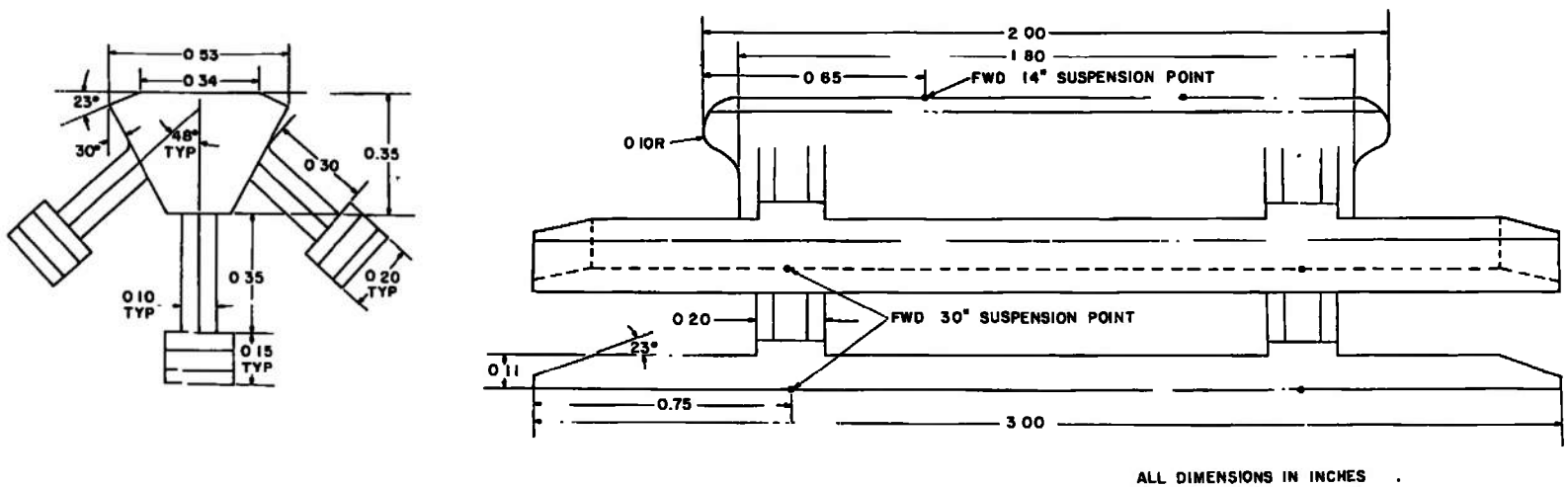

d. TRL 4
Fig. 4 Continued

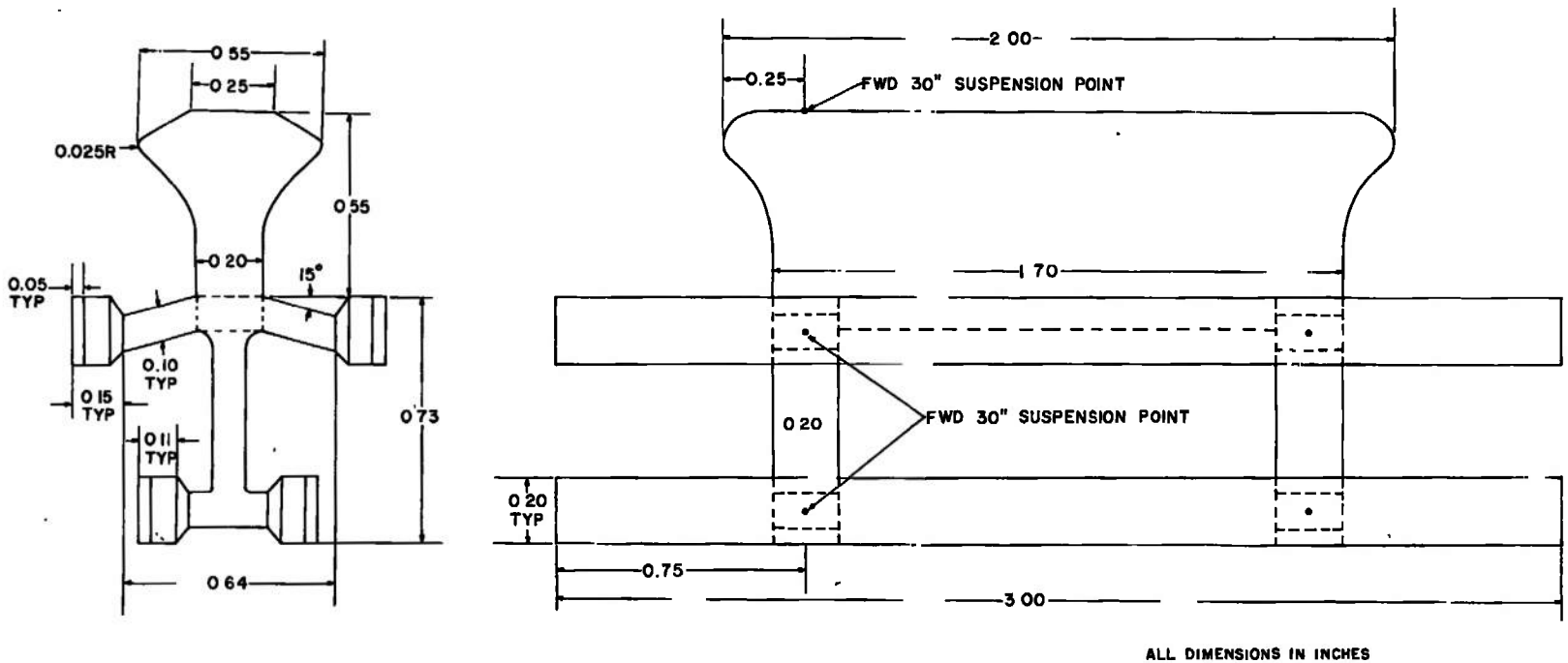

e. QRL 1
Fig. 4 Continued

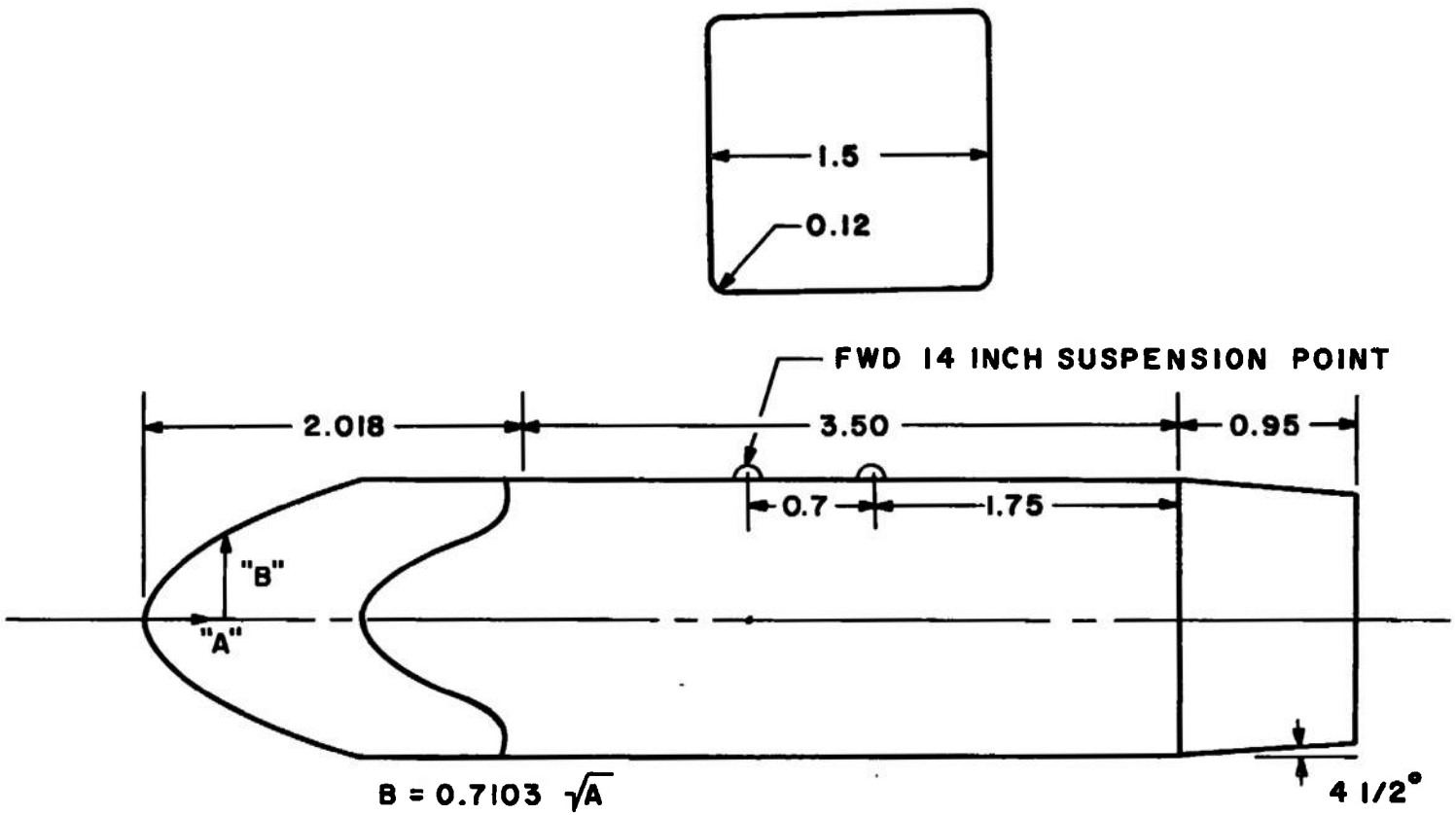

ALL DIMENSIONS IN INCHES

f. ATRL 30 x 30
Fig. 4 Concluded

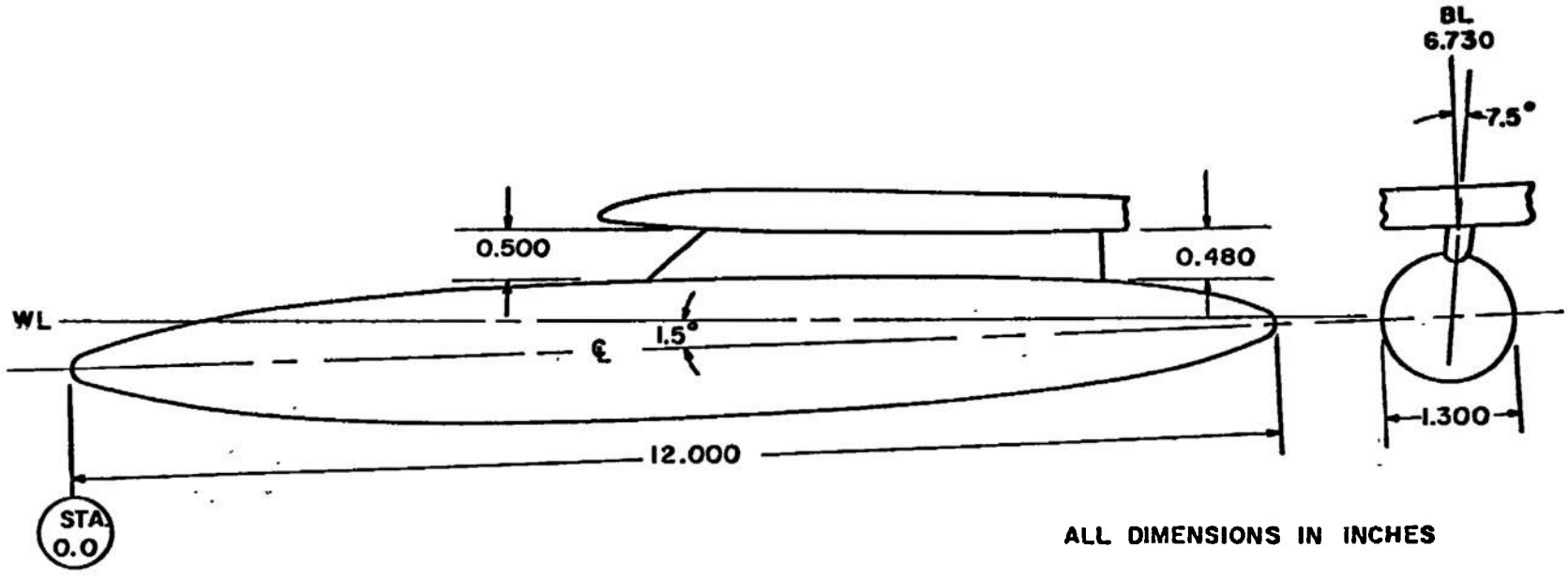

BODY CONTOUR, TYPICAL BOTH ENDS

STATION	BODY DIAM	STATION	BODY DIAM
0.000	0.000	2.500	1.116
0.025	0.100	2.750	1.156
0.050	0.144	3.000	1.190
0.150	0.258	3.250	1.218
0.250	0.340	3.500	1.242
0.500	0.498	3.750	1.260
0.750	0.622	4.000	1.274
1.000	0.724	4.250	1.286
1.250	0.812	4.500	1.294
1.500	0.890	4.750	1.298
1.750	0.958	5.000	1.300
2.000	1.016	6.000	1.300
2.250	1.070		

Fig. 5 Details and Dimensions of the 370-gal Fuel Tank Model on the Outboard Pylon

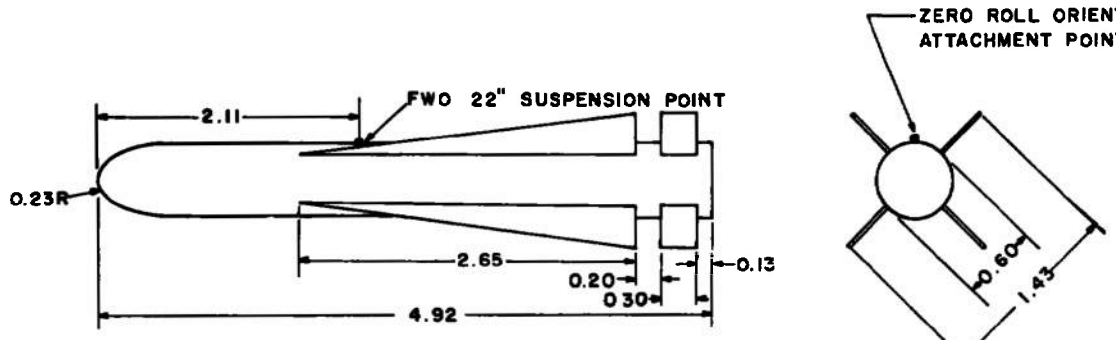

a. M1

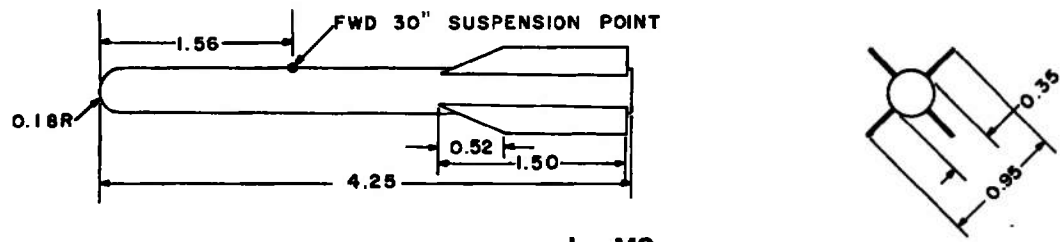

b. M2

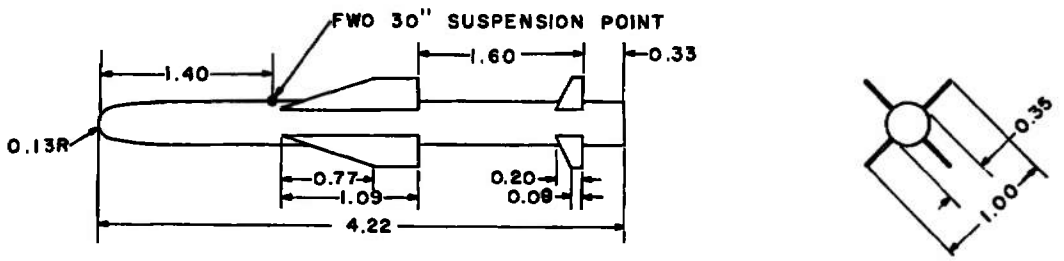

c. M3

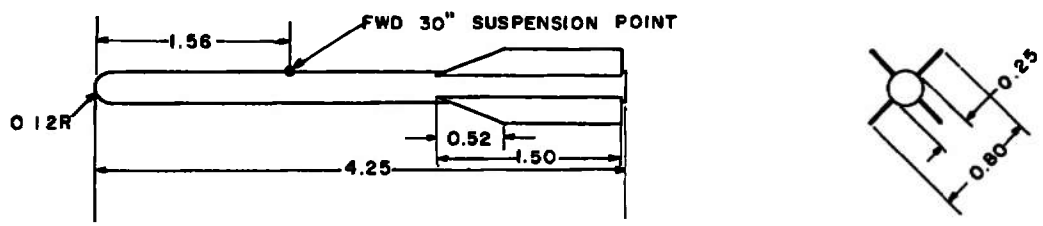

ALL DIMENSIONS IN INCHES

d. M4

Fig. 6 Details and Dimensions of the Weapon Store Models

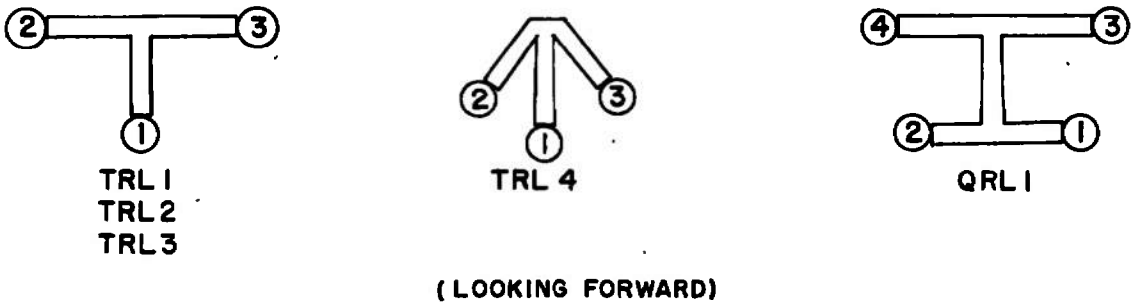

TYPE RACK	STATION	STORE ROLL ORIENTATION (DEGREES)
TRL 1, TRL 2 OR TRL 3	1	0
	2	+90
	3	-90
TRL 4	1	0
	2	+48
	3	-48
QRL 1	1	-90
	2	+90
	3	-90
	4	+90

Fig. 7 Schematic of the Launcher Rack Store Stations and Orientation

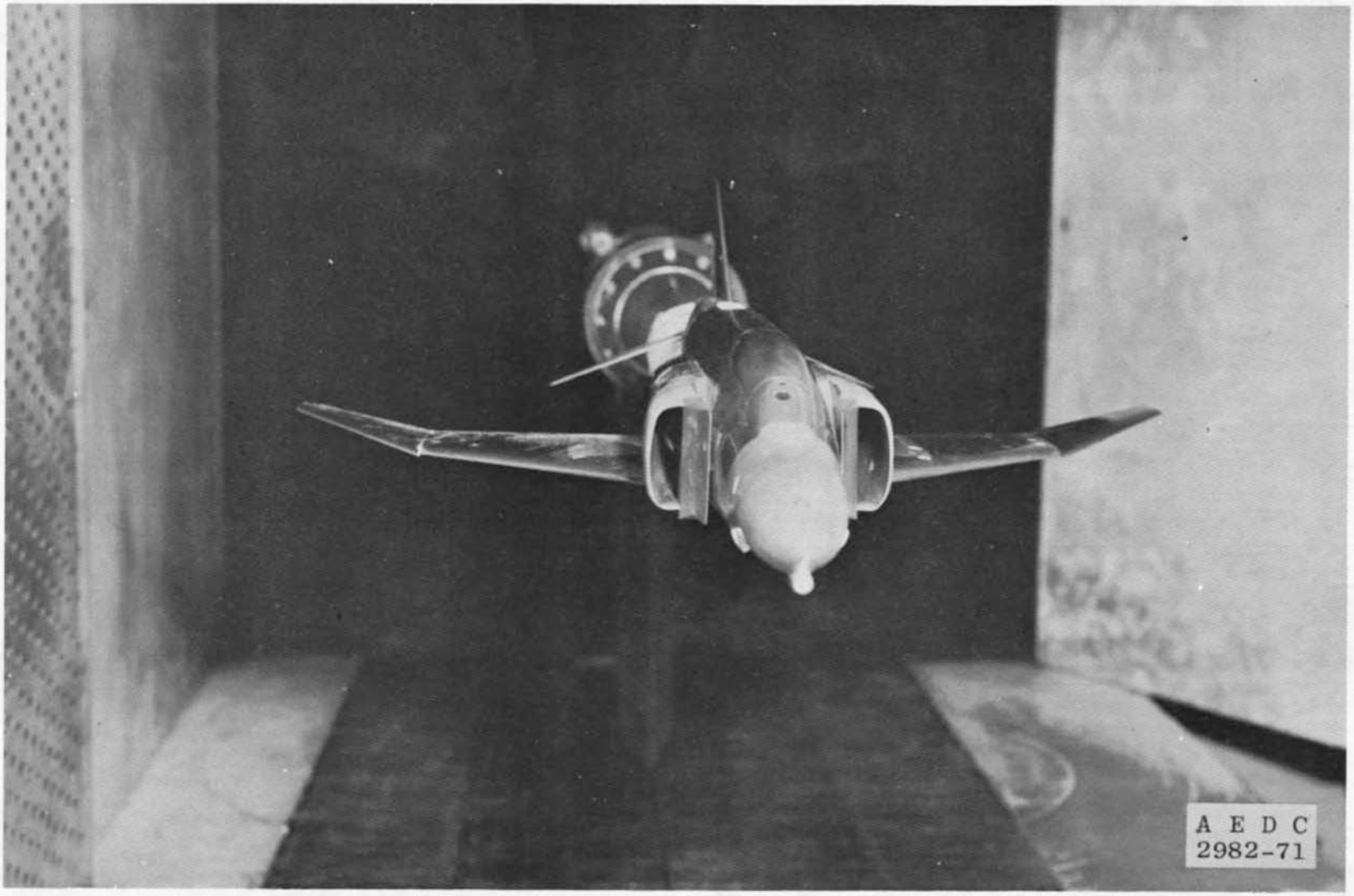

a. Configuration F401

Fig. 8 F-4D Model with Different Store Configurations Installed in the Tunnel Test Section

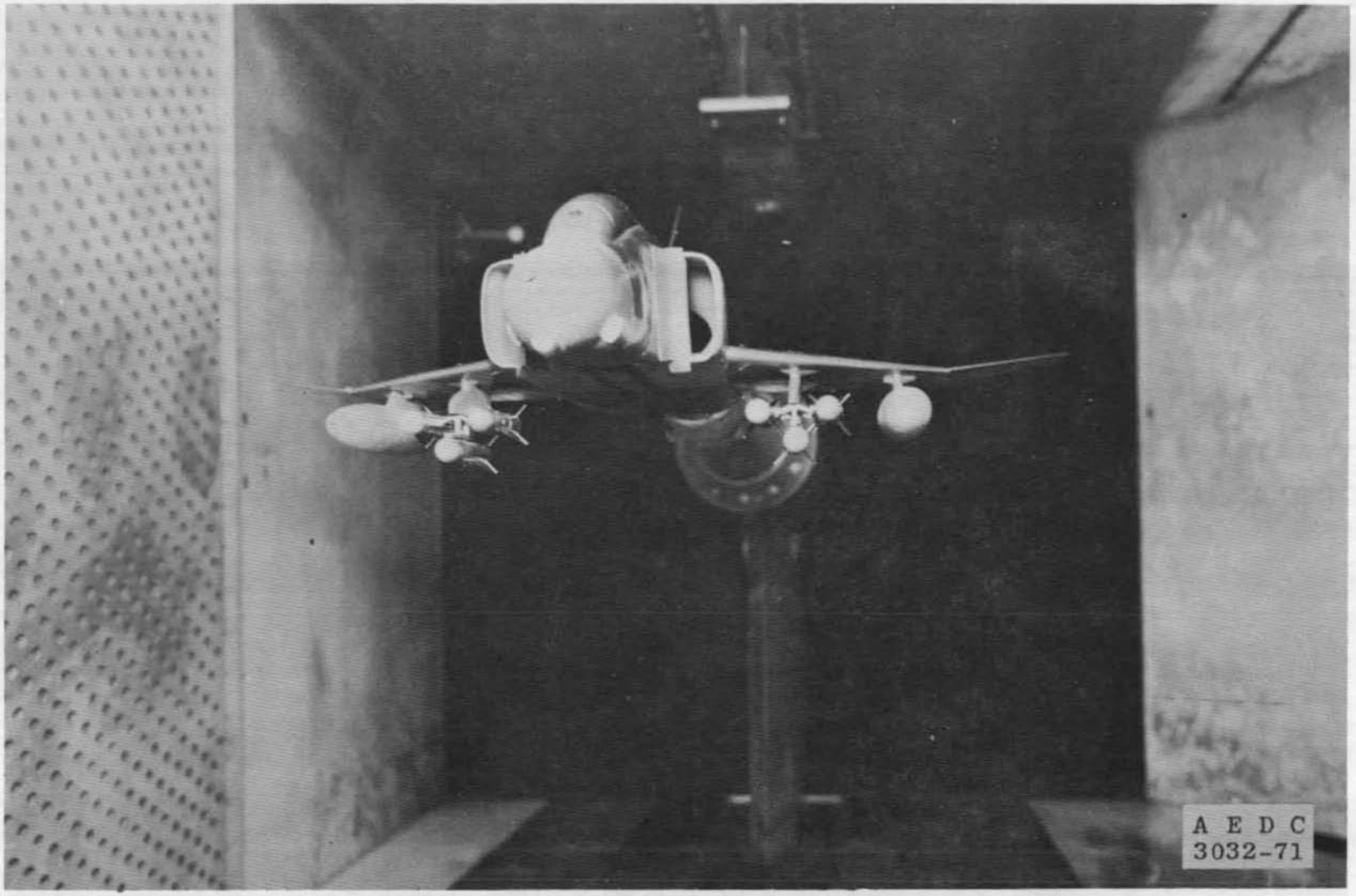

b. Configuration F408
Fig. 8 Continued

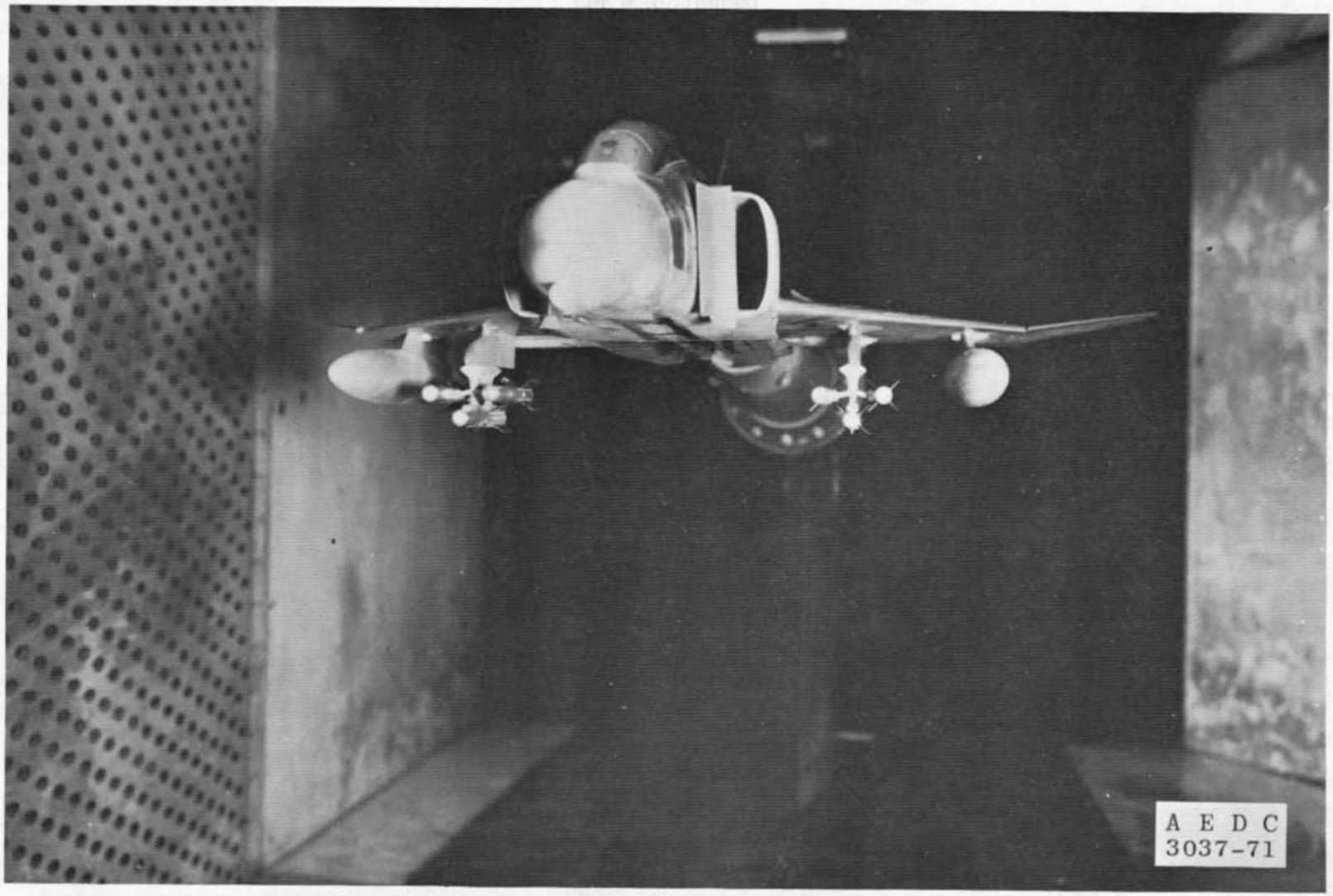

c. Configuration F422
Fig. 8 Continued

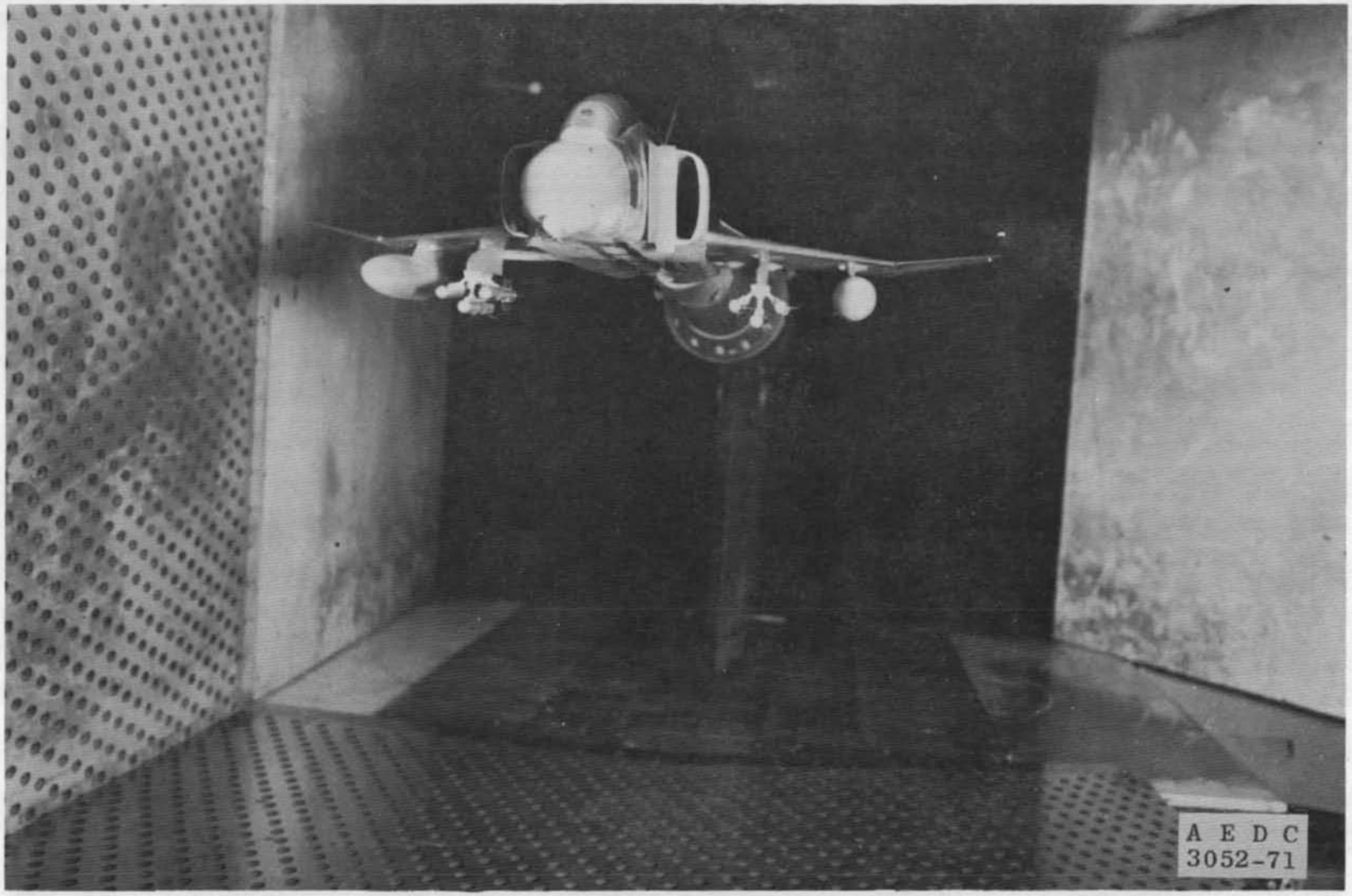

d. Configuration F429
Fig. 8 Continued

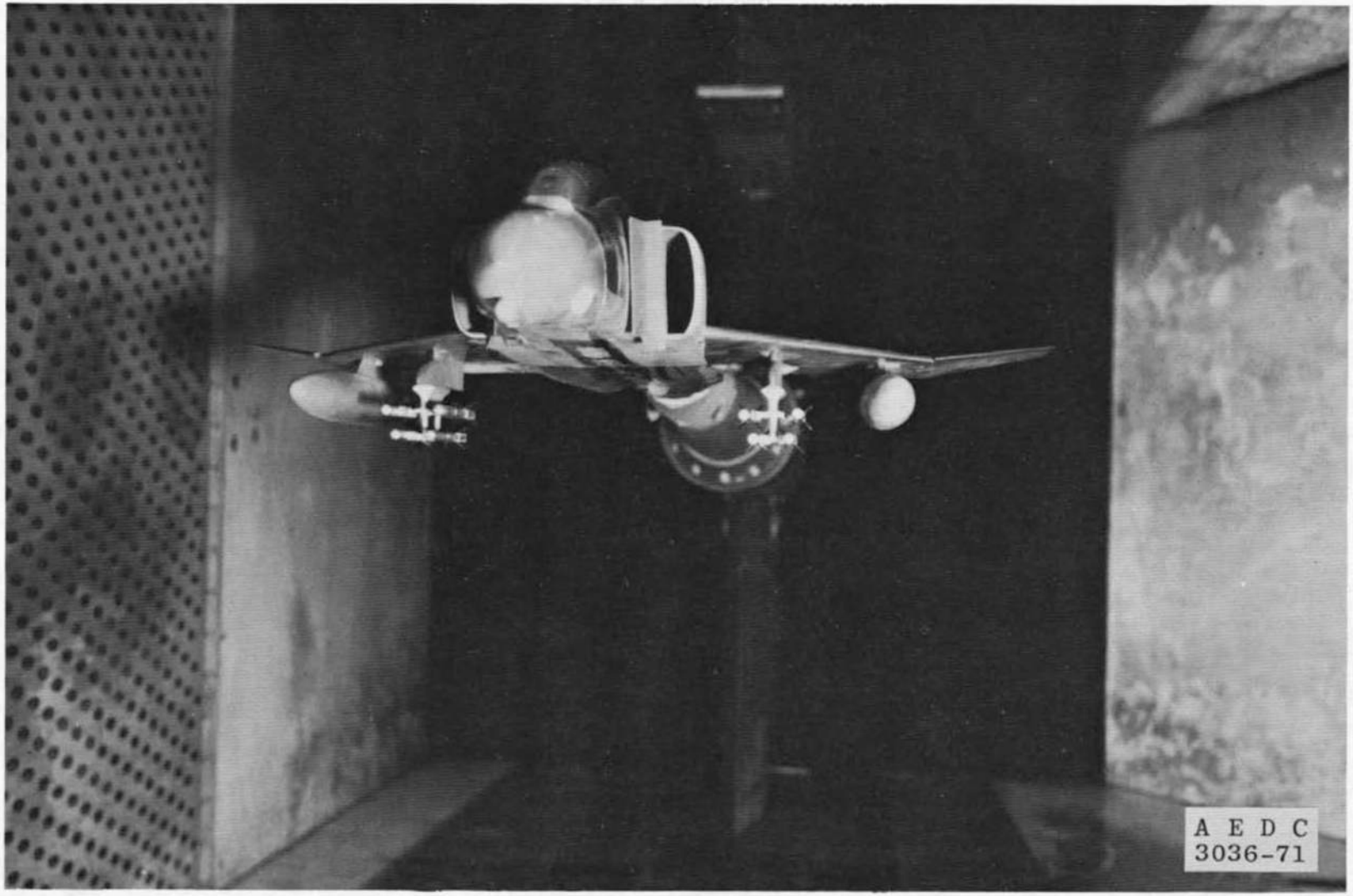

e. Configuration F435
Fig. 8 Continued

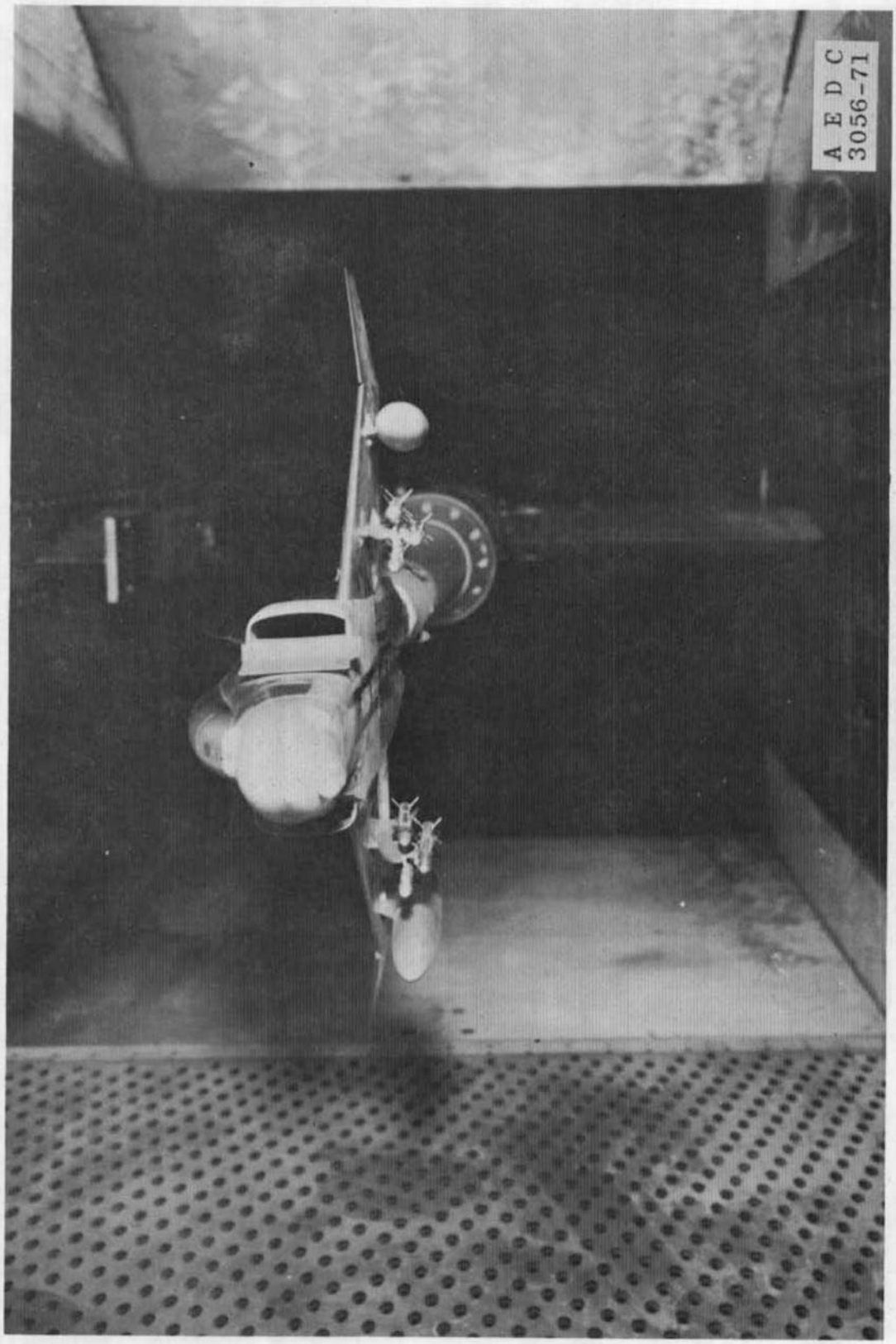

f. Configuration F438
Fig. 8 Continued

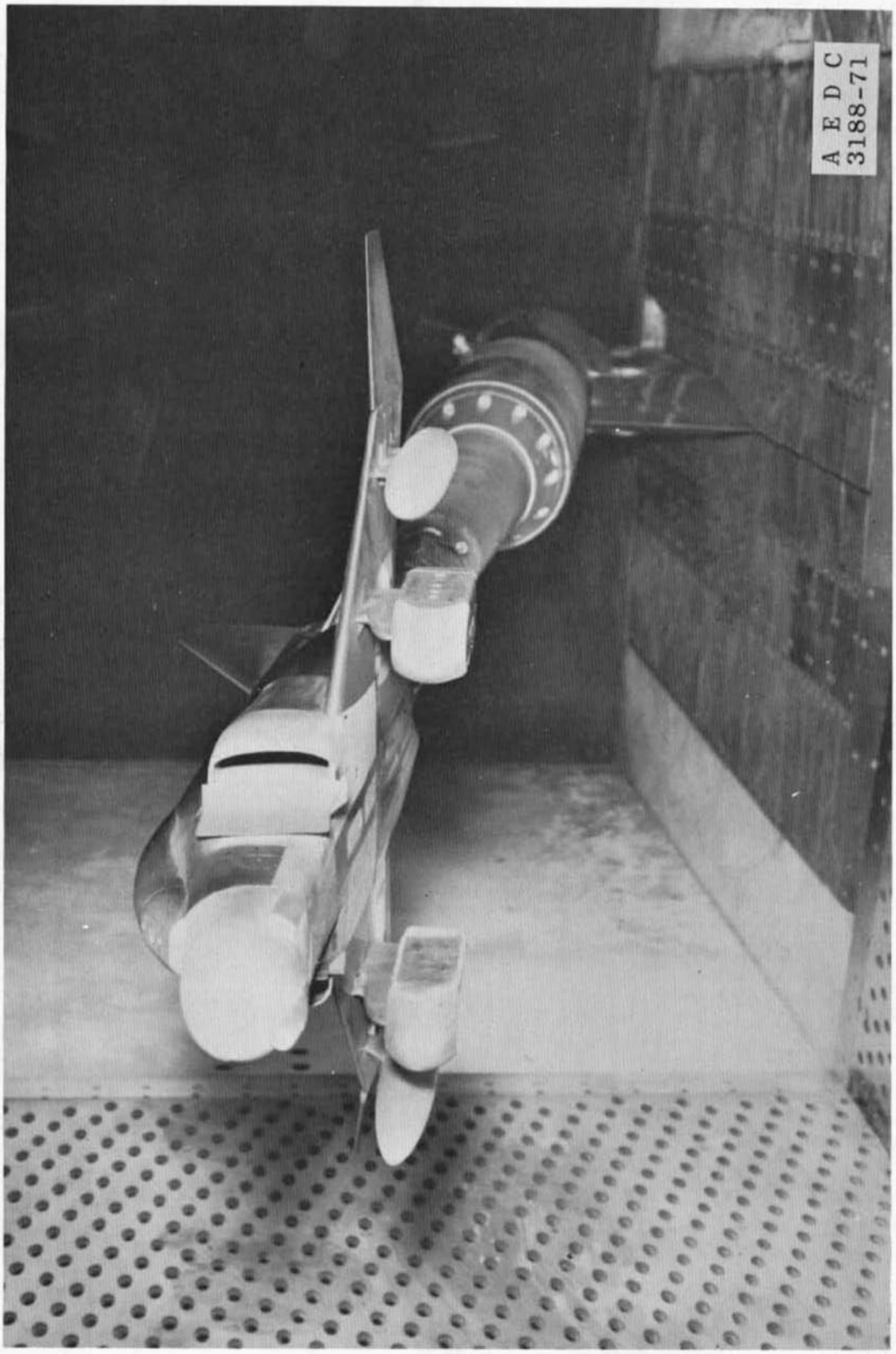

g. Configuration F456

Fig. 8 Concluded

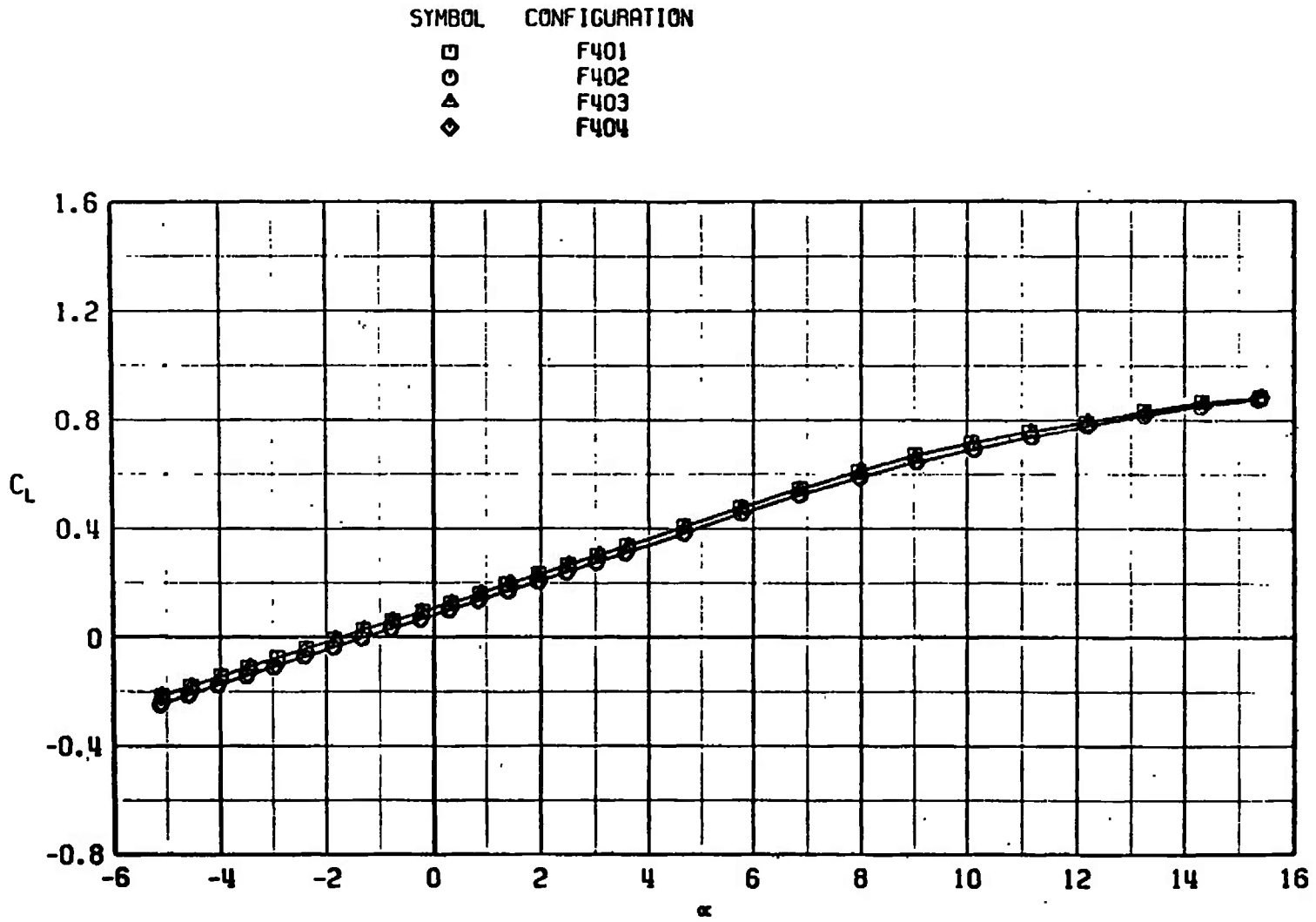

a. $M_\infty = 0.75$

Fig. 9 Lift Coefficient Variation with Angle of Attack for Configurations F401, F402, F403, and F404

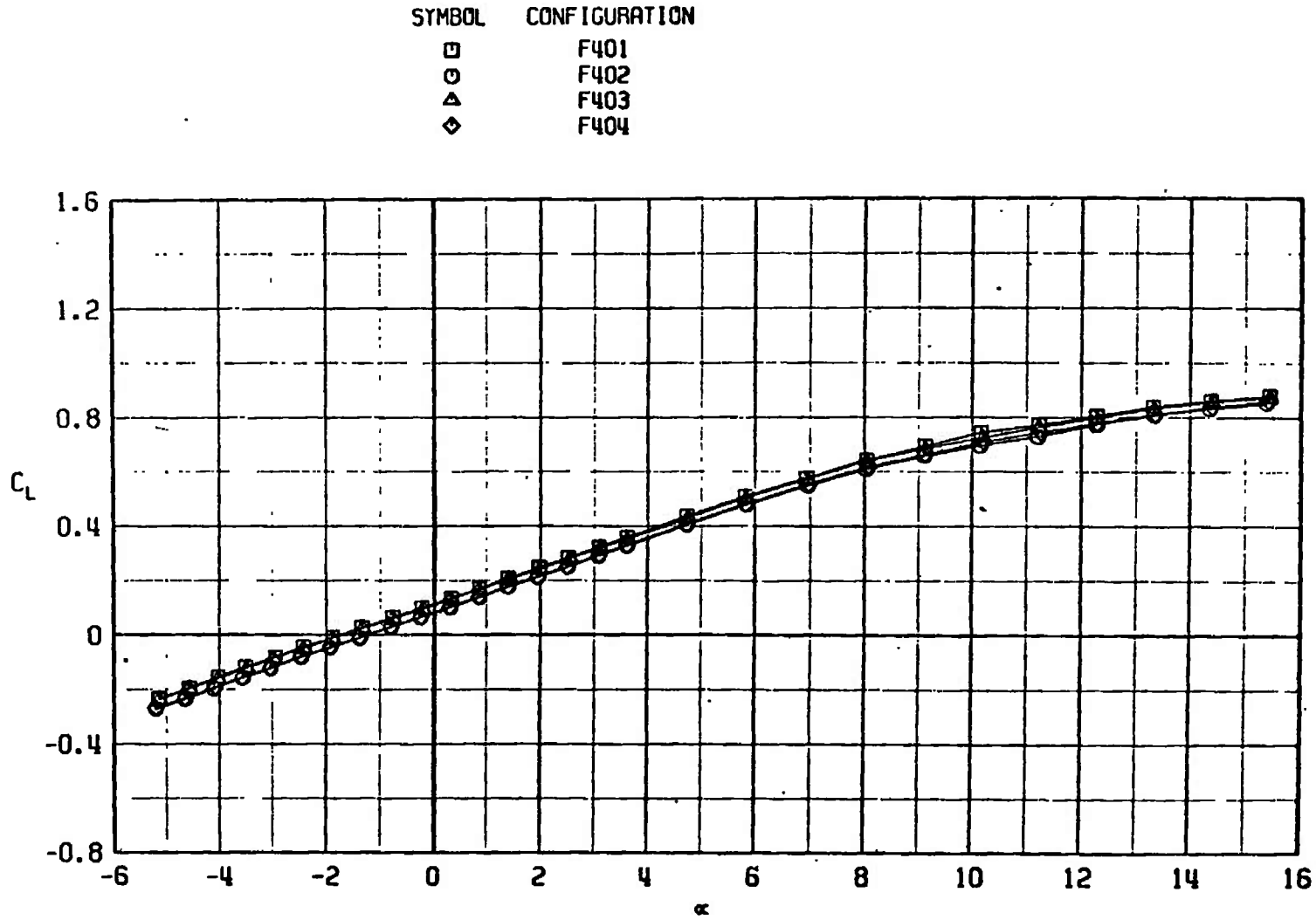

b. $M_\infty = 0.85$

Fig. 9 Continued

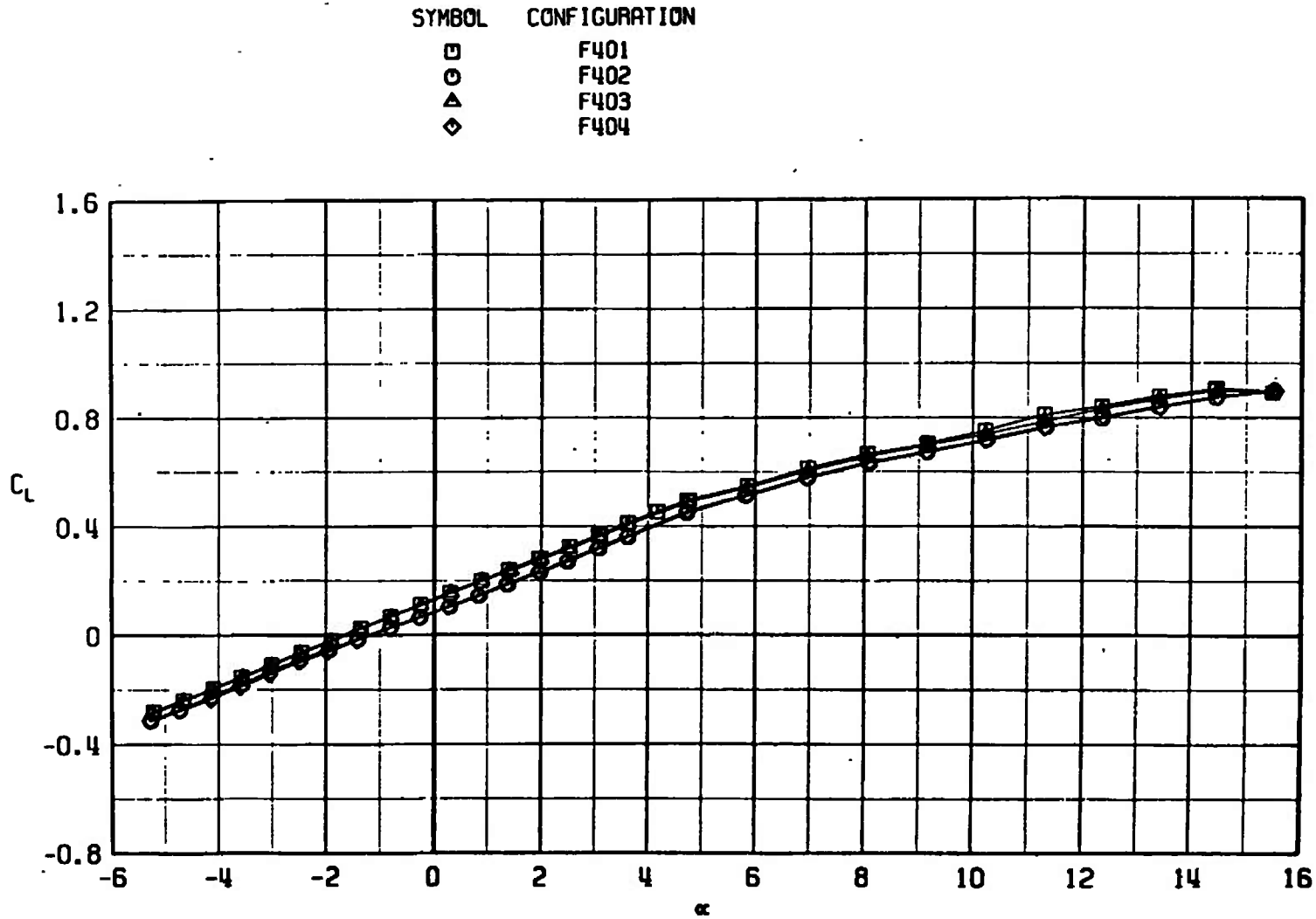

c. $M_\infty = 0.95$

Fig. 9 Continued

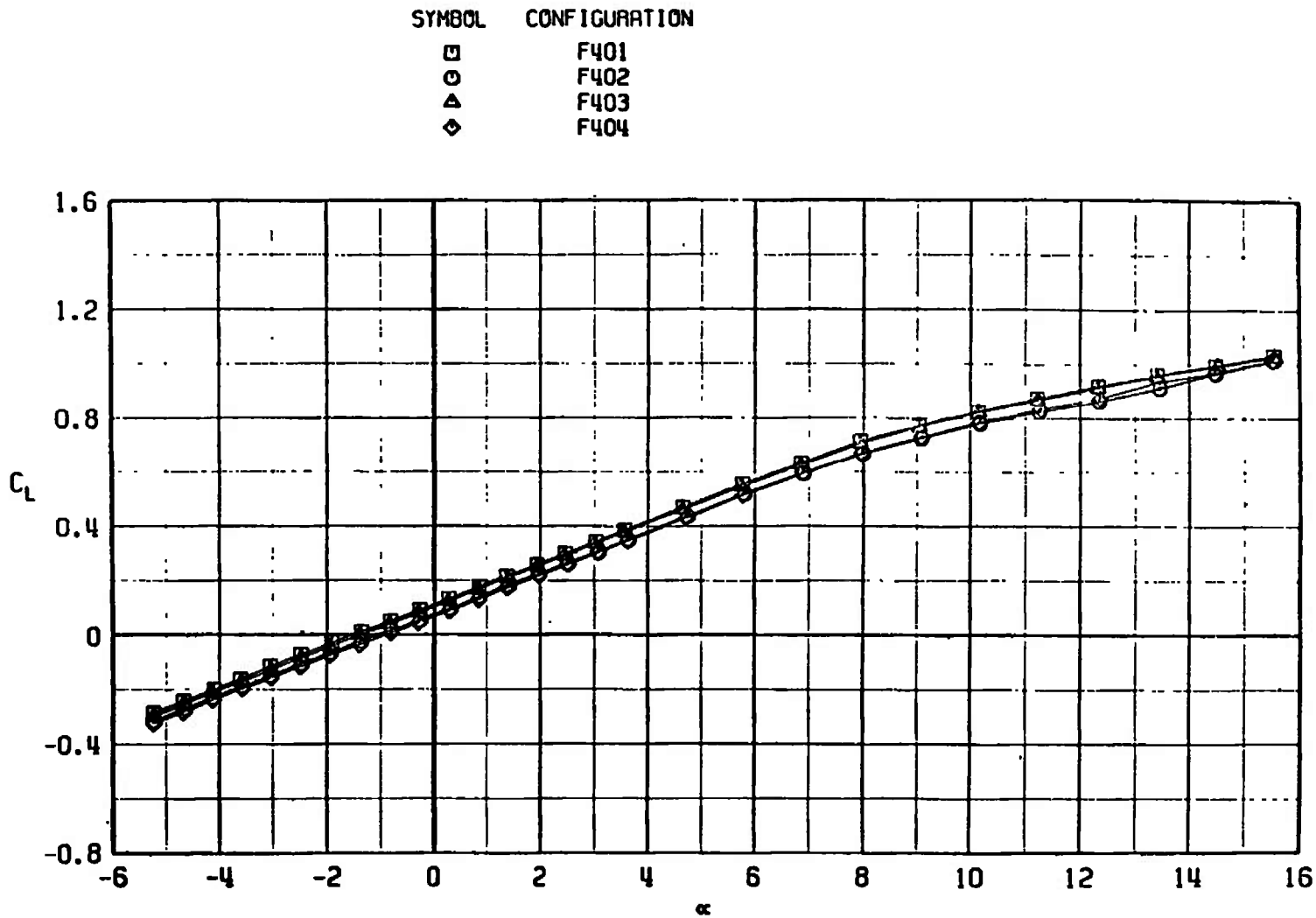

d. $M_\infty = 1.10$

Fig. 9 Continued

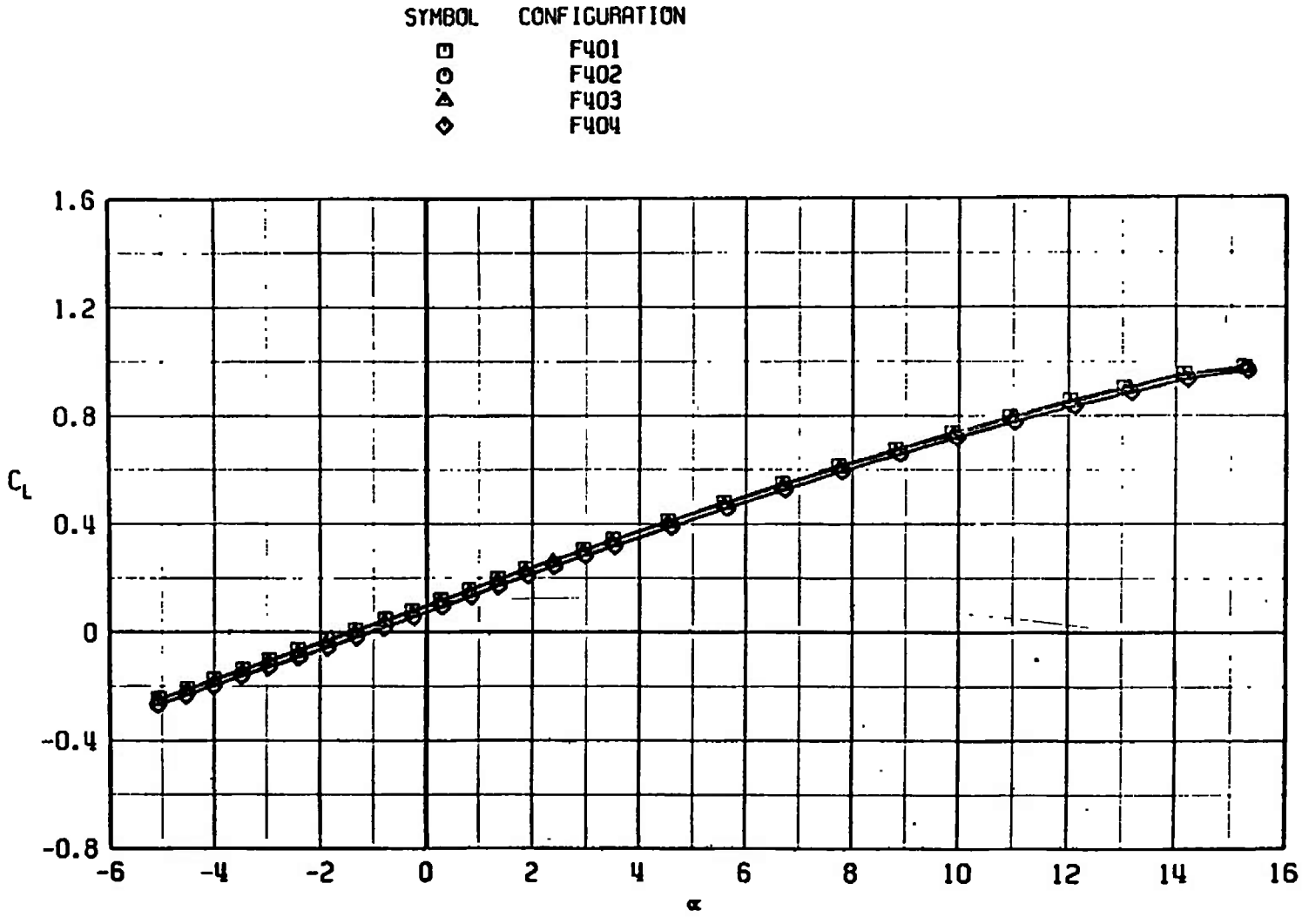

e. $M_\infty = 1.30$

Fig. 9 Concluded

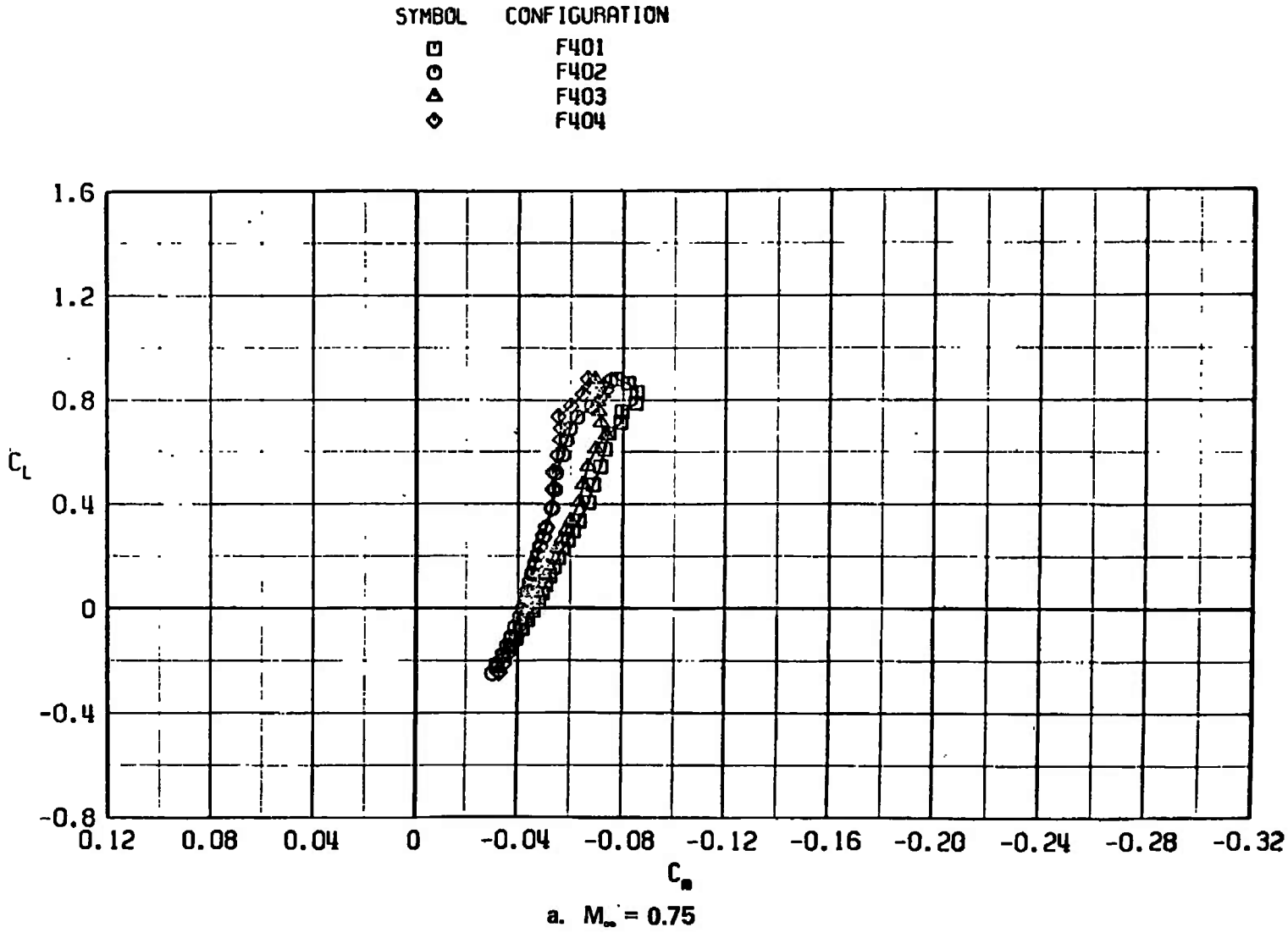

a. $M_\infty = 0.75$

Fig. 10 Pitching-Moment Coefficient Variation with Lift Coefficient for Configurations F401, F402, F403, and F404

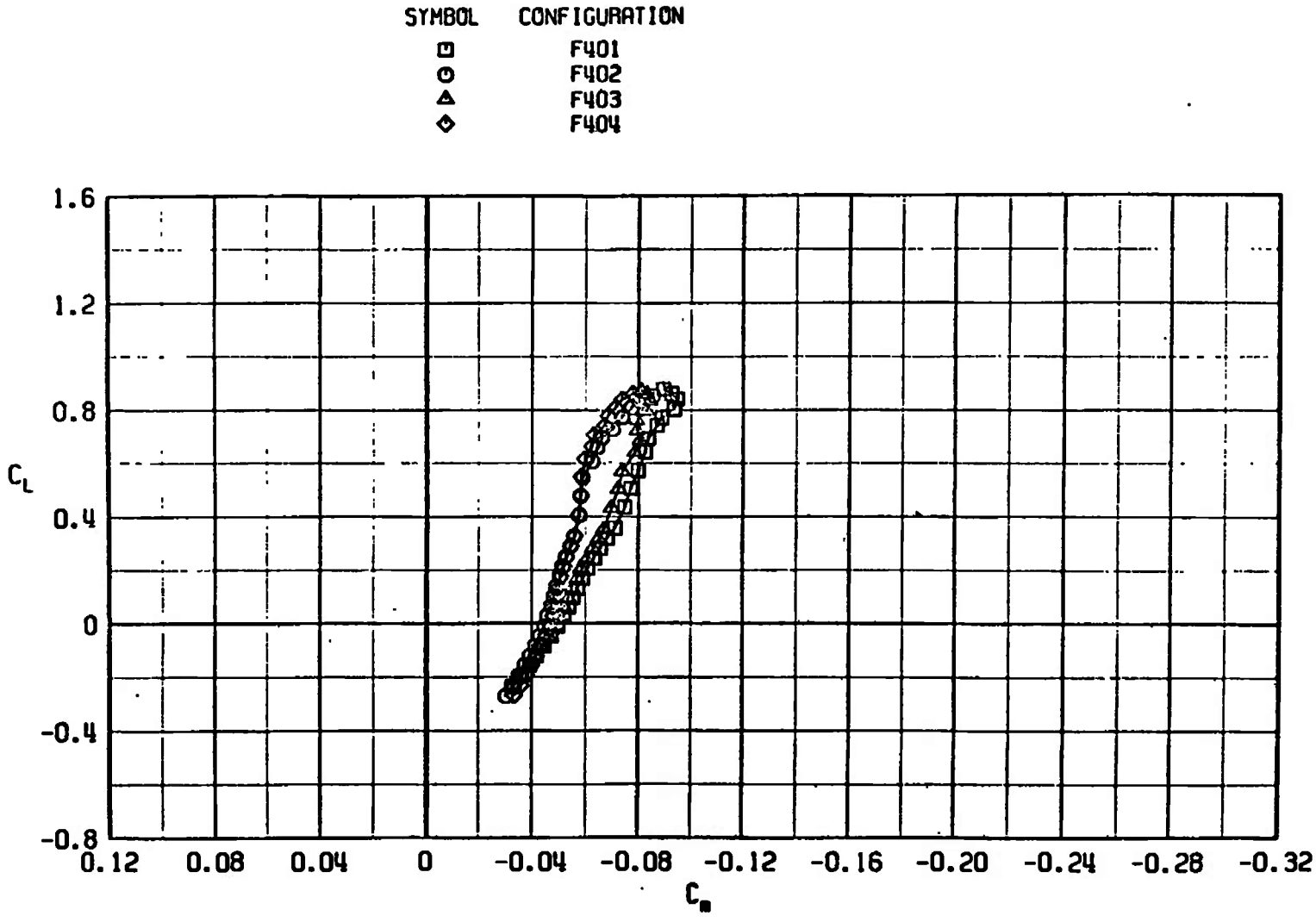

b. $M_\infty = 0.85$

Fig. 10 Continued

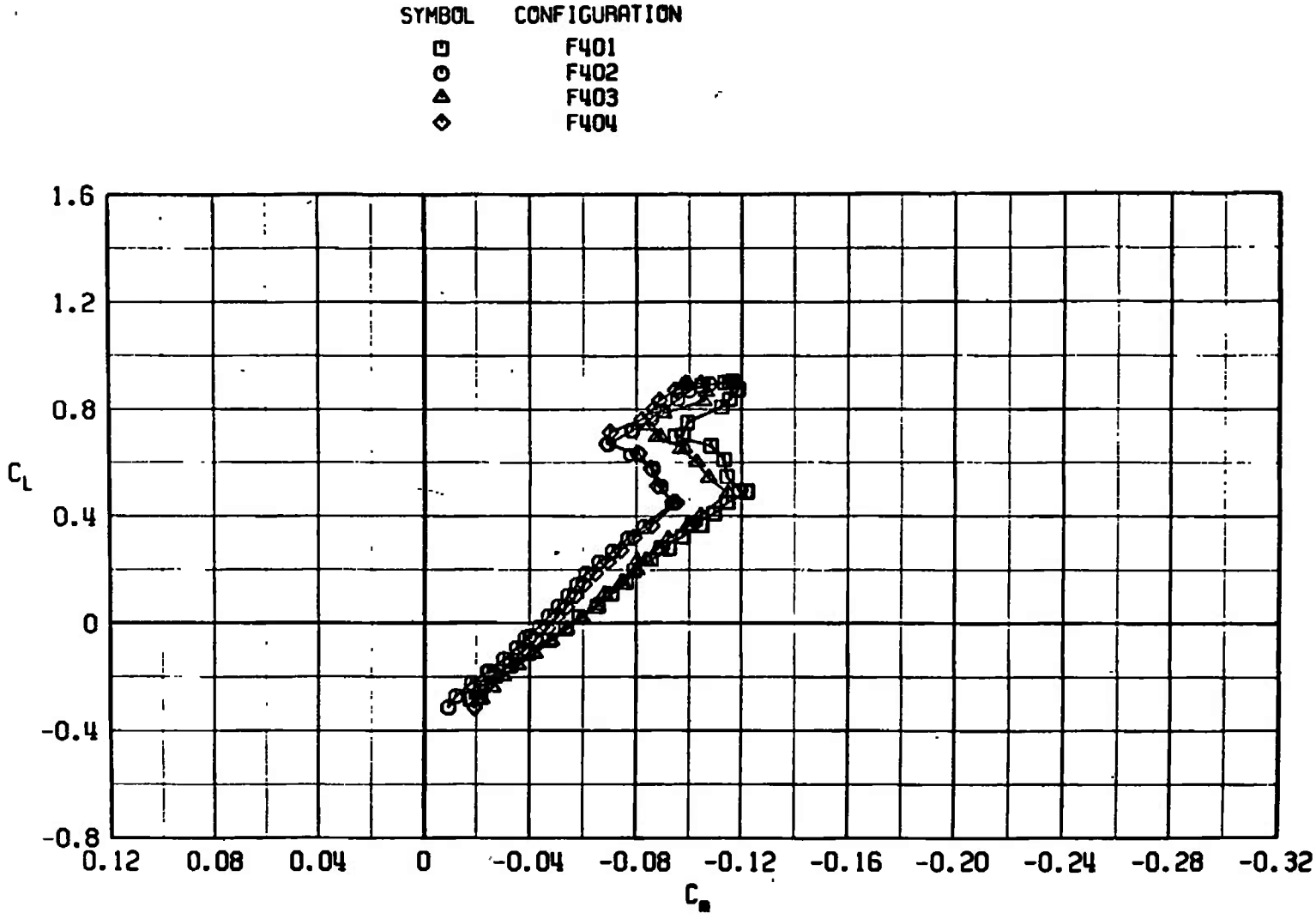

c. $M_\infty = 0.95$

Fig. 10 Continued

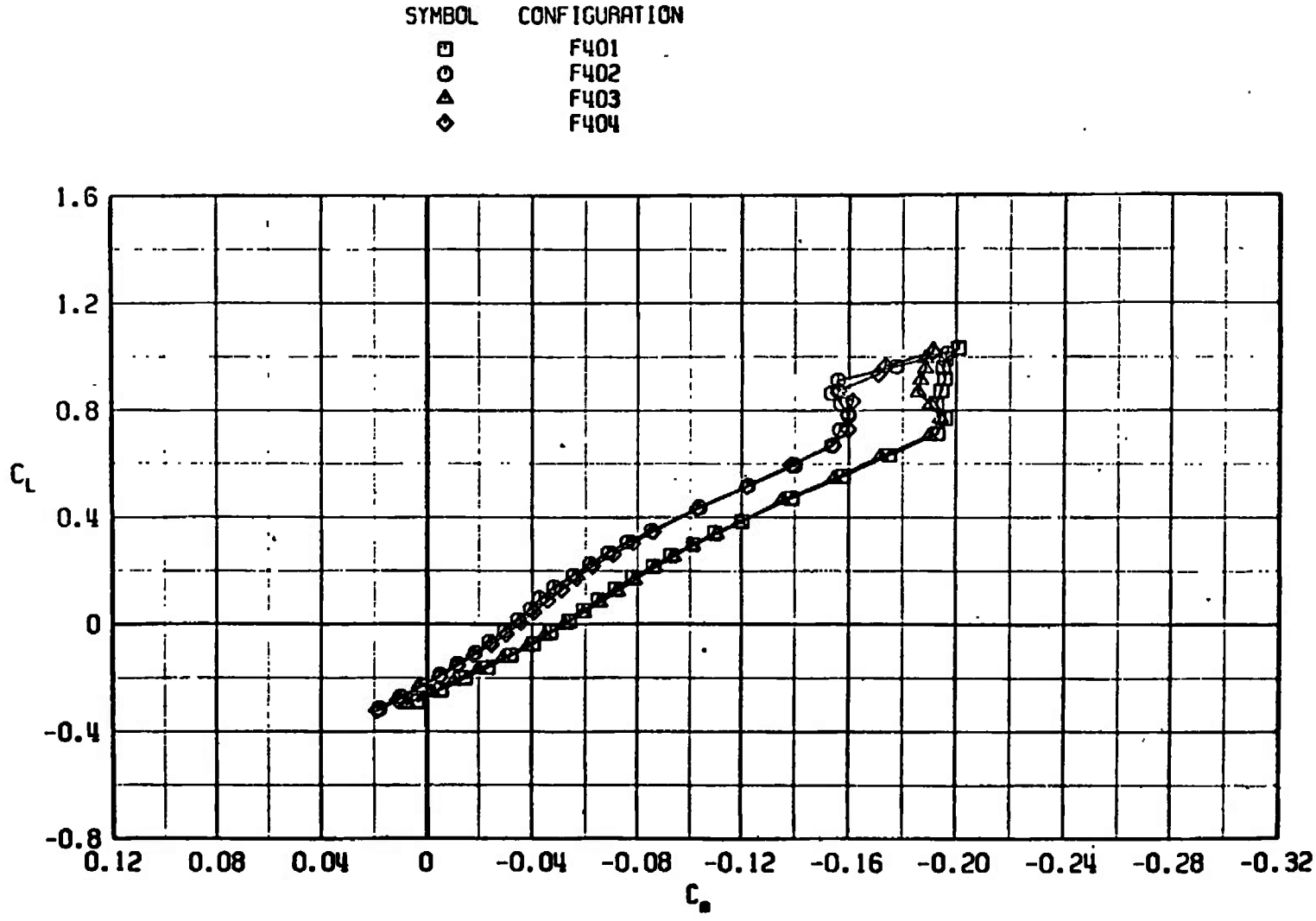

d. $M_\infty = 1.10$

Fig. 10 Continued

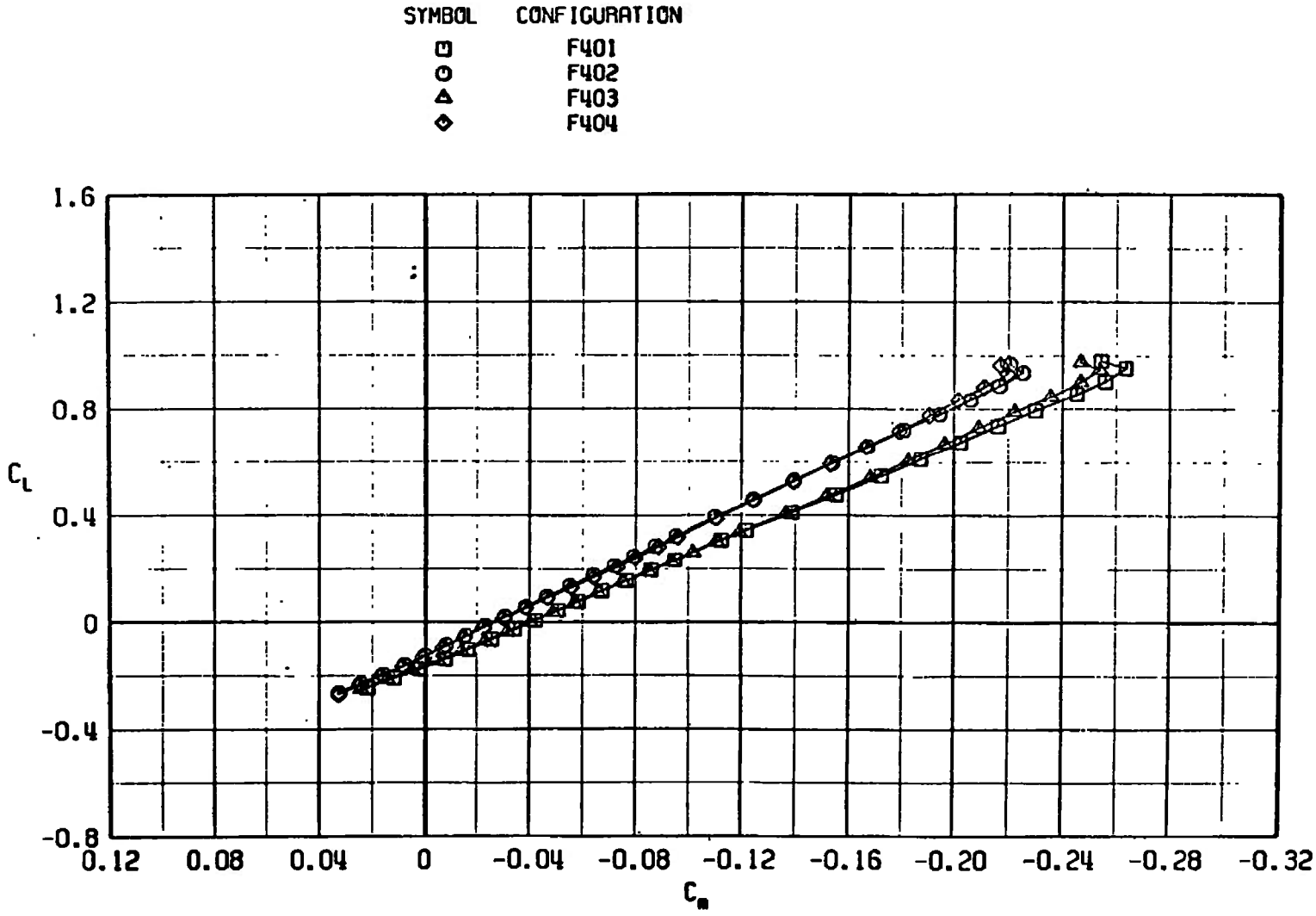

e. $M_\infty = 1.30$

Fig. 10 Concluded

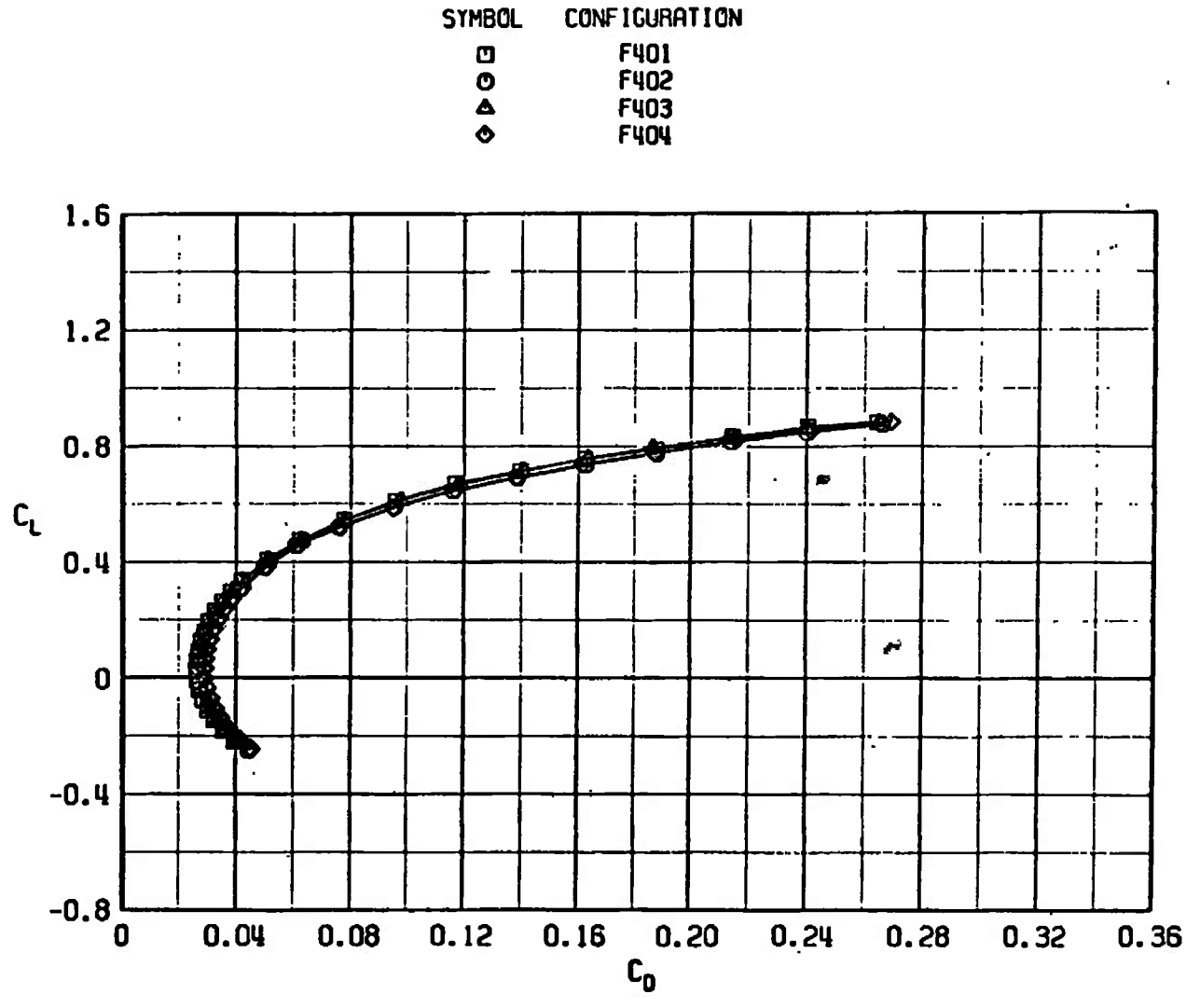

a. $M_\infty = 0.75$

Fig. 11 Drag Coefficient Variation with Lift Coefficient for Configurations F401, F402, F403, and F404

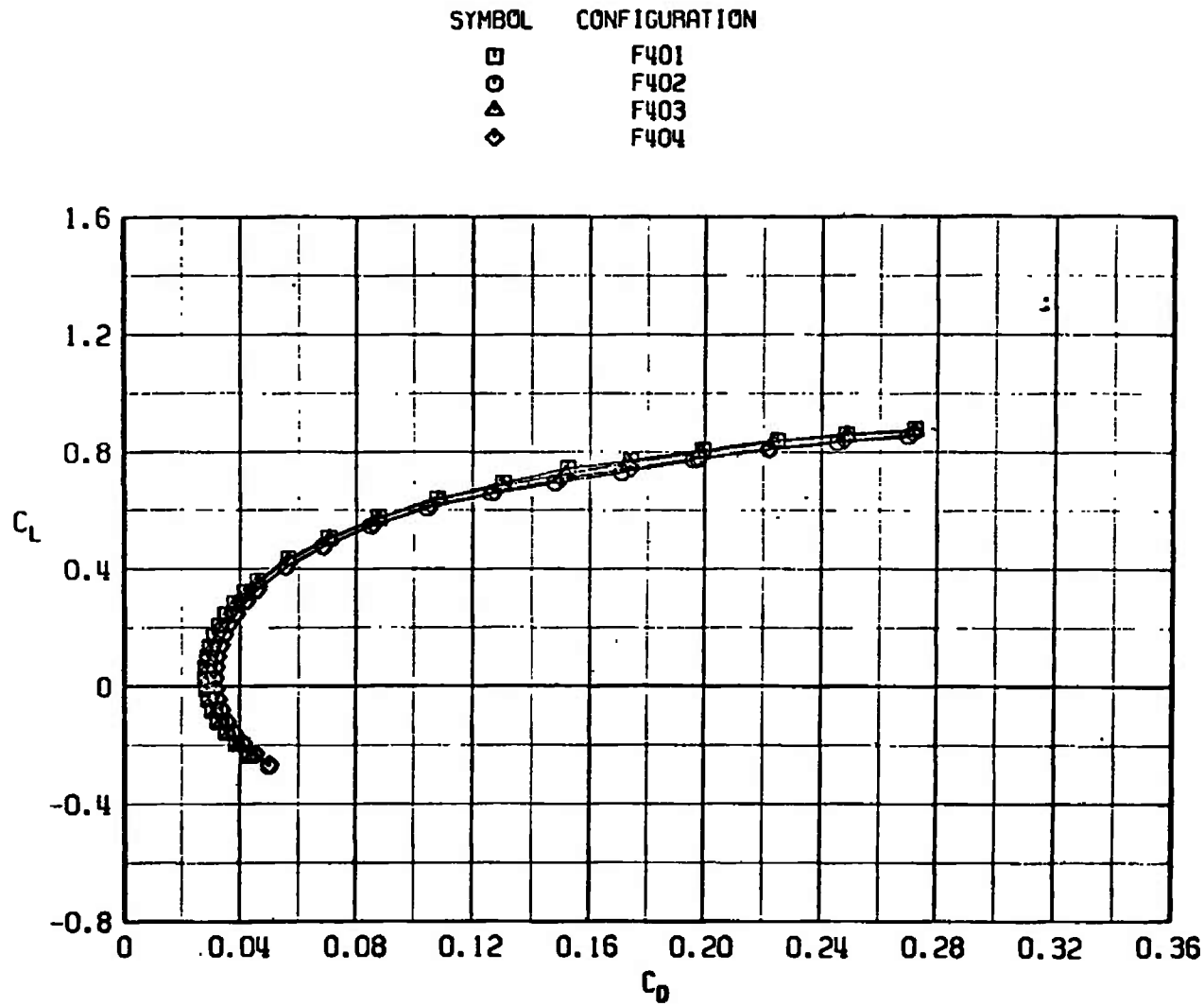

b. $M_\infty = 0.85$

Fig. 11 Continued

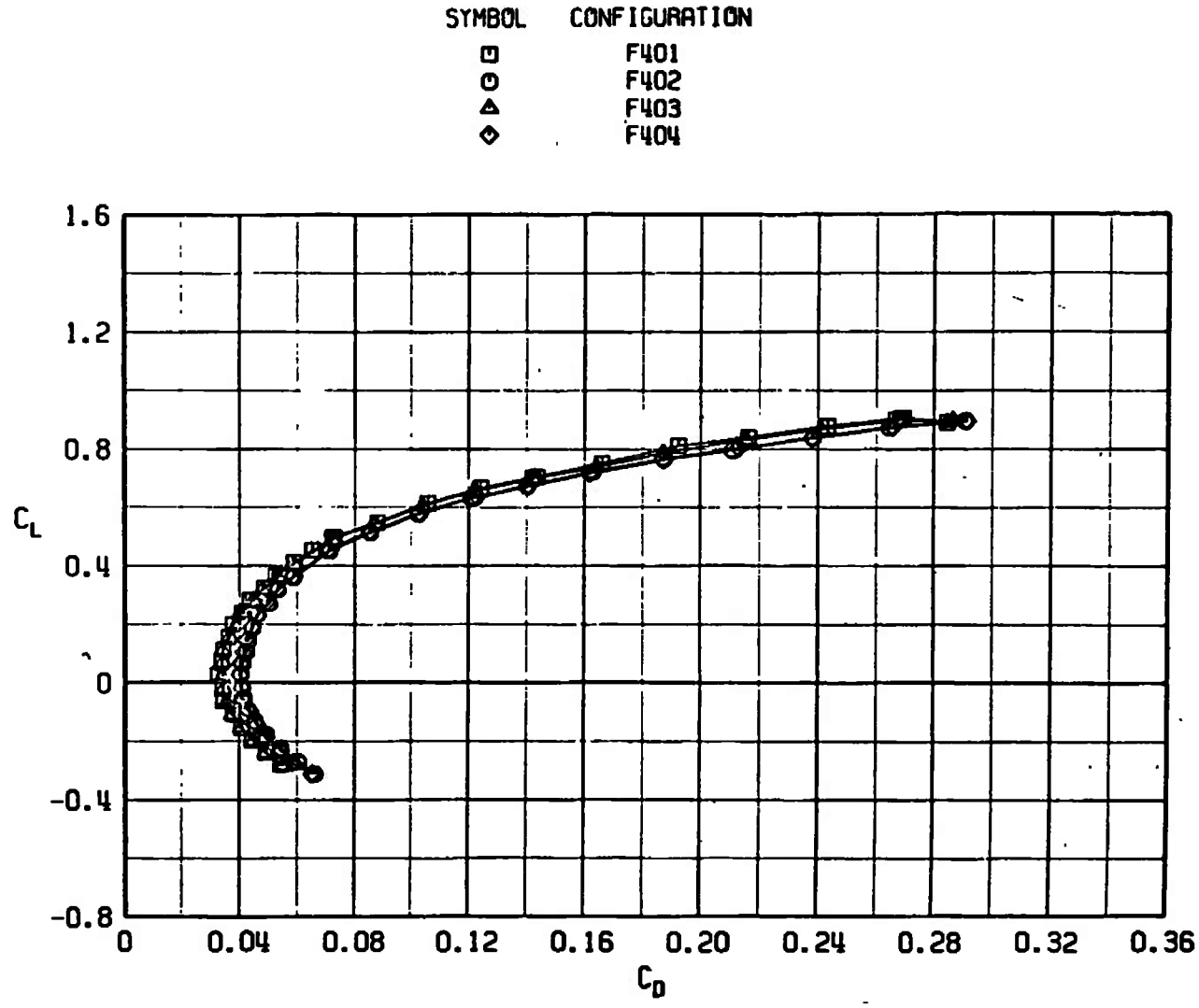

c. $M_\infty = 0.95$

Fig. 11 Continued

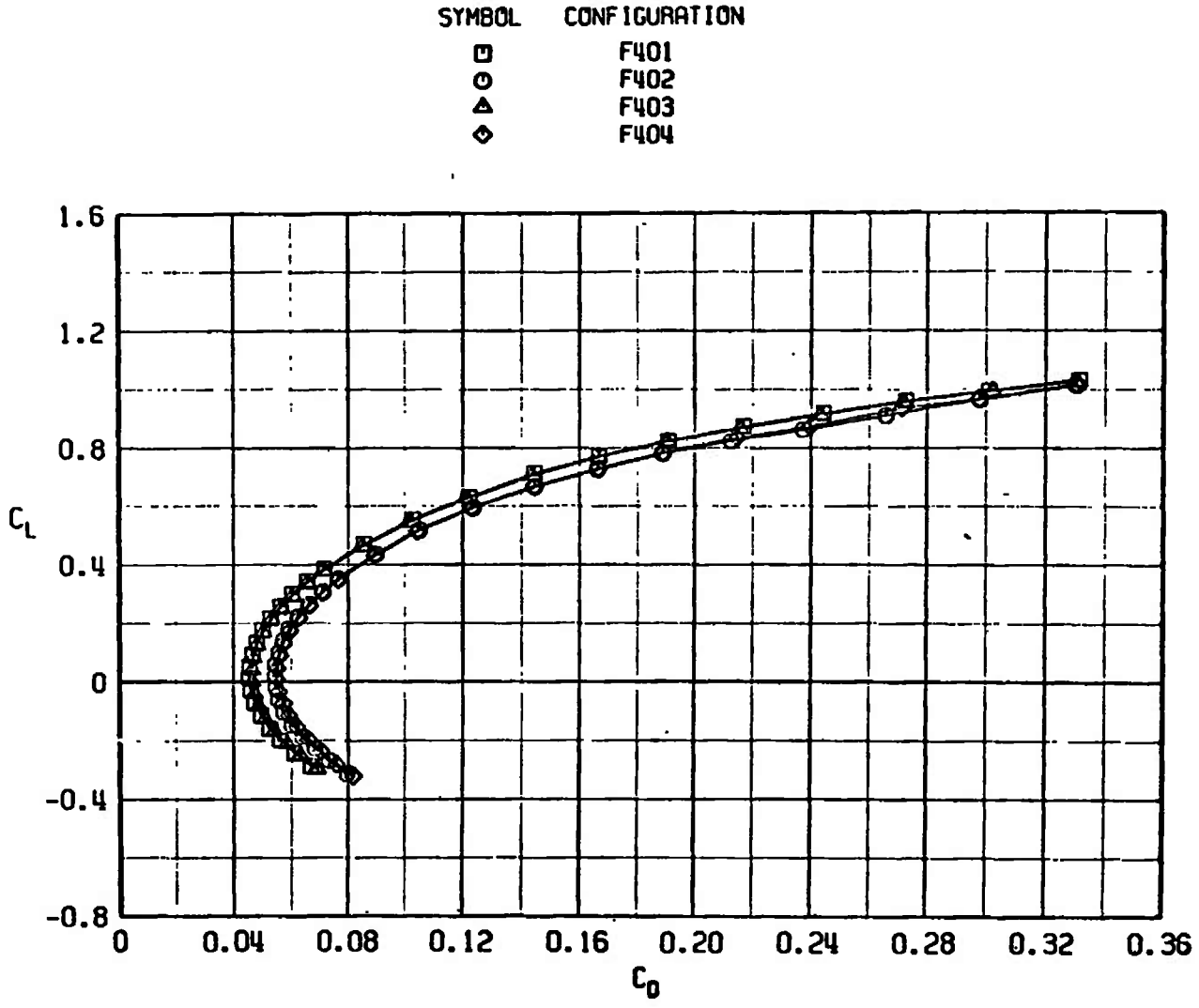

d. $M_\infty = 1.10$

Fig. 11 Continued

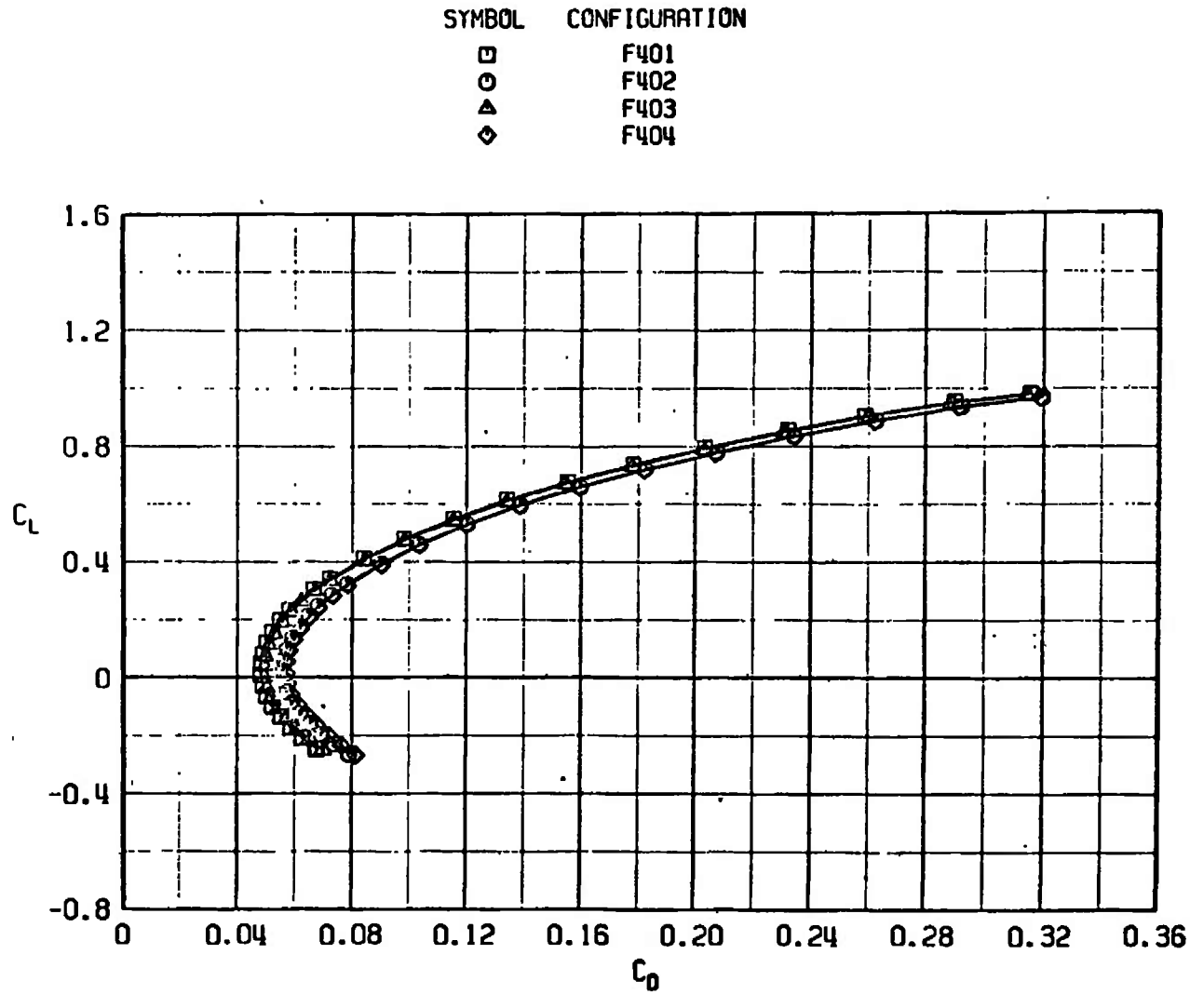

e. $M_\infty = 1.30$

Fig. 11 Concluded

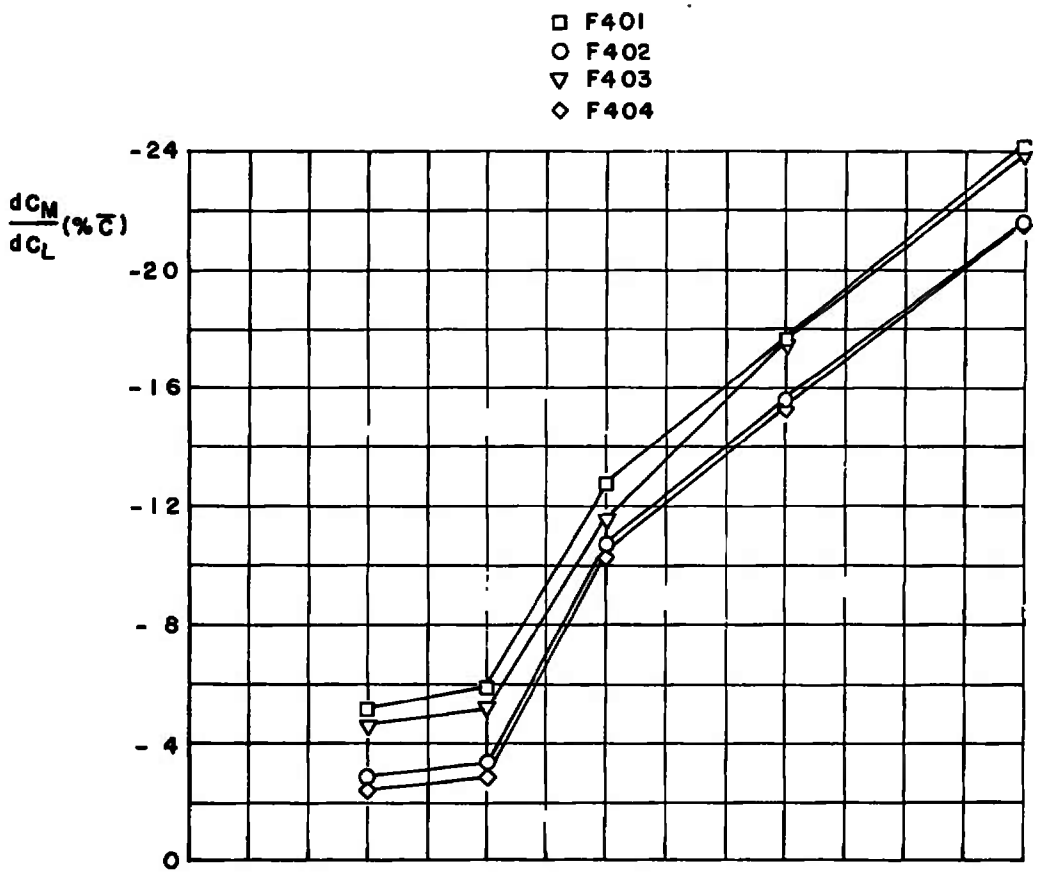

a. dC_m/dC_L versus M_∞ at $C_L = 0.2$ in percentage of $\bar{c}$

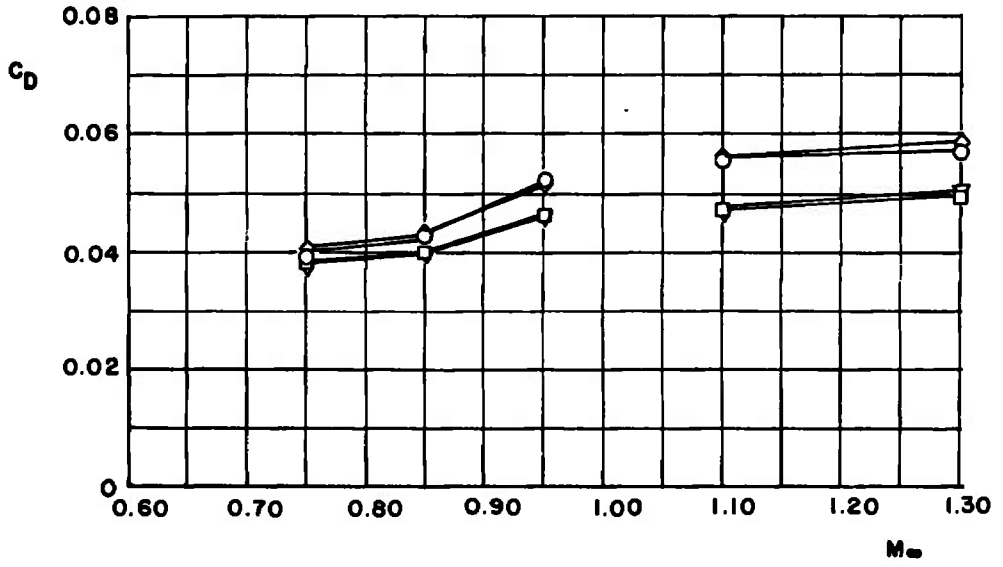

b. C_D versus M_∞ at $C_L = 0.3$, $M_\infty < 1.0$, and $C_L = 0.1$, $M_\infty > 1.0$

Fig. 12 Drag Coefficient and dC_m/dC_L Variation with Mach Number for Configurations F401, F402, F403, and F404

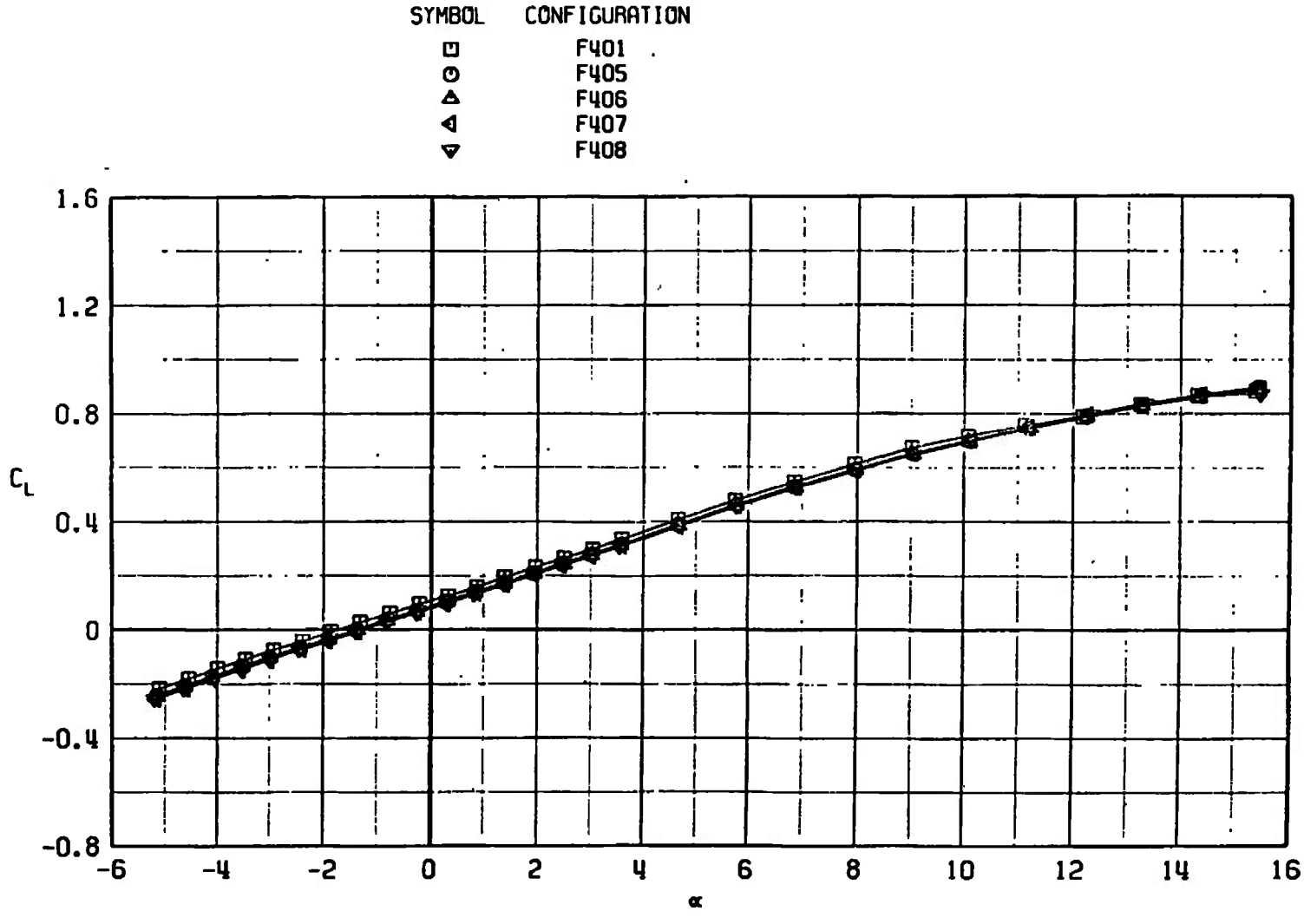

a. $M_\infty = 0.75$

Fig. 13 Lift Coefficient Variation with Angle of Attack for Configurations F401, F405, F406, F407, and F408

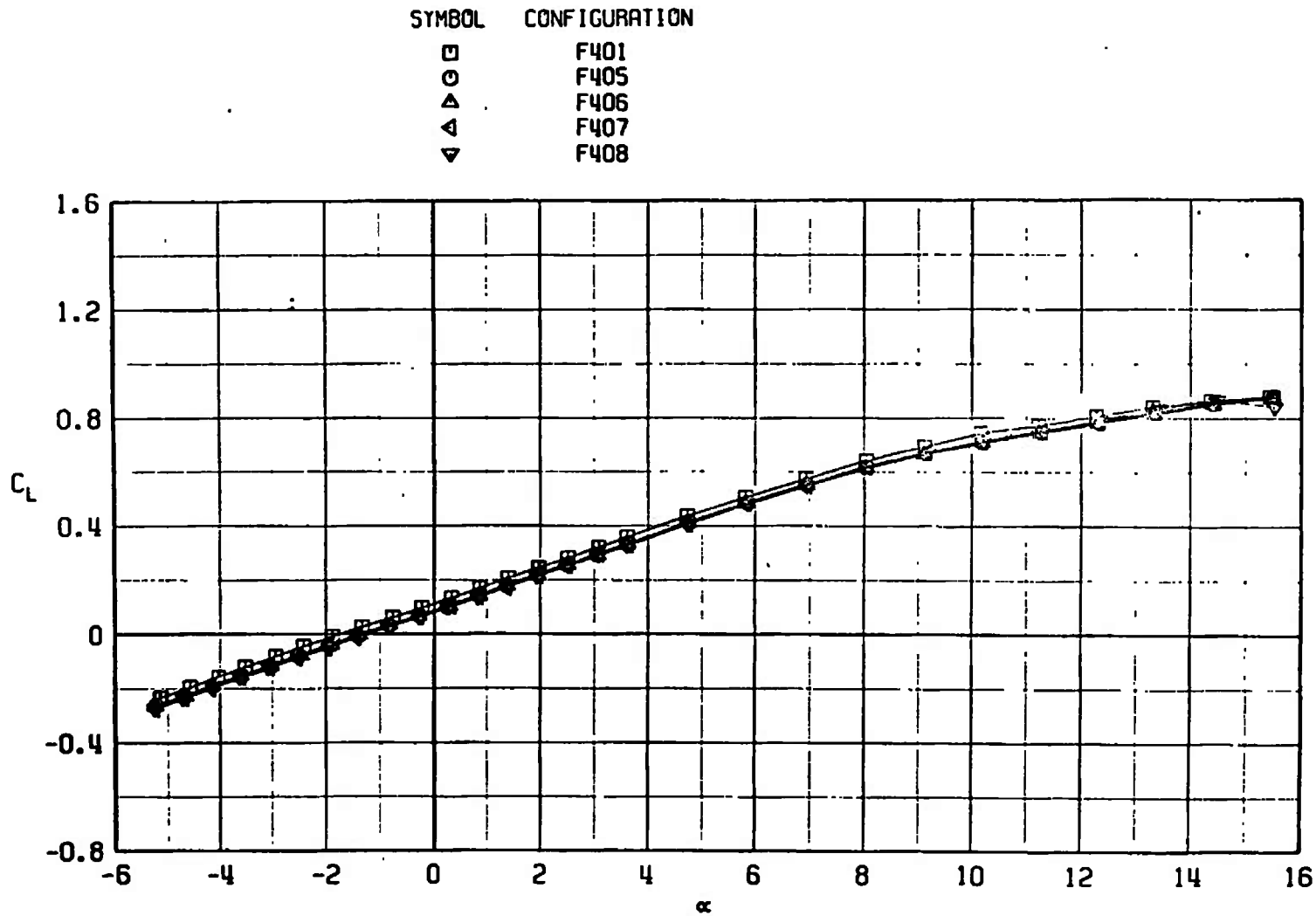

b. $M_\infty = 0.85$

Fig. 13 Continued

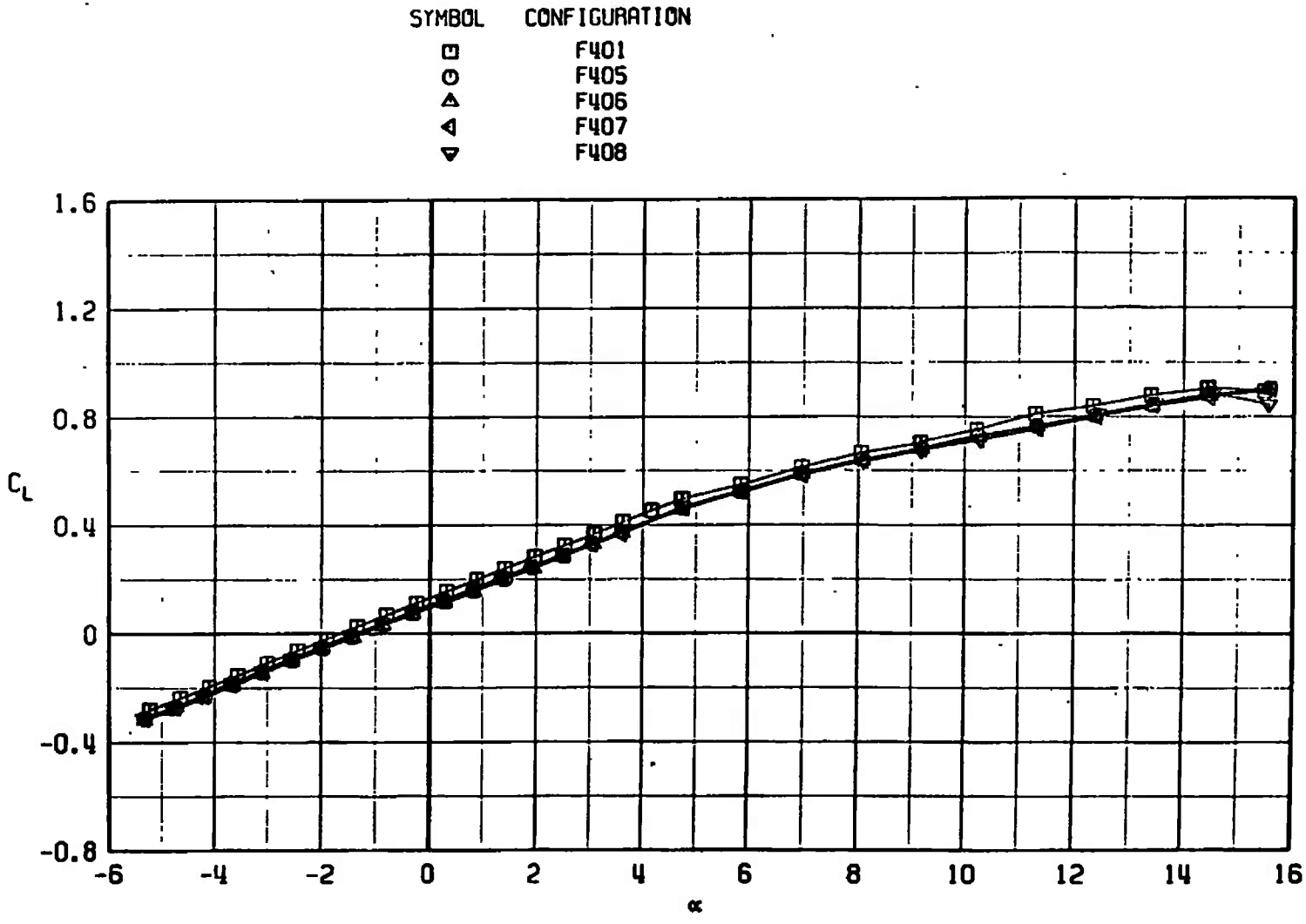

c. $M_\infty = 0.95$

Fig. 13 Continued

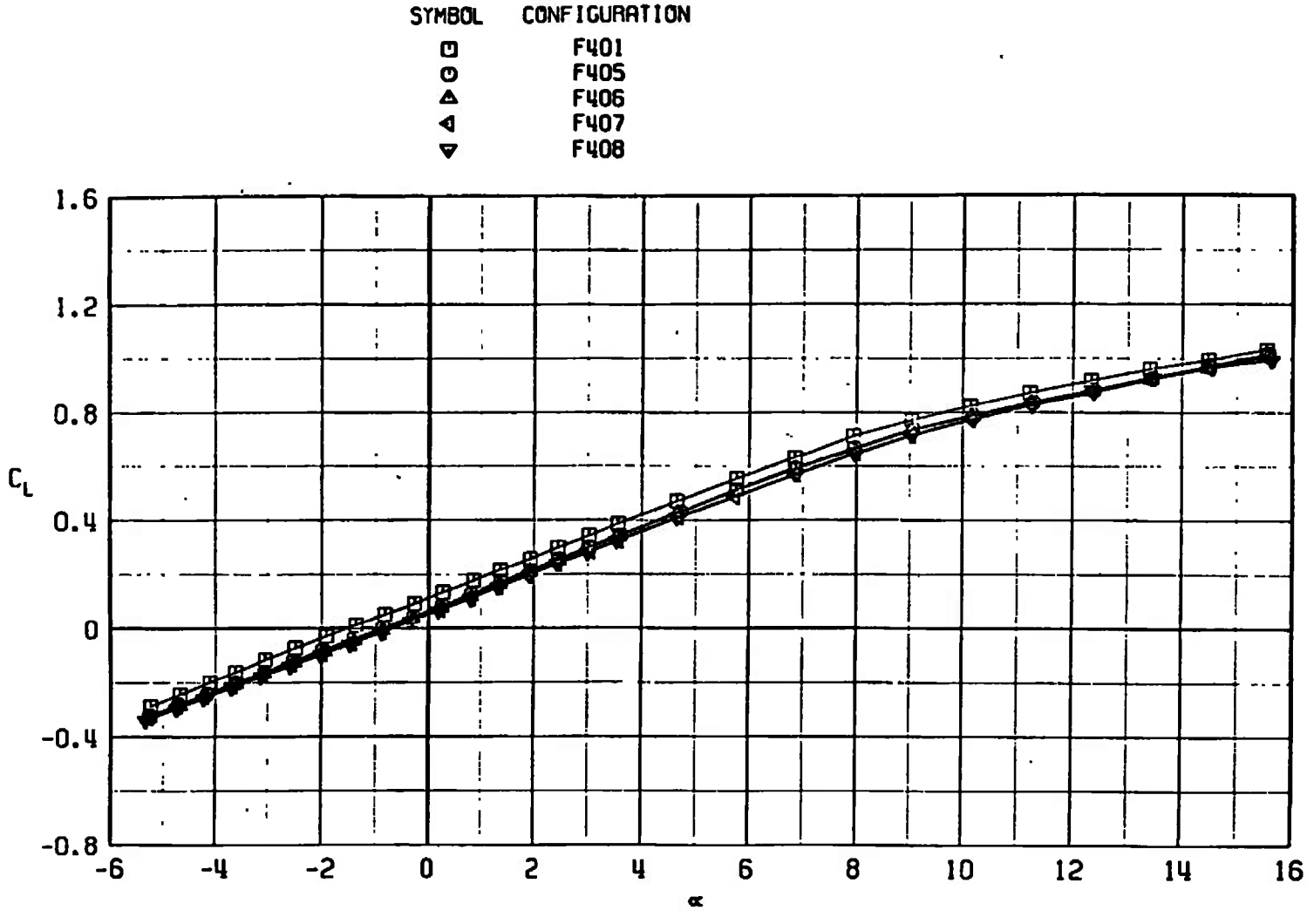

d. $M_\infty = 1.10$

Fig. 13 Continued

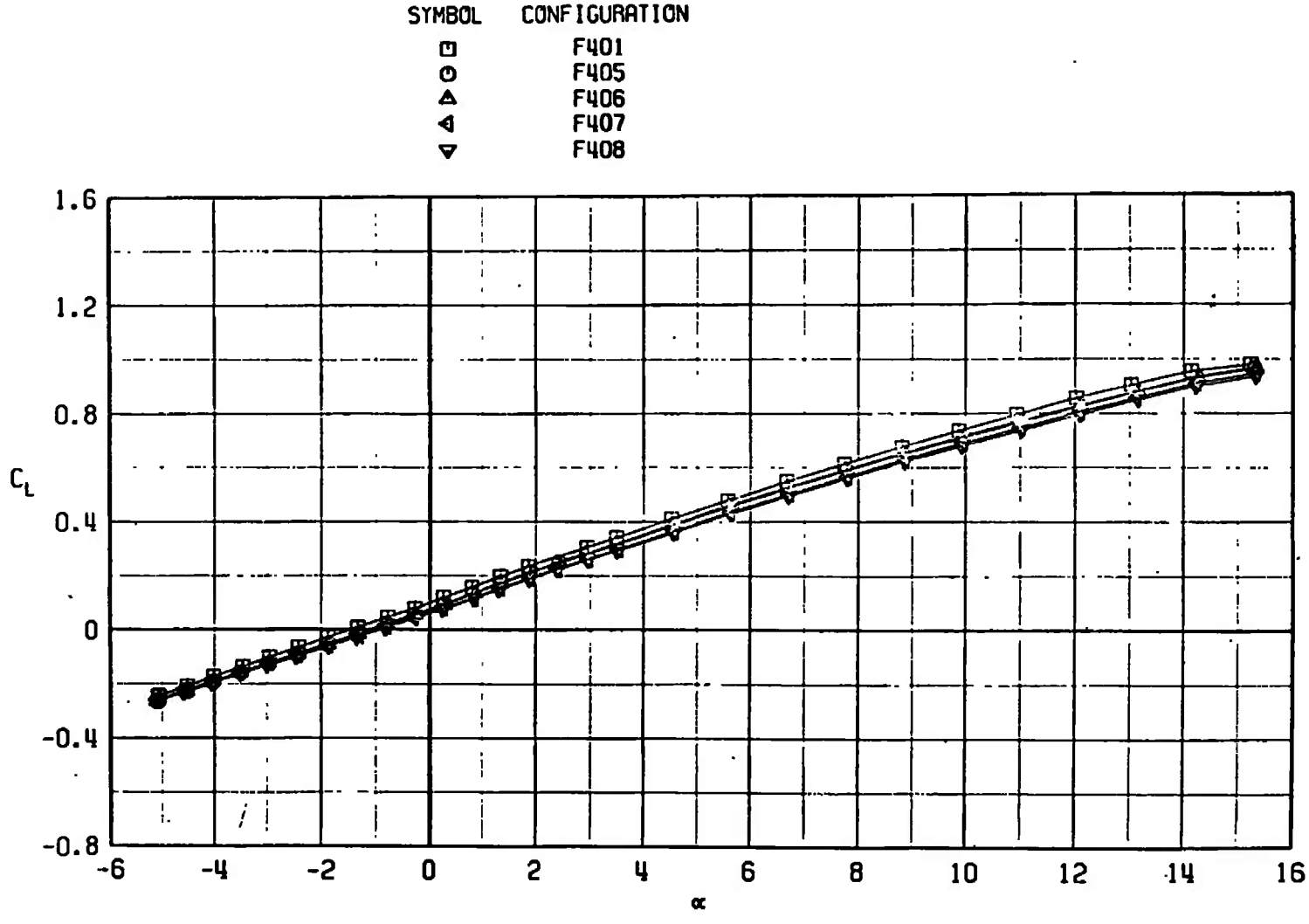

e. $M_\infty = 1.30$

Fig. 13 Concluded

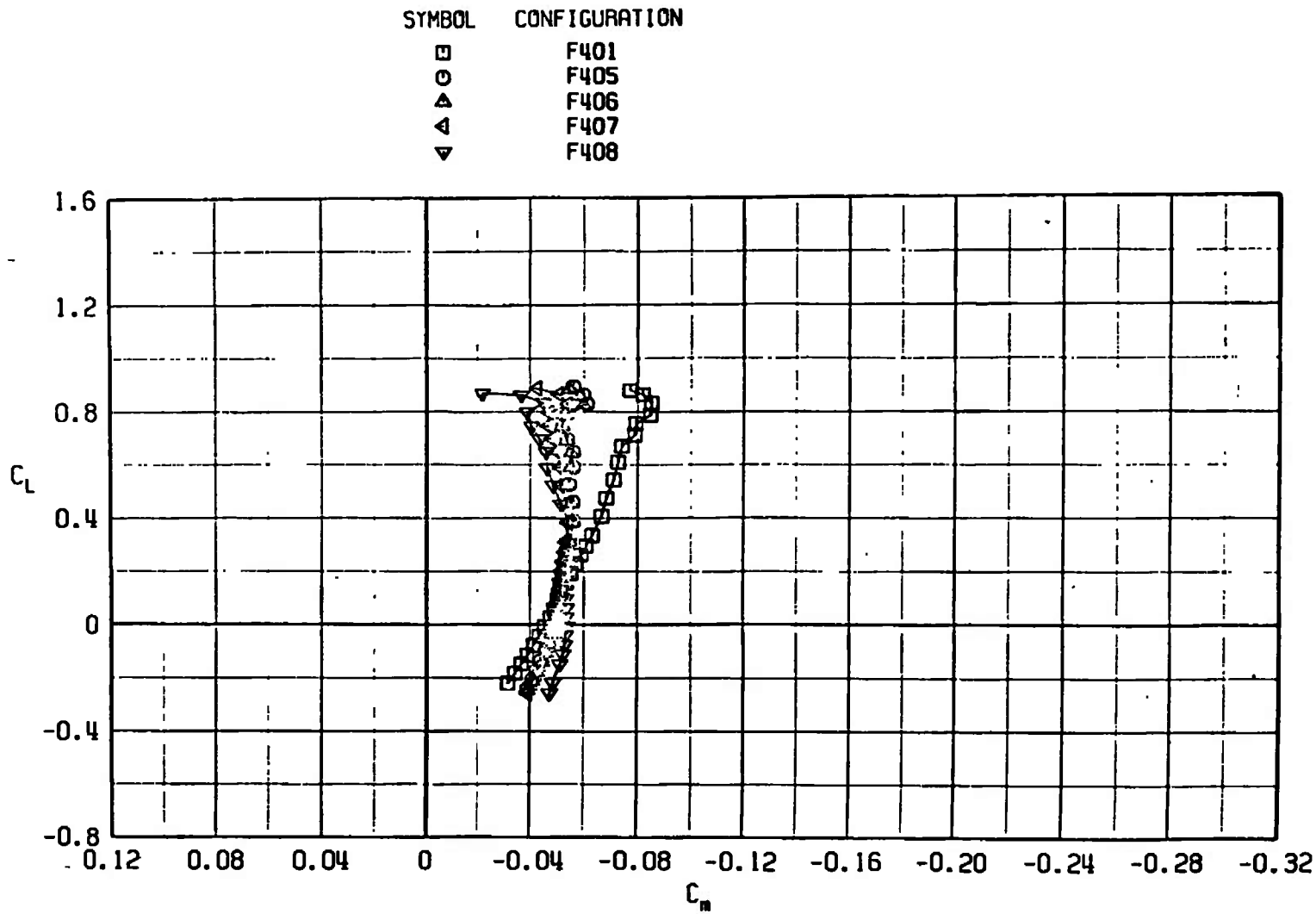

a. $M_\infty = 0.75$

Fig. 14 Pitching-Moment Coefficient Variation with Lift Coefficient for Configurations F401, F405, F406, F407, and F408

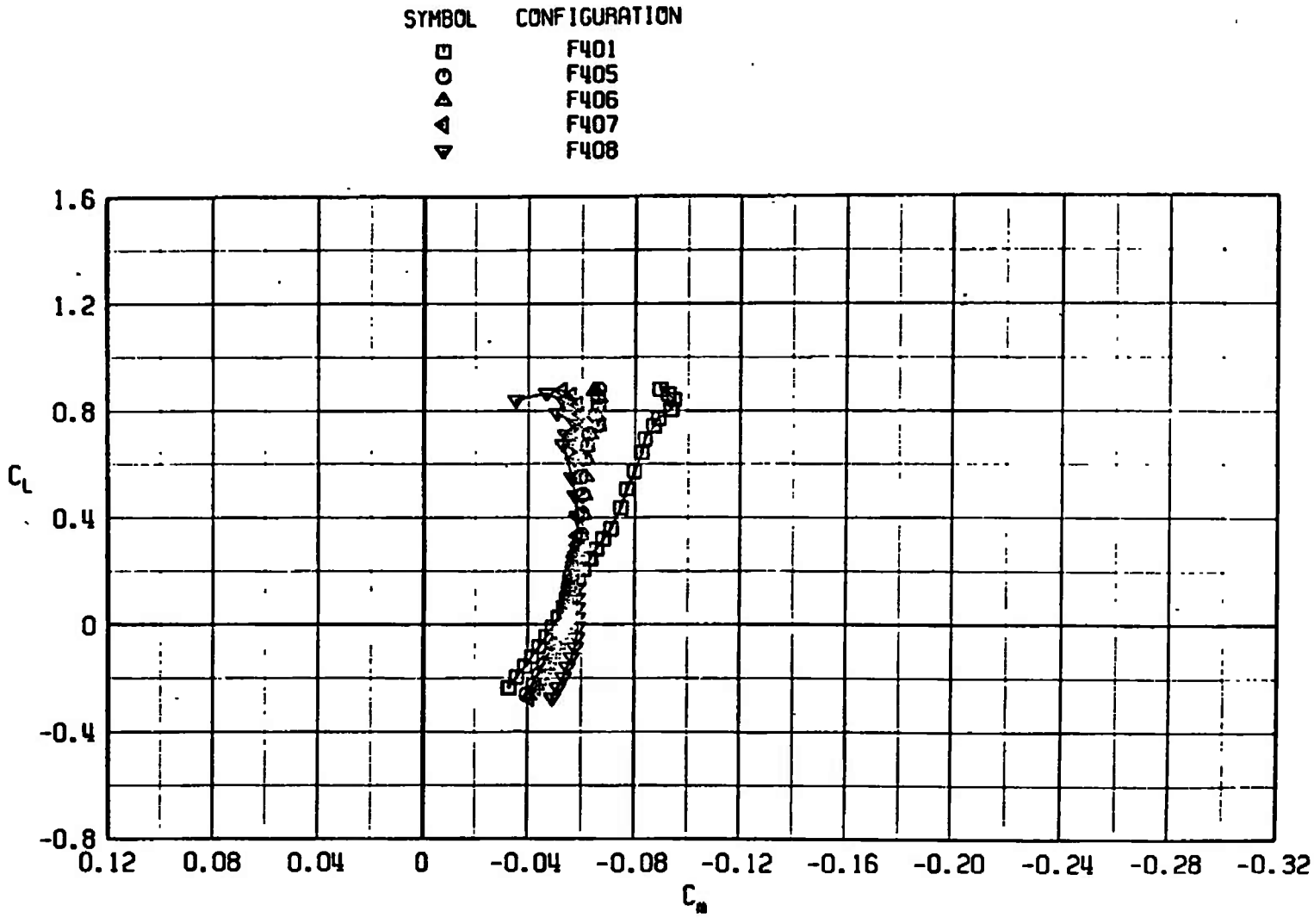

b. $M_\infty = 0.85$

Fig. 14 Continued

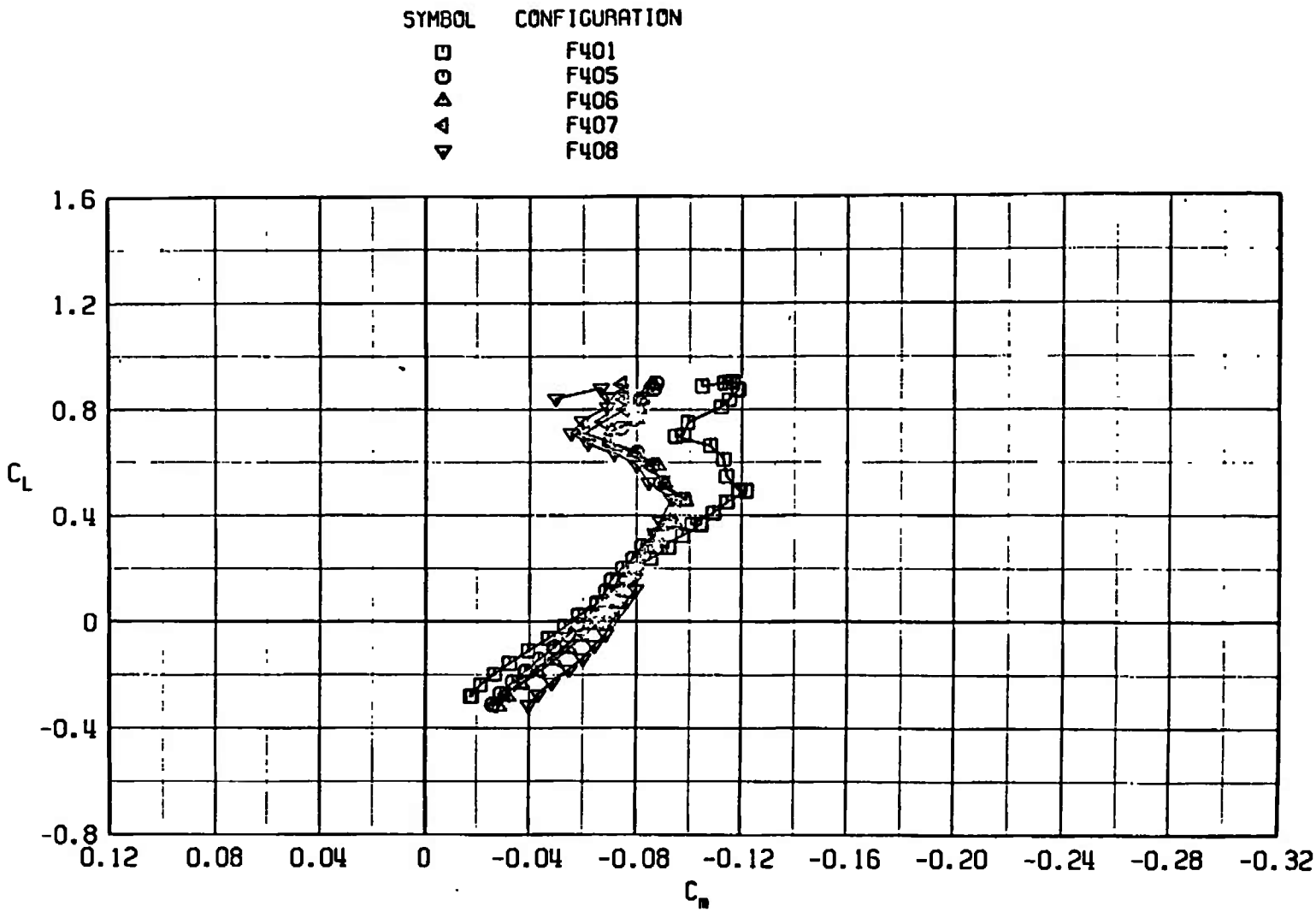

c. $M_\infty = 0.95$

Fig. 14 Continued

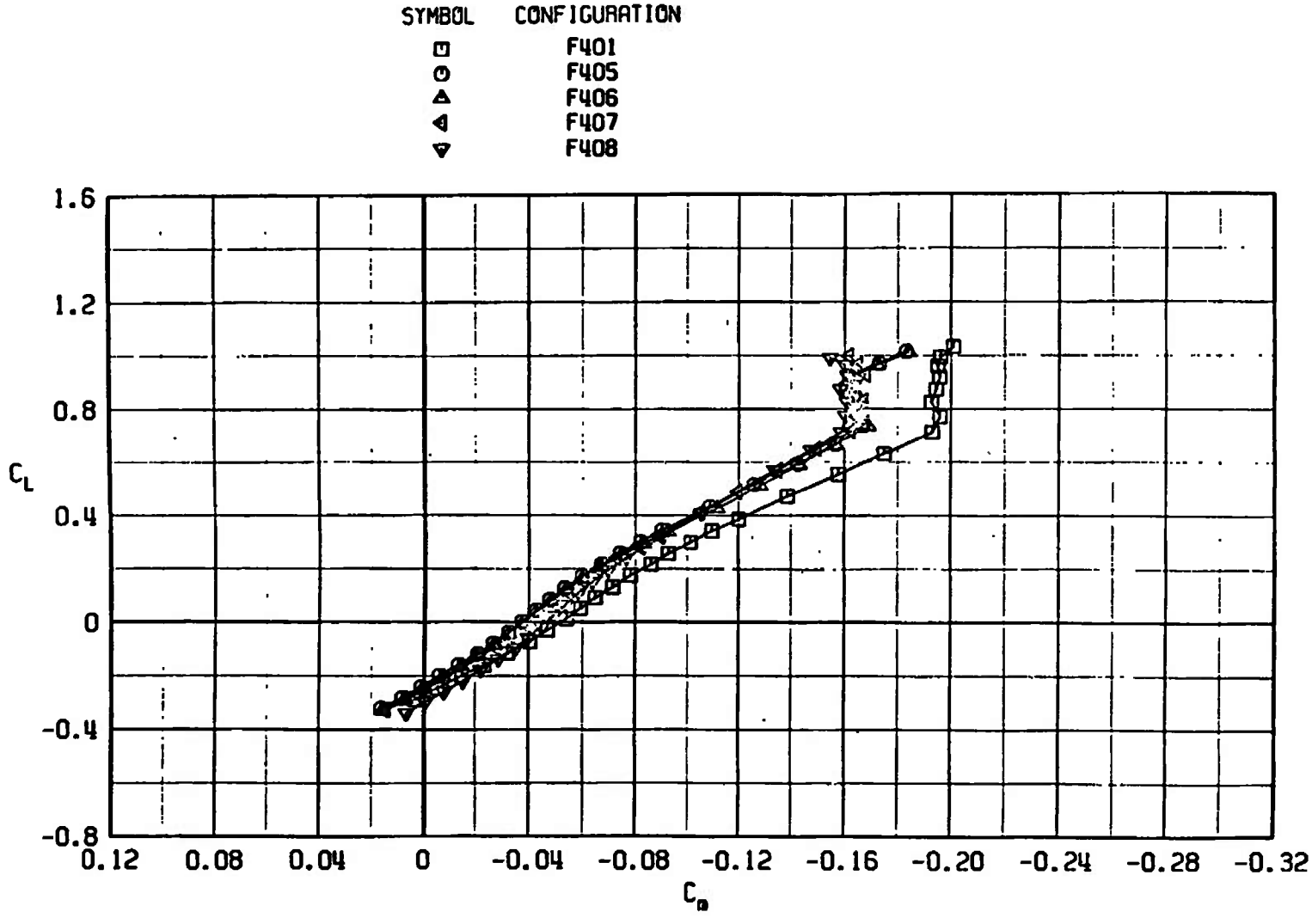

d. $M_\infty = 1.10$

Fig. 14 Continued

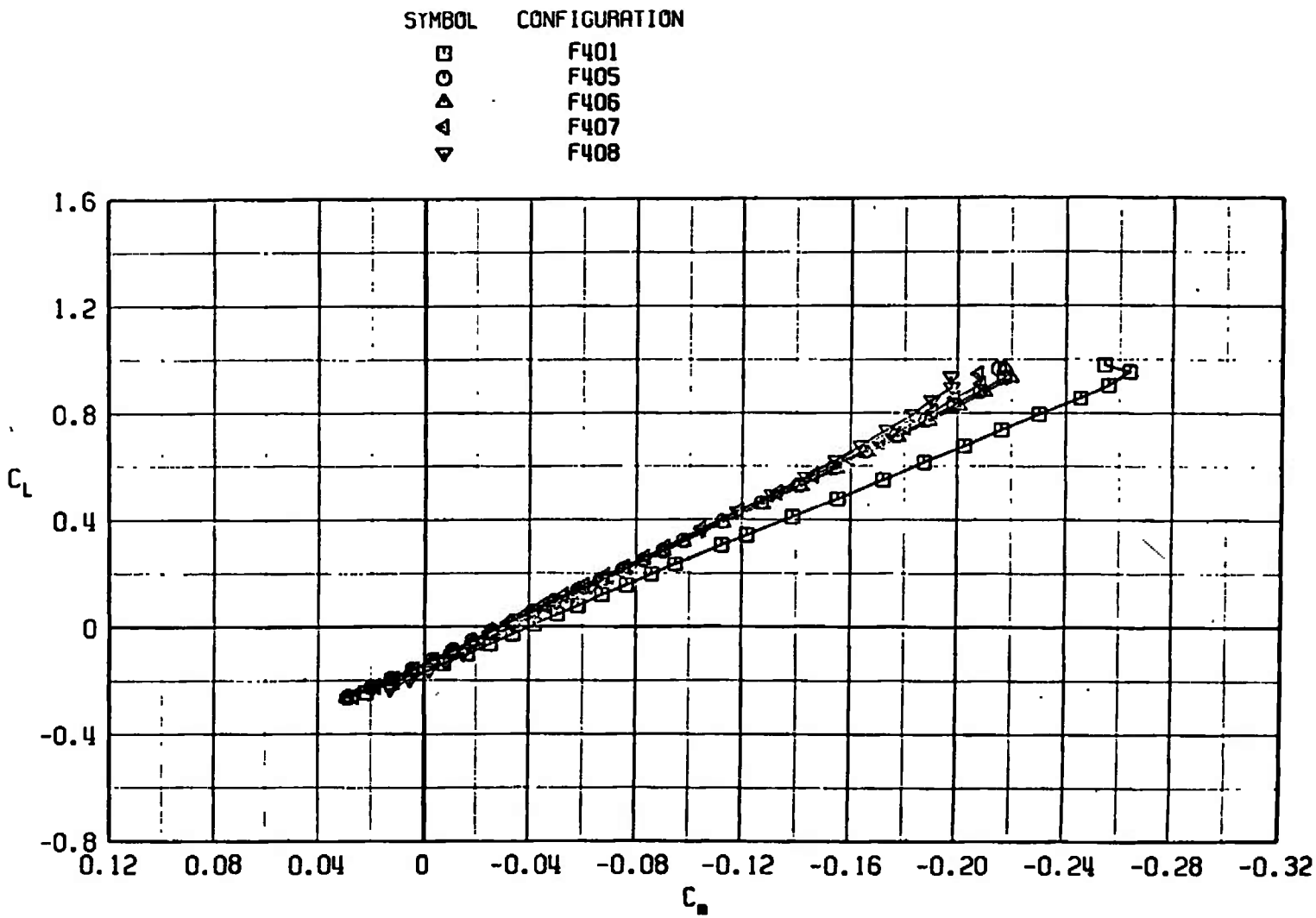

e. $M_\infty = 1.30$

Fig. 14 Concluded

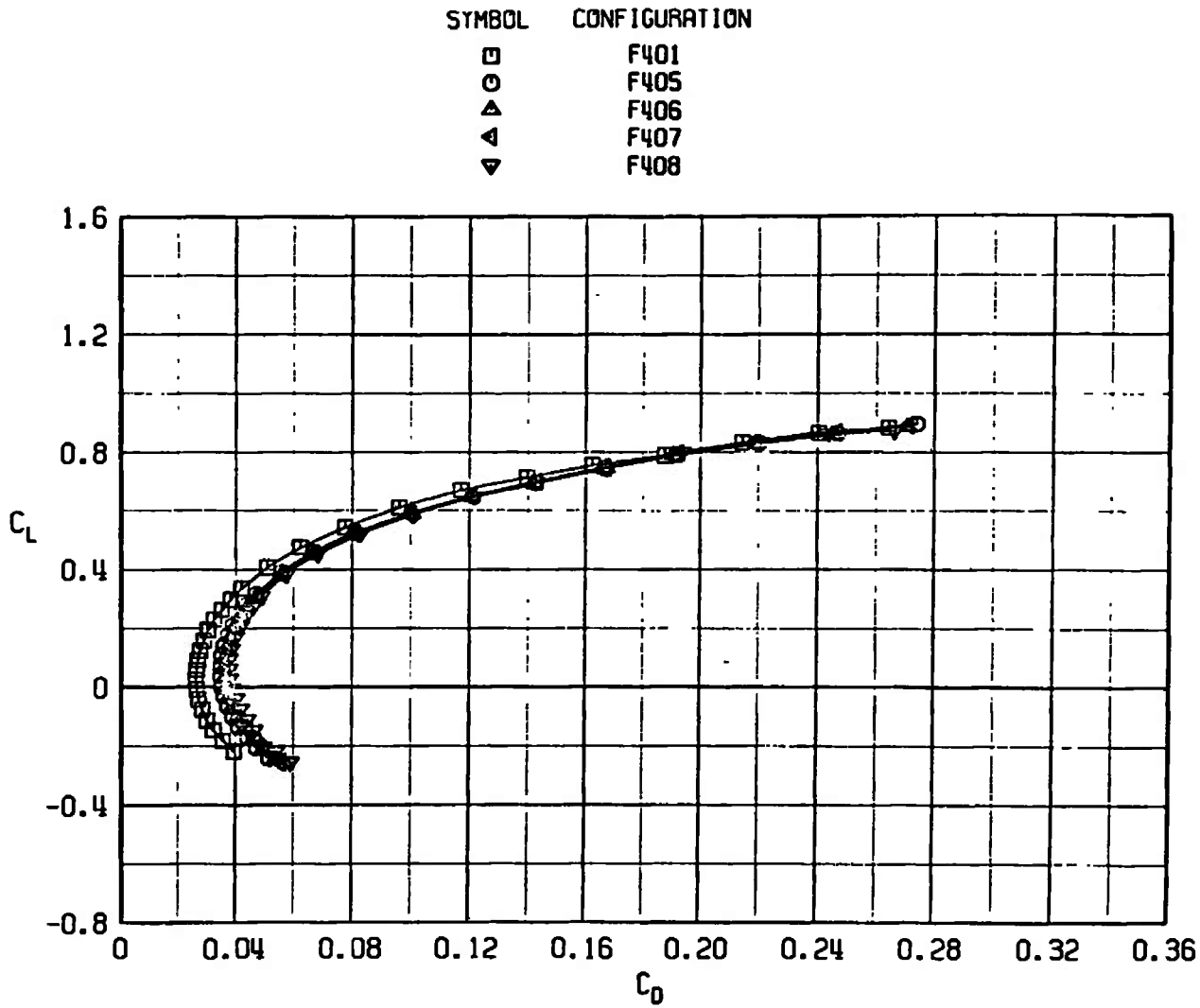

a. $M_\infty = 0.75$

Fig. 15 Drag Coefficient Variation with Lift Coefficient for Configurations F401, F405, F406, F407, and F408

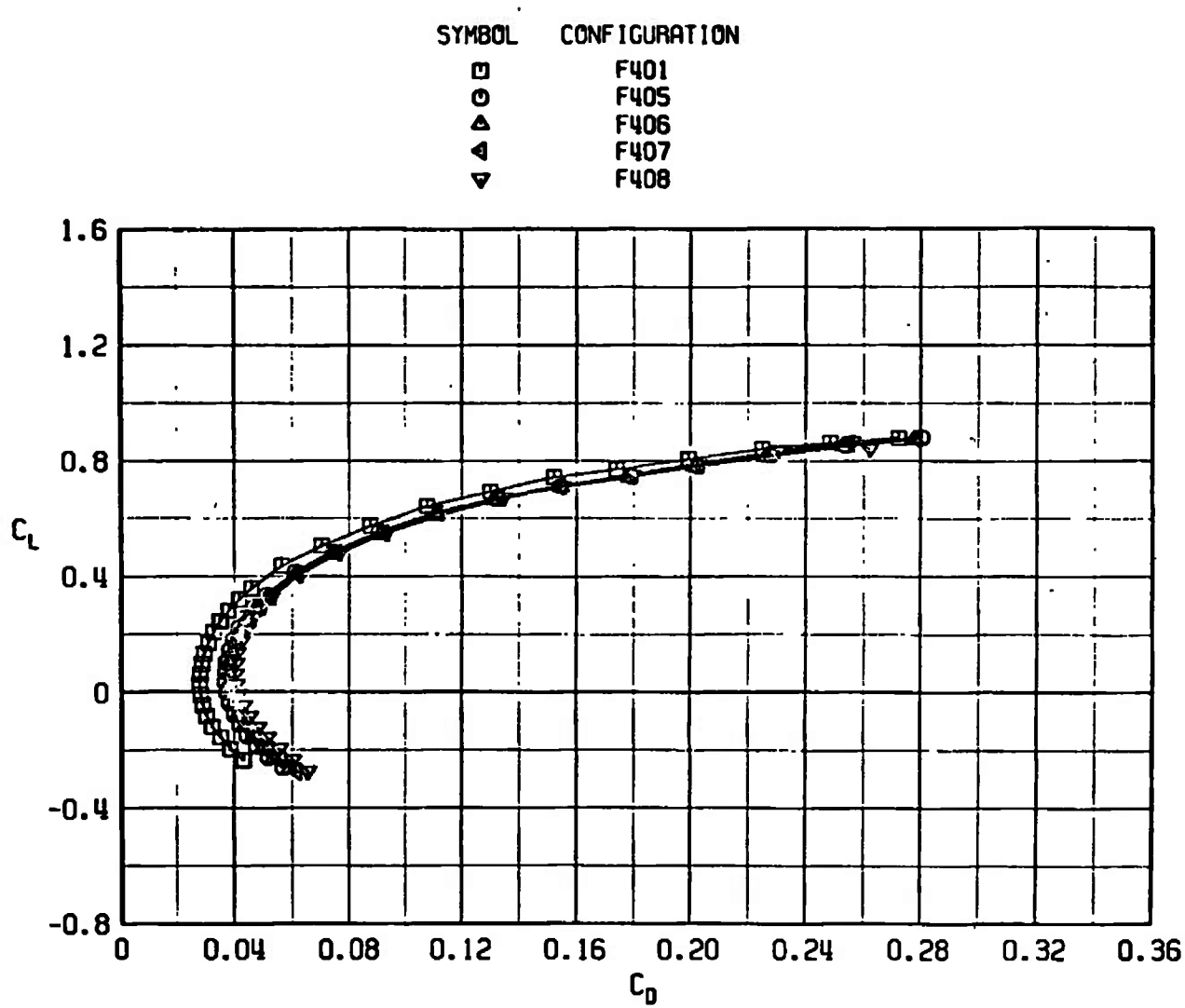

b. $M_\infty = 0.85$

Fig. 15 Continued

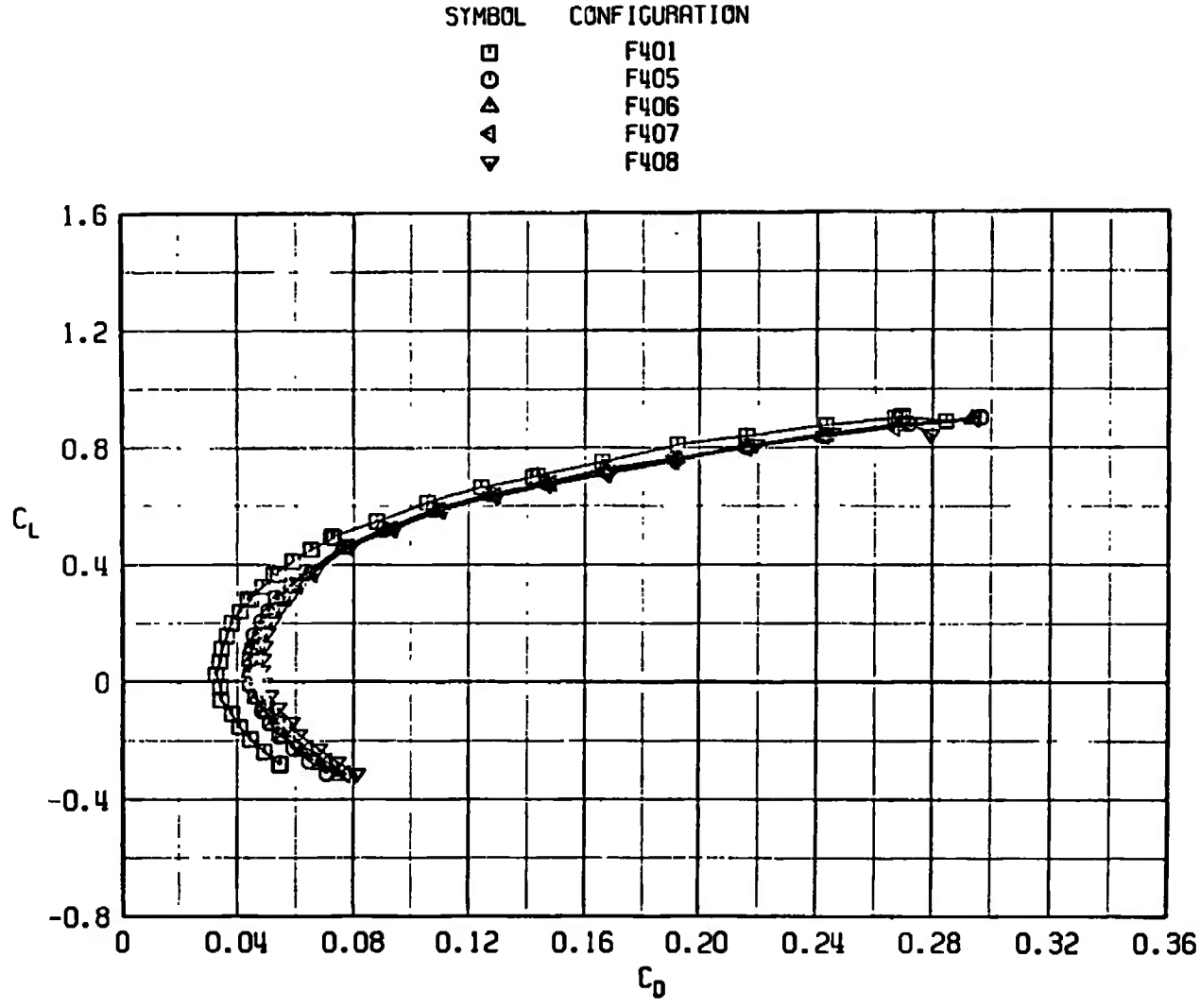

c. $M_\infty = 0.95$

Fig. 15 Continued

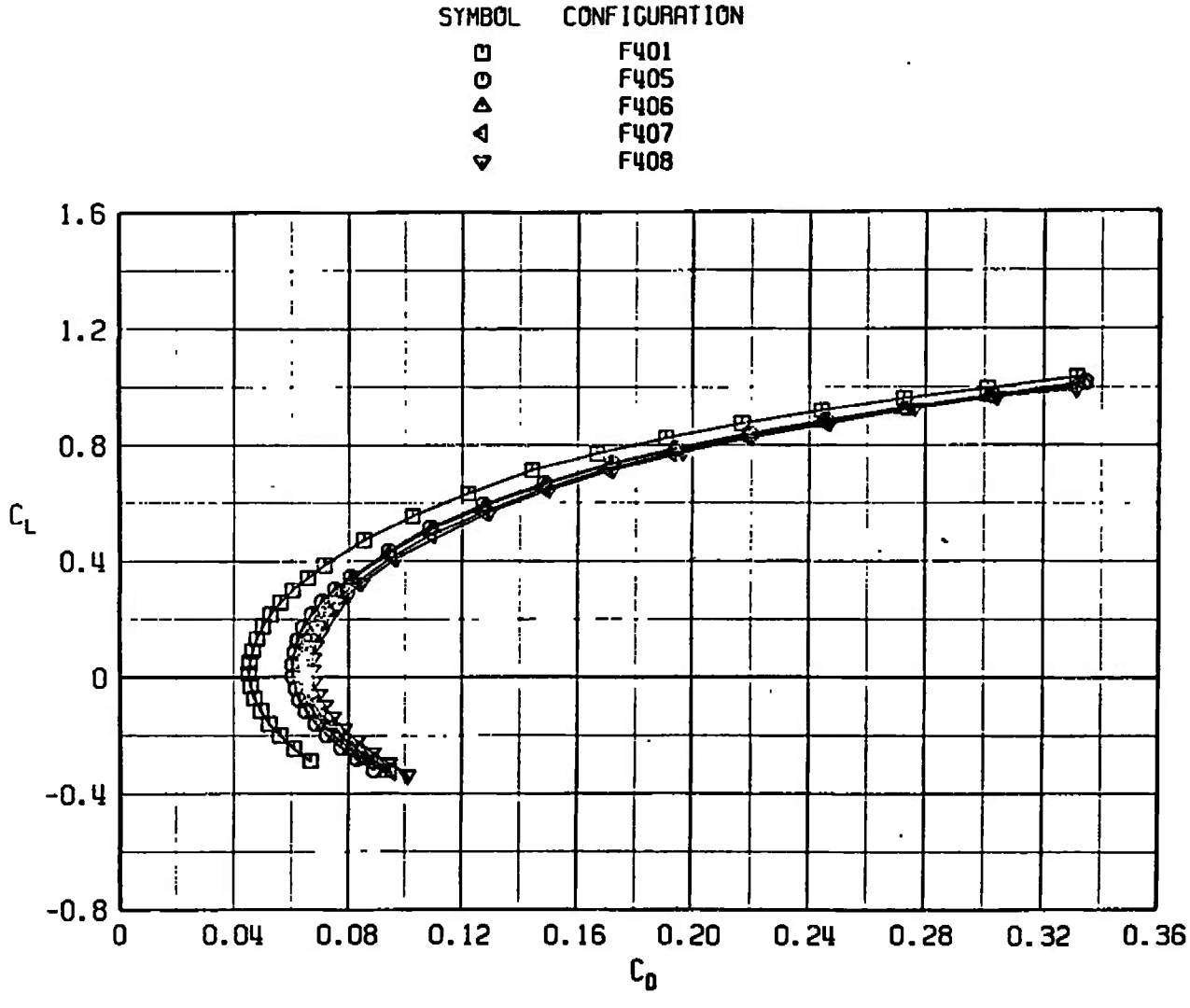

d. $M_\infty = 1.10$

Fig. 15 Continued

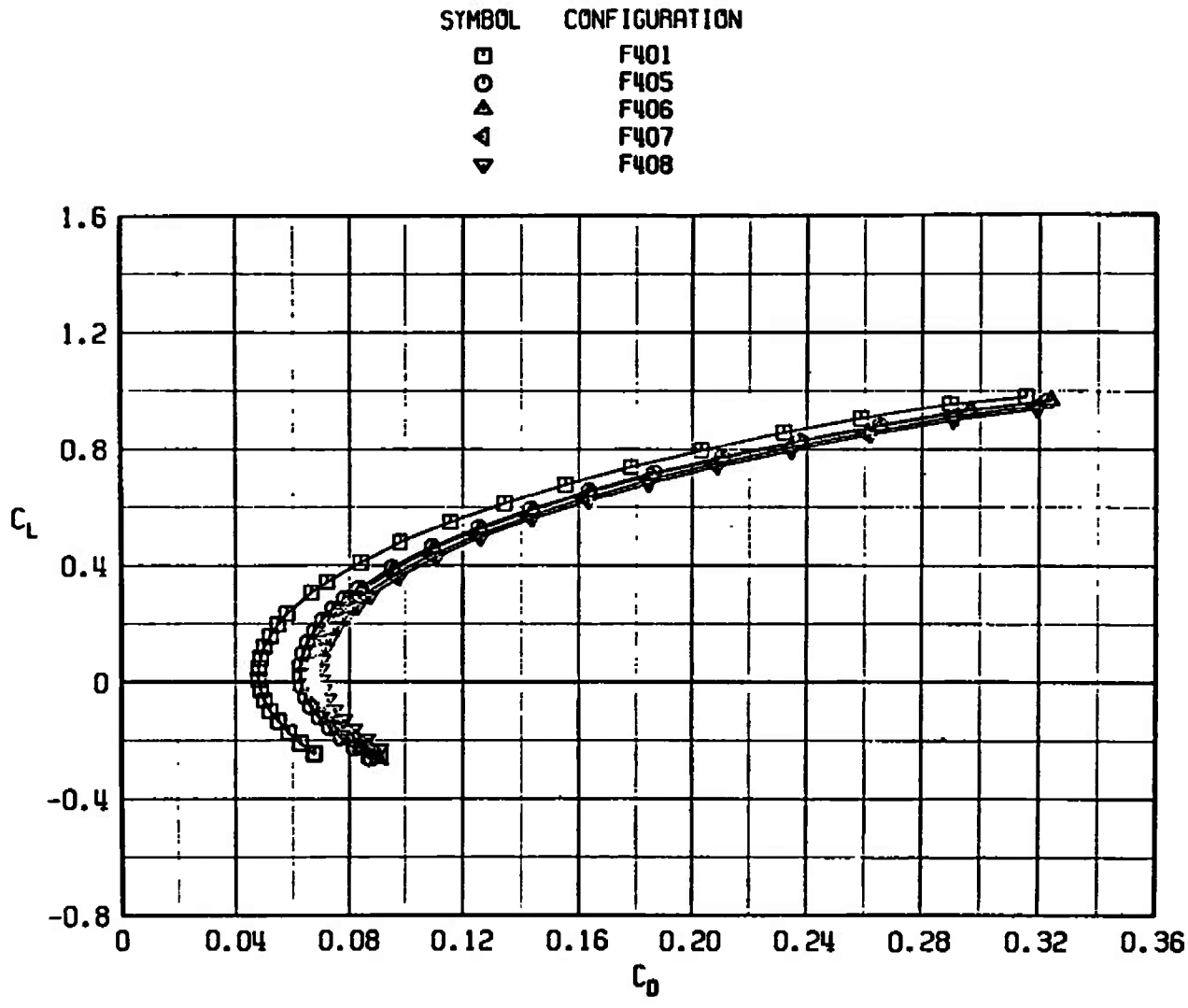

e. $M_\infty = 1.30$

Fig. 15 Concluded

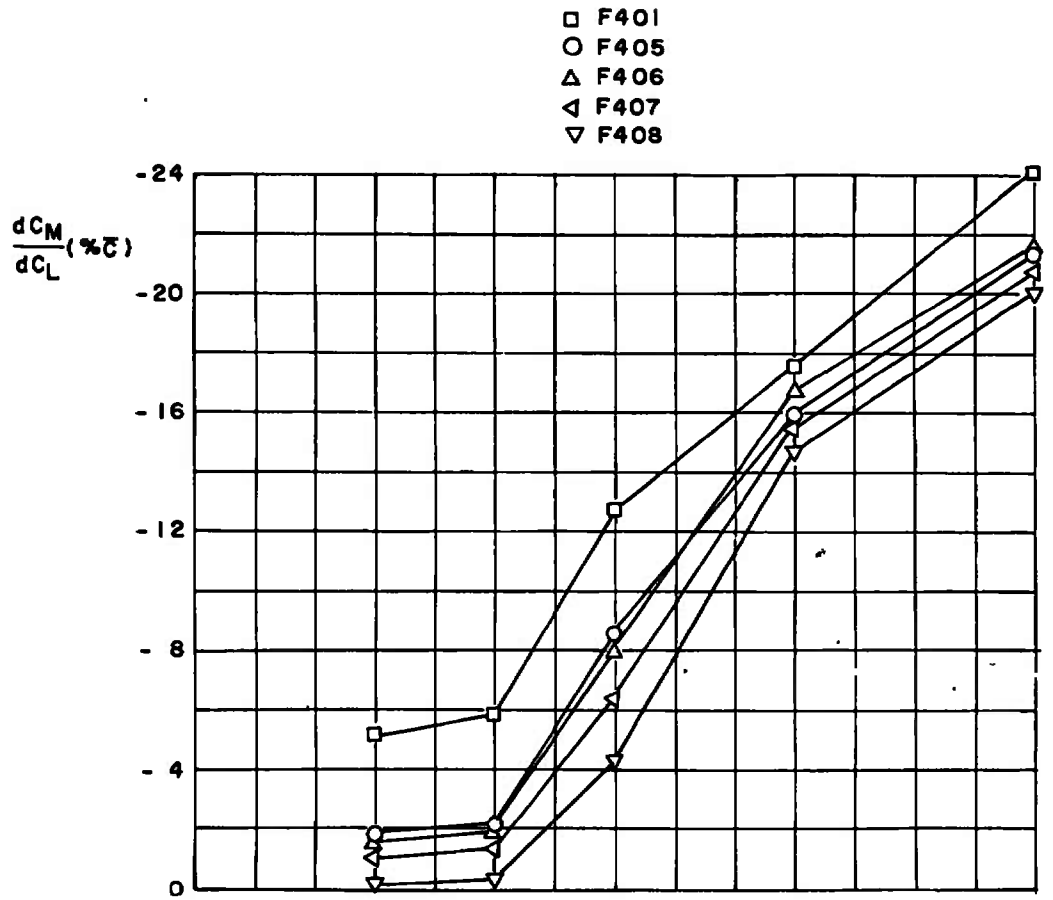

a. dC_m/dC_L versus M_∞ at $C_L = 0.2$ in percentage $\bar{c}$

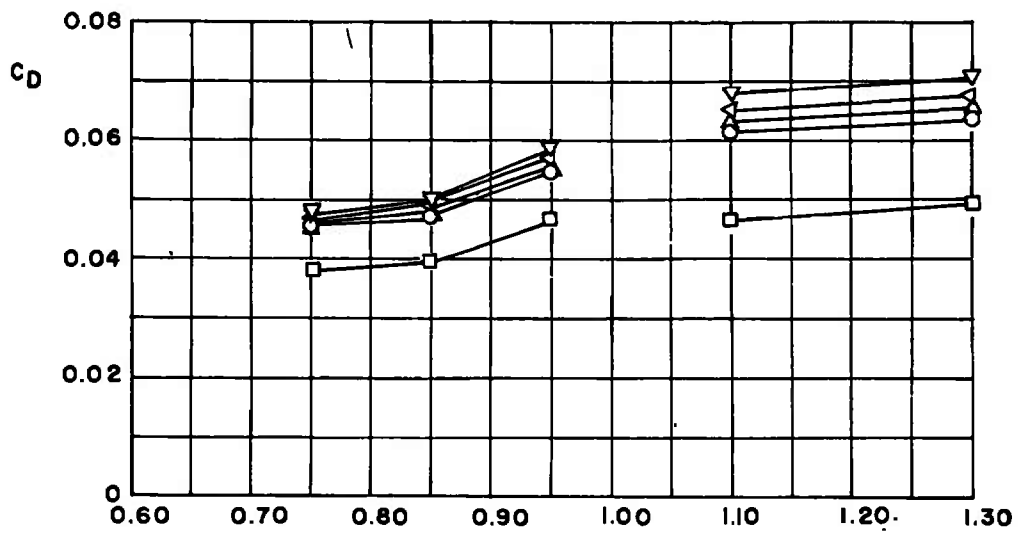

b. C_D versus M_∞ at $C_L = 0.3$, $M_\infty < 1.0$, and $C_L = 0.1$, $M_\infty > 1.0$

Fig. 16 Drag Coefficient and dC_m/dC_L Variation with Mach Number for Configurations F401, F405, F406, F407, and F408

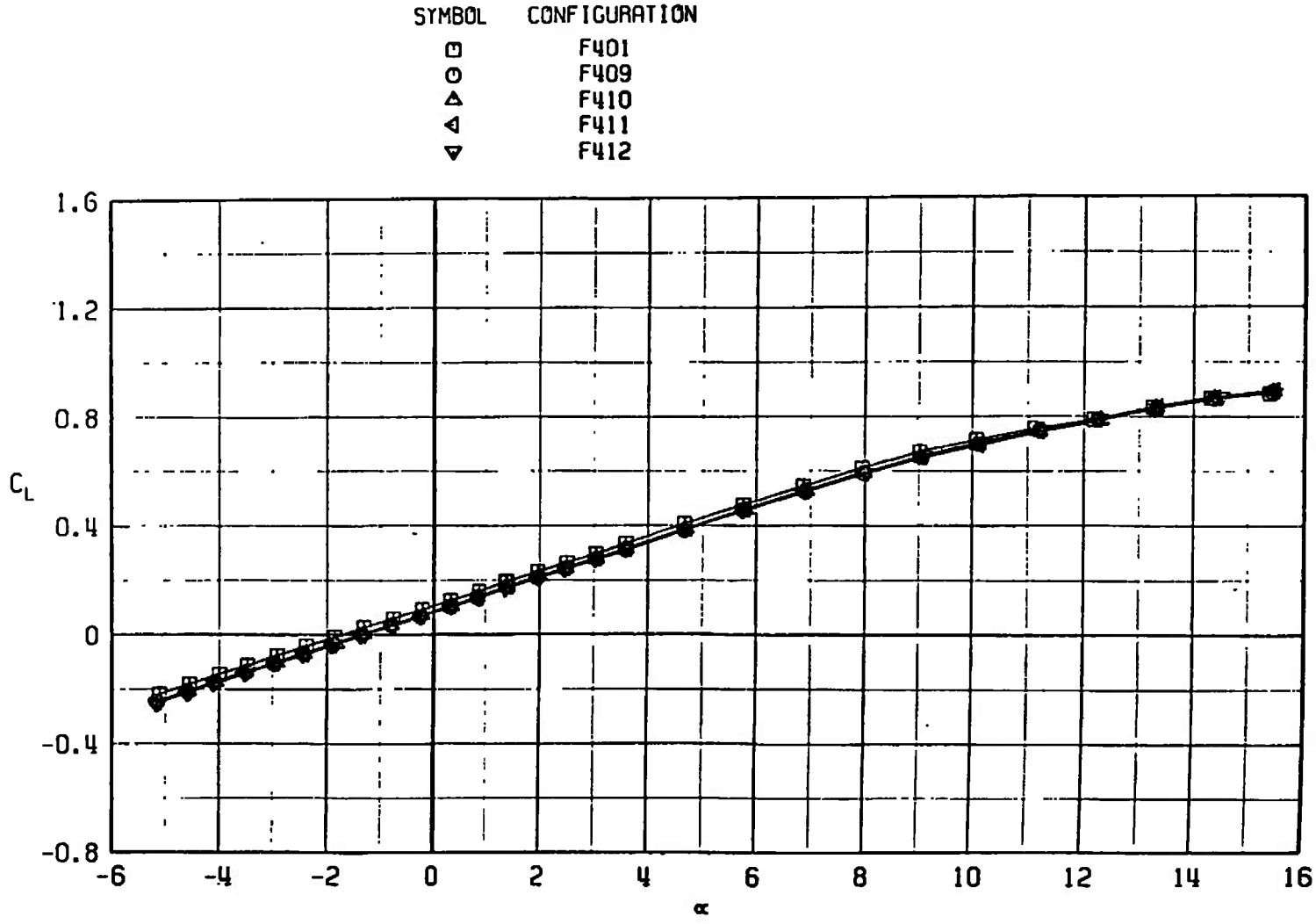

a. $M_\infty = 0.75$.

Fig. 17 Lift Coefficient Variation with Angle of Attack for Configurations F401, F409, F410, F411, and F412

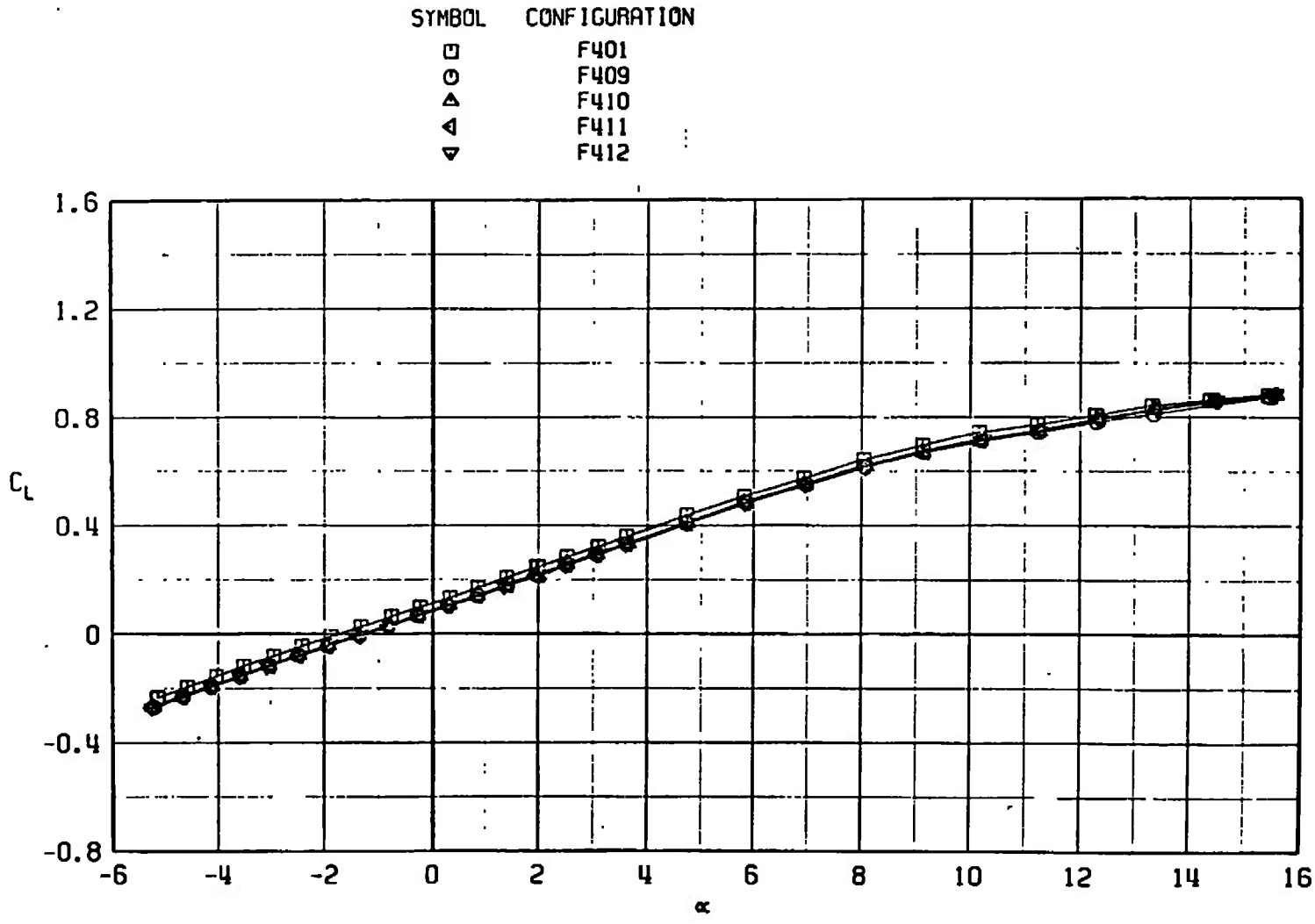

b. $M_\infty = 0.85$

Fig. 17 Continued

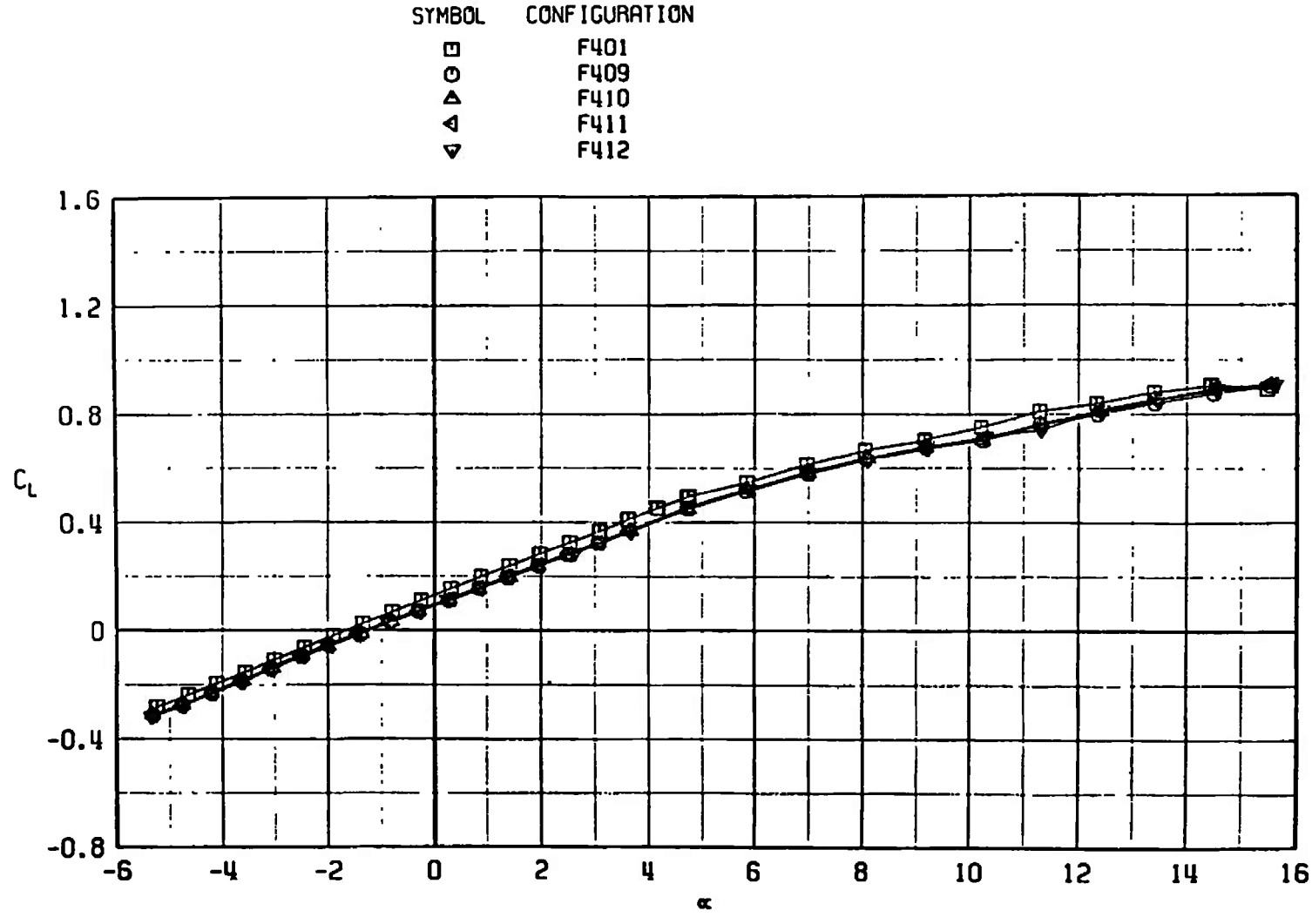

c. $M_\infty = 0.95$

Fig. 17 Continued

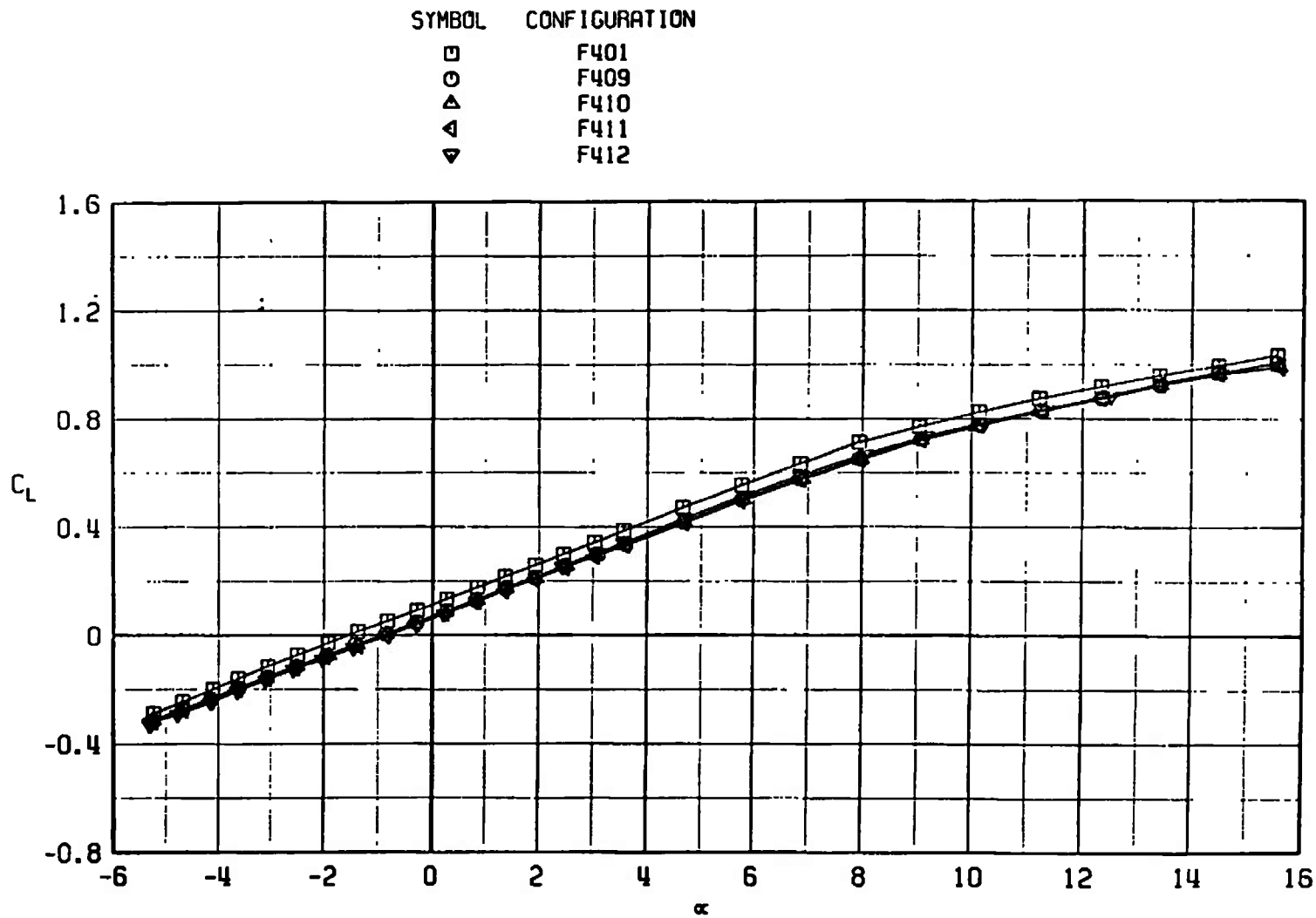

d. $M_\infty = 1.10$

Fig. 17 Continued

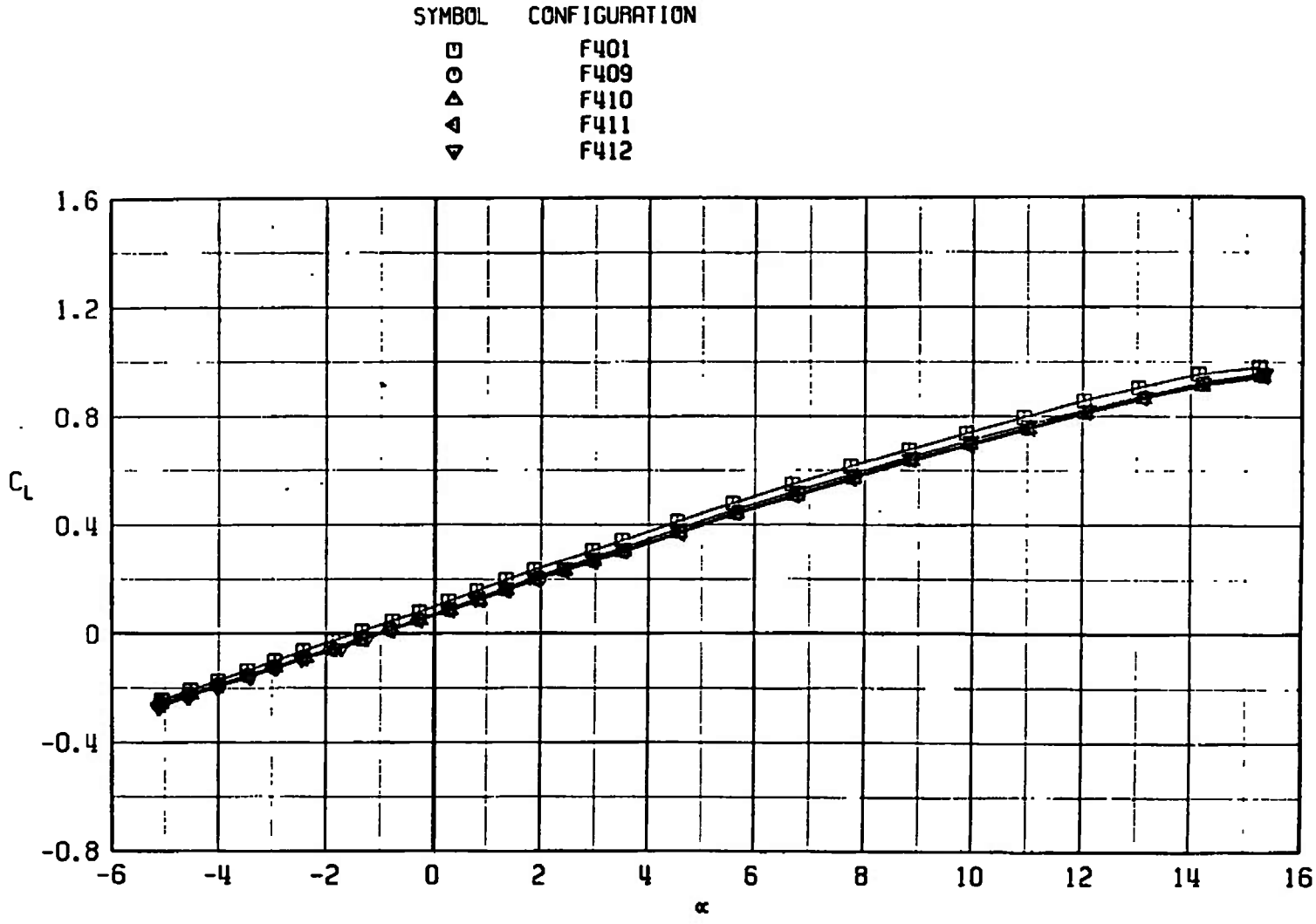

e. $M_\infty = 1.30$

Fig. 17 Concluded

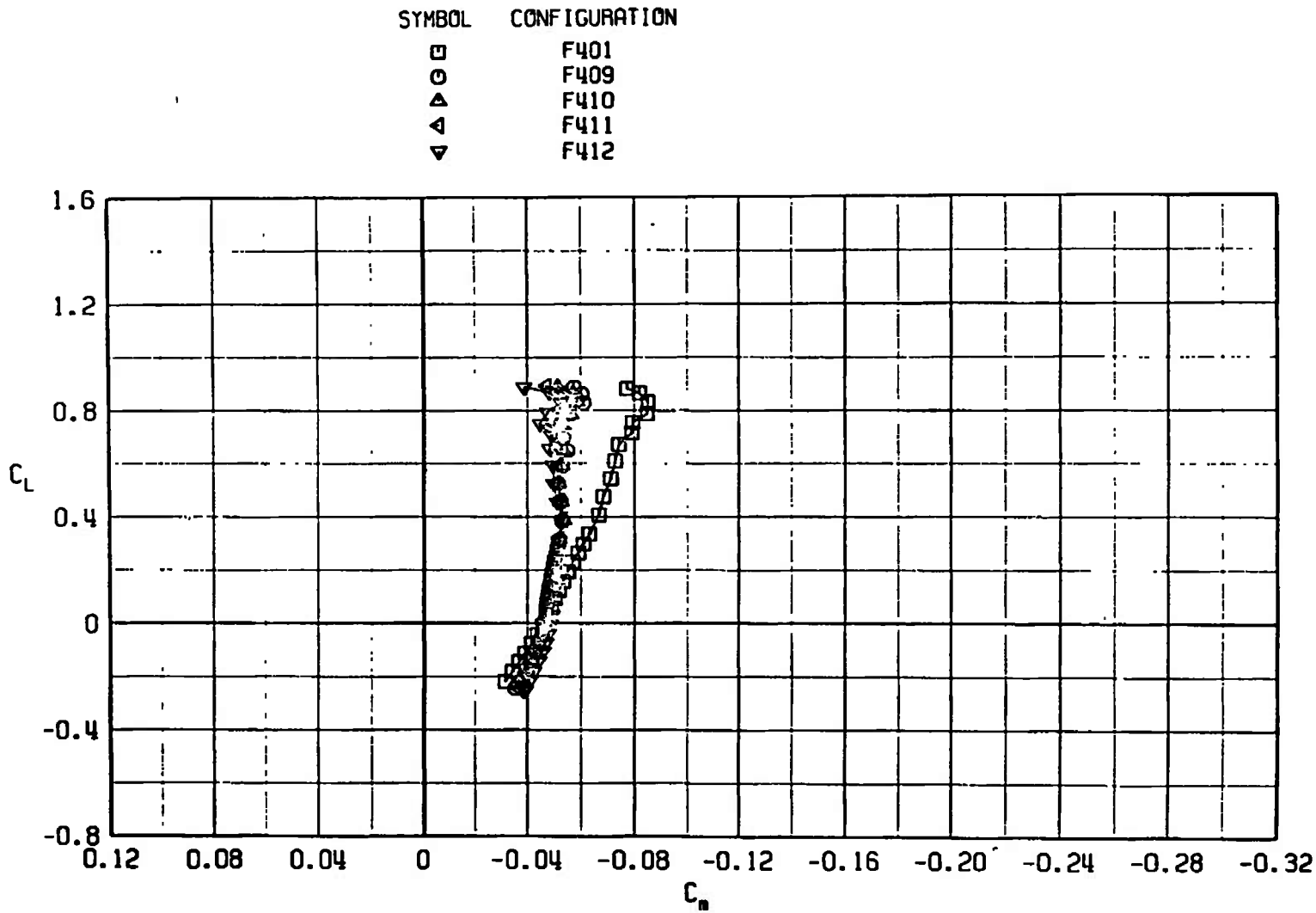

a. $M_\infty = 0.75$

Fig. 18 Pitching-Moment Coefficient Variation with Lift Coefficient for Configurations F401, F409, F410, F411, and F412

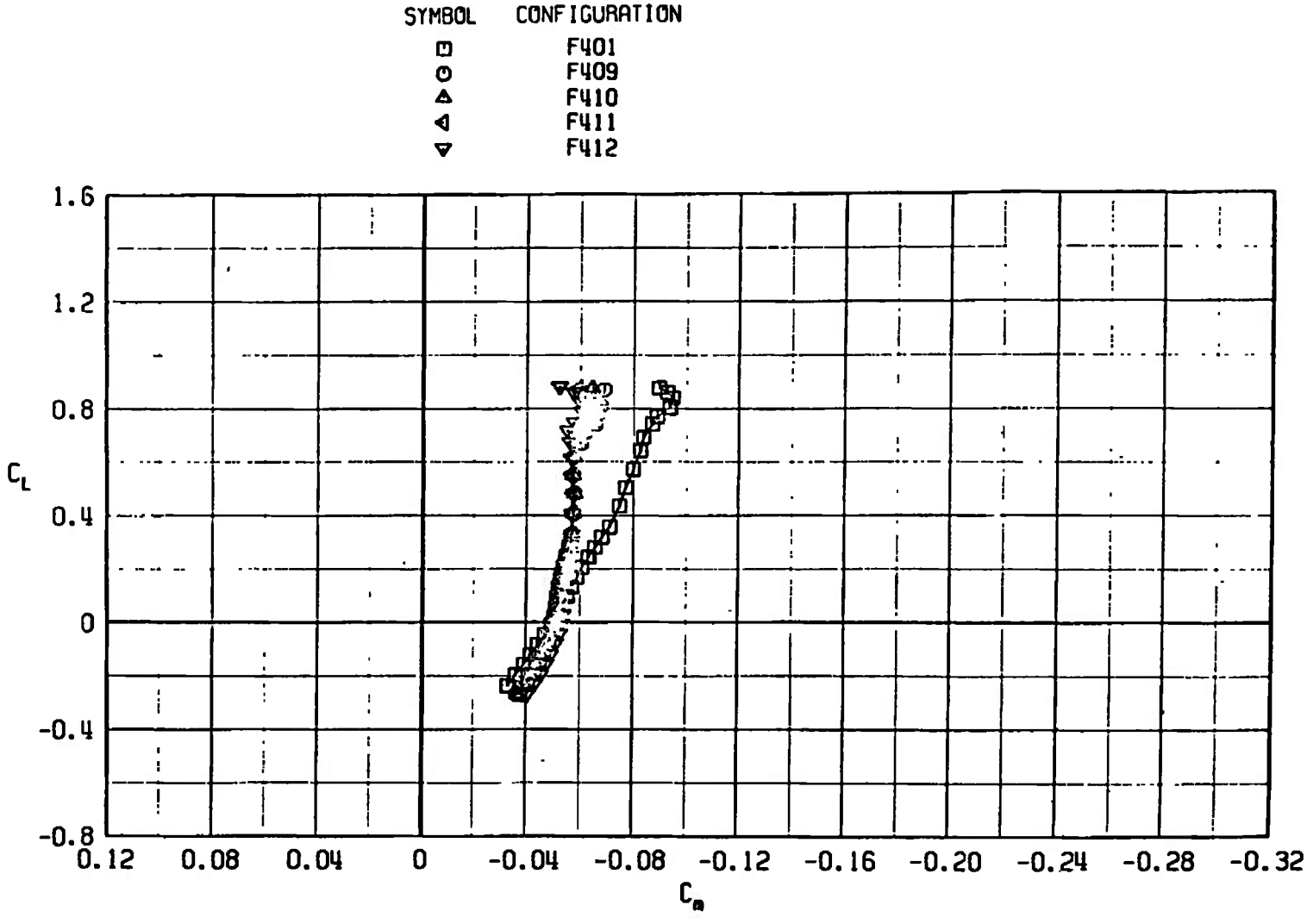

b. $M_\infty = 0.85$

Fig. 18 Continued

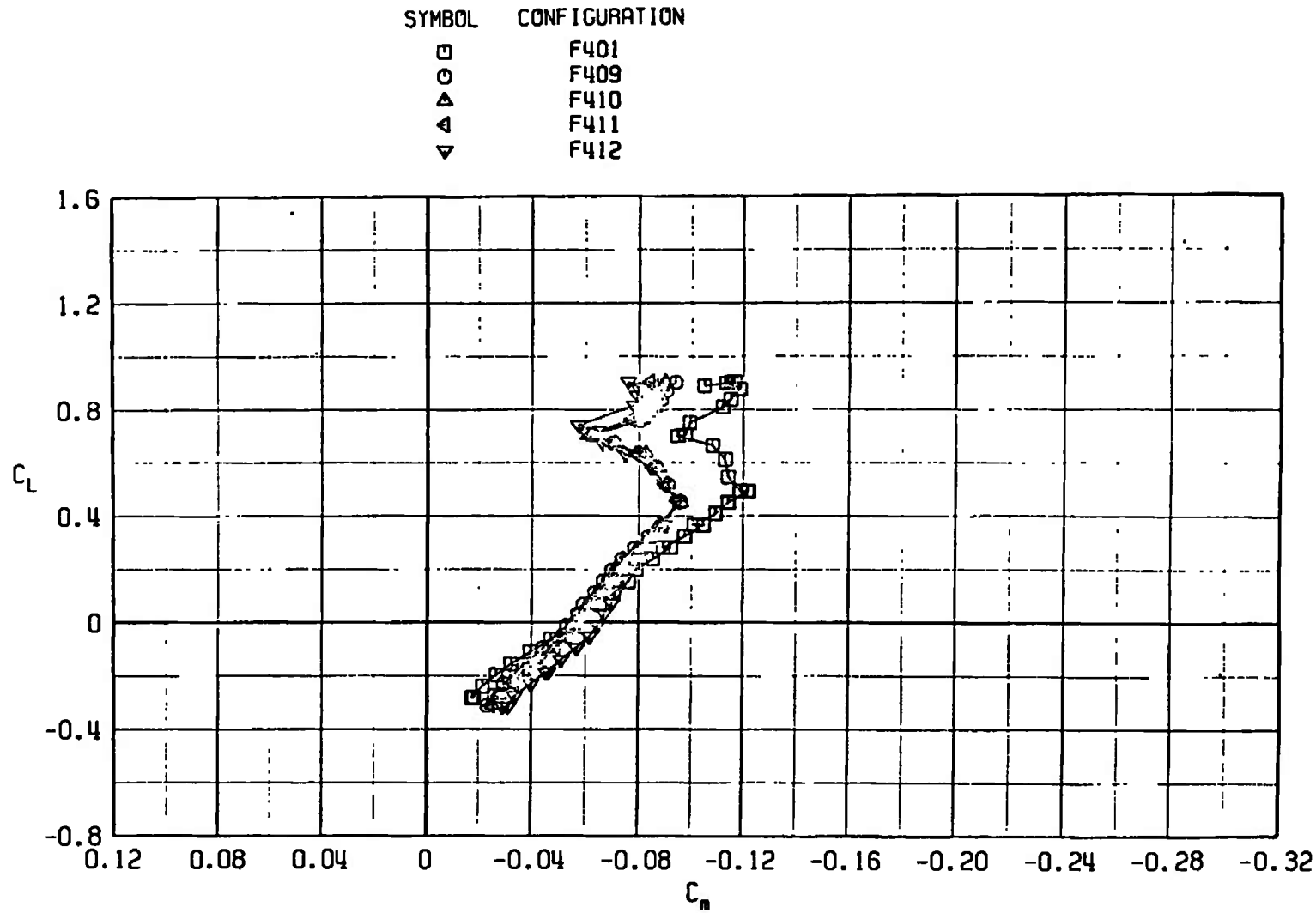

c. $M_\infty = 0.95$

Fig. 18 Continued

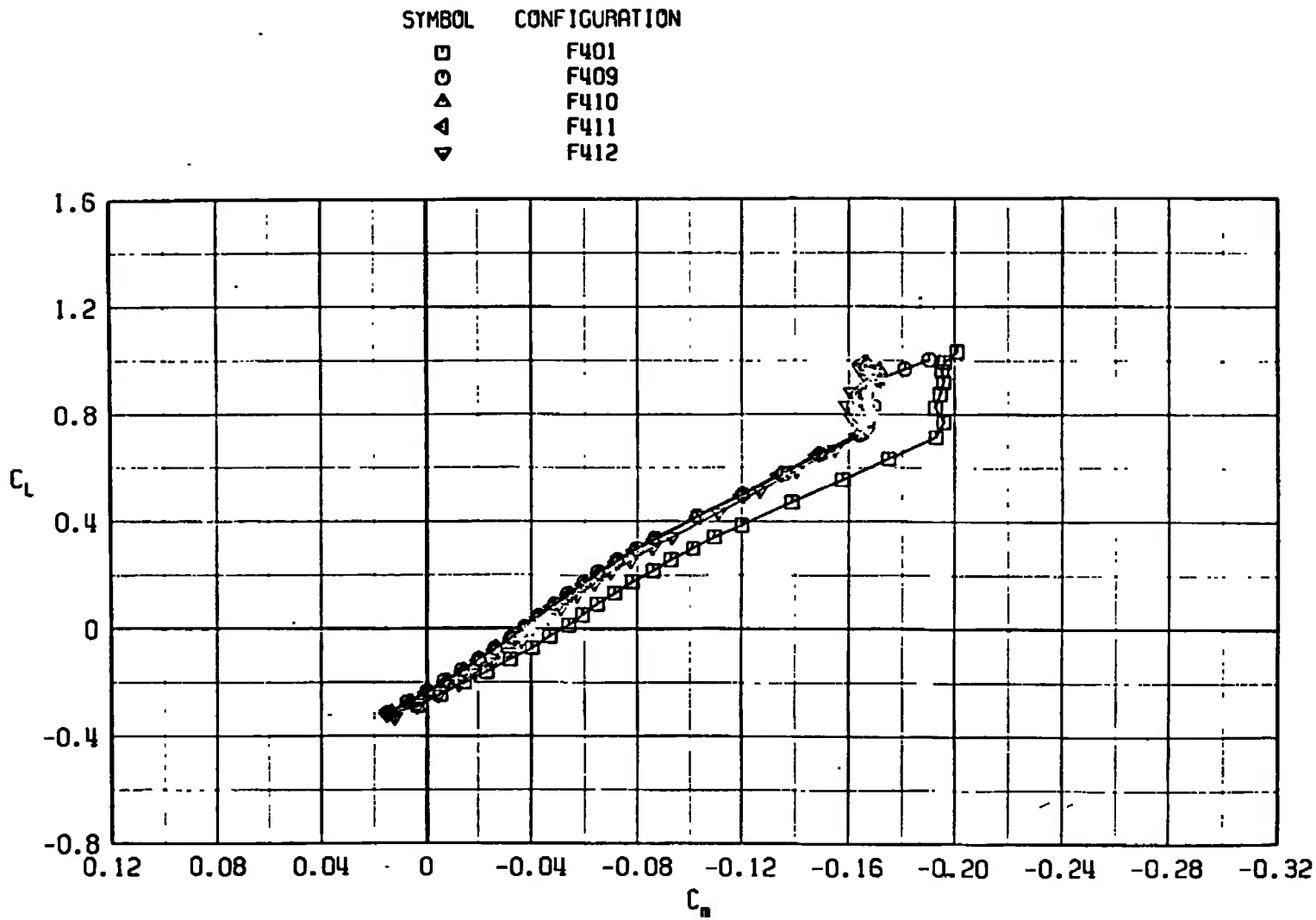

d. $M_\infty = 1.10$

Fig. 18 Continued

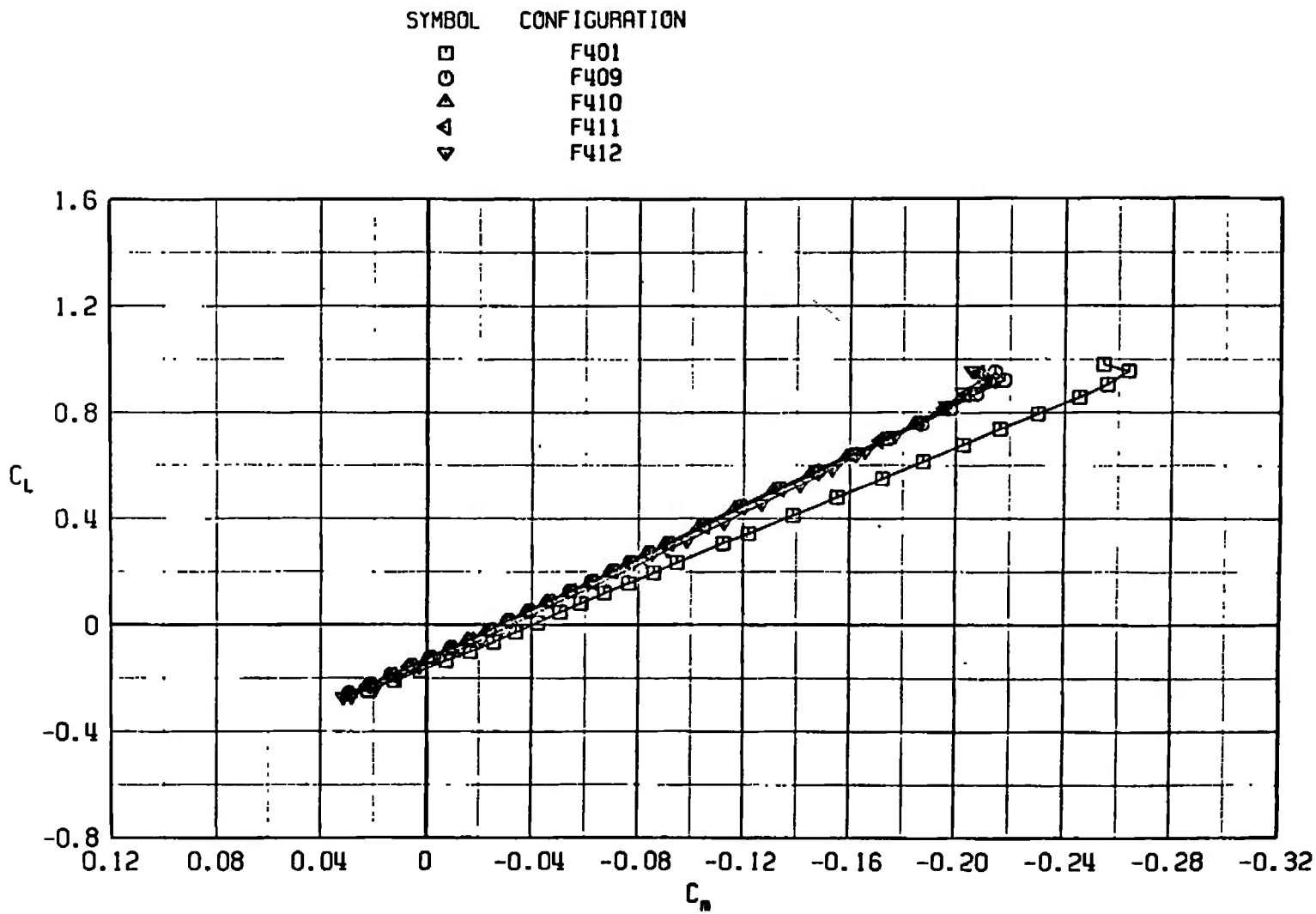

e. $M_\infty = 1.30$

Fig. 18 Concluded

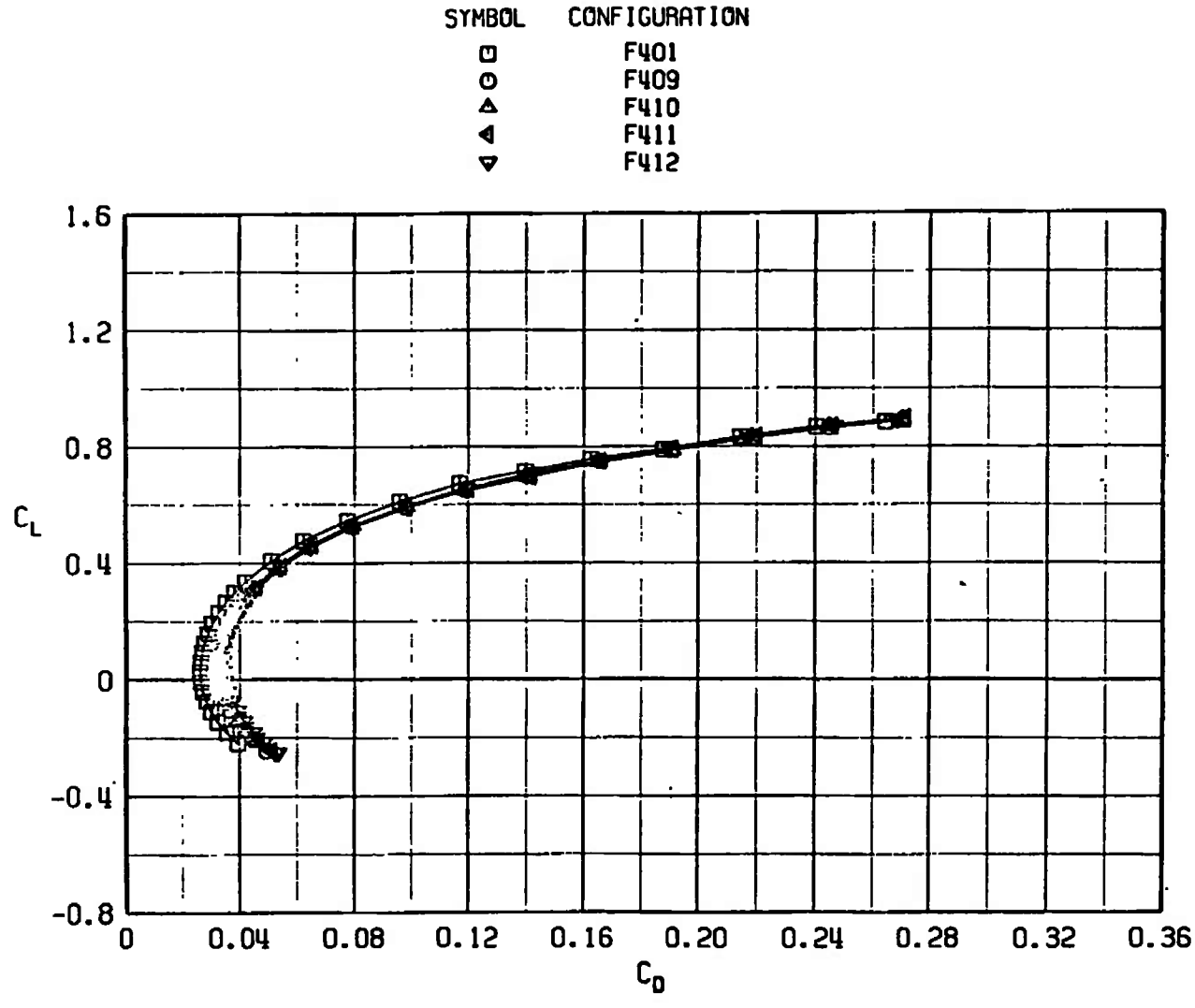

a. $M_\infty = 0.75$

Fig. 19 Drag Coefficient Variation with Lift Coefficient for Configurations F401, F409, F410, F411, and F412

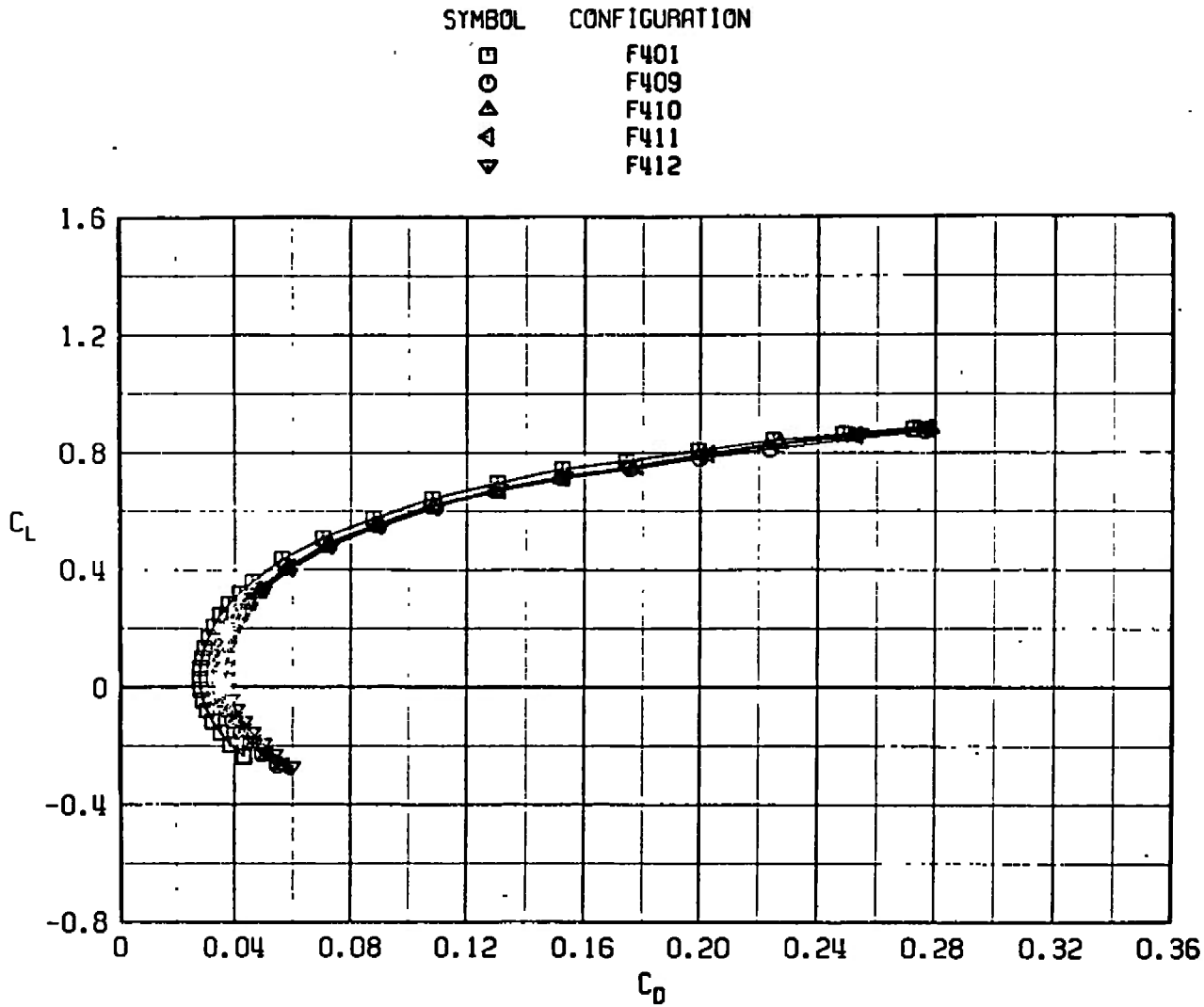

b. $M_\infty = 0.85$

Fig. 19 Continued

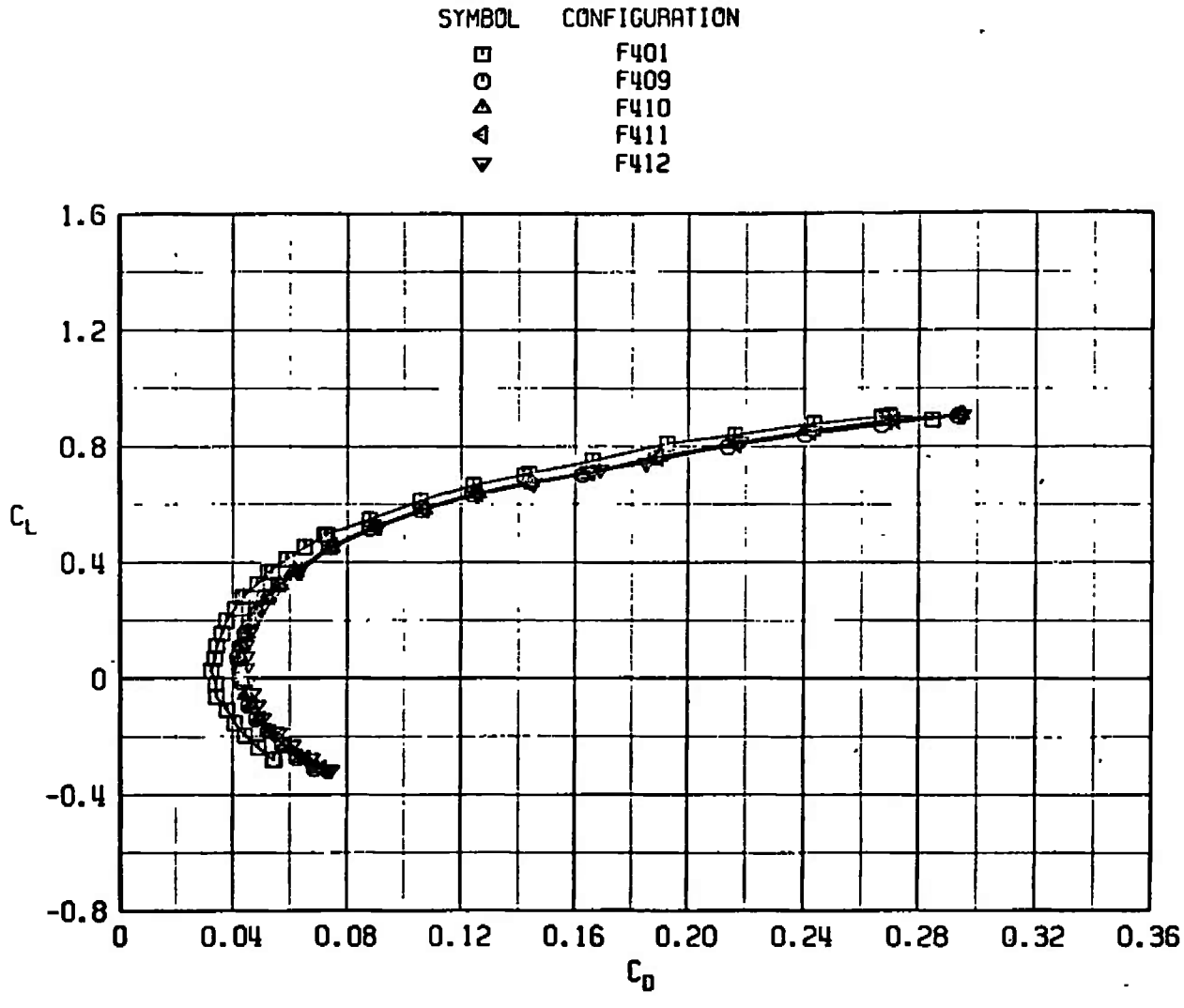

c. $M_\infty = 0.95$

Fig. 19 Continued

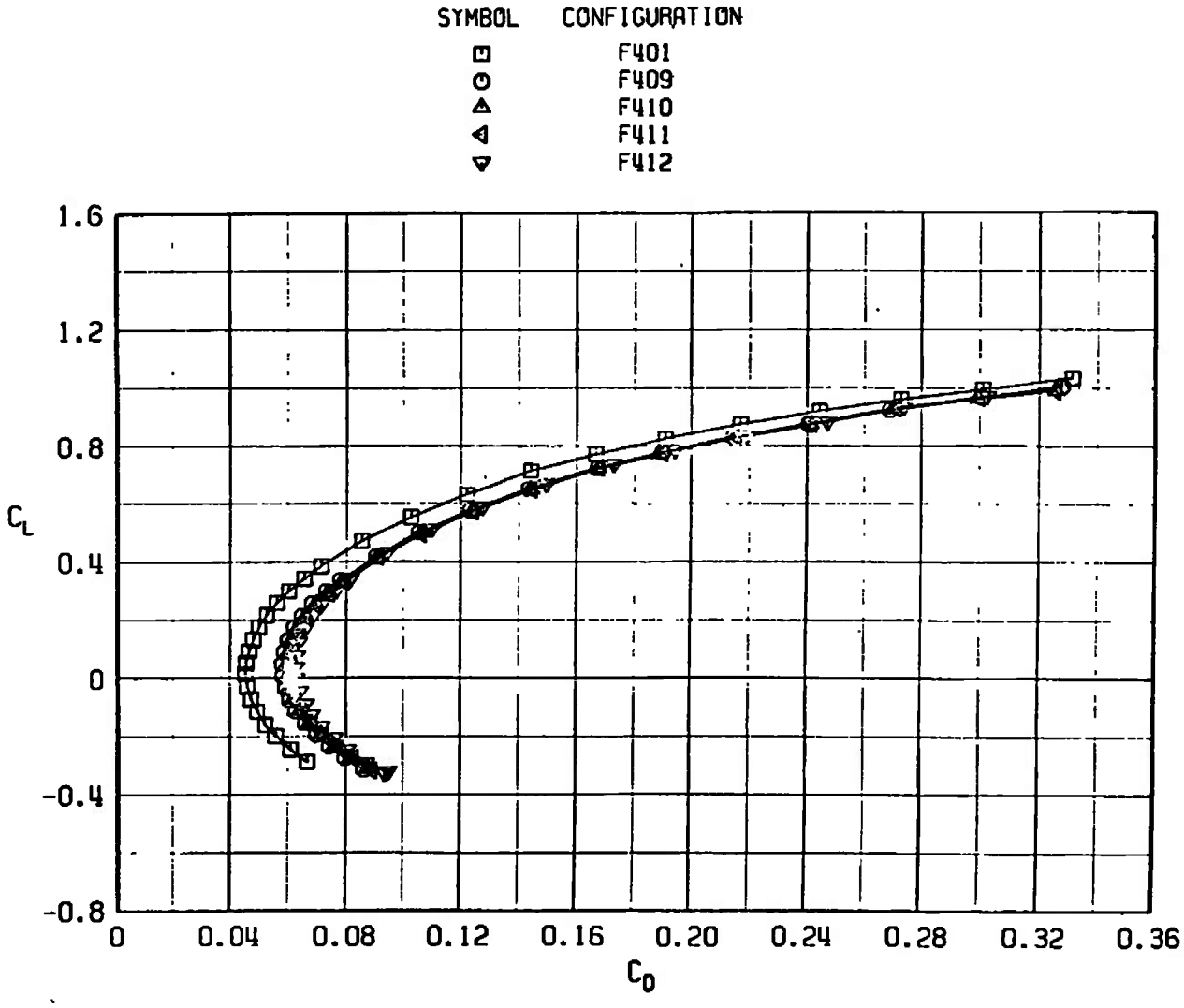

d. $M_\infty = 1.10$

Fig. 19 Continued

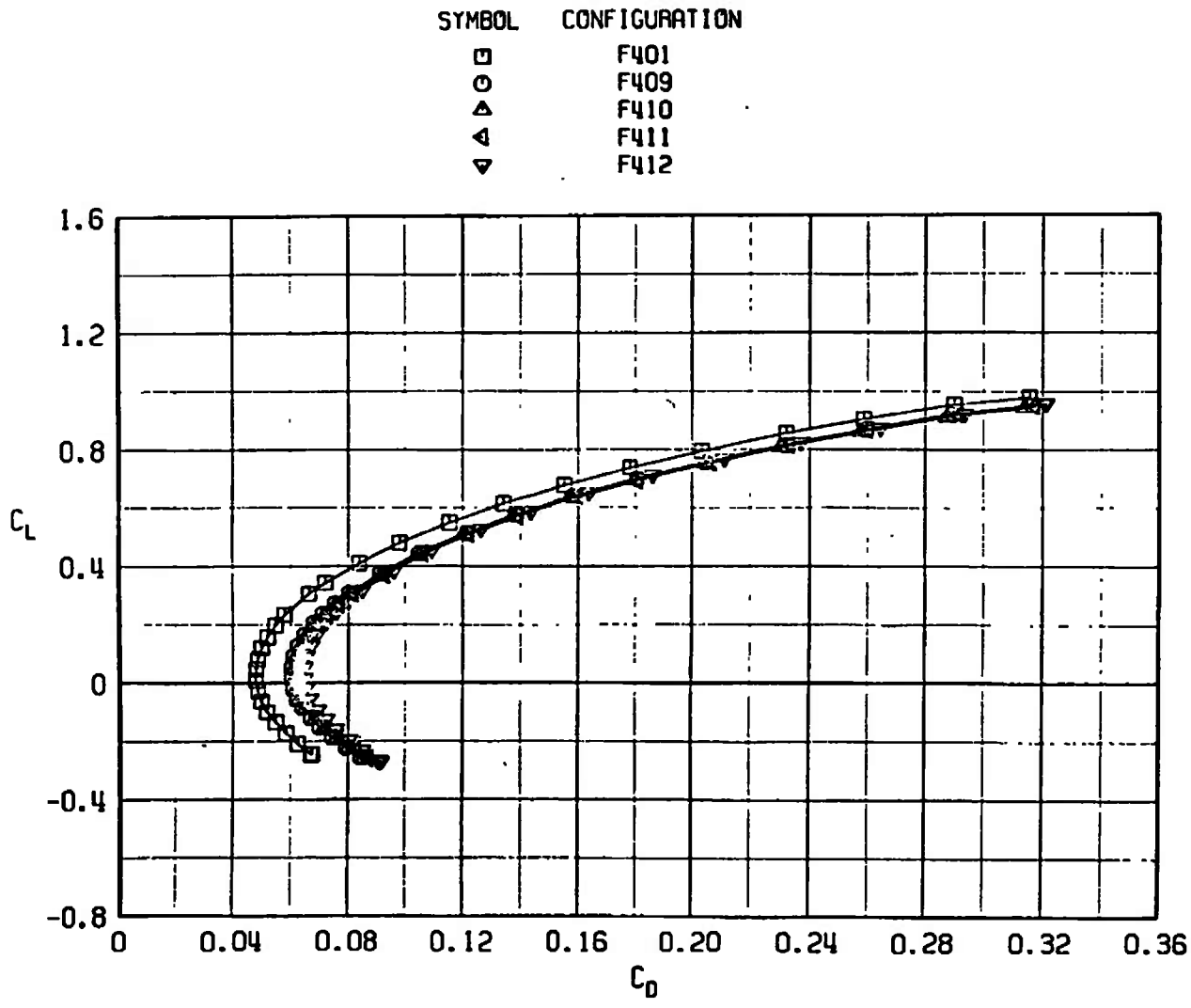

e. $M_\infty = 1.30$

Fig. 19 Concluded

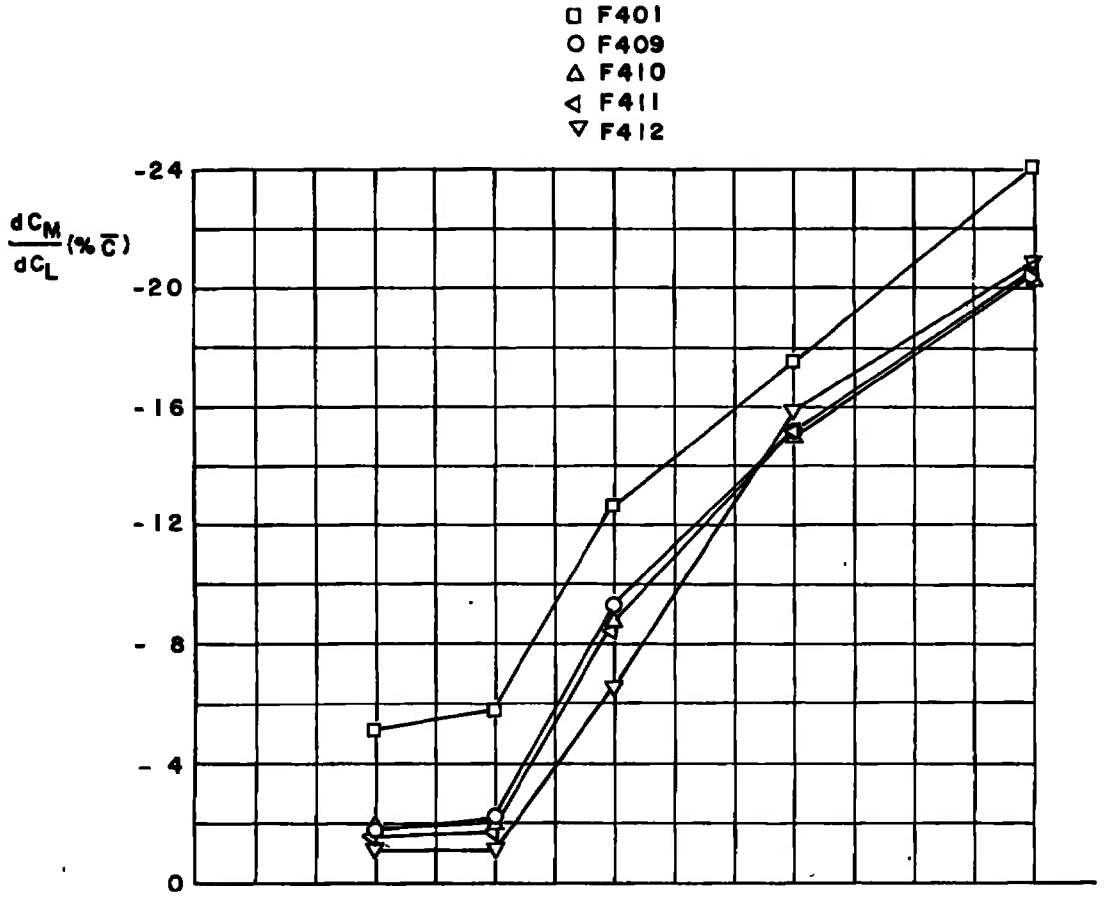

a. dC_m/dC_L versus M_∞ at C_L = 0.2 in percentage of $\bar{c}$

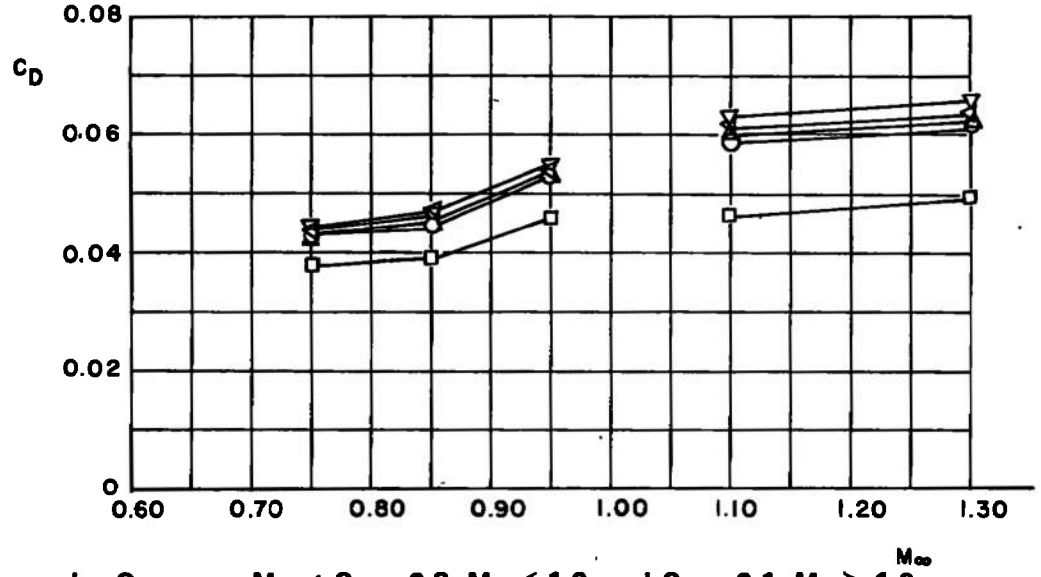

b. C_D versus M_∞ at C_L = 0.3, $M_\infty < 1.0$, and C_L = 0.1, $M_\infty > 1.0$

Fig. 20 Drag Coefficient and dC_m/dC_L Variation with Mach Number for Configurations F401, F409, F410, F411, and F412

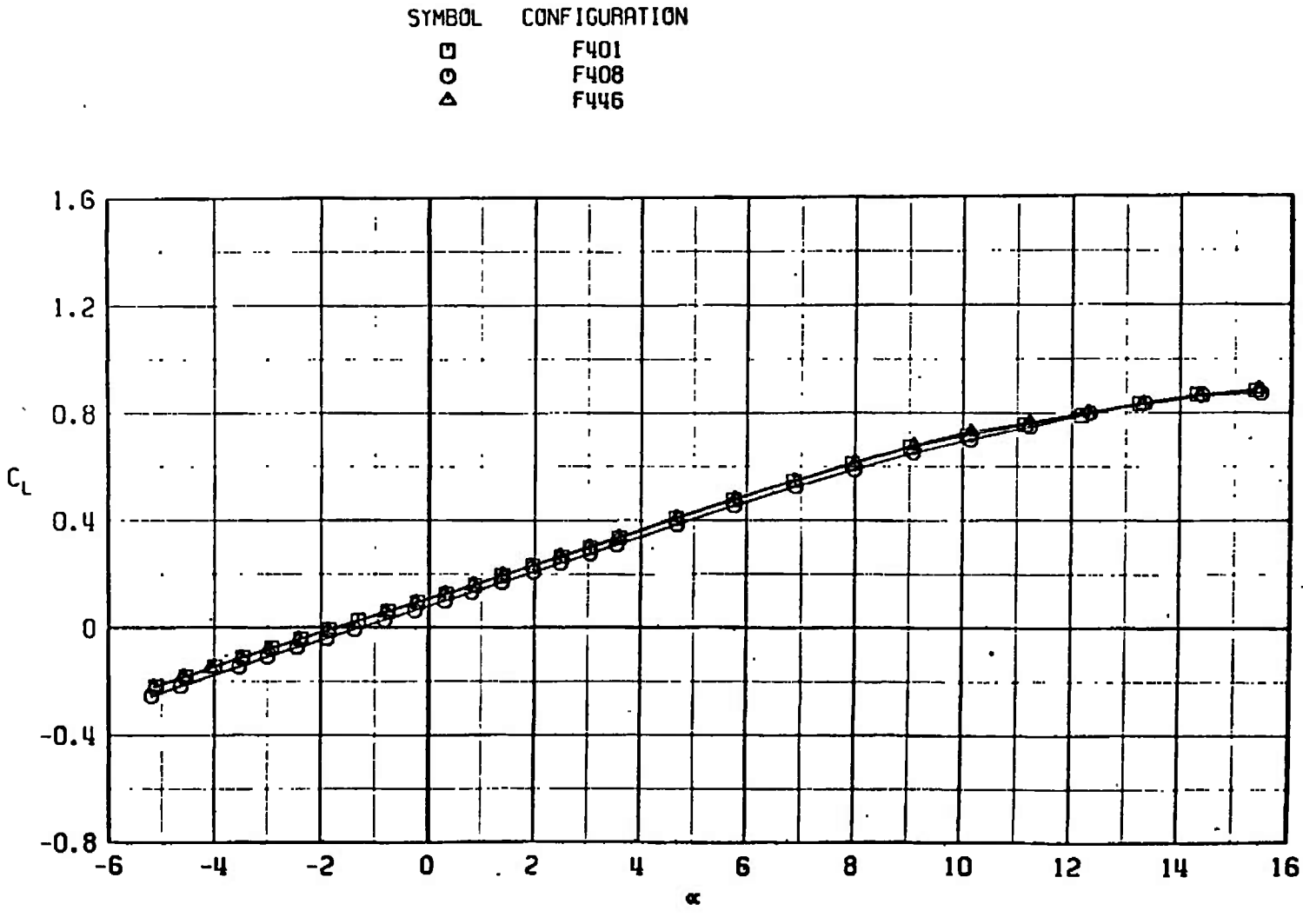

a. $M_\infty = 0.75$

Fig. 21 Lift Coefficient Variation with Angle of Attack for Configurations F401, F408, and F446

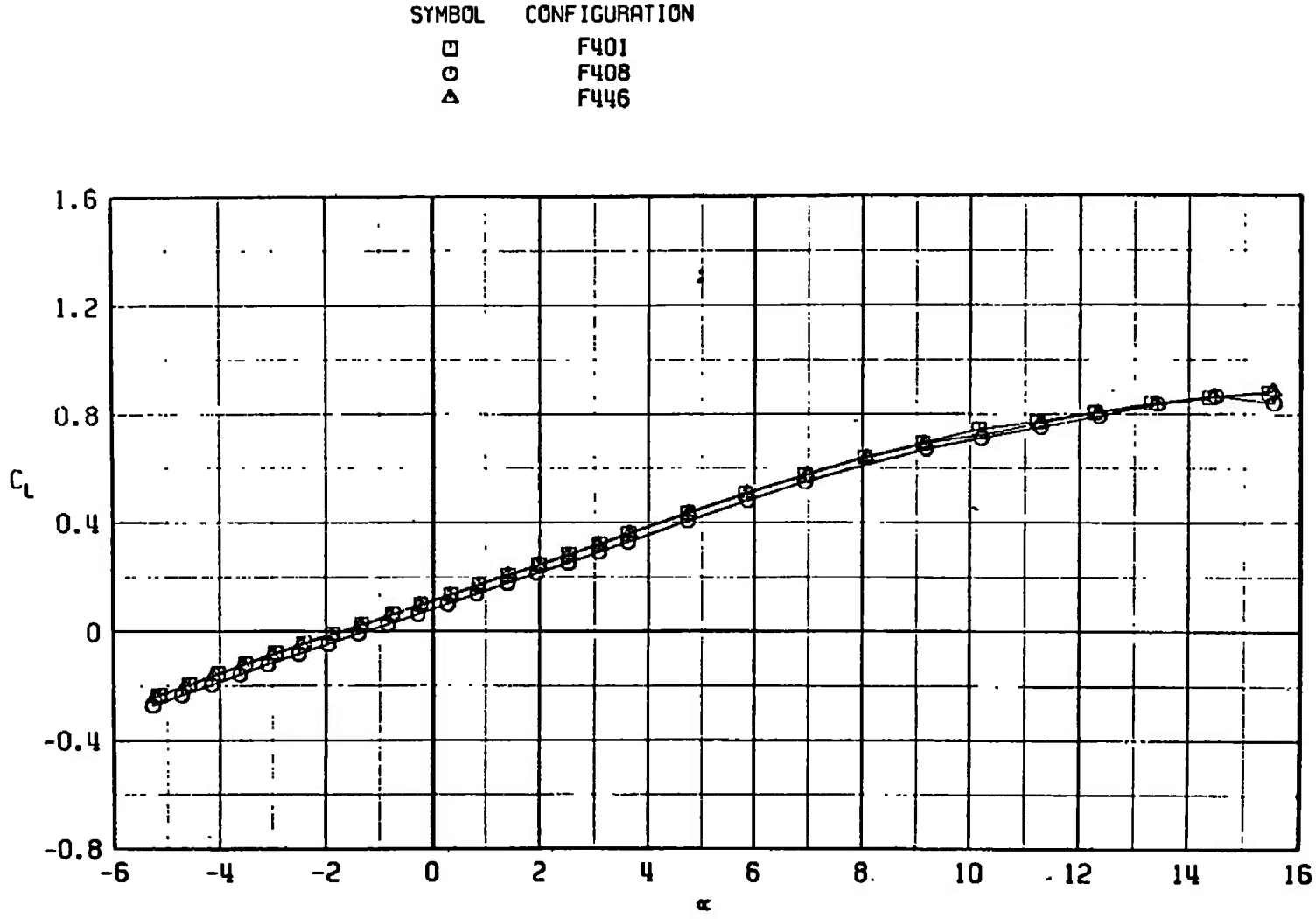

b. $M_\infty = 0.85$

Fig. 21 Continued

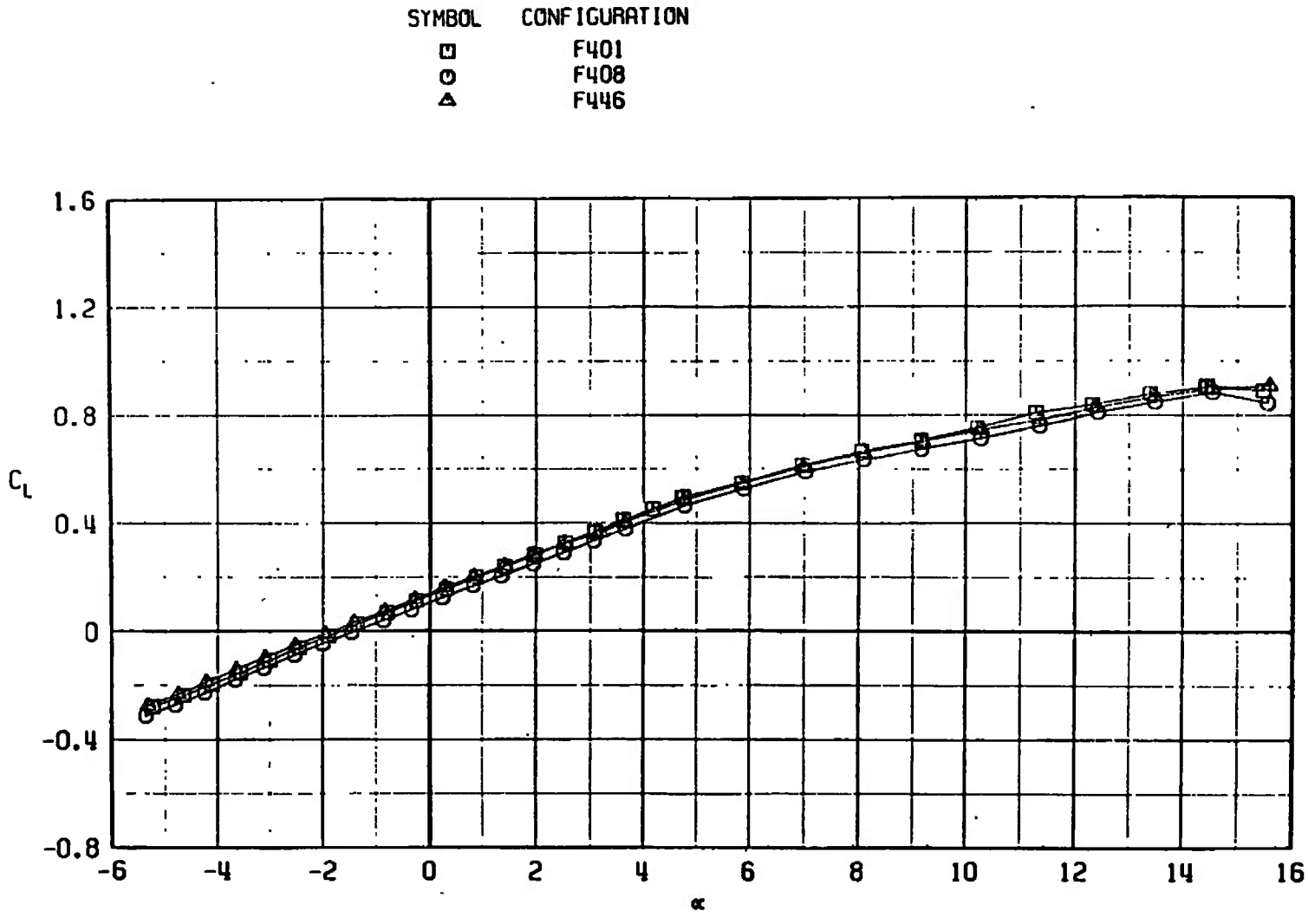

c. $M_\infty = 0.95$

Fig. 21 Continued

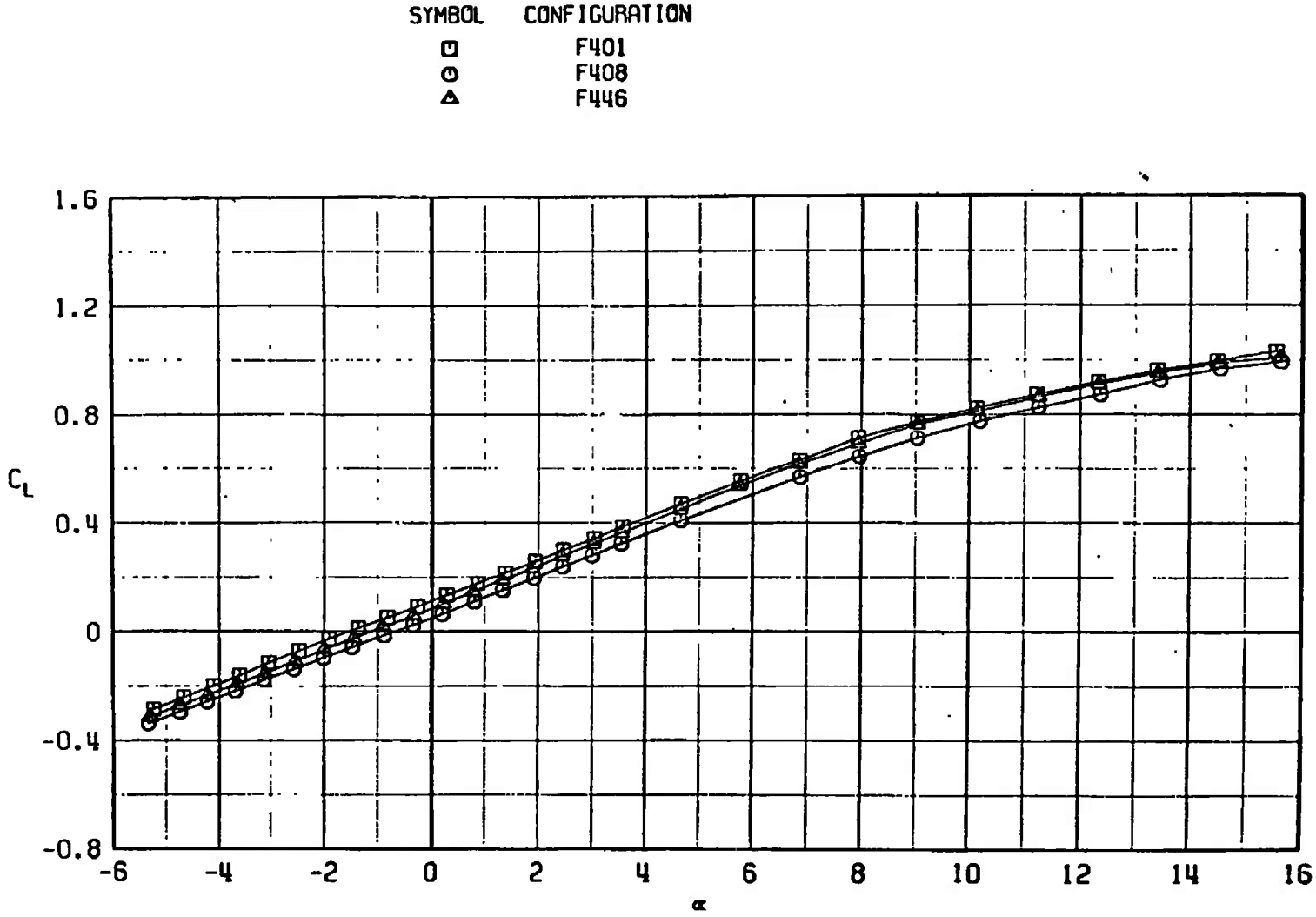

d. $M_\infty = 1.10$
Fig. 21 Continued

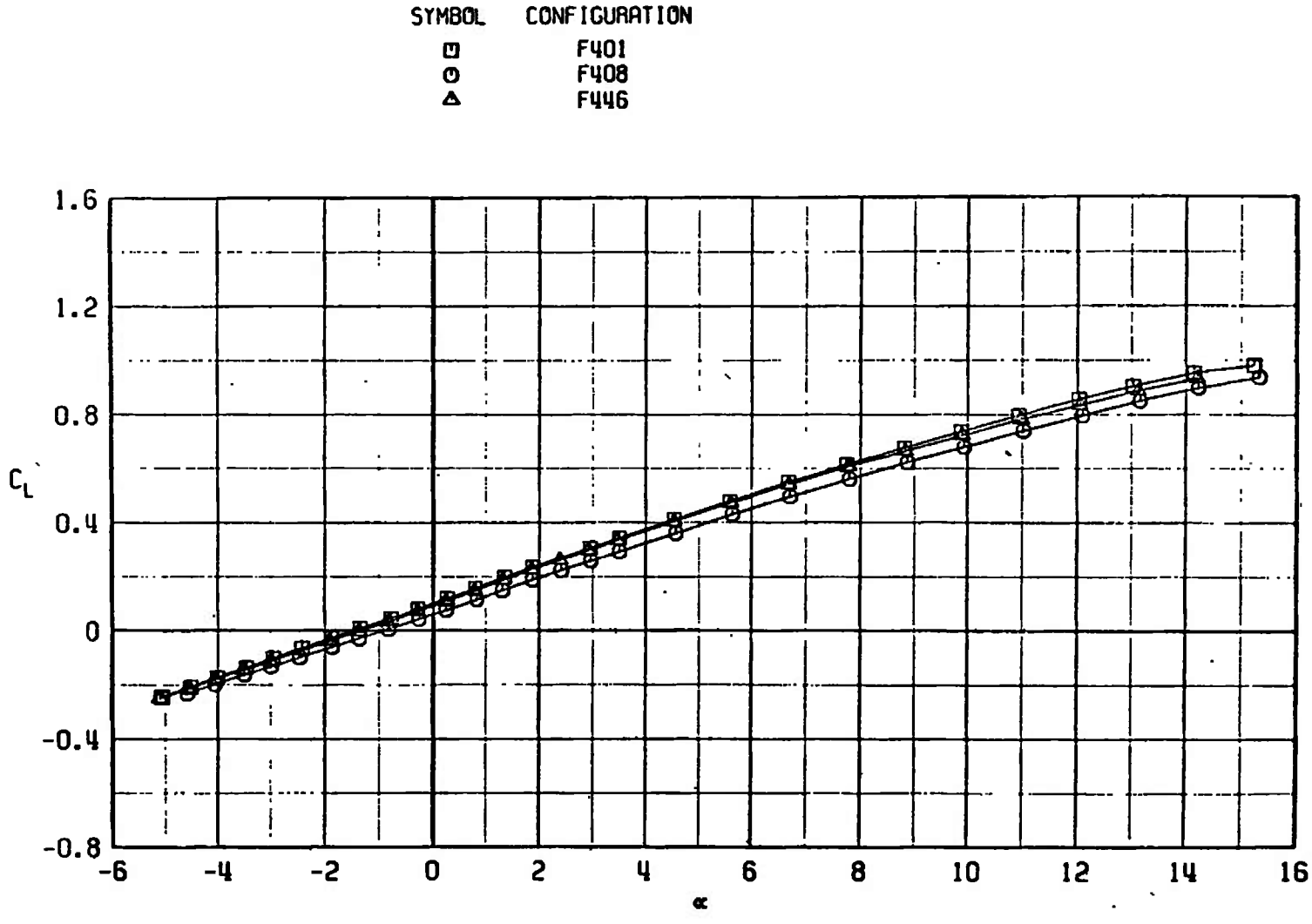

e. $M_\infty = 1.30$

Fig. 21 Concluded

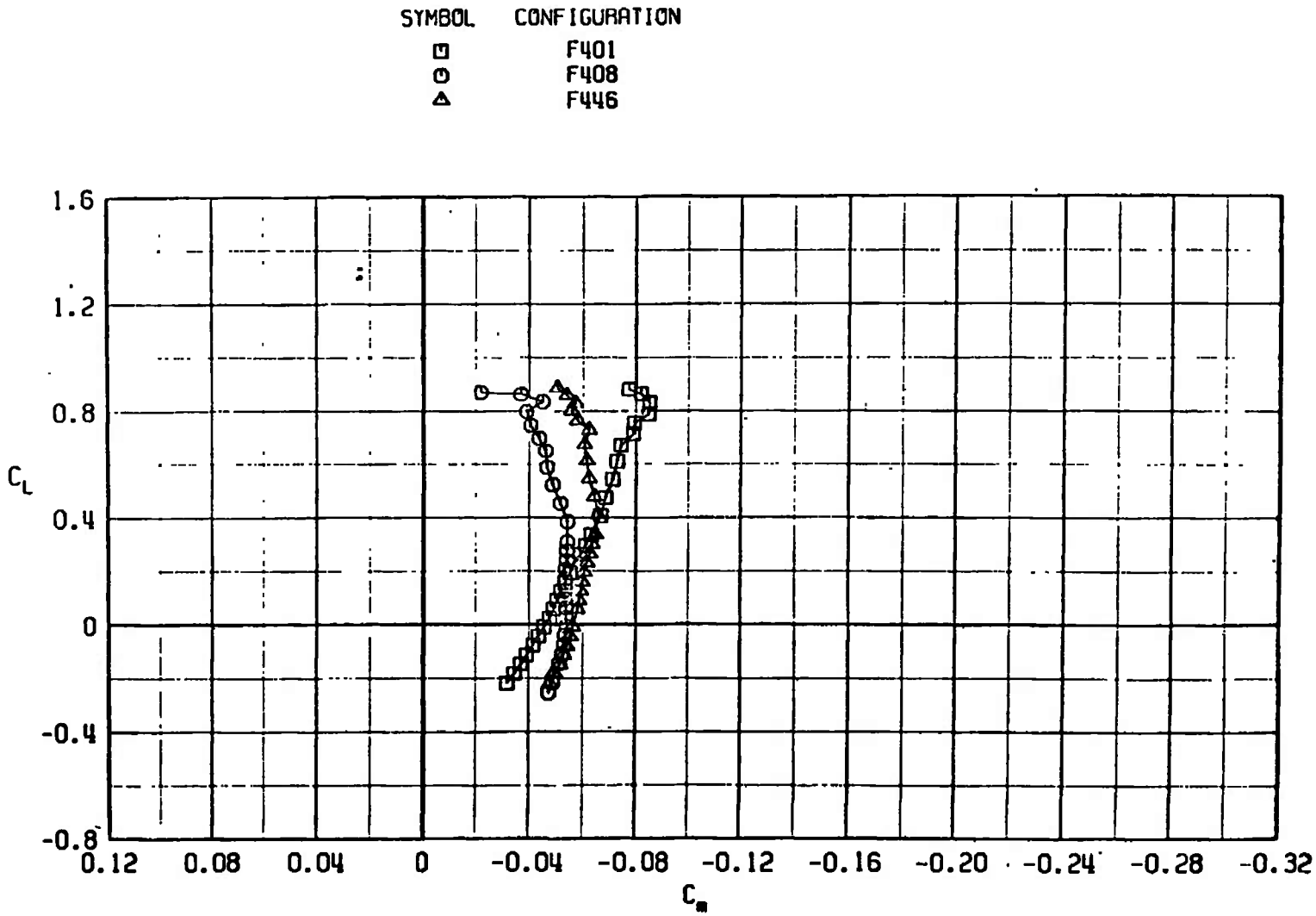

a. $M_\infty = 0.75$

Fig. 22 Pitching-Moment Coefficient Variation with Lift Coefficient for Configurations F401, F408, and F446

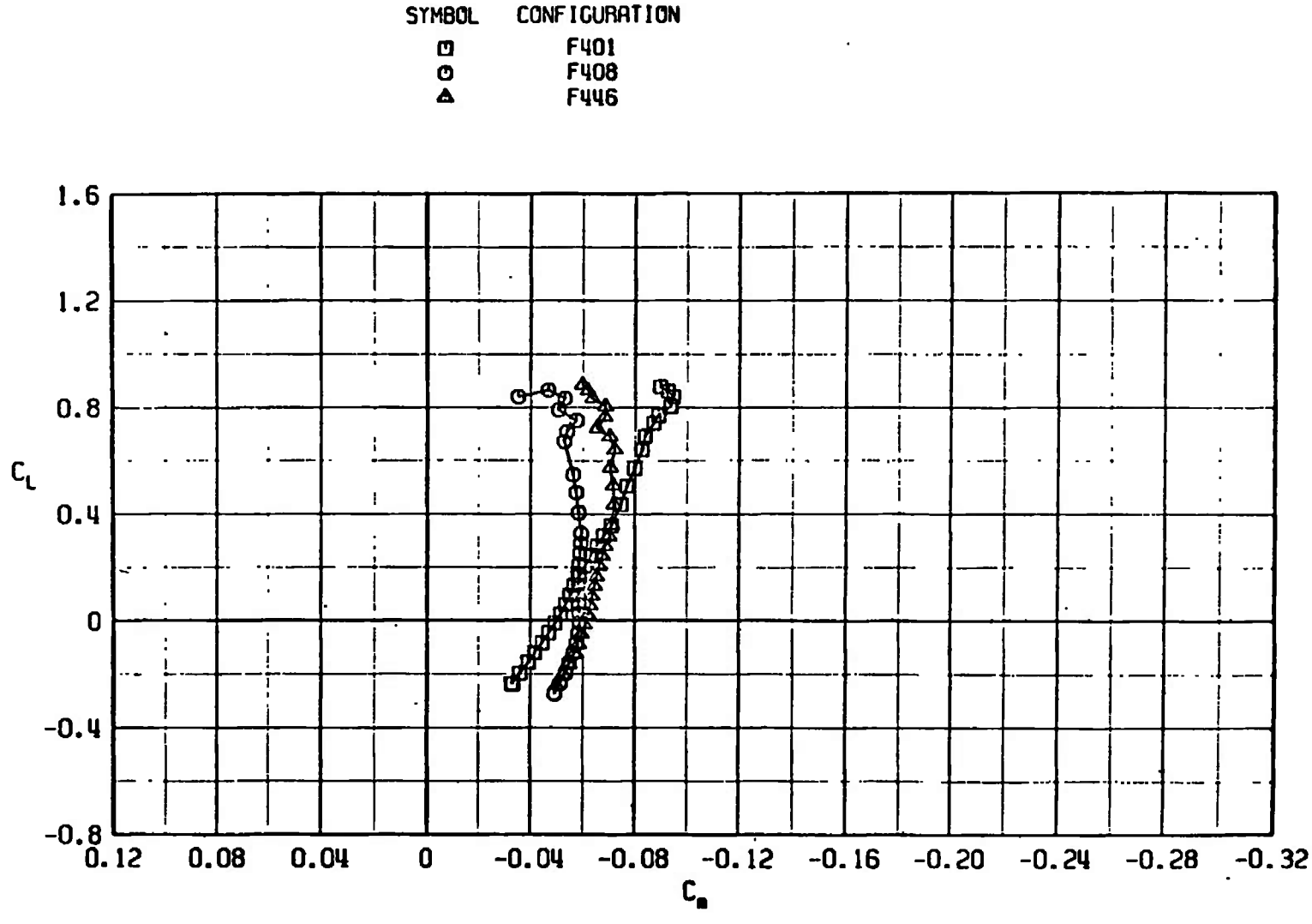

b. $M_\infty = 0.85$

Fig. 22 Continued

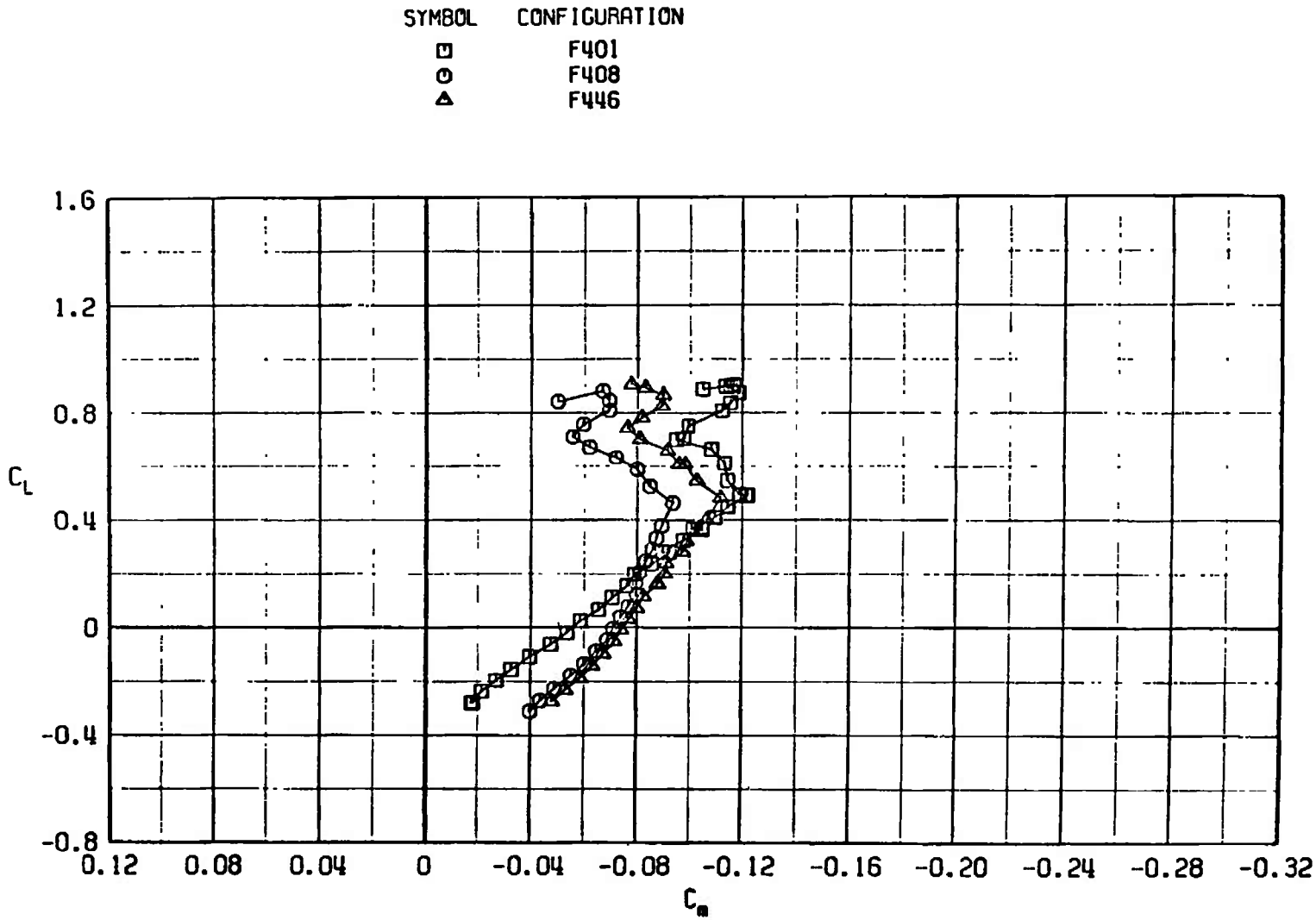

c. $M_\infty = 0.95$

Fig. 22 Continued

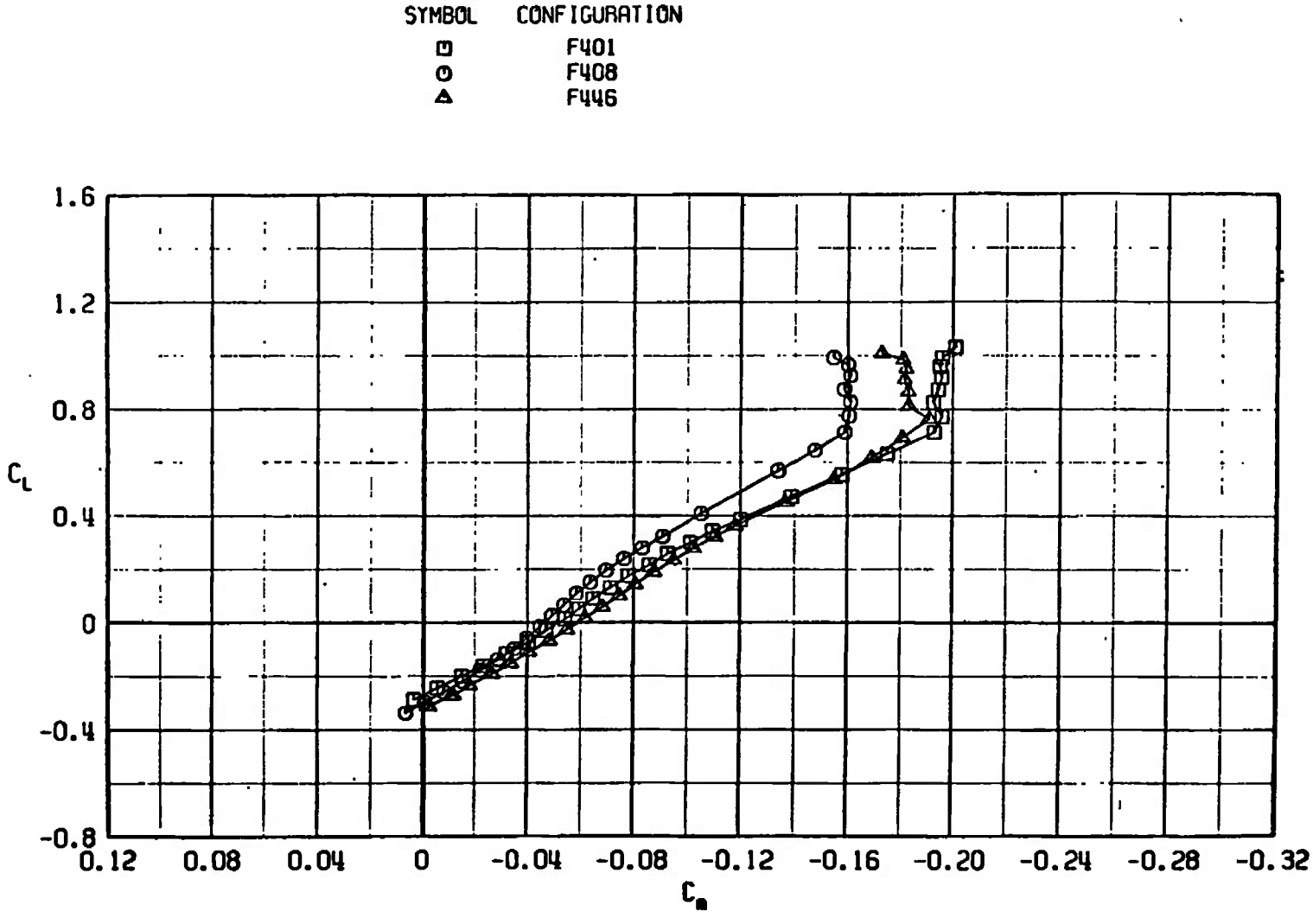

d. $M_\infty = 1.10$

Fig. 22 Continued

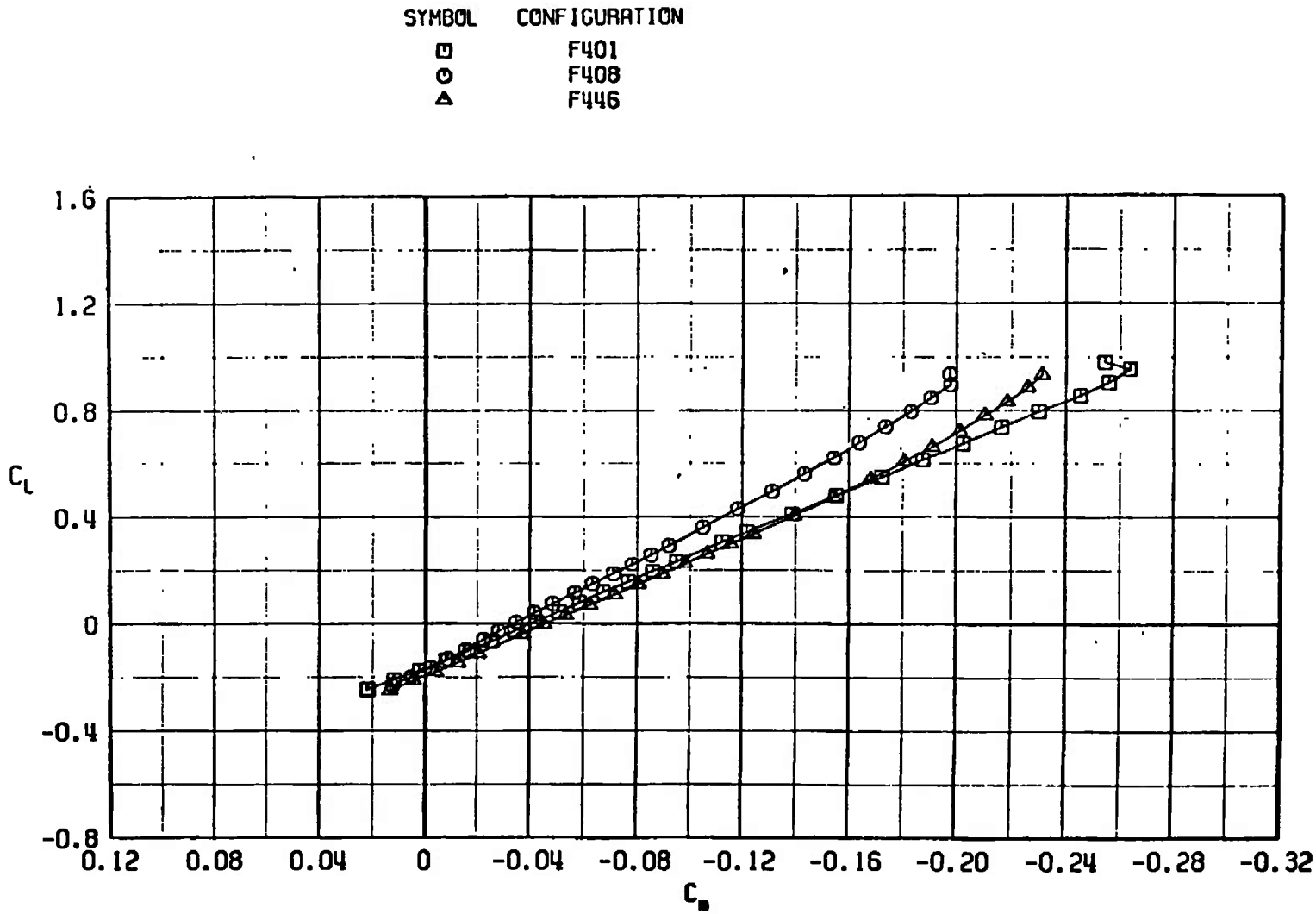

e. $M_\infty = 1.30$

Fig. 22 Concluded

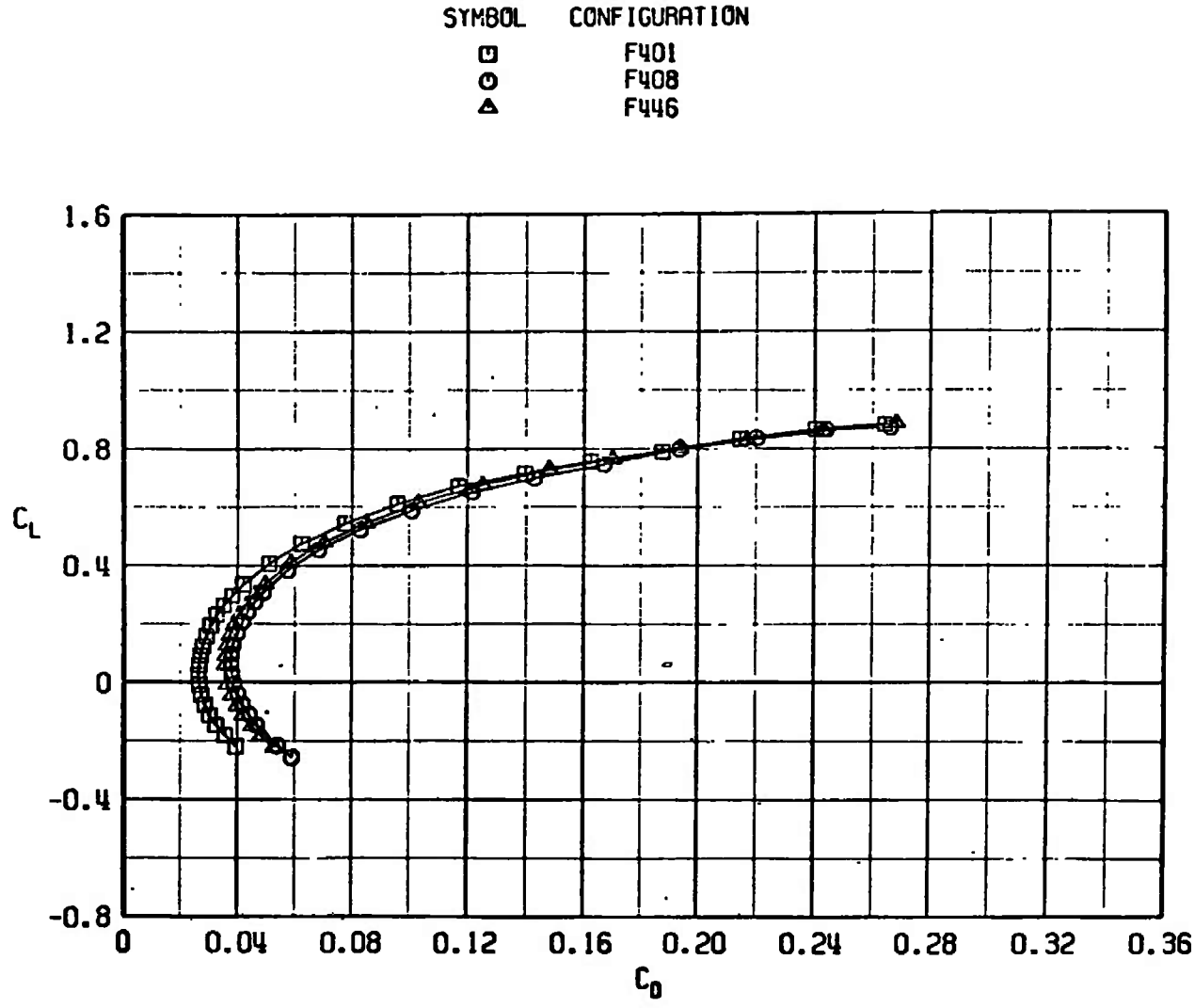

a. $M_\infty = 0.75$

Fig. 23 Drag Coefficient Variation with Lift Coefficient for Configurations F401, F408, and F446

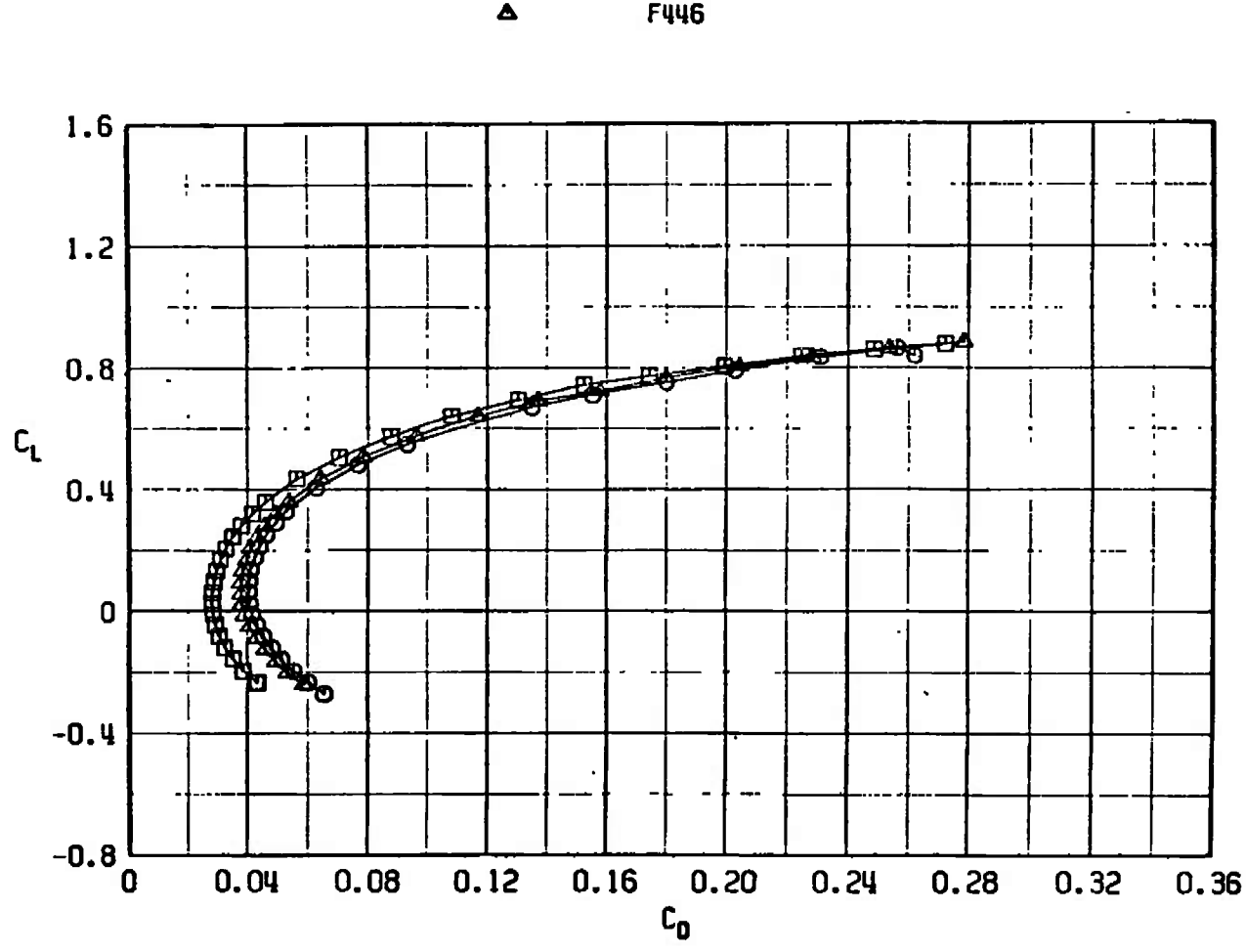

b. $M_\infty = 0.85$

Fig. 23 Continued

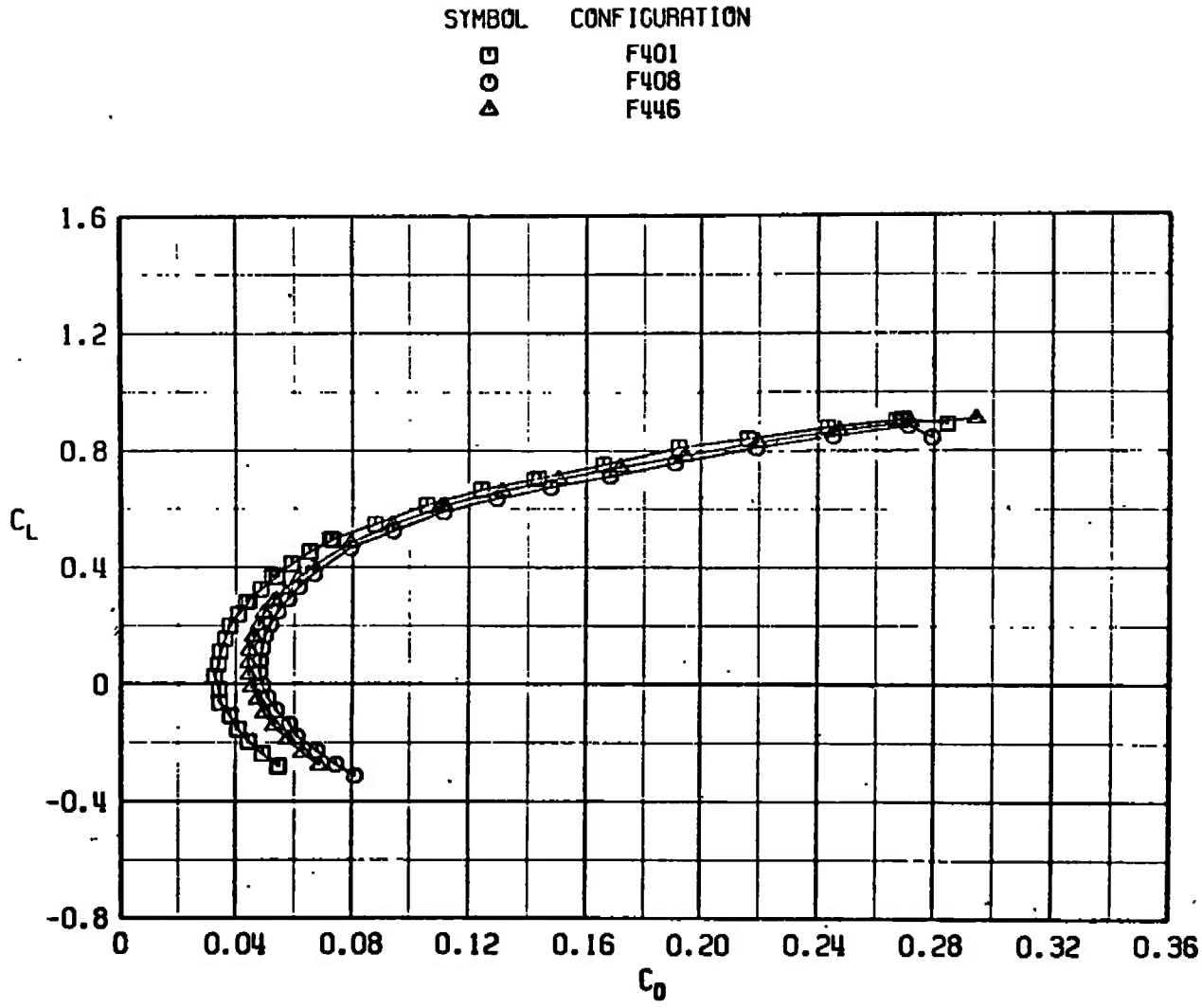

c. $M_\infty = 0.95$

Fig. 23 Continued

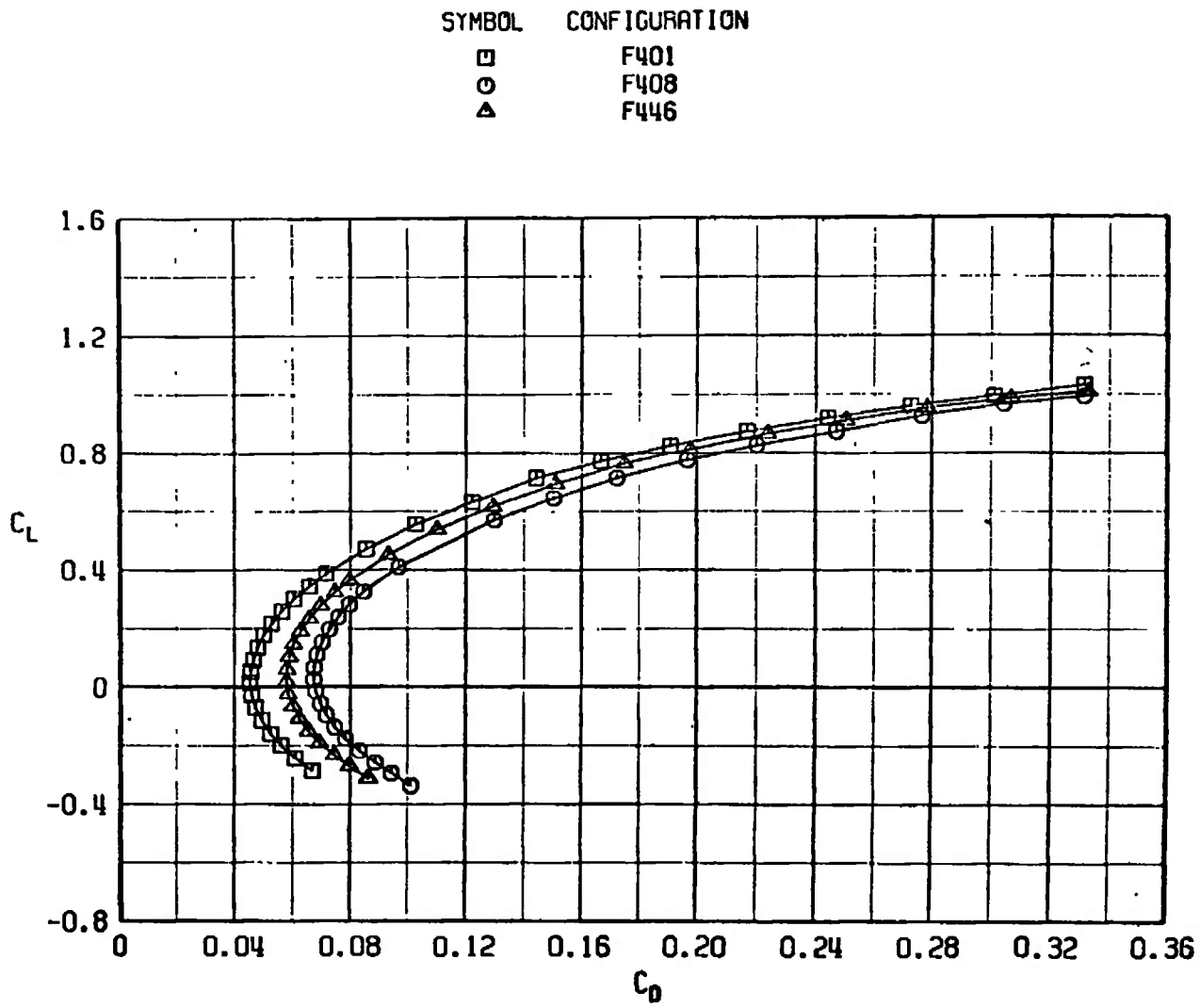

d. $M_\infty = 1.10$

Fig. 23 Continued

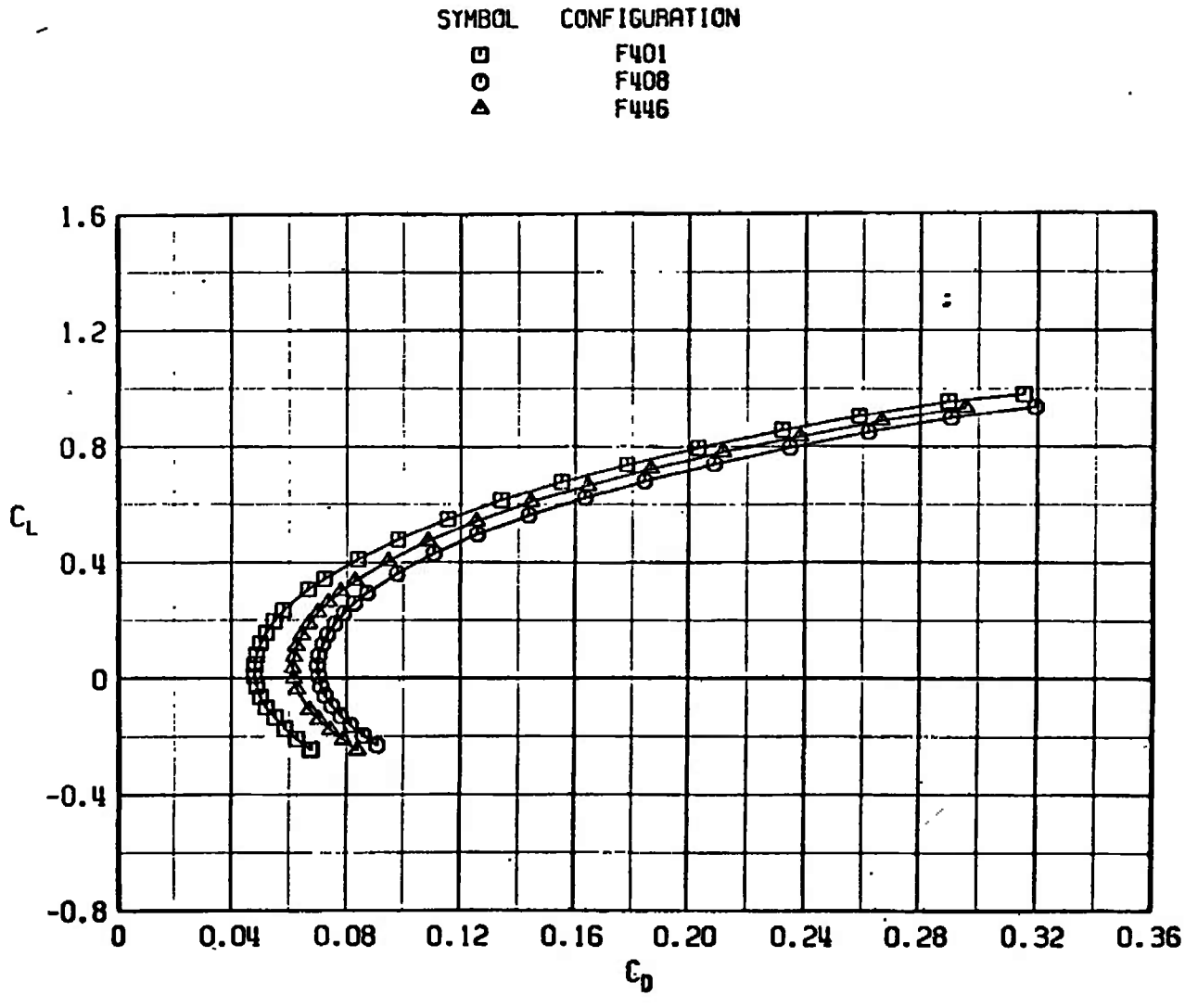

e. $M_\infty = 1.30$

Fig. 23 Concluded

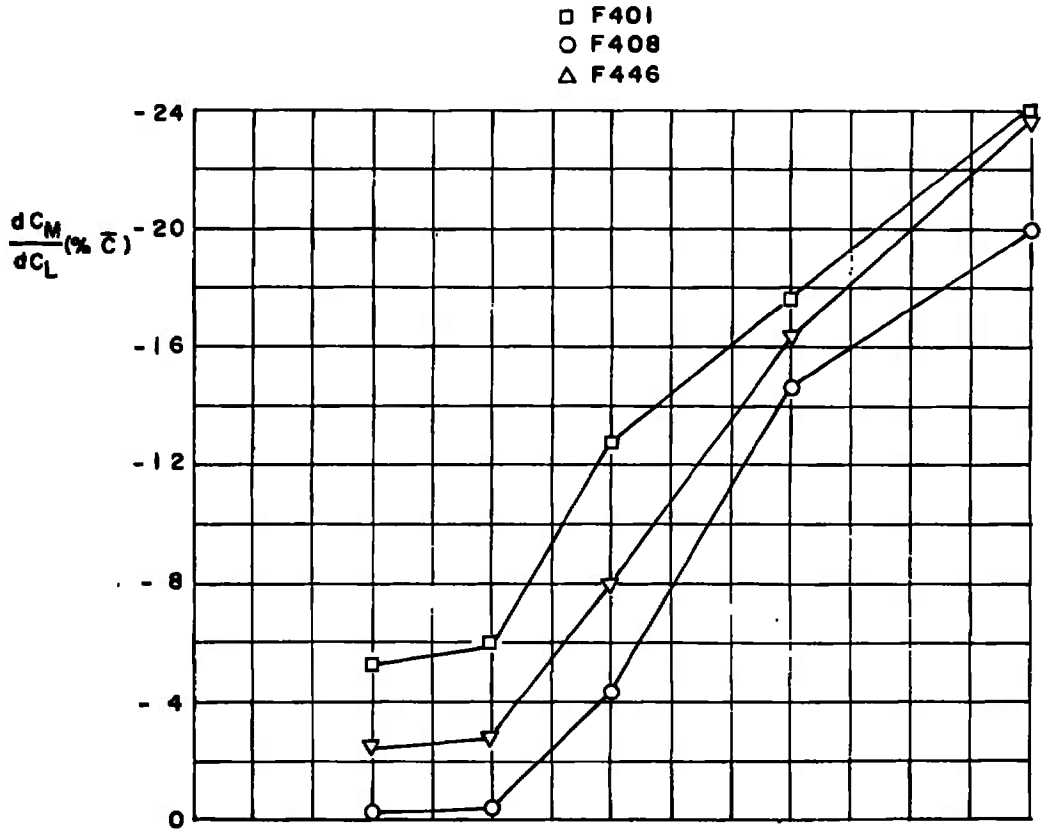

a. dC_m/dC_L versus M_∞ at $C_L = 0.2$ in percentage of $\bar{c}$

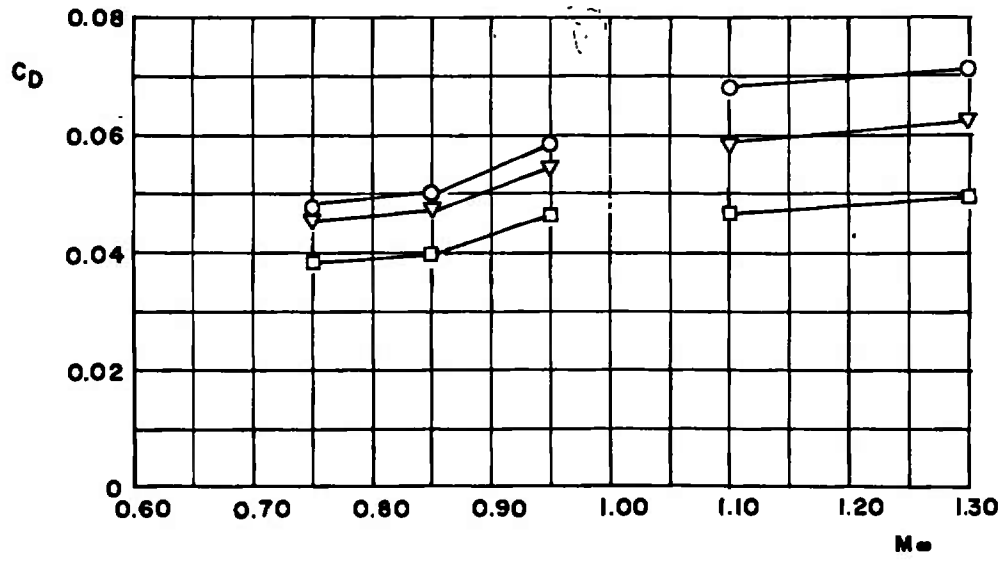

b. C_D versus M_∞ at $C_L = 0.3$, $M_\infty < 1.0$, and $C_D = 0.1$, $M_\infty > 1.0$

Fig. 24 Drag Coefficient and dC_m/dC_L Variation with Lift Coefficient for Configurations F401, F408, and F446

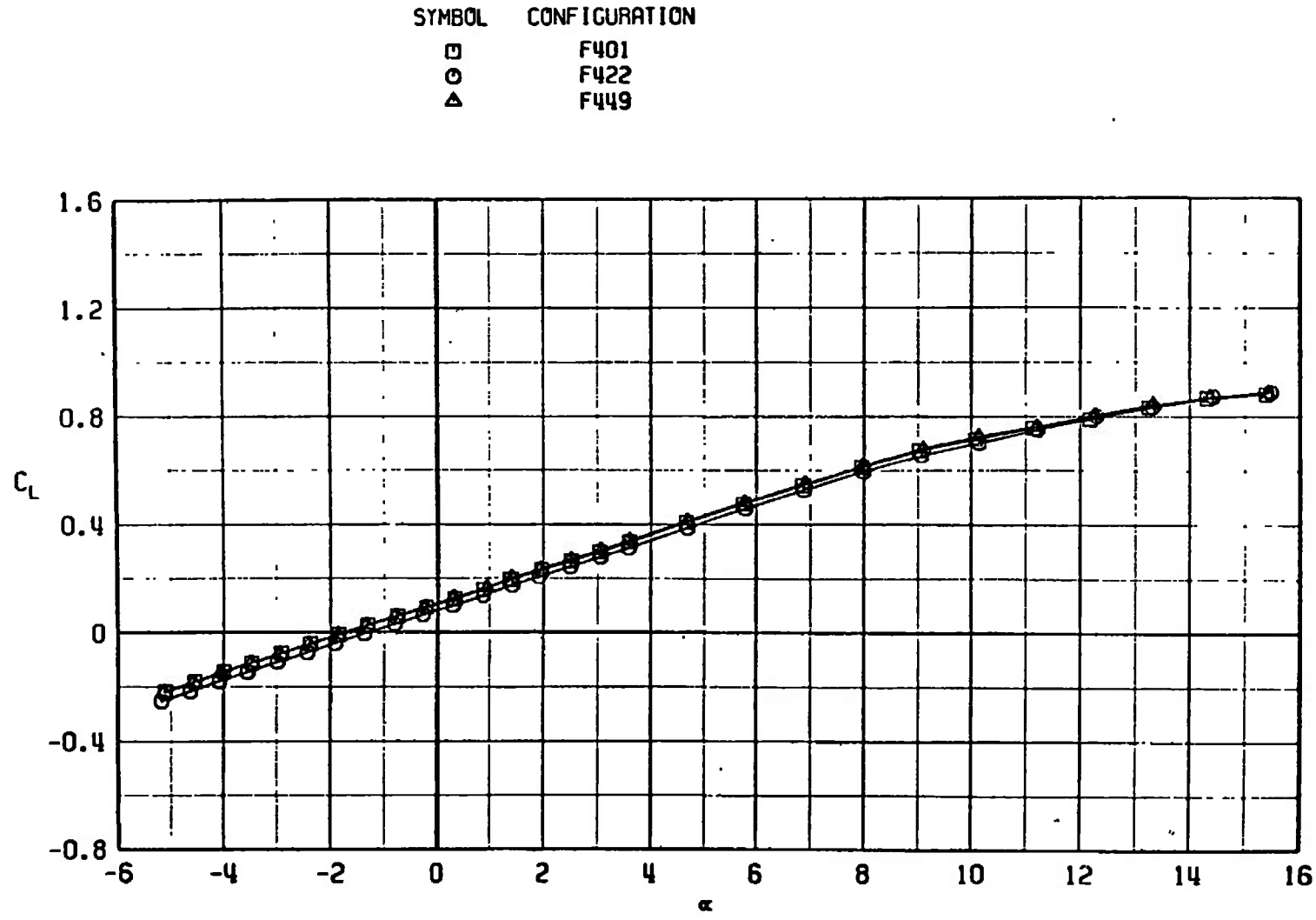

a. $M_\infty = 0.75$

Fig. 25 Lift Coefficient Variation with Angle of Attack for Configurations F401, F422, and F449

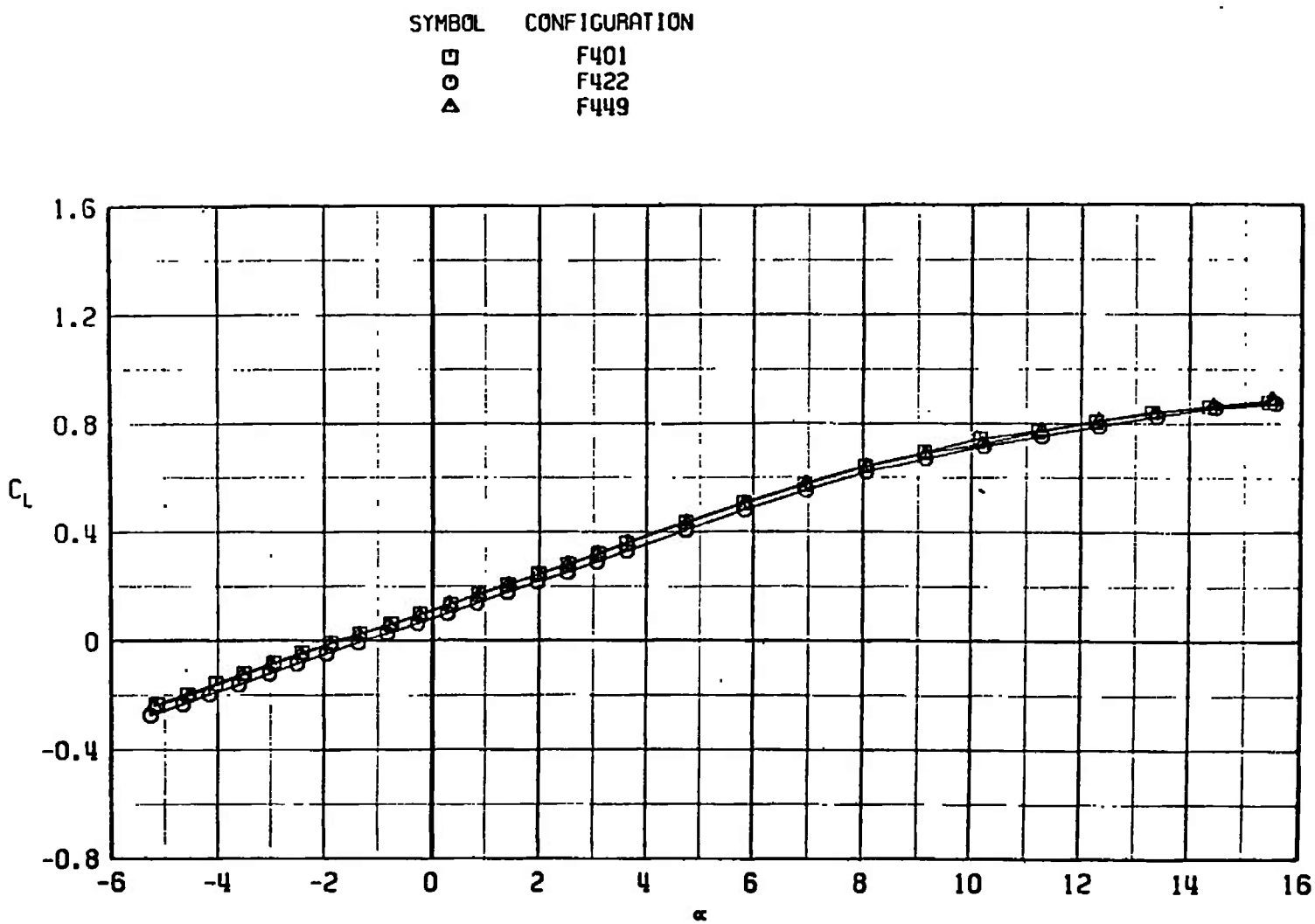

b. $M_\infty = 0.85$

Fig. 25 Continued

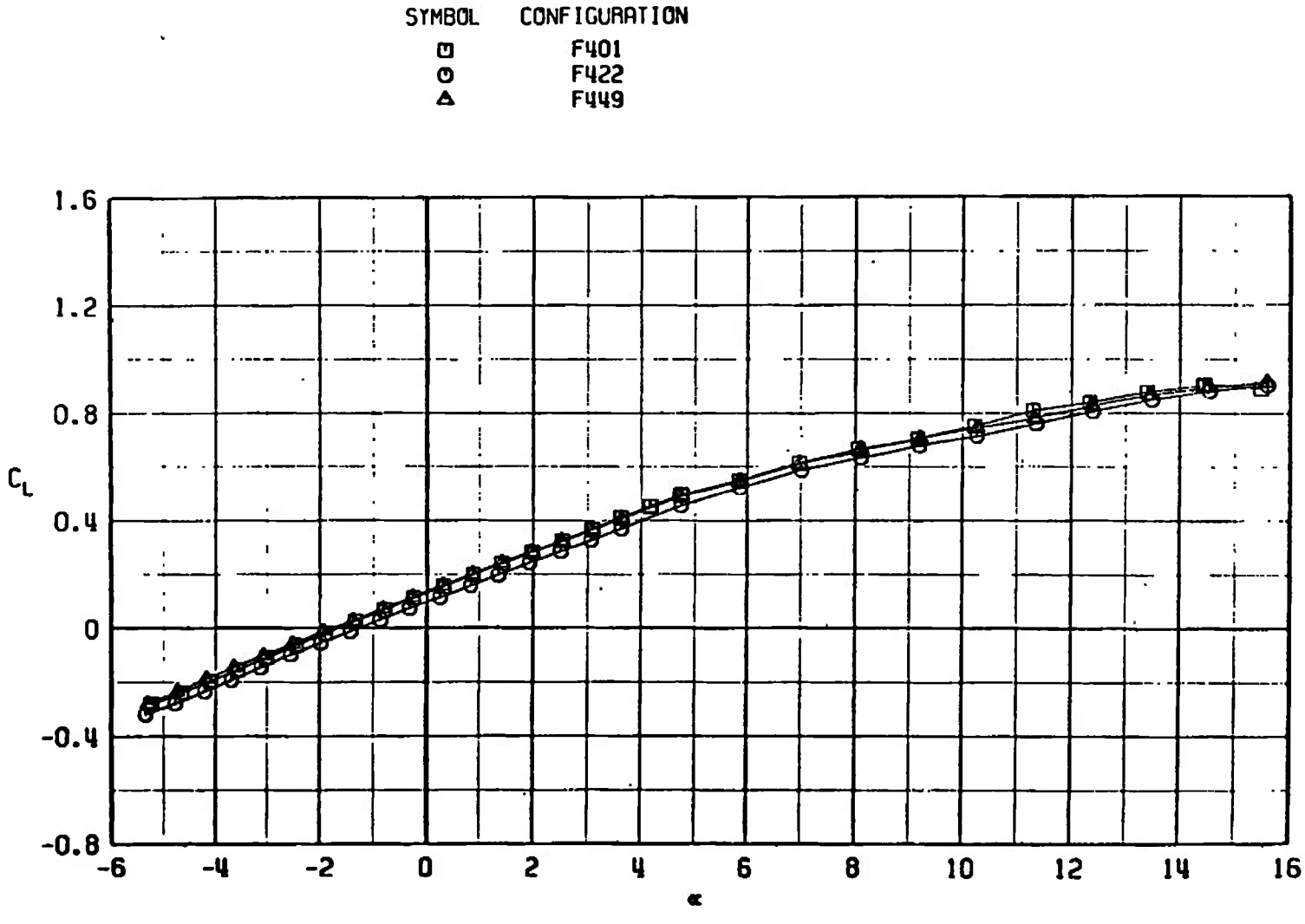

c. $M_\infty = 0.95$
Fig. 25 Continued

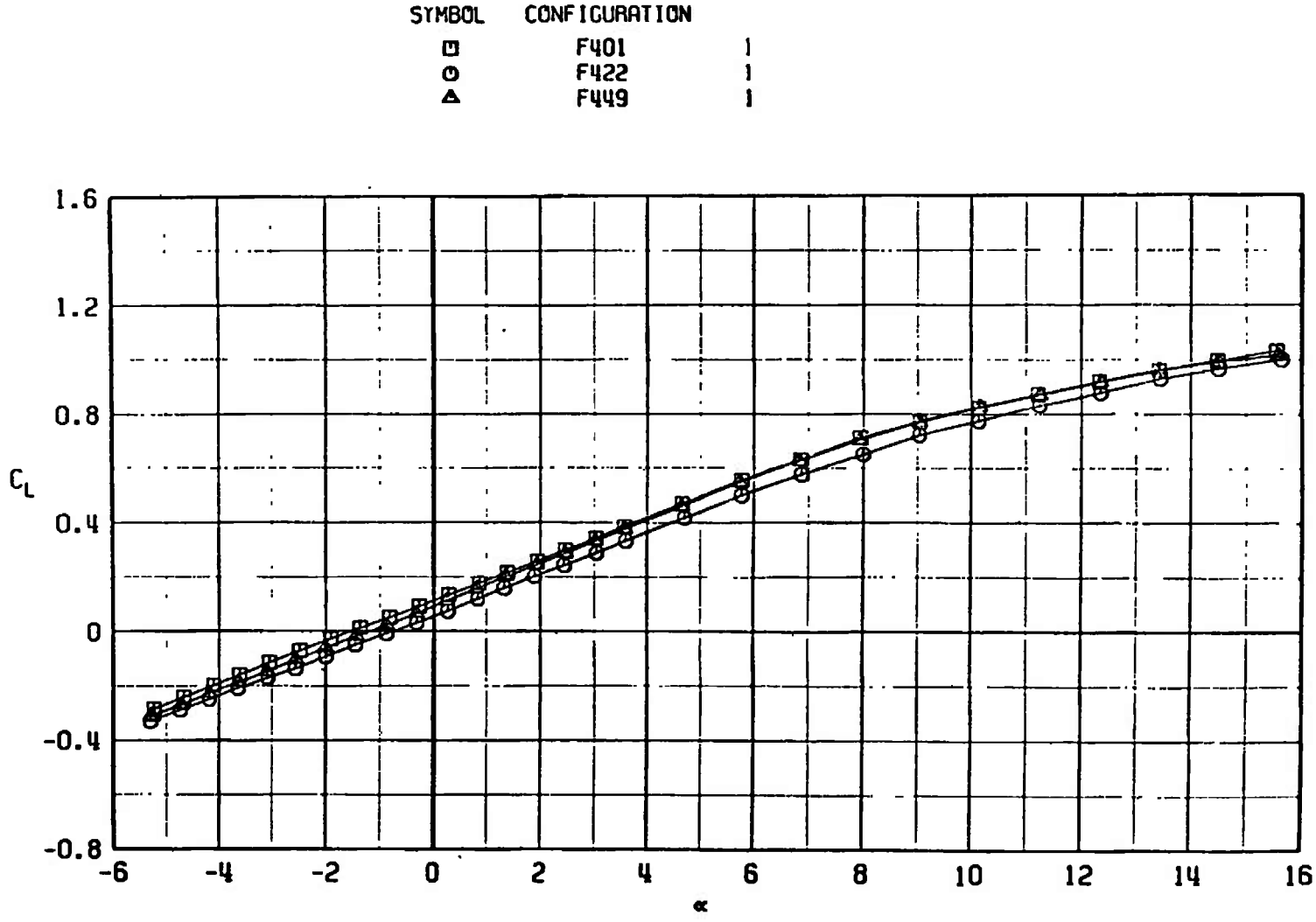

d. $M_\infty = 1.10$

Fig. 25 Continued

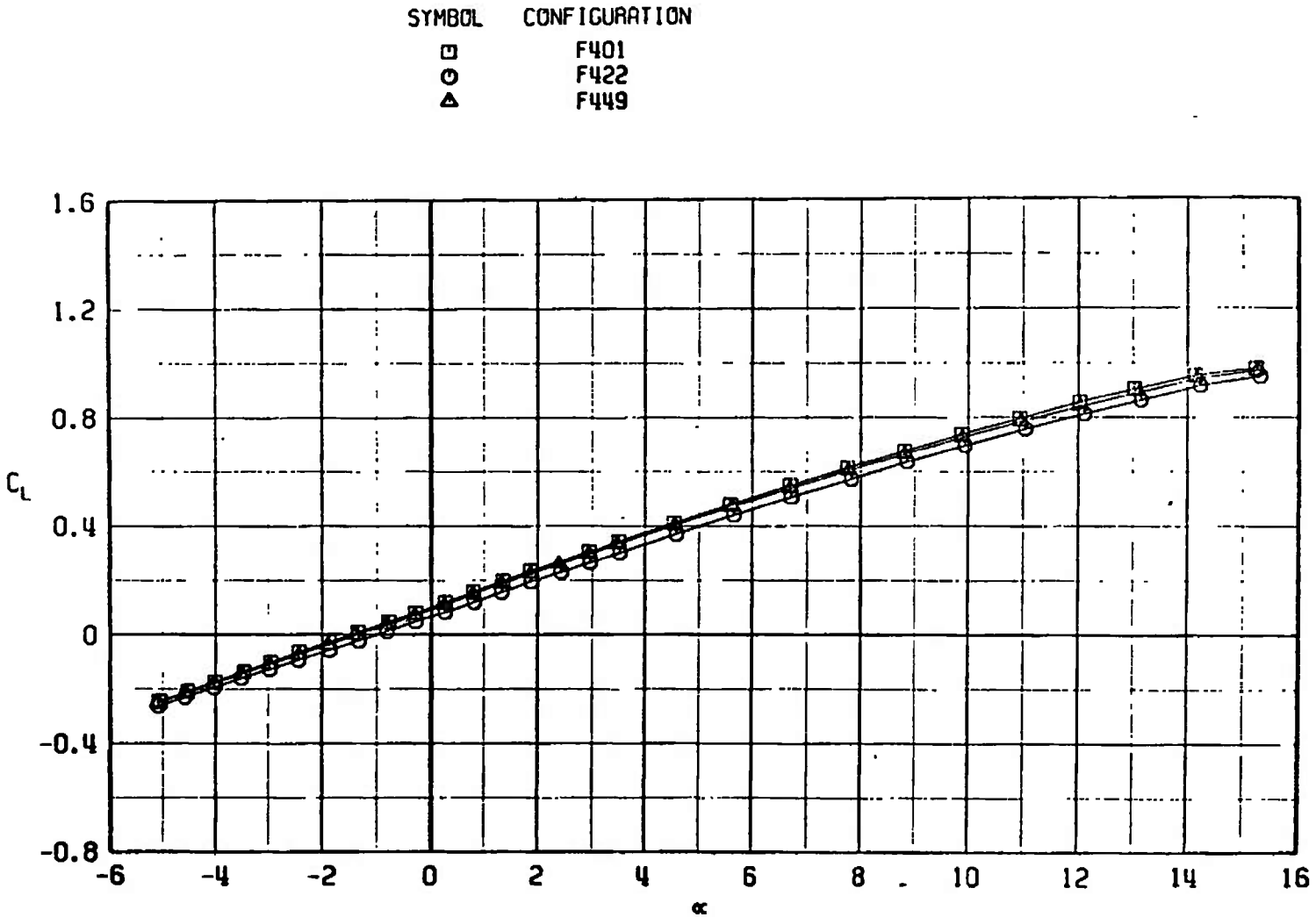

e. $M_\infty = 1.30$

Fig. 25 Concluded

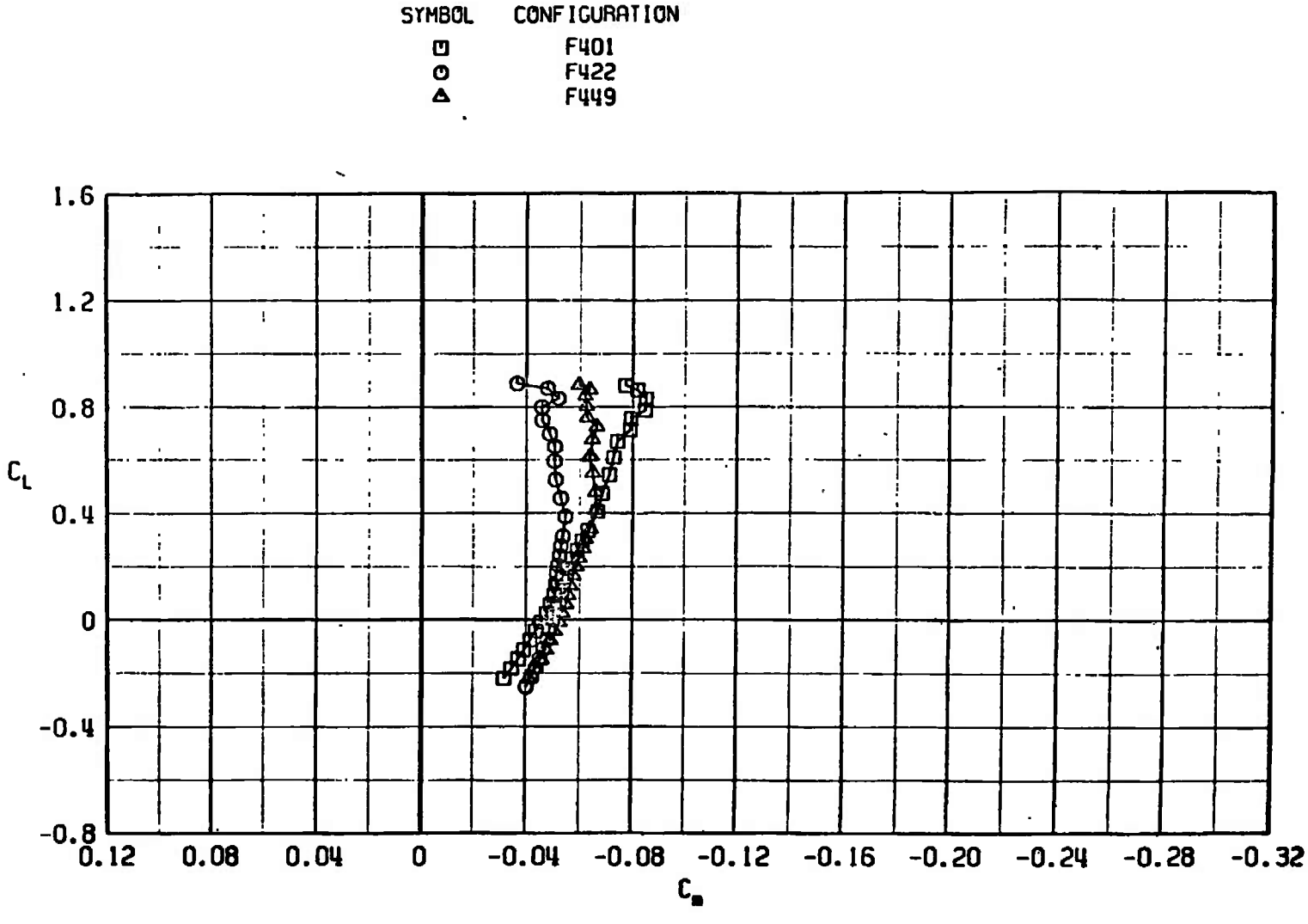

a. $M_\infty = 0.75$

Fig. 26 Pitching-Moment Coefficient Variation with Lift Coefficient for Configurations F401, F422, and F449

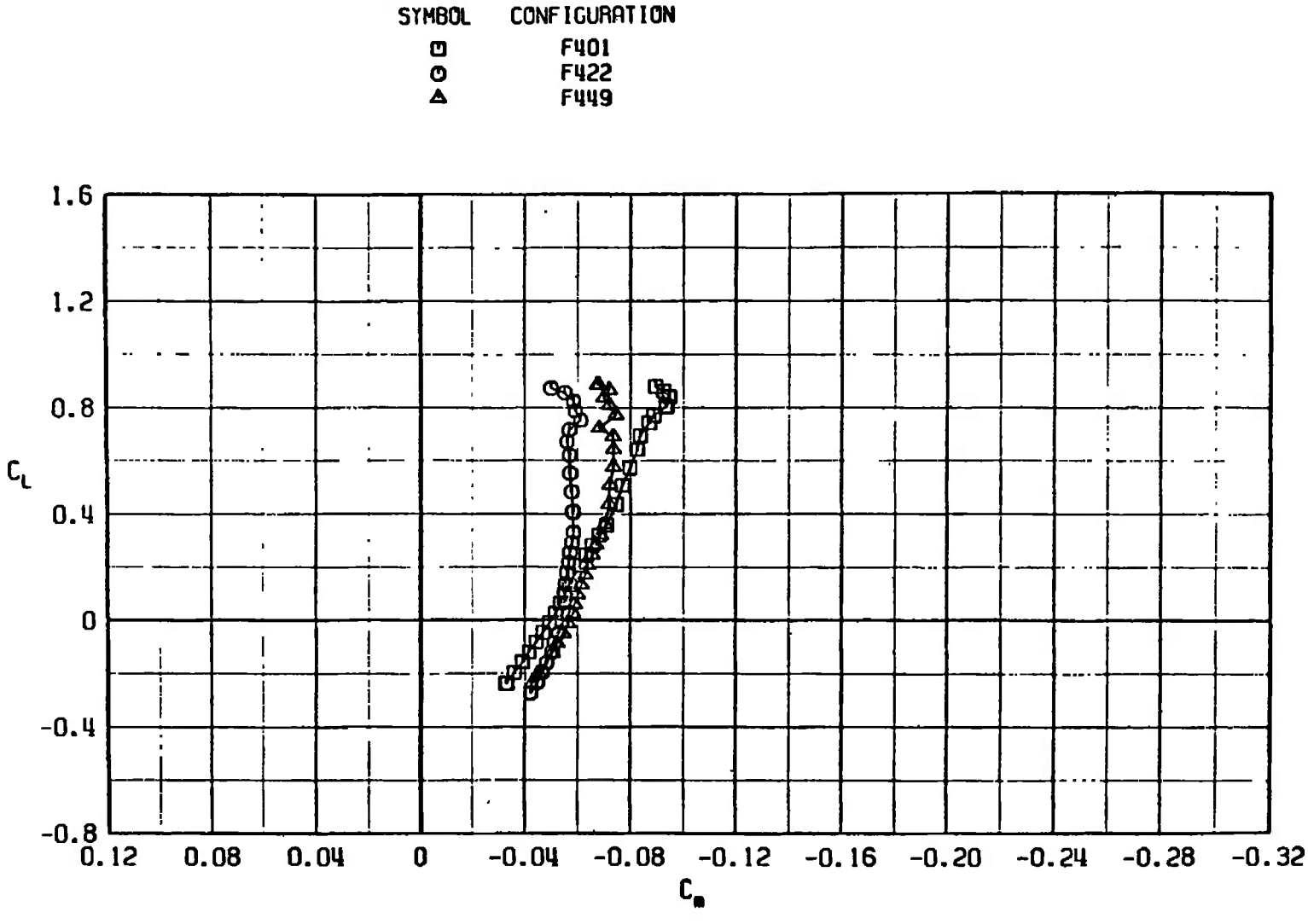

b. $M_\infty = 0.85$

Fig. 26 Continued

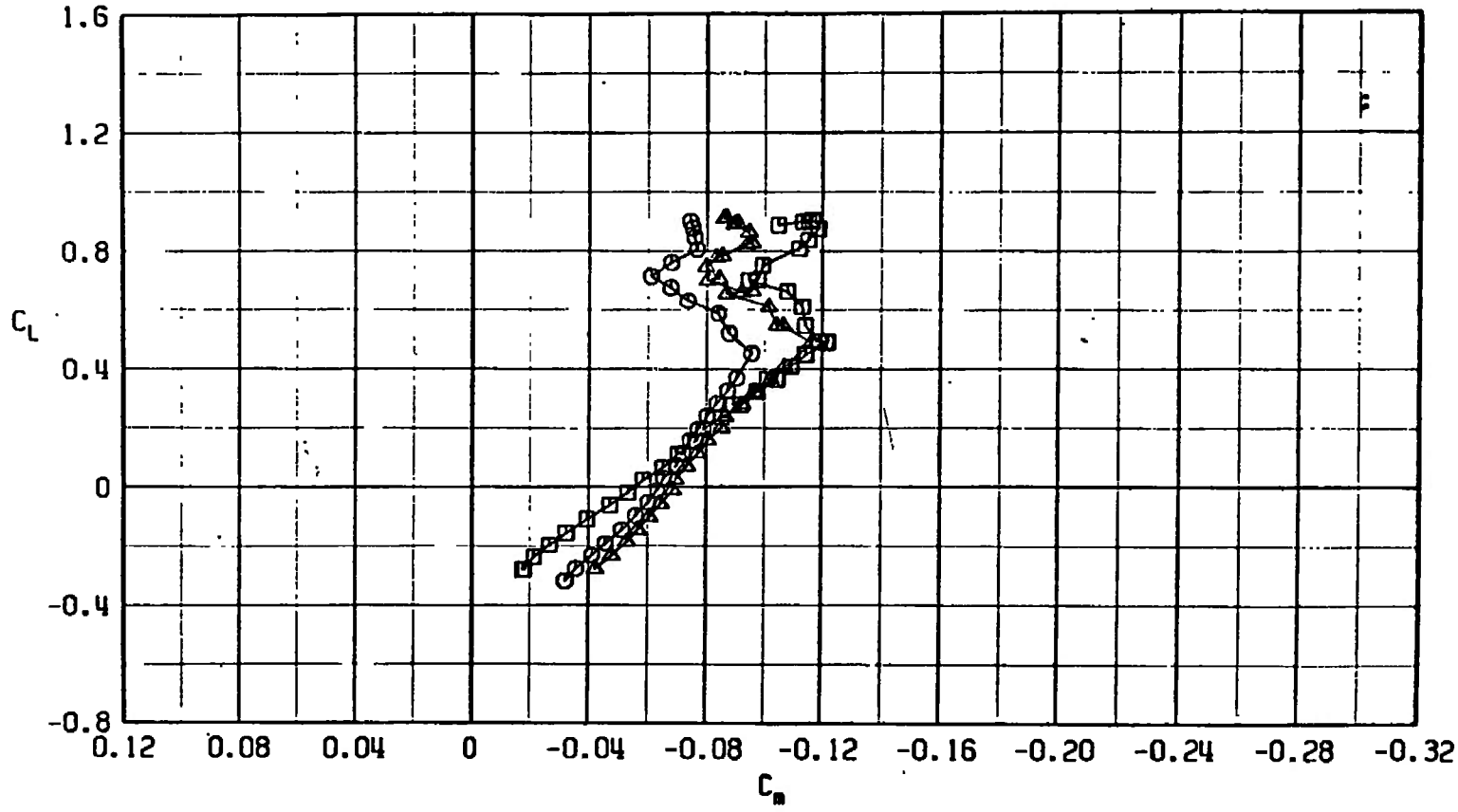

c. $M_\infty = 0.95$

Fig. 26 Continued

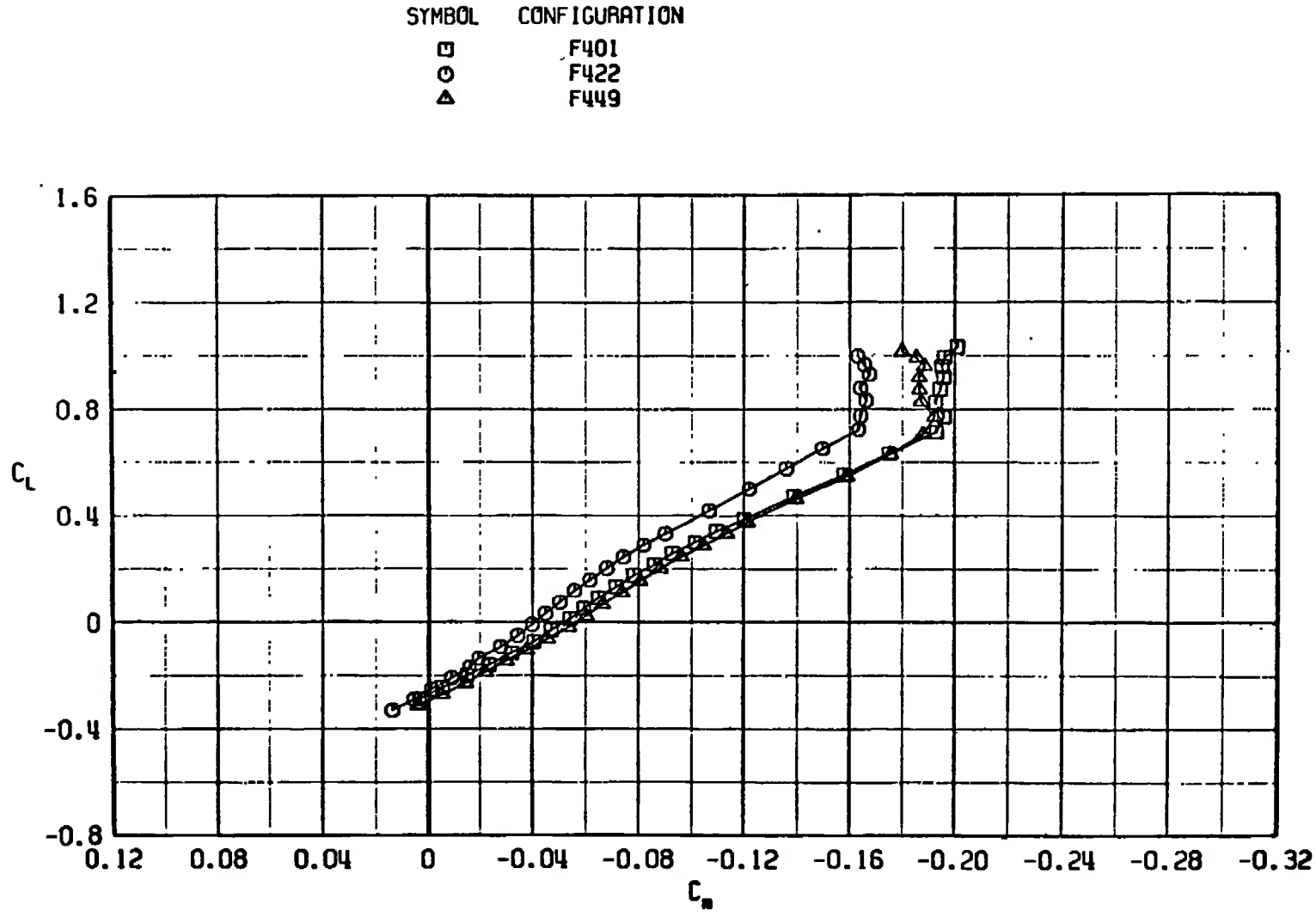

d. $M_\infty = 1.10$

Fig. 26 Continued

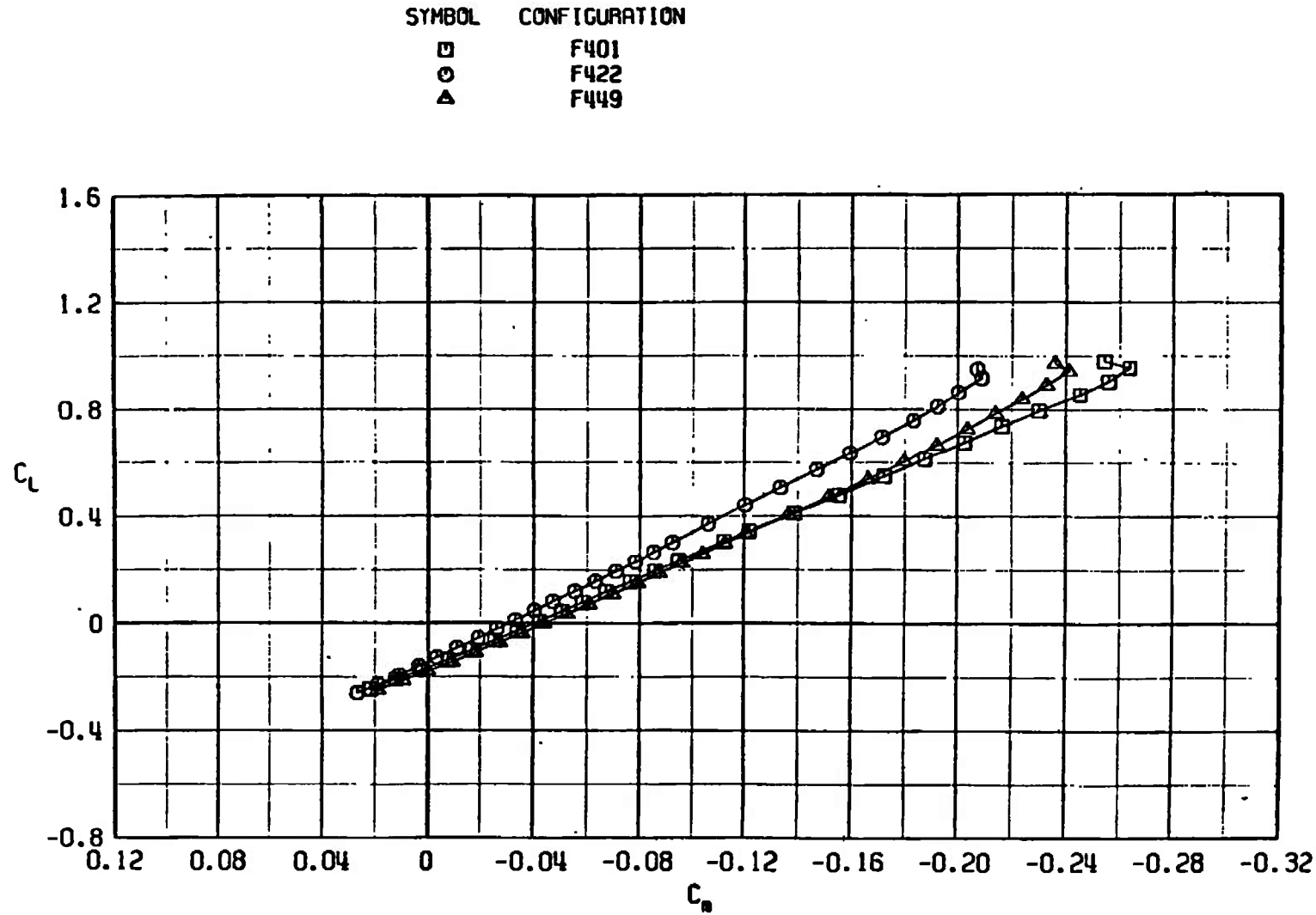

e. $M_\infty = 1.30$

Fig. 26 Concluded

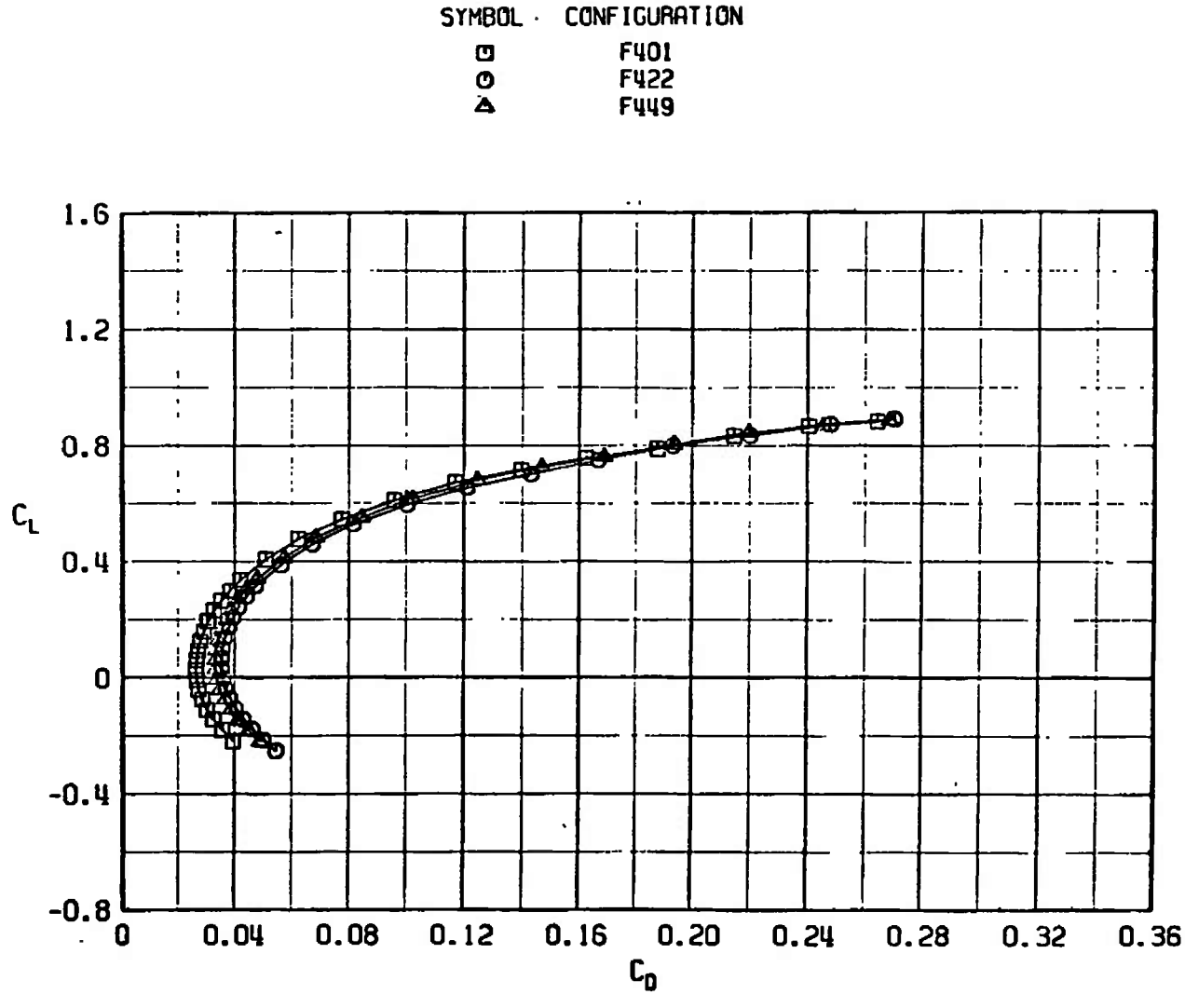

a. $M_\infty = 0.75$

Fig. 27 Drag Coefficient Variation with Lift Coefficient for Configurations F401, F422, and F449

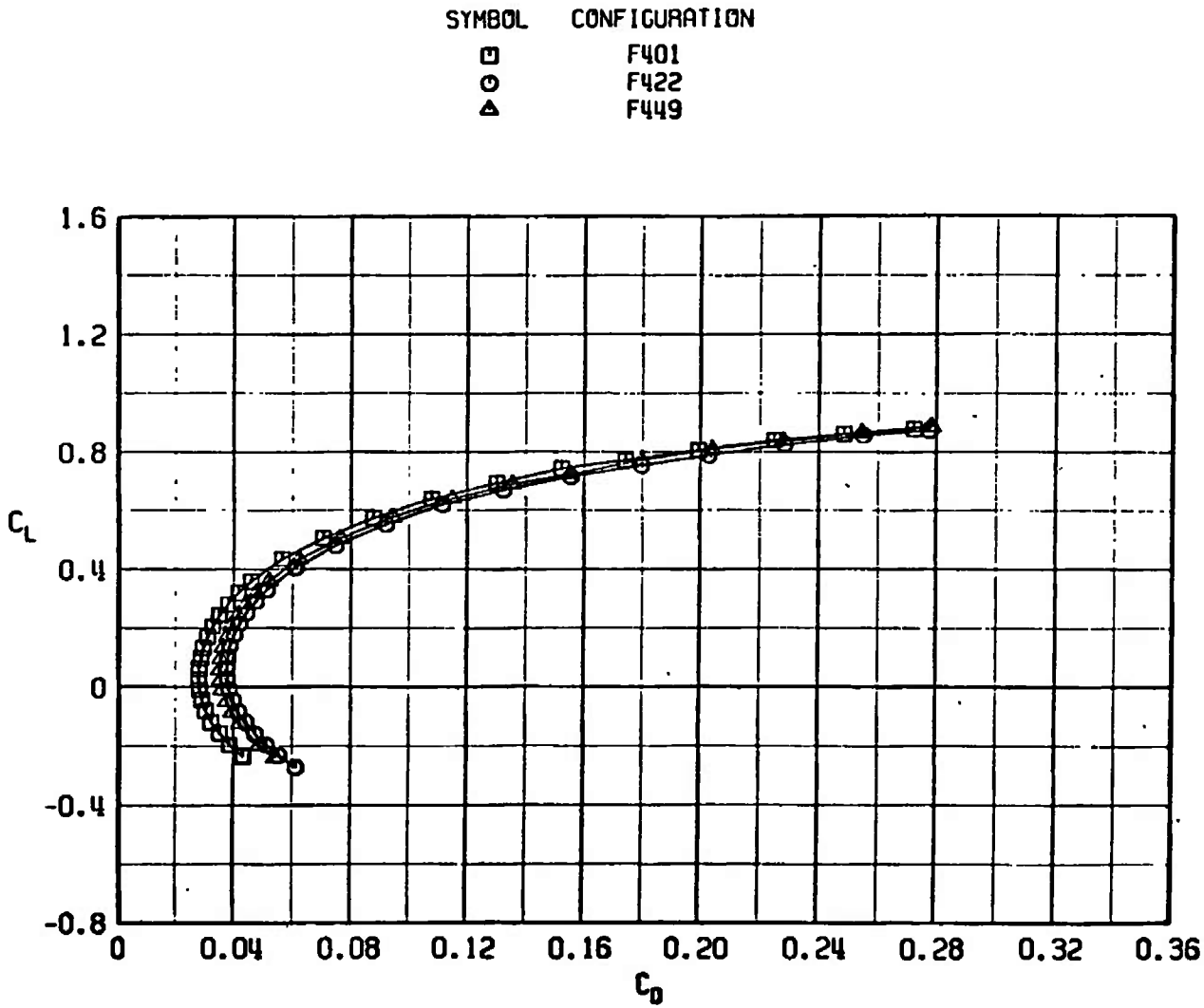

b. $M_\infty = 0.85$

Fig. 27 Continued

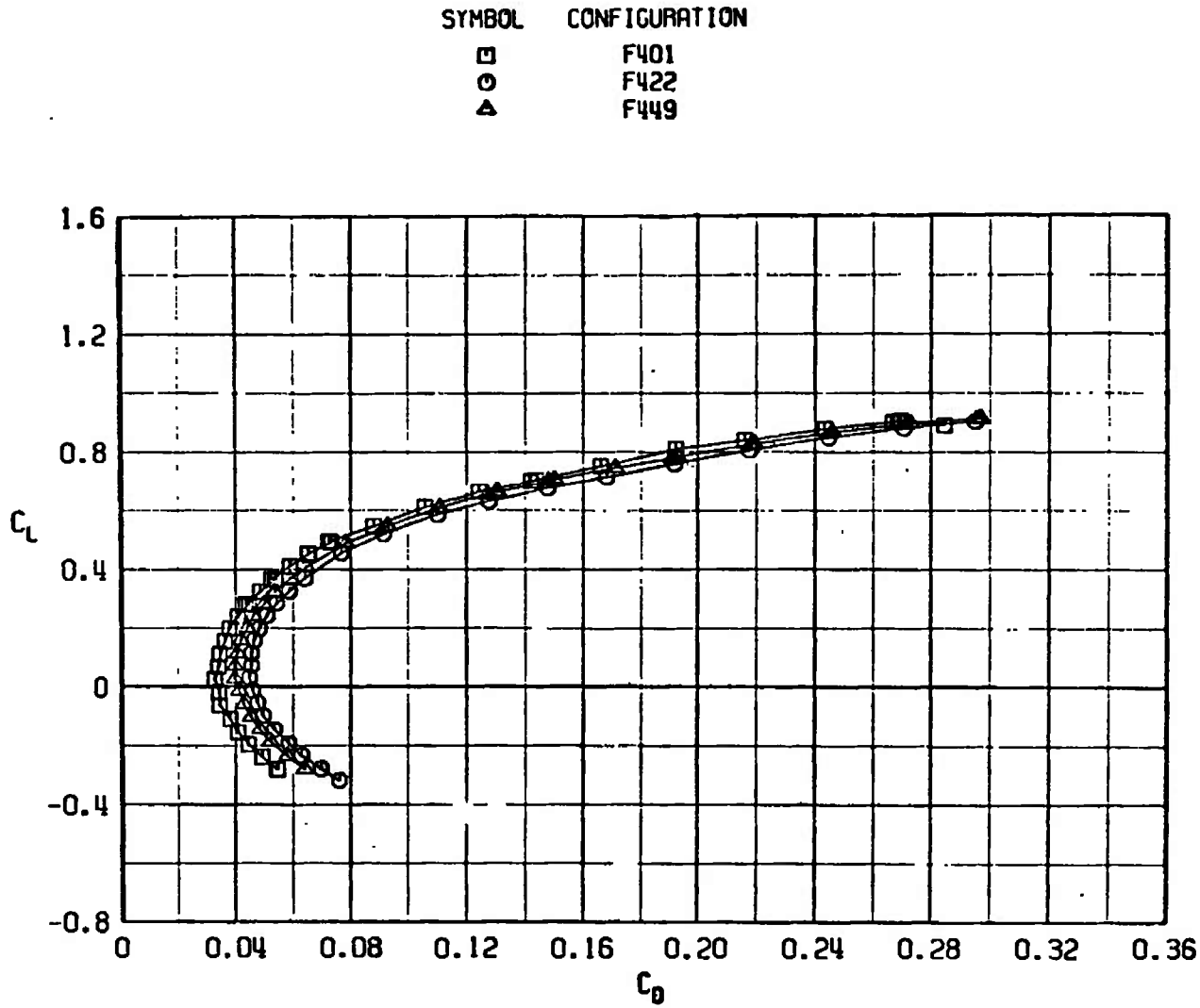

c. $M_\infty = 0.95$

Fig. 27 Continued

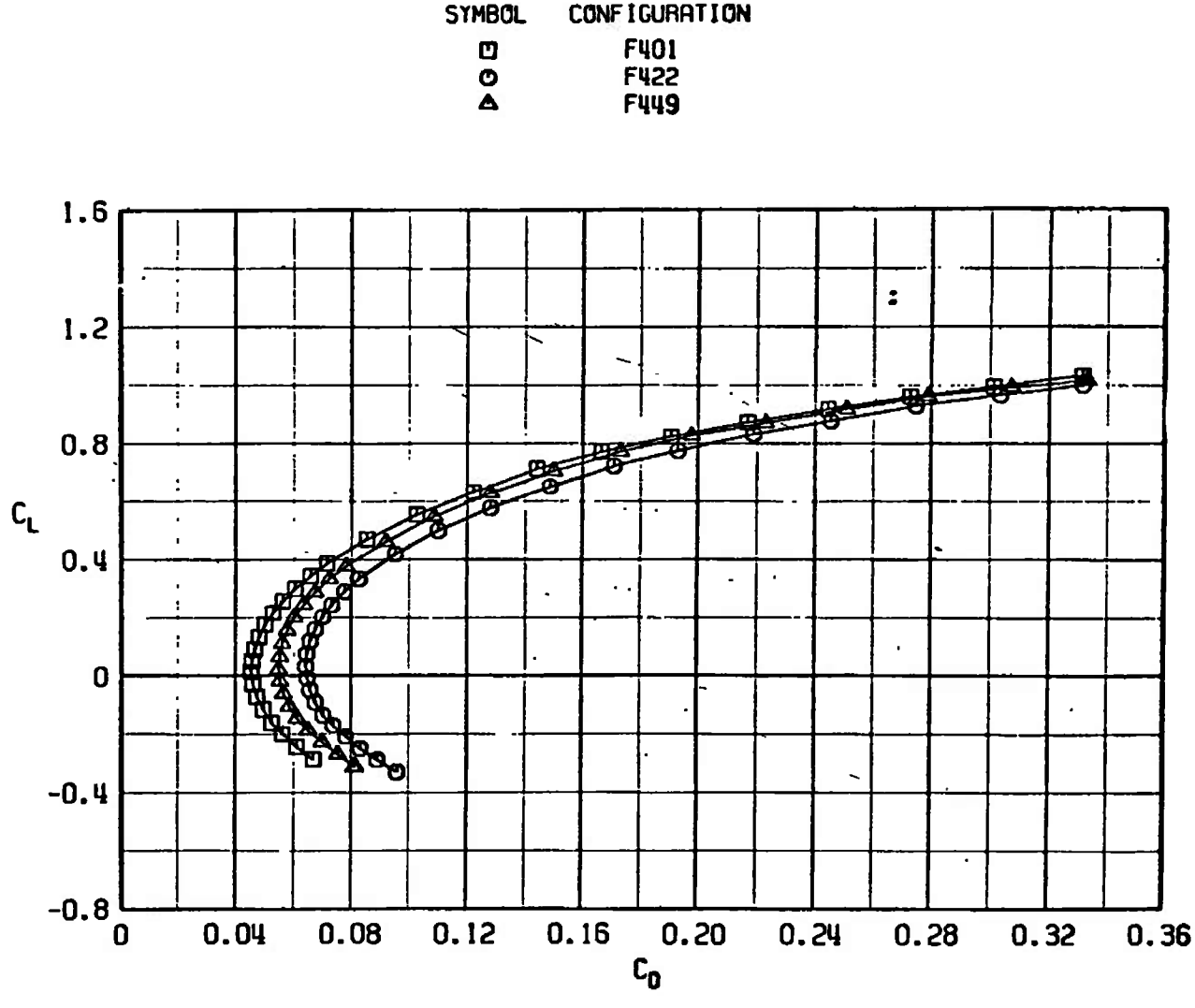

d. $M_\infty = 1.10$

Fig. 28 Continued

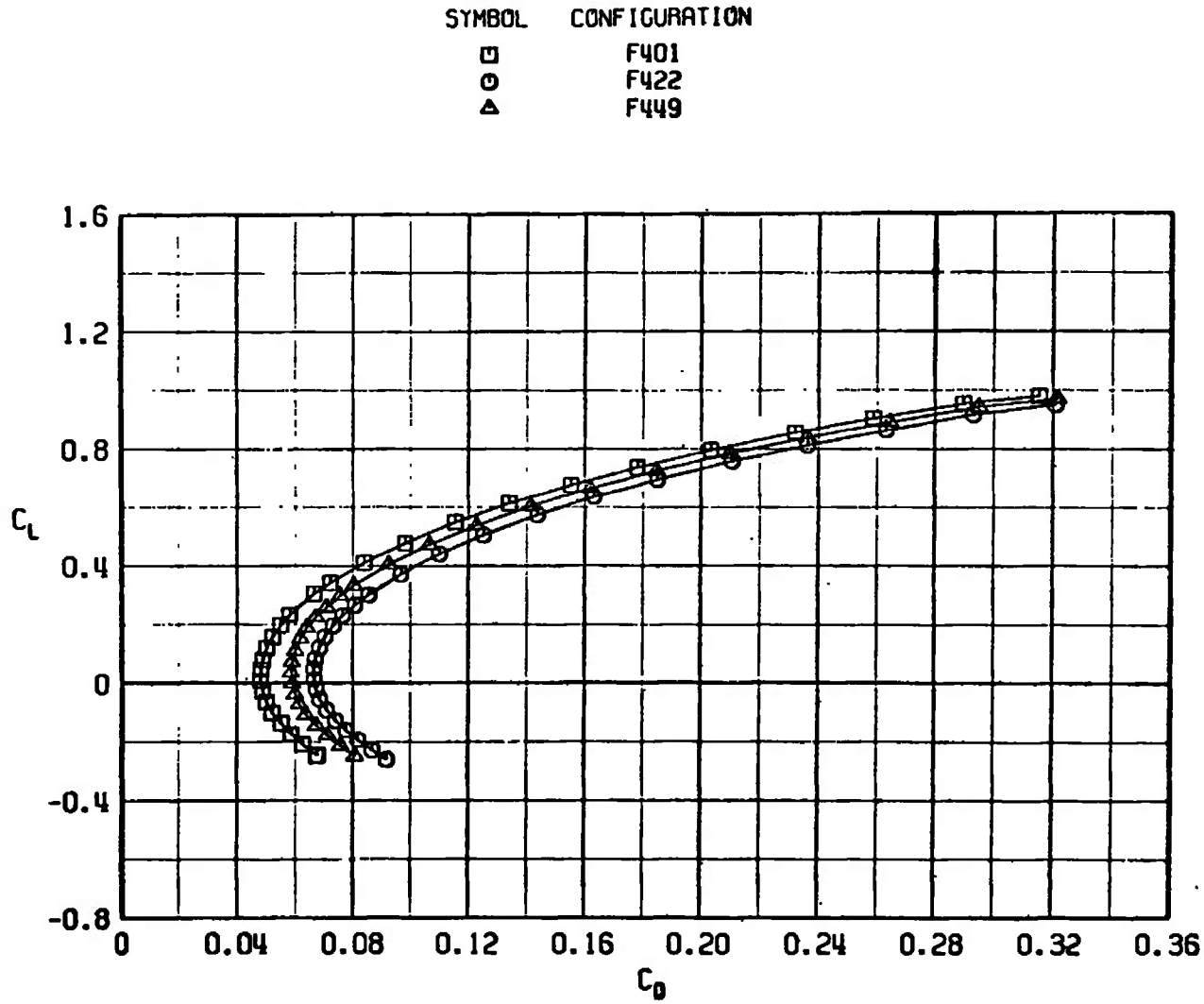

e. $M_\infty = 1.30$

Fig. 27 Concluded

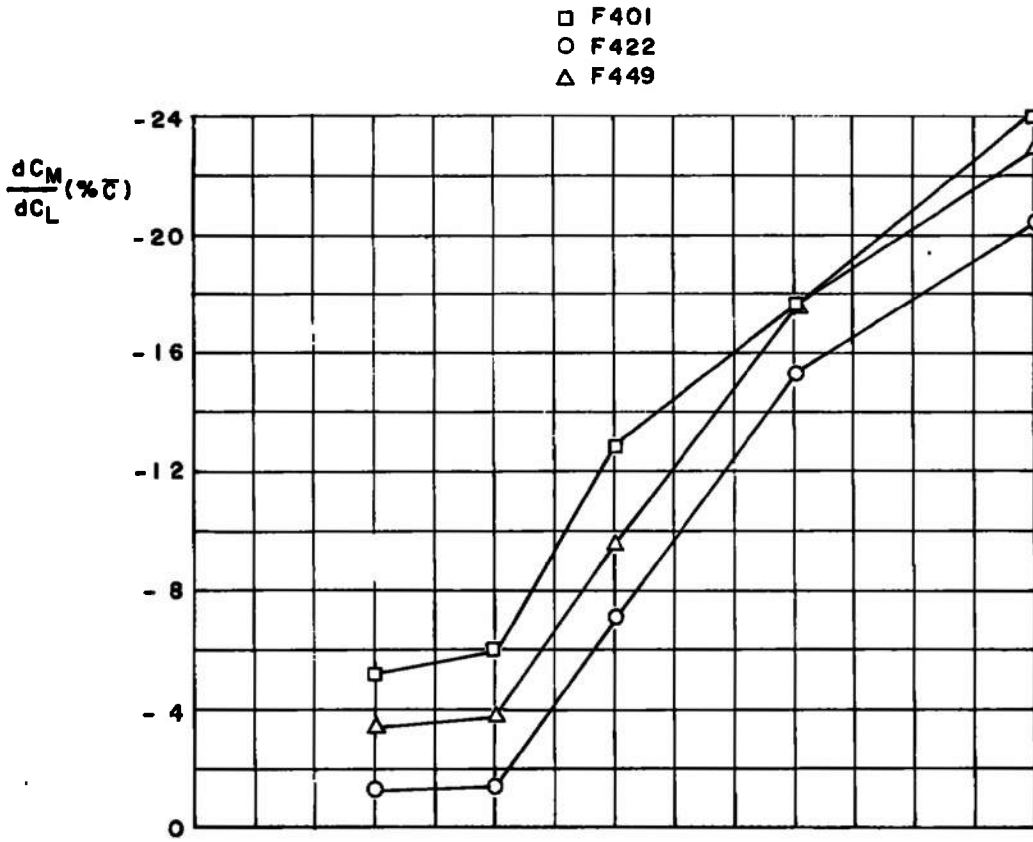

a. dC_m/dC_L versus M_∞ at $C_L = 0.20$ in percentage $\bar{c}$

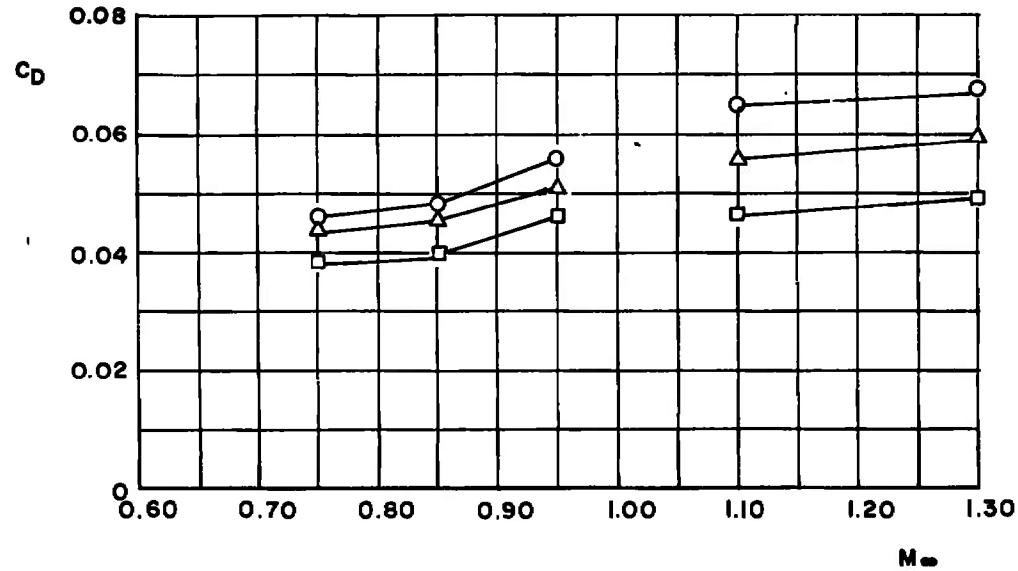

b. C_D versus M_∞ at $C_L = 0.30$, $M_\infty < 1.0$, and $C_L = 0.10$, $M_\infty > 1.0$

Fig. 28 Drag Coefficient and dC_m/dC_L Variation with Mach Number for Configurations F401, F422, and F449

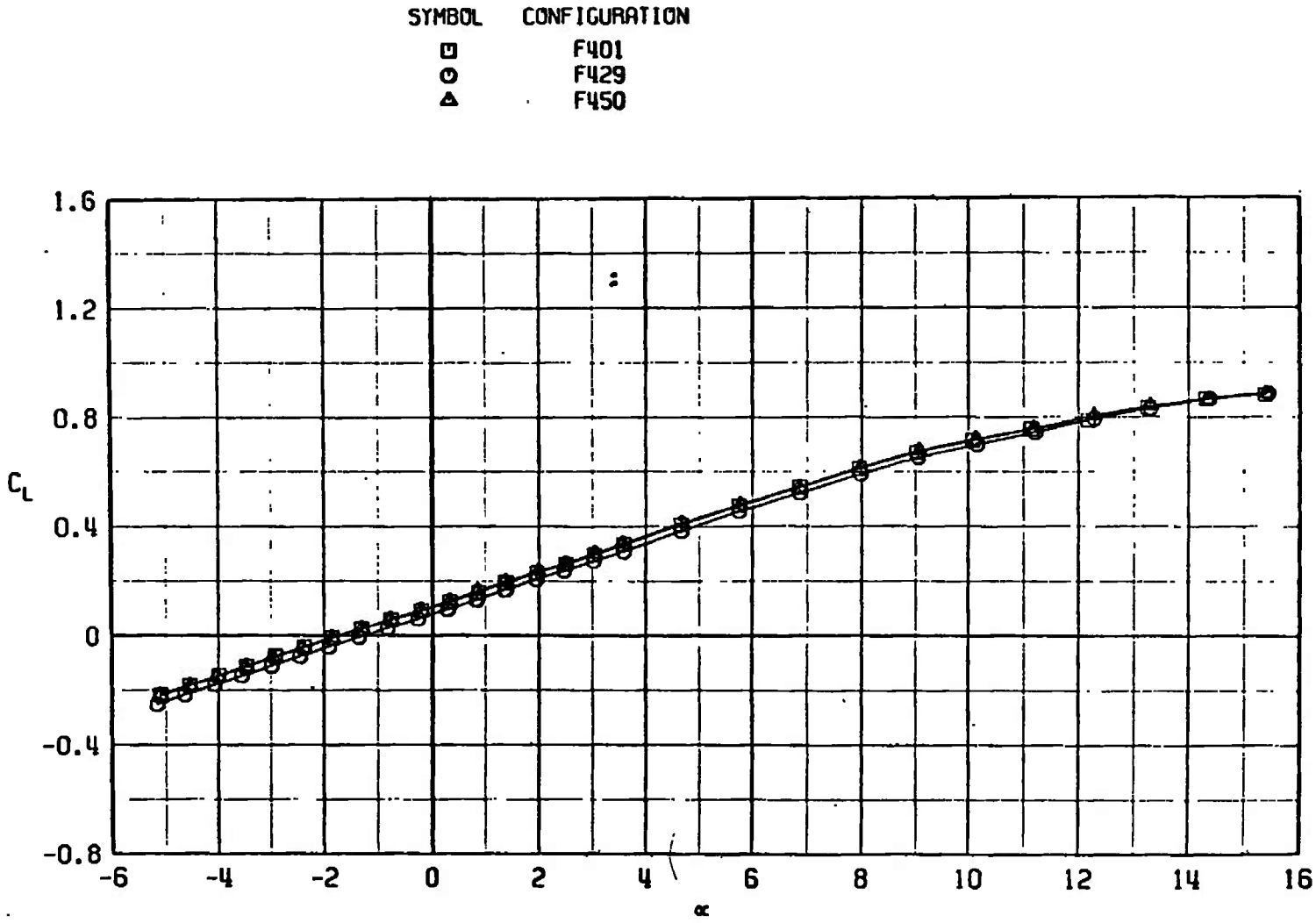

a. $M_\infty = 0.75$

Fig. 29 Lift Coefficient Variation with Angle of Attack for Configurations F401, F429, and F450

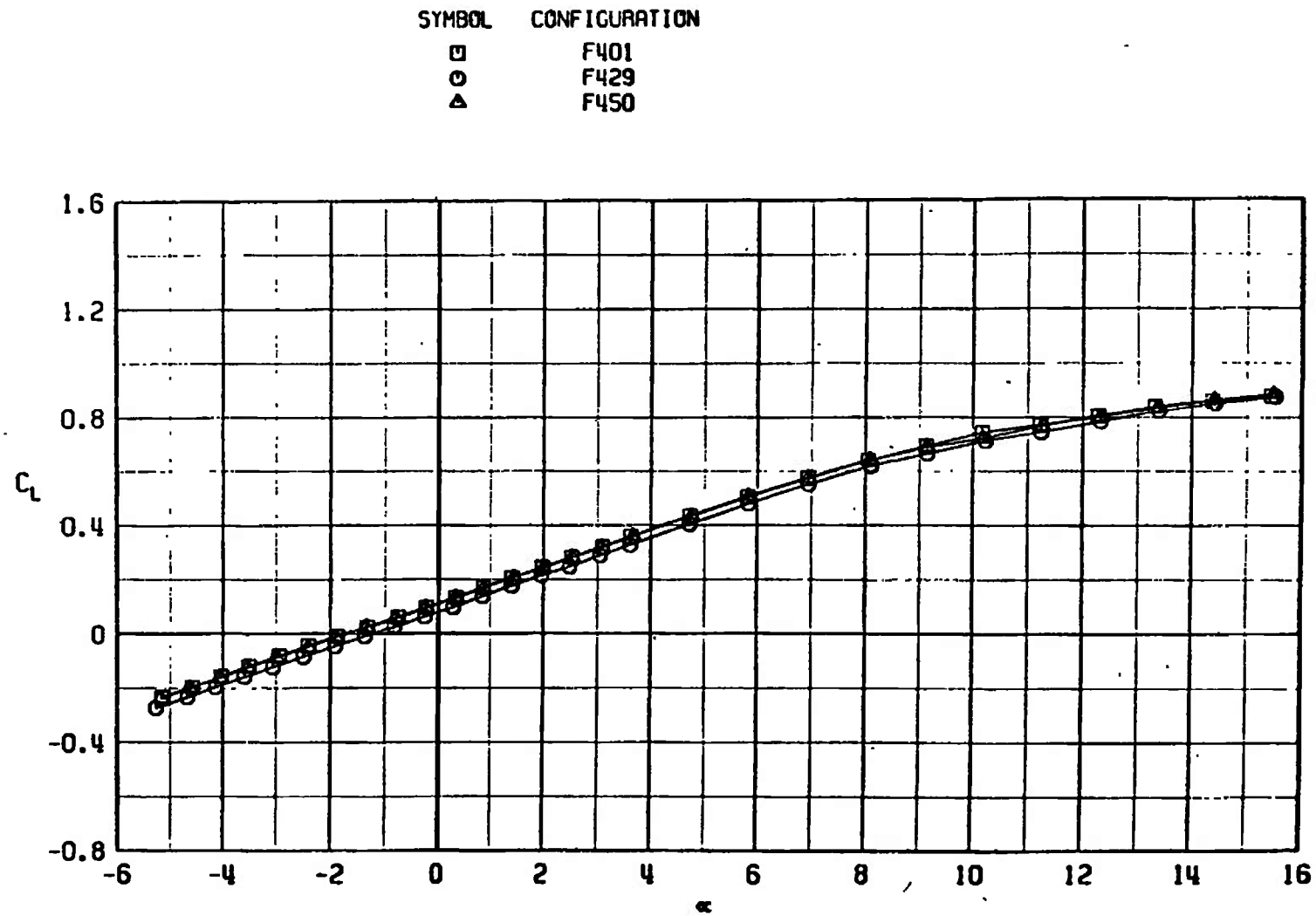

b. $M_\infty = 0.85$

Fig. 29 Continued

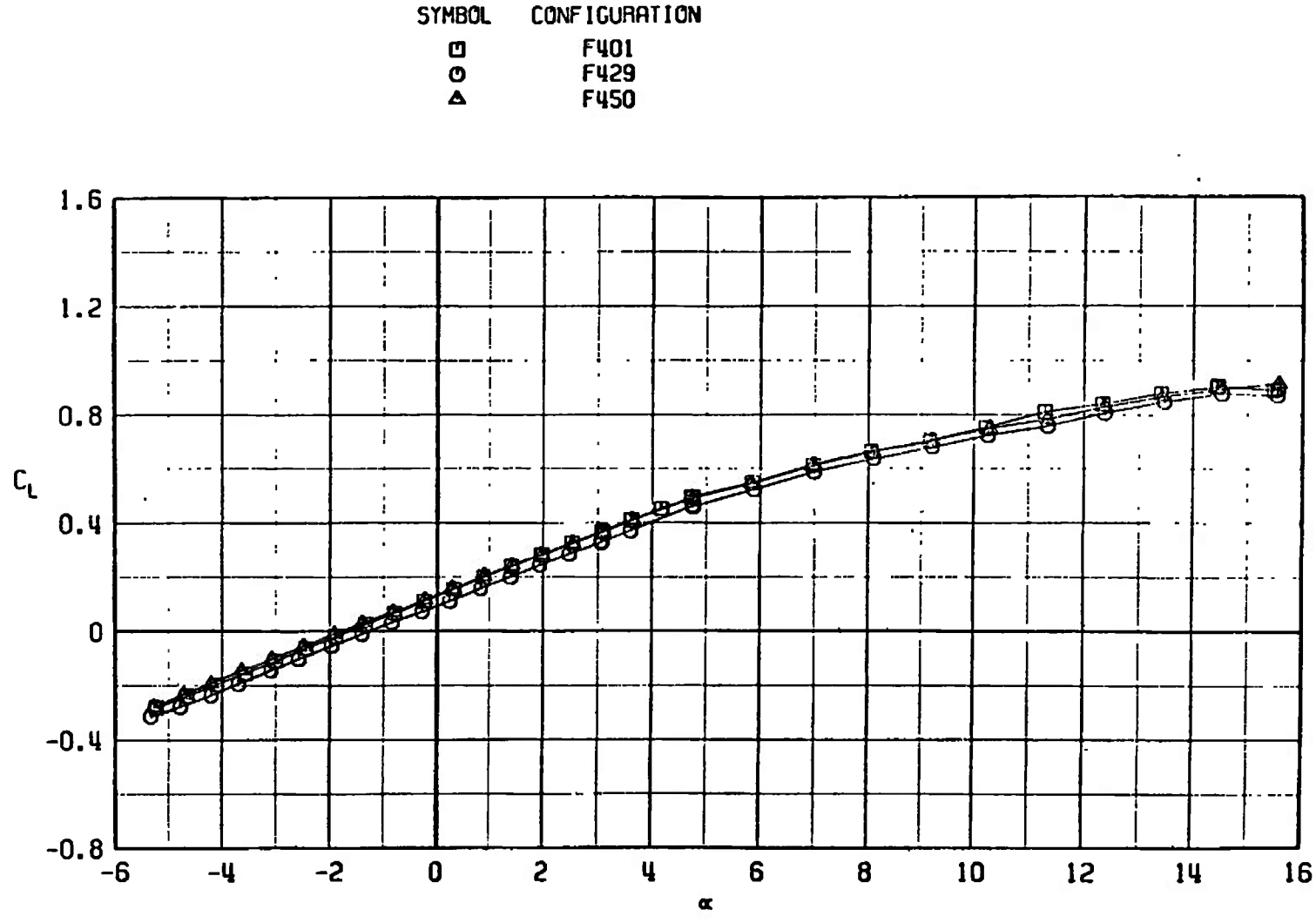

c. $M_\infty = 0.95$

Fig. 29 Continued

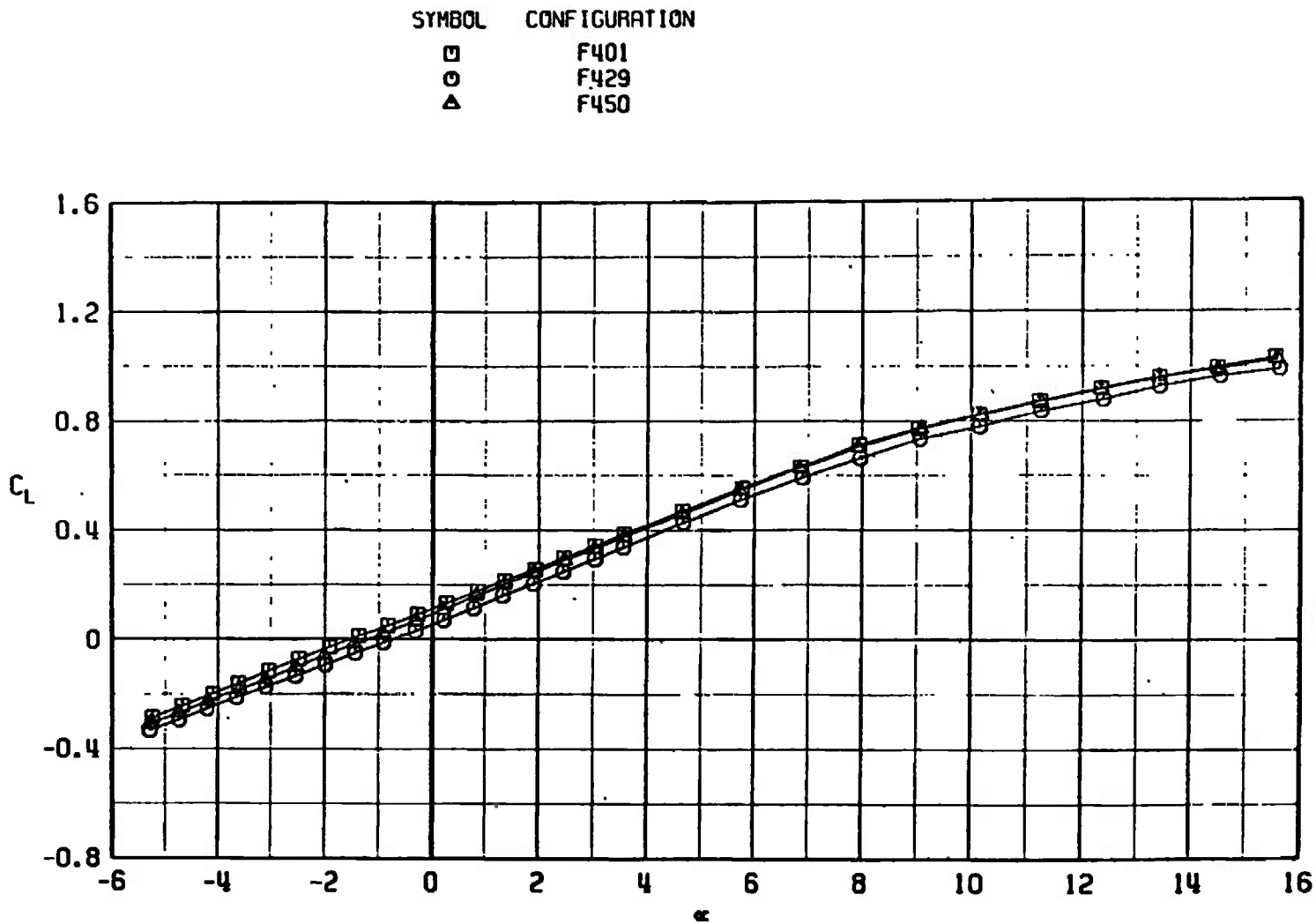

d. $M_\infty = 1.10$

Fig. 29 Continued

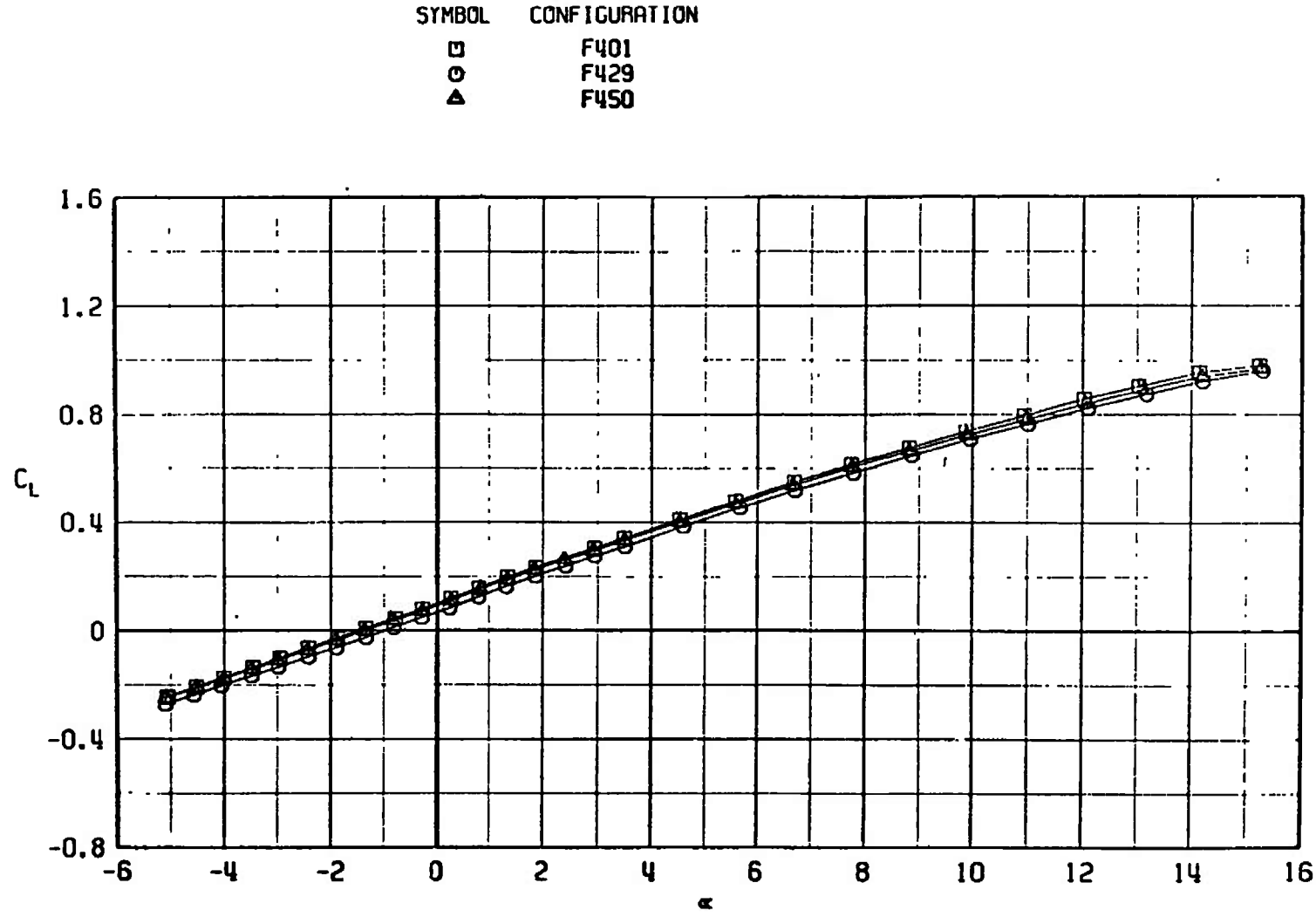

e. $M_\infty = 1.30$

Fig. 29 Concluded

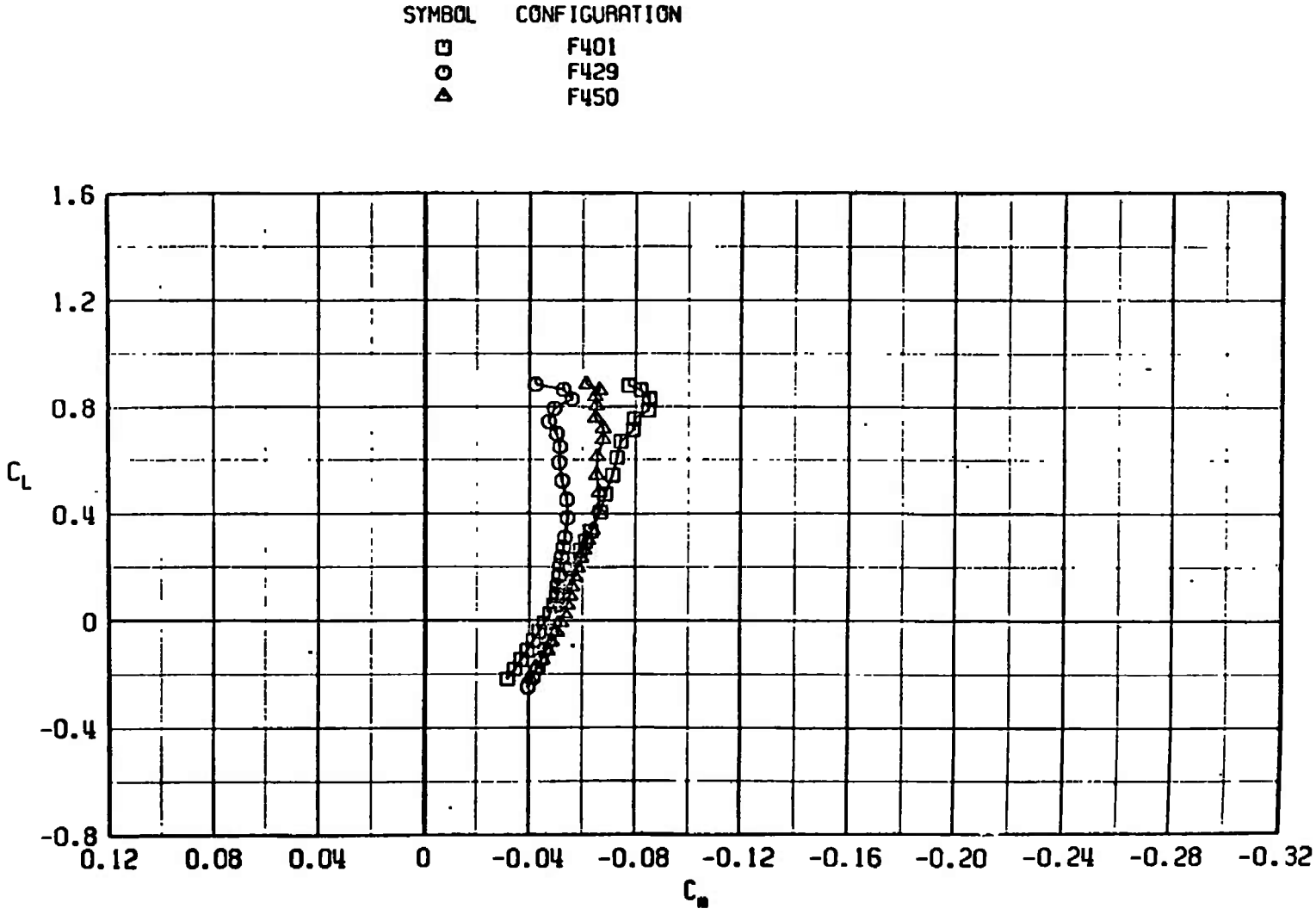

a. $M_\infty = 0.75$

Fig. 30 Pitching-Moment Coefficient Variation with Lift Coefficient for Configurations F401, F429, and F450

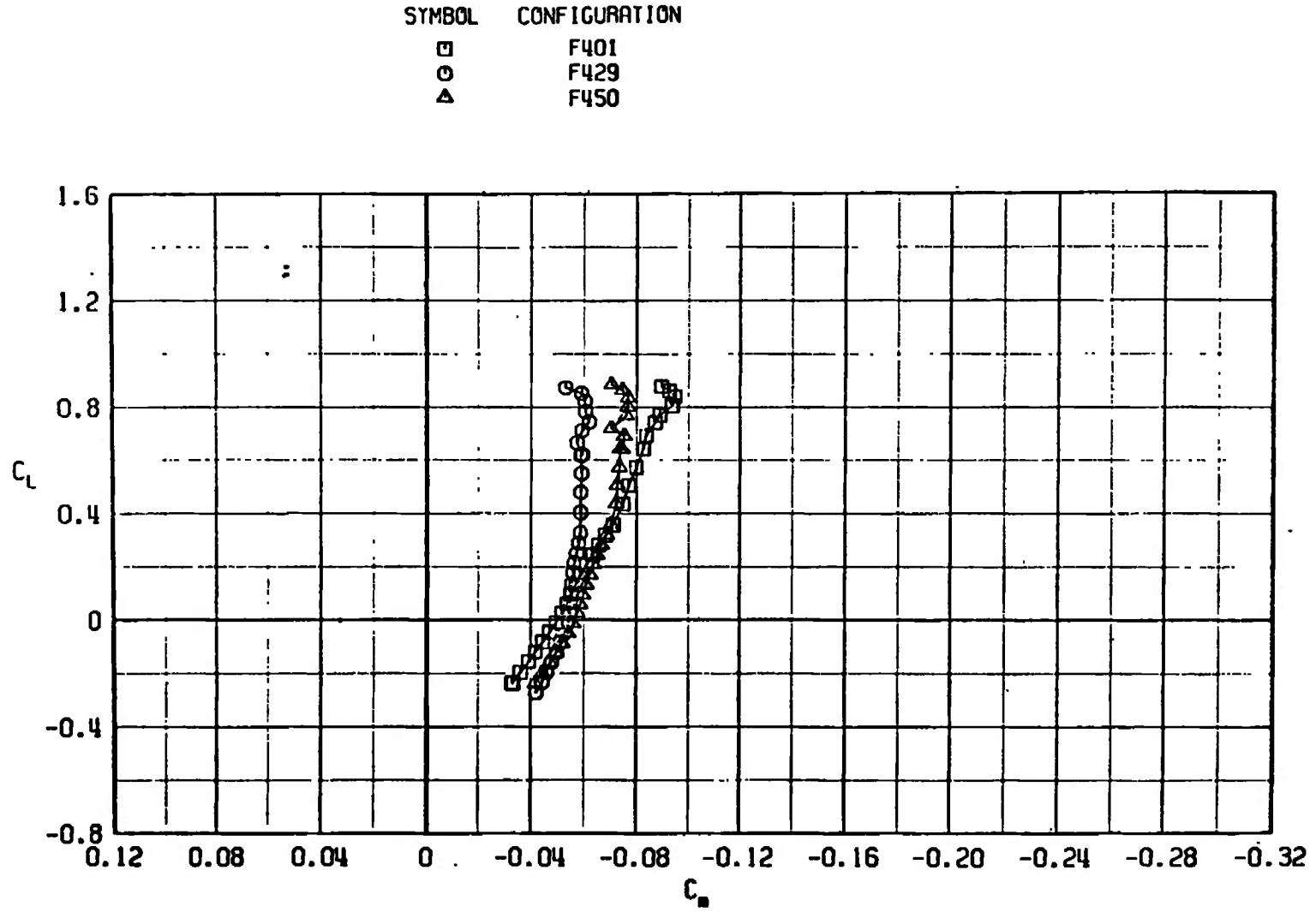

b. $M_\infty = 0.85$

Fig. 30 Continued

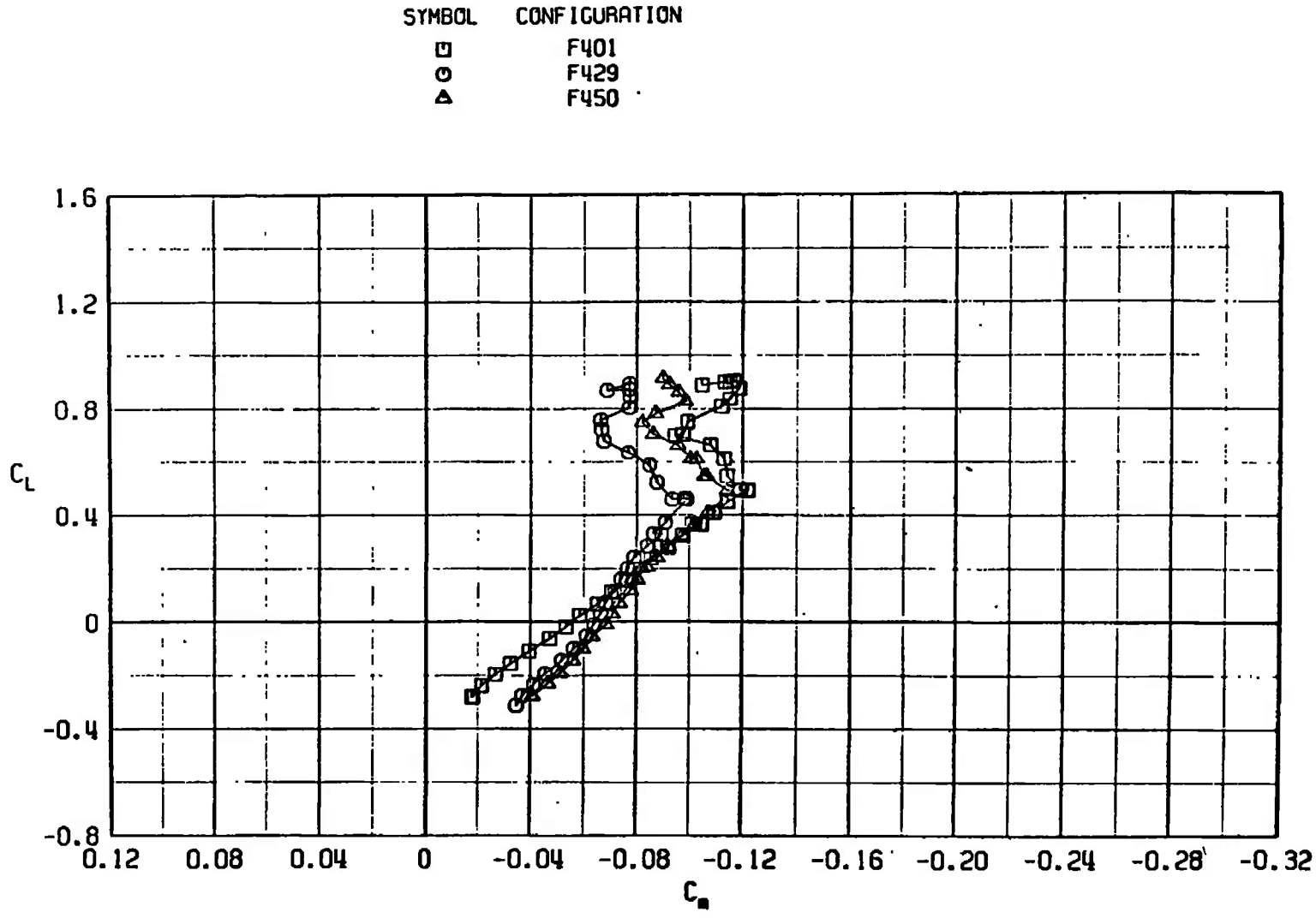

c. $M_\infty = 0.95$

Fig. 30 Continued

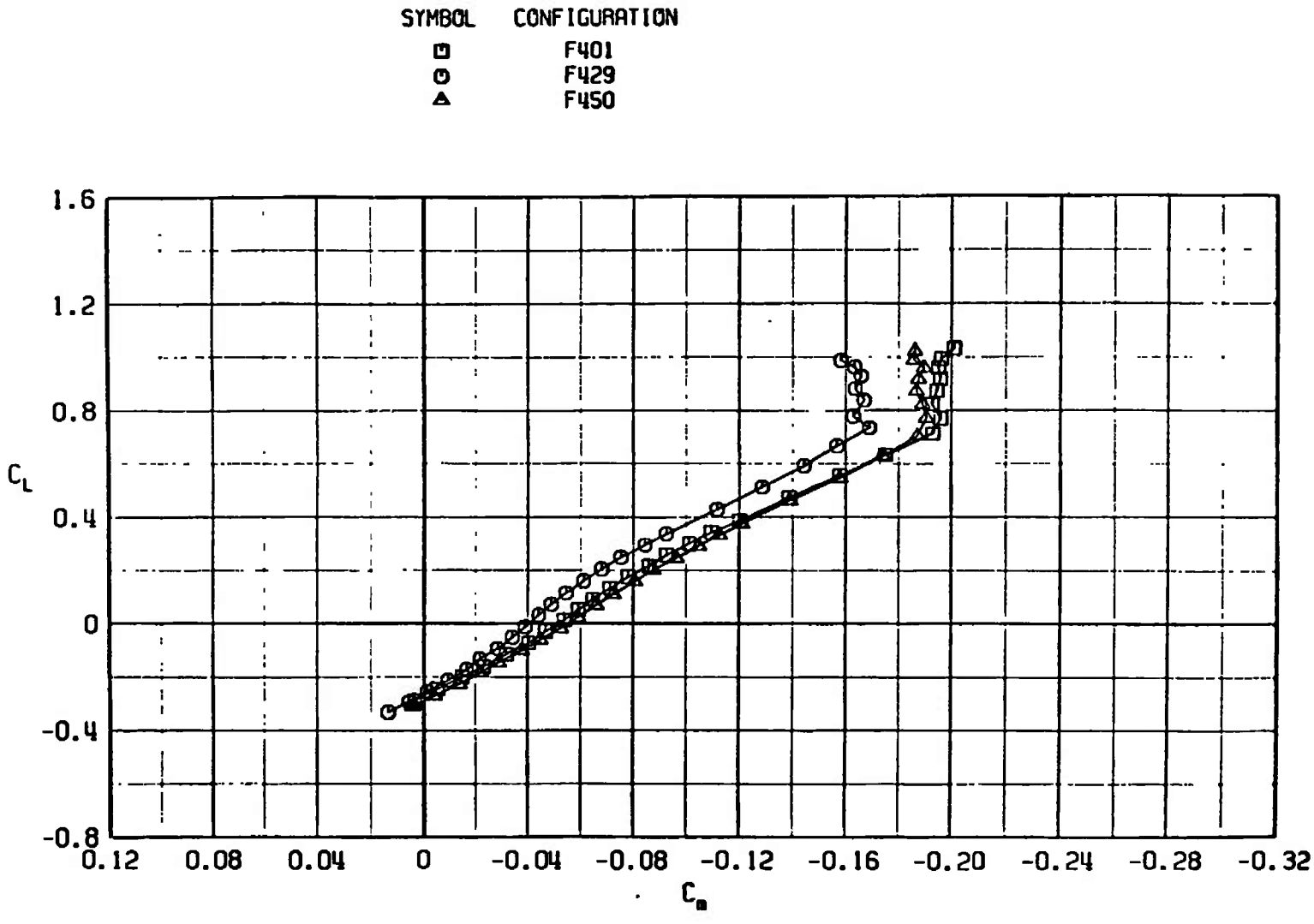

d. $M_\infty = 1.10$

Fig. 30 Continued

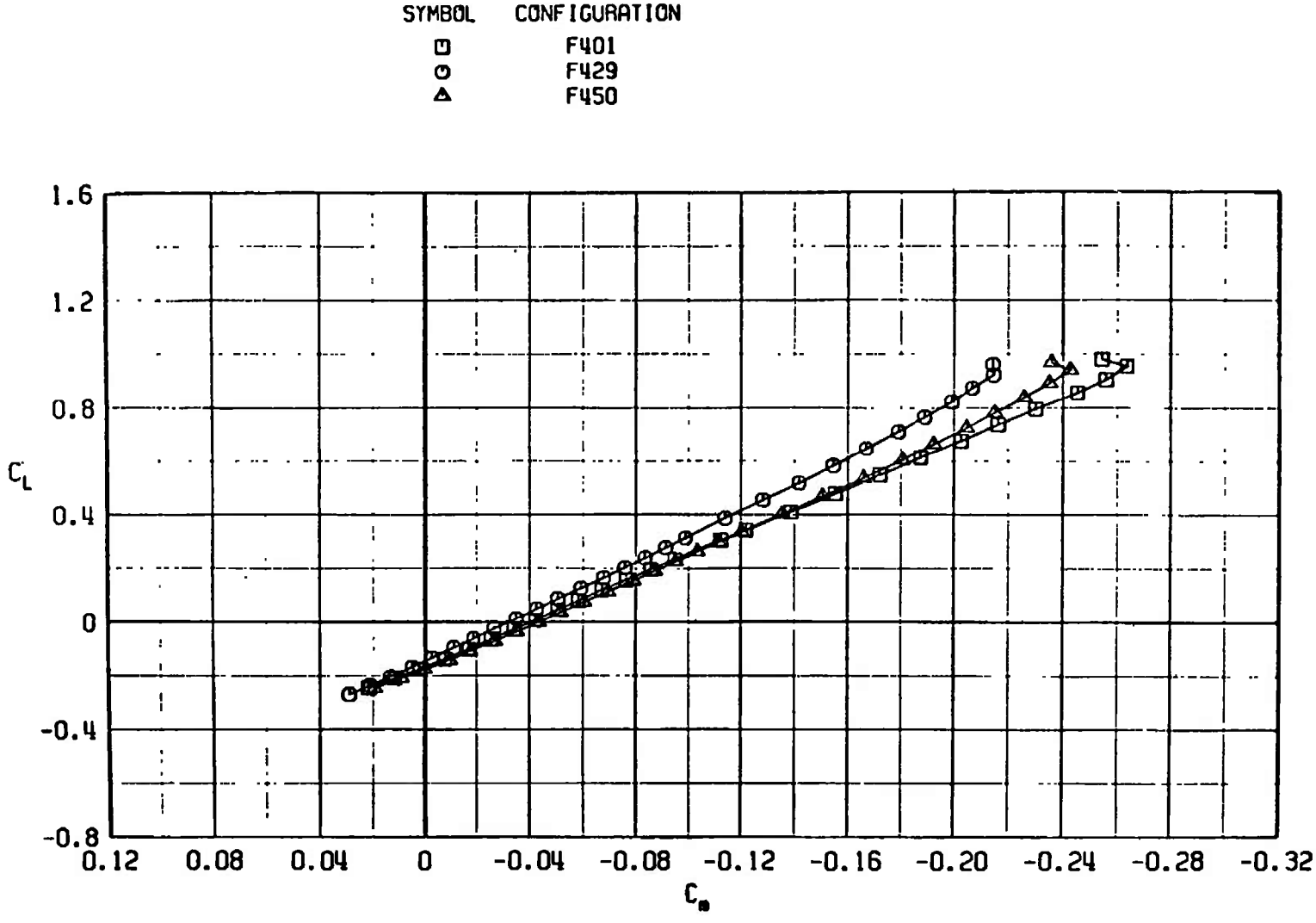

e. $M_\infty = 1.30$

Fig. 30 Concluded

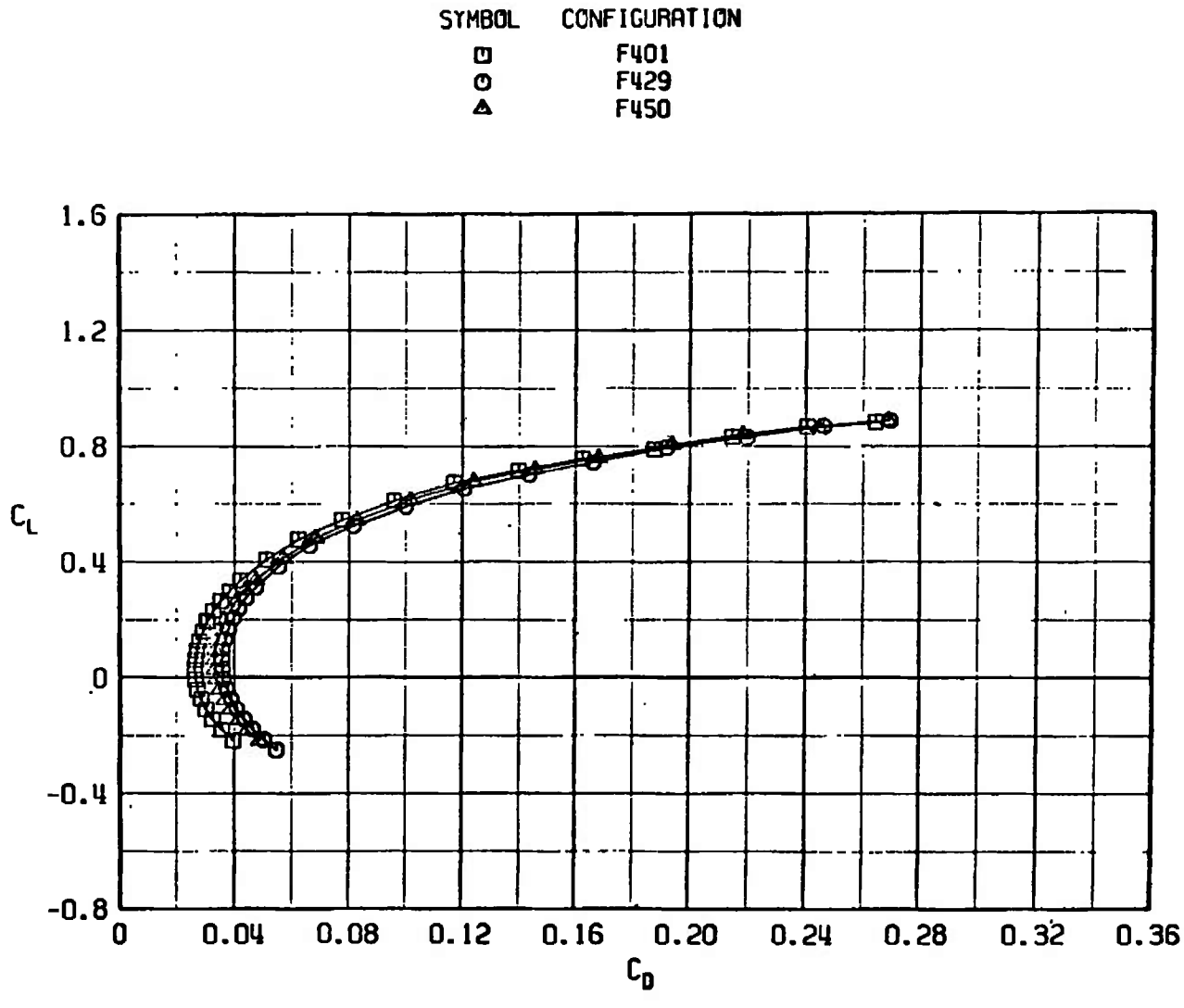

a. $M_\infty = 0.75$

Fig. 31 Drag Coefficient Variation with Lift Coefficient for Configurations F401, F429, and F450

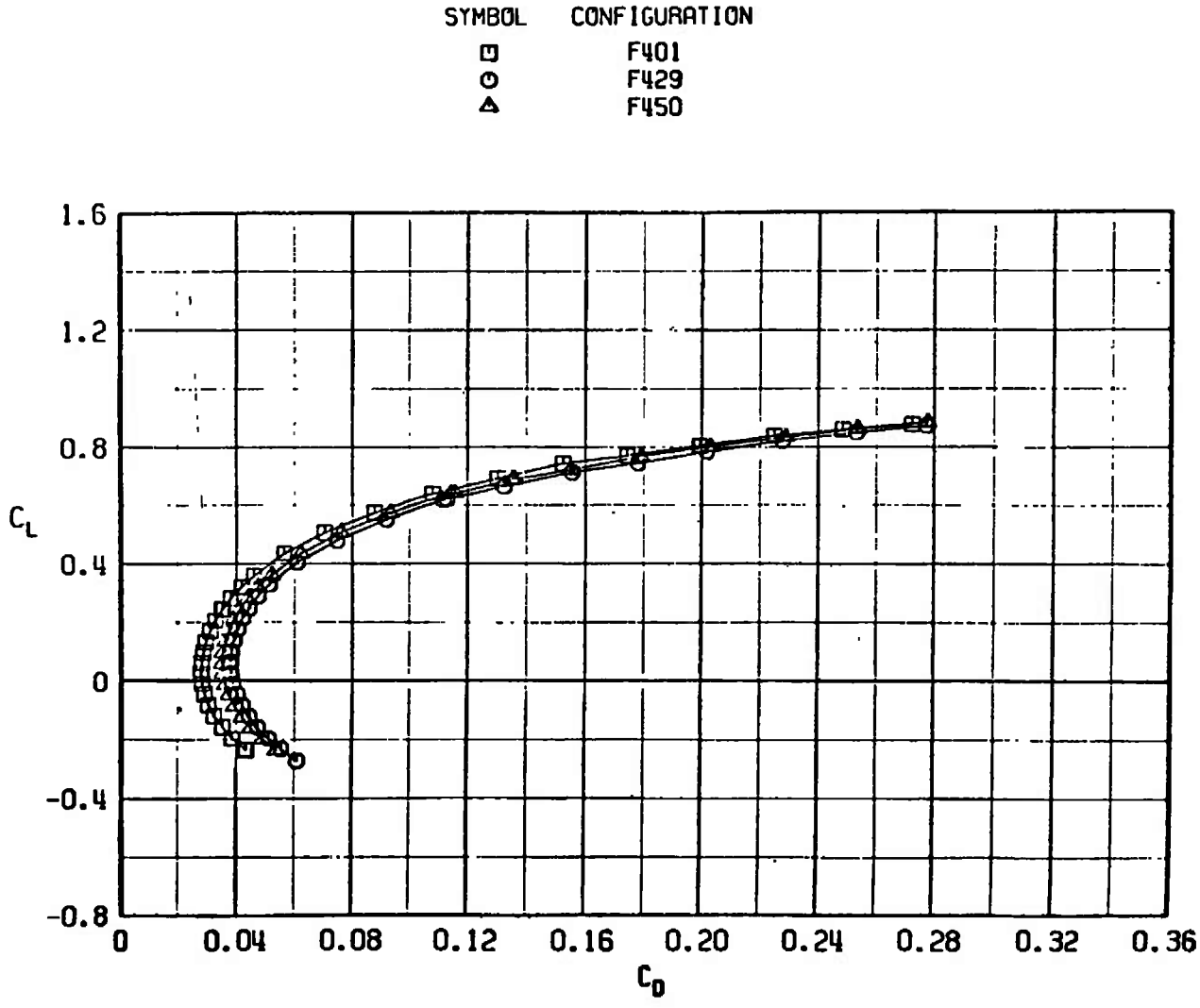

b. $M_\infty = 0.85$

Fig. 31 Continued

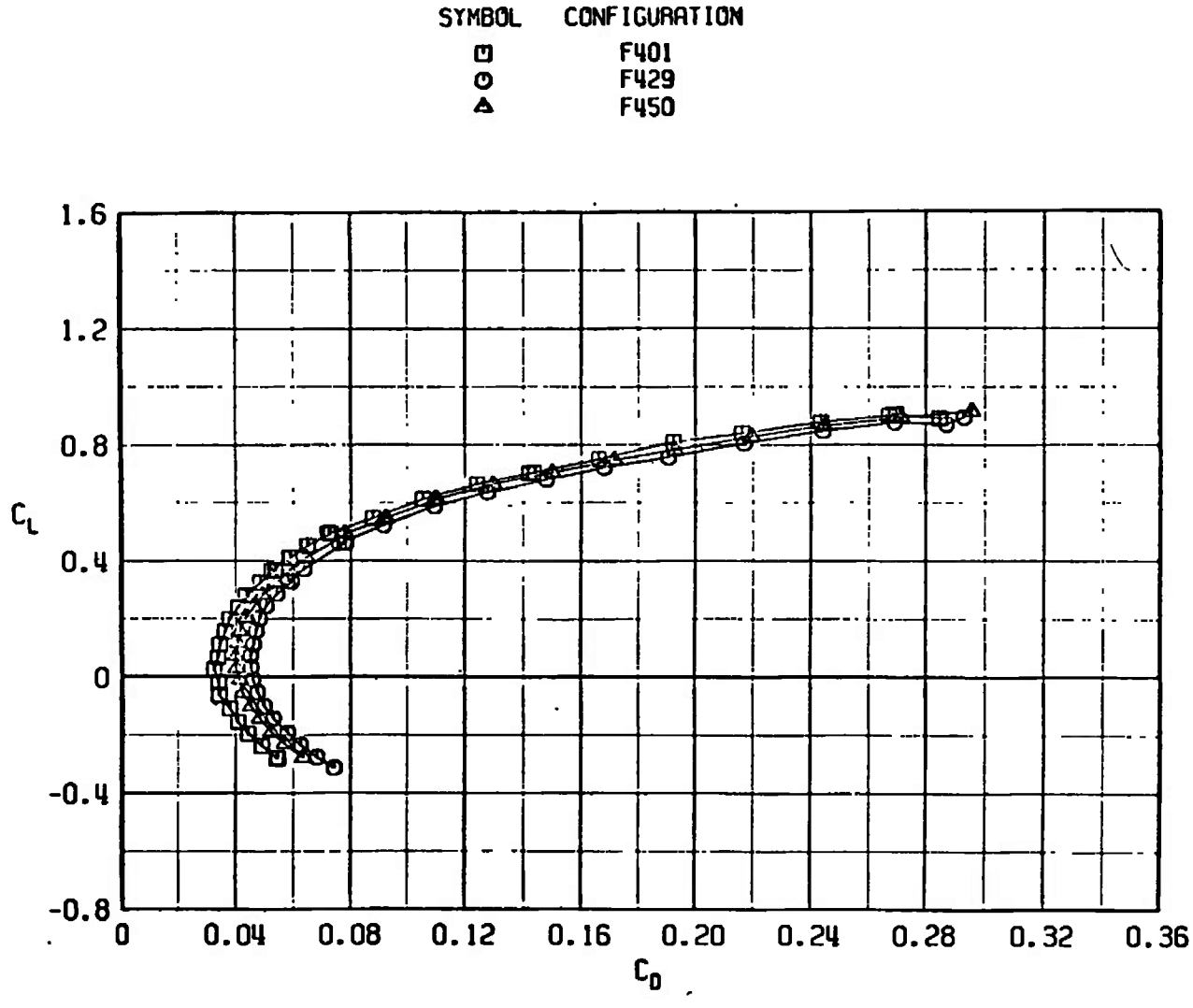

c. $M_\infty = 0.95$

Fig. 31 Continued

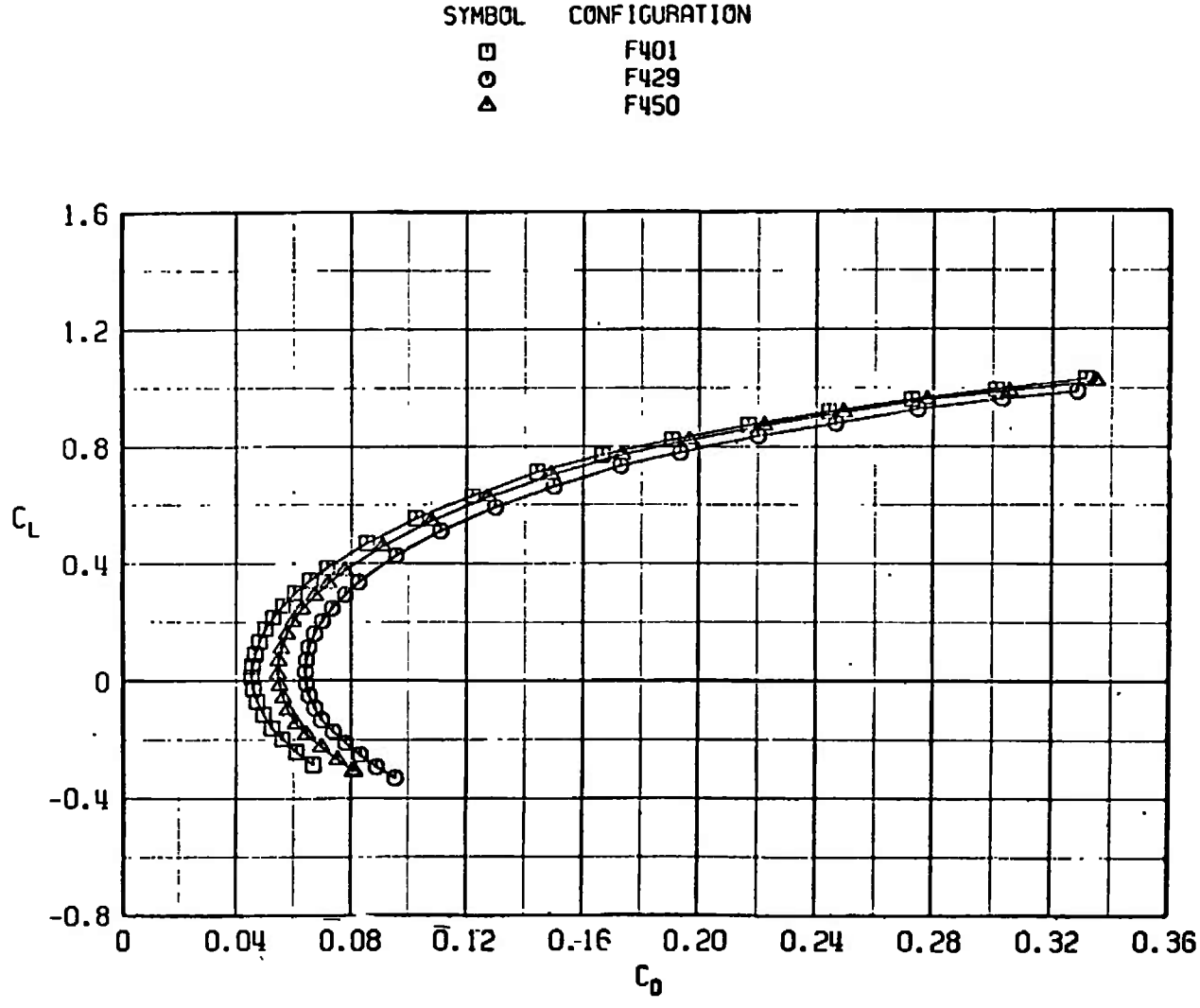

d. $M_\infty = 1.10$

Fig. 31 Continued

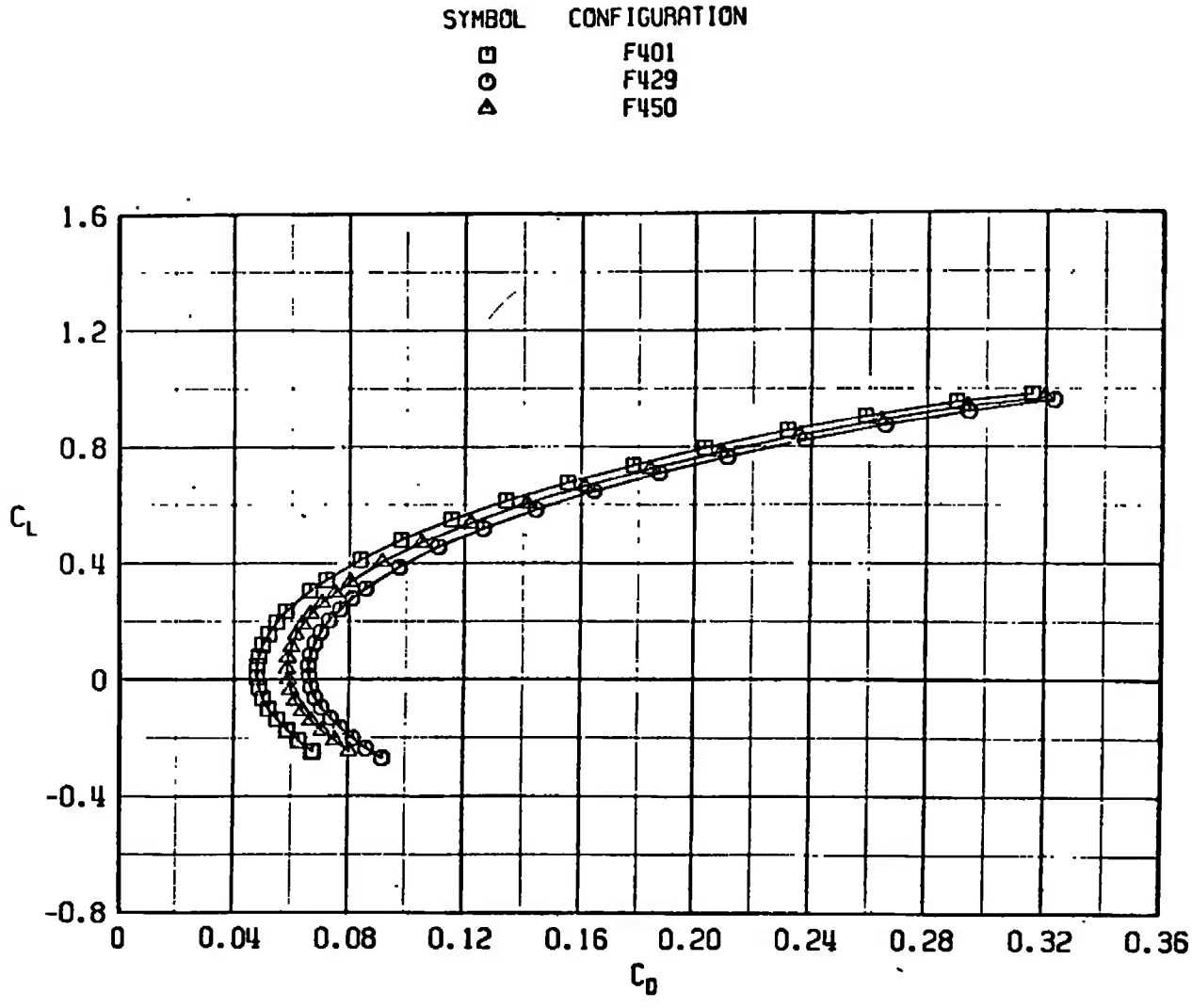

e. $M_\infty = 1.30$

Fig. 31 Concluded

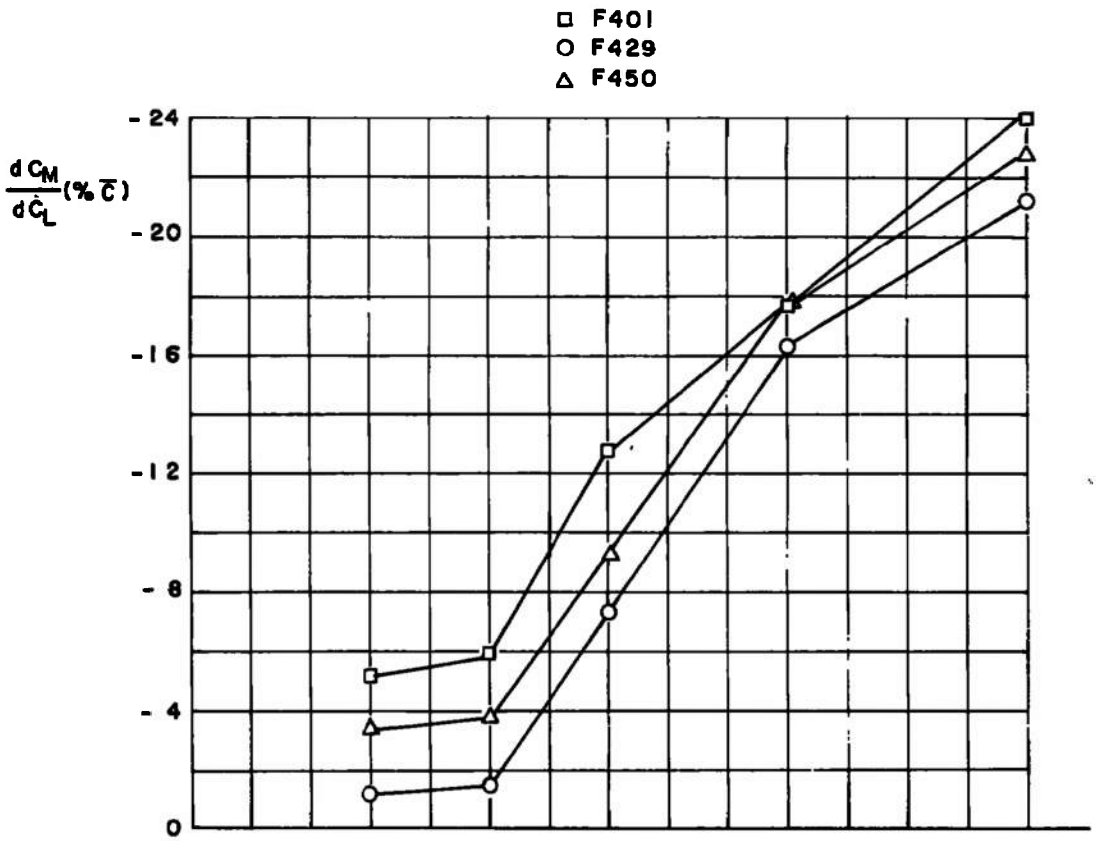

a. dC_m/dC_L versus M_∞ at $C_L = 0.20$ in percentage of $\bar{c}$

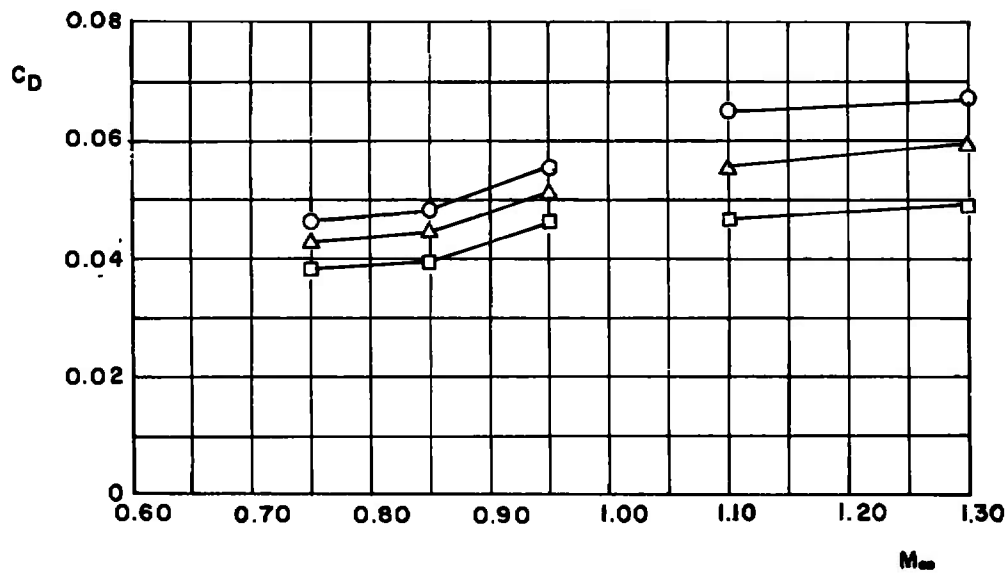

b. C_D versus M_∞ at $C_L = 0.30$, $M_\infty < 1.0$, and $C_L = 0.10$, $M_\infty > 1.0$

Fig. 32 Drag Coefficient and dC_m/dC_L Variation with Mach Number for Configurations F401, F429, and F450

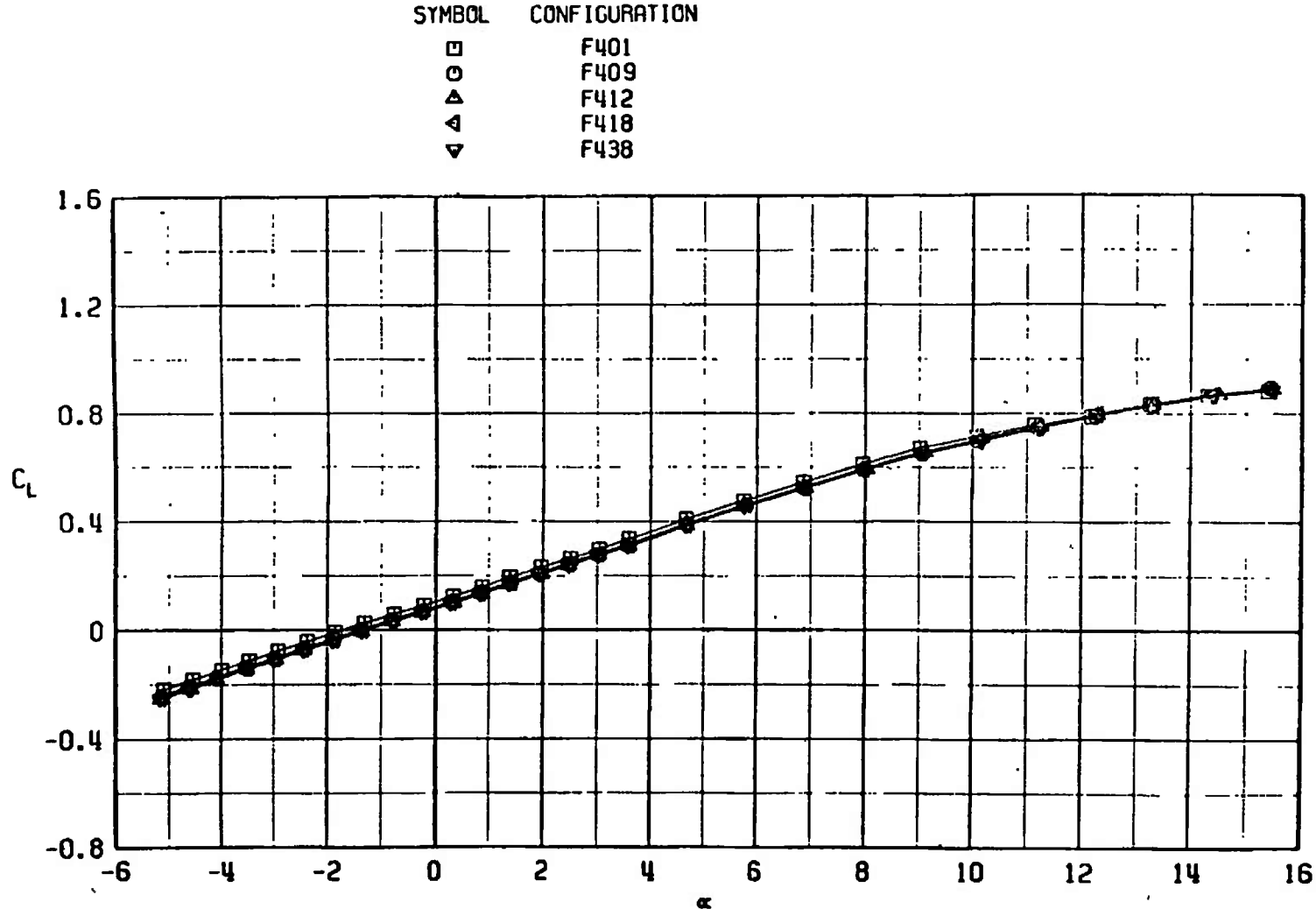

a. $M_\infty = 0.75$

Fig. 33 Lift Coefficient Variation with Angle of Attack for Configurations F401, F409, F412, F418, and F438

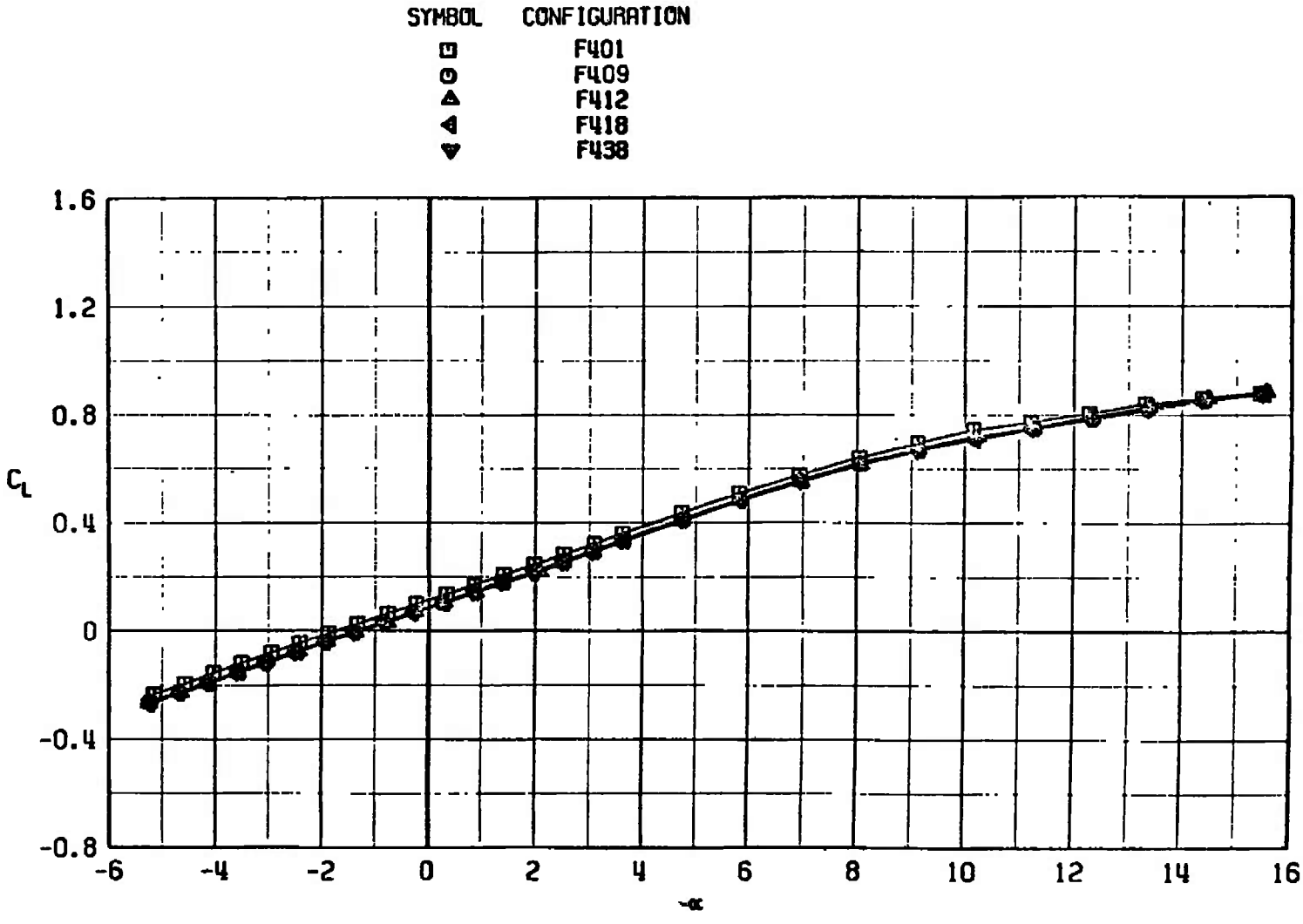

b. $M_\infty = 0.85$

Fig. 33 Continued

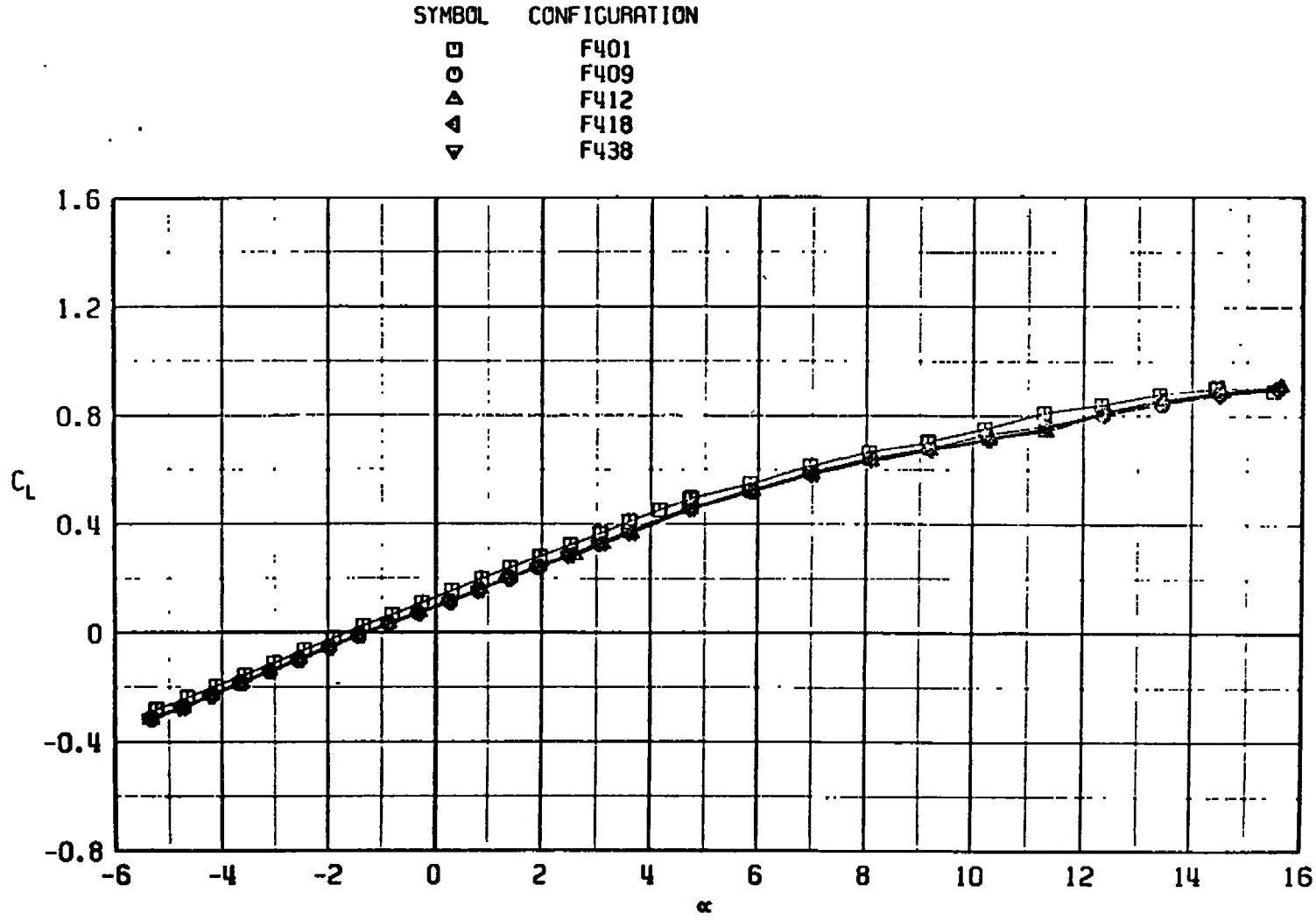

c. $M_\infty = 0.95$

Fig. 33 Continued

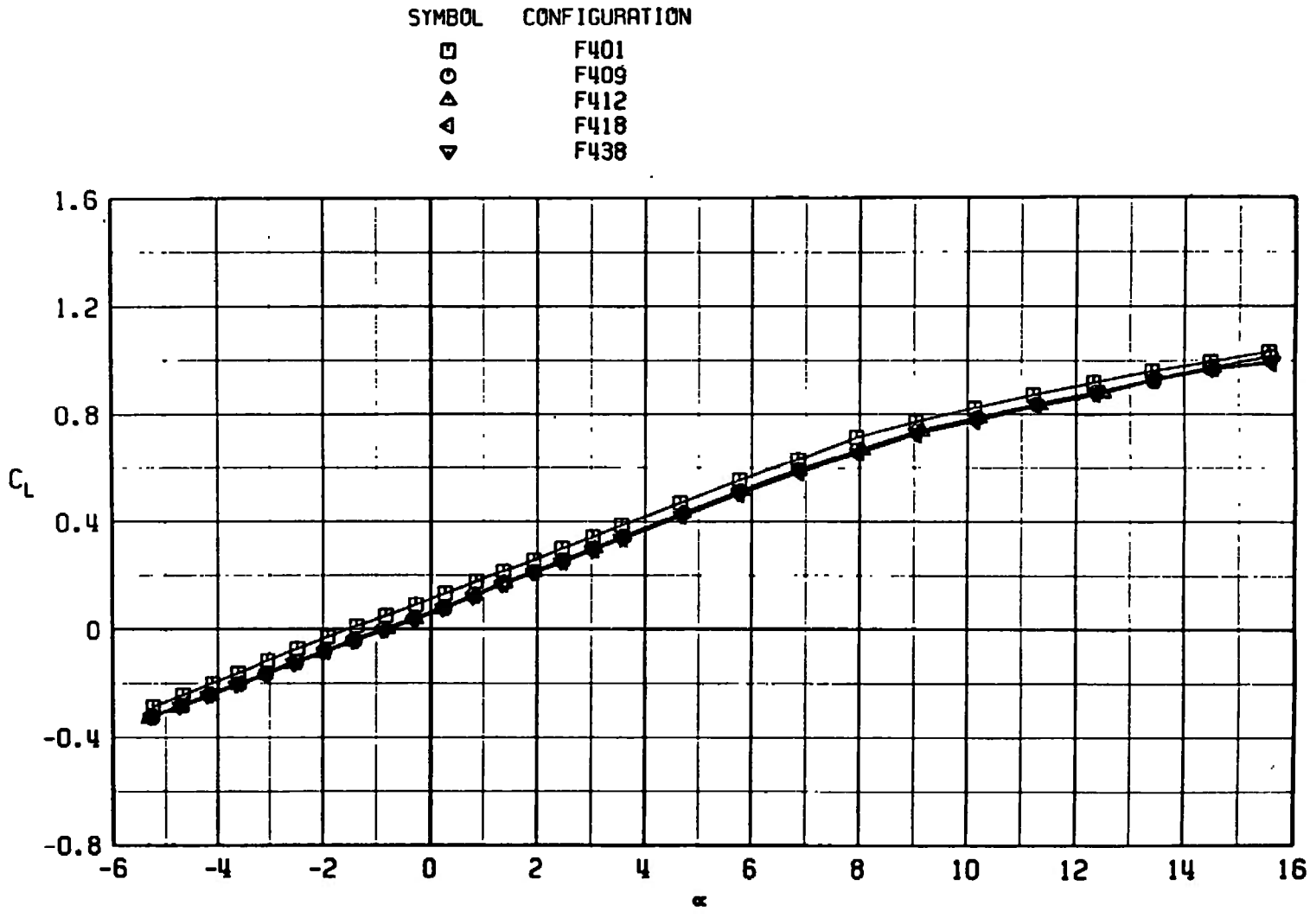

d. $M_\infty = 1.10$
Fig. 33 Continued

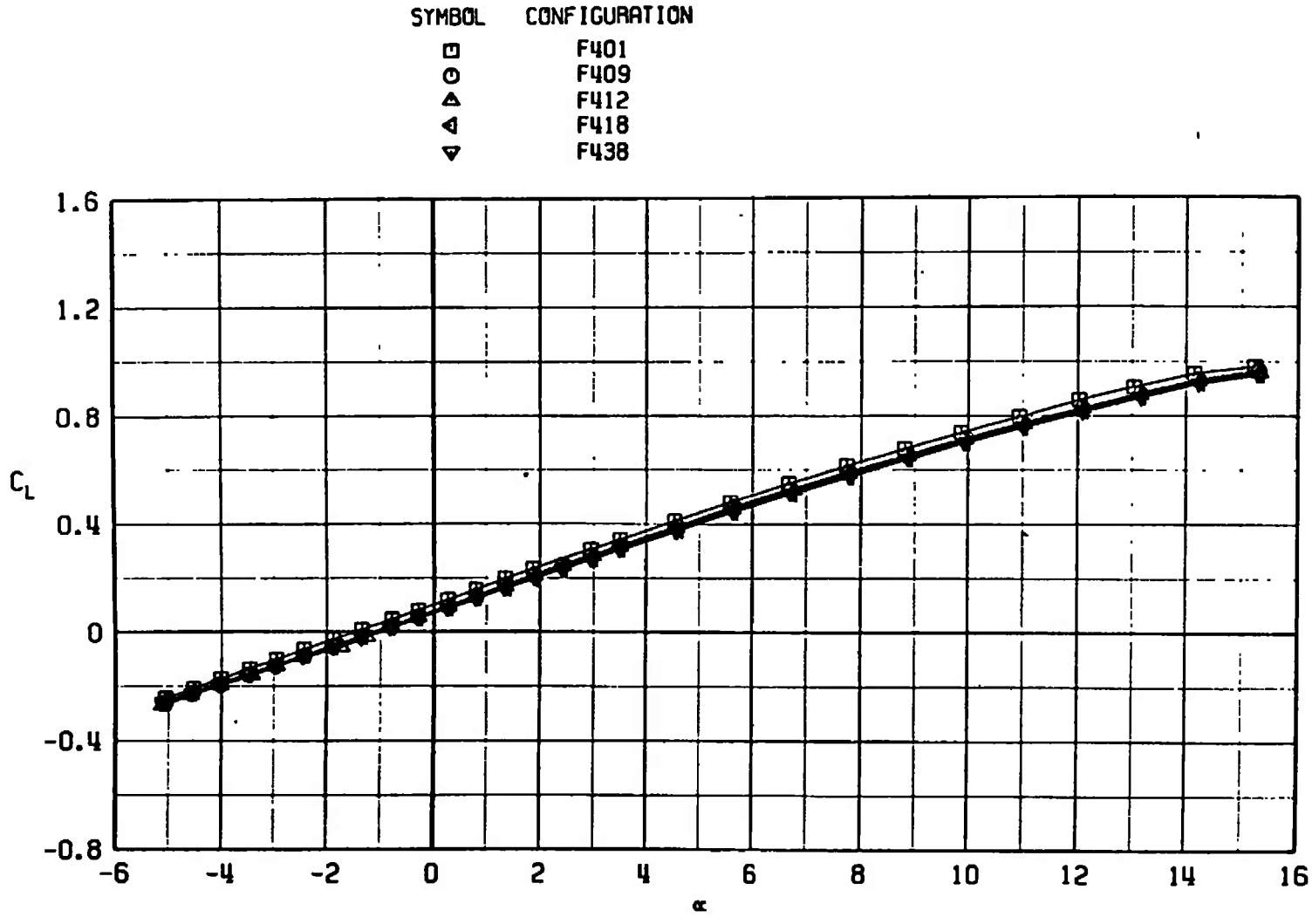

e. $M_\infty = 1.30$

Fig. 33 Concluded

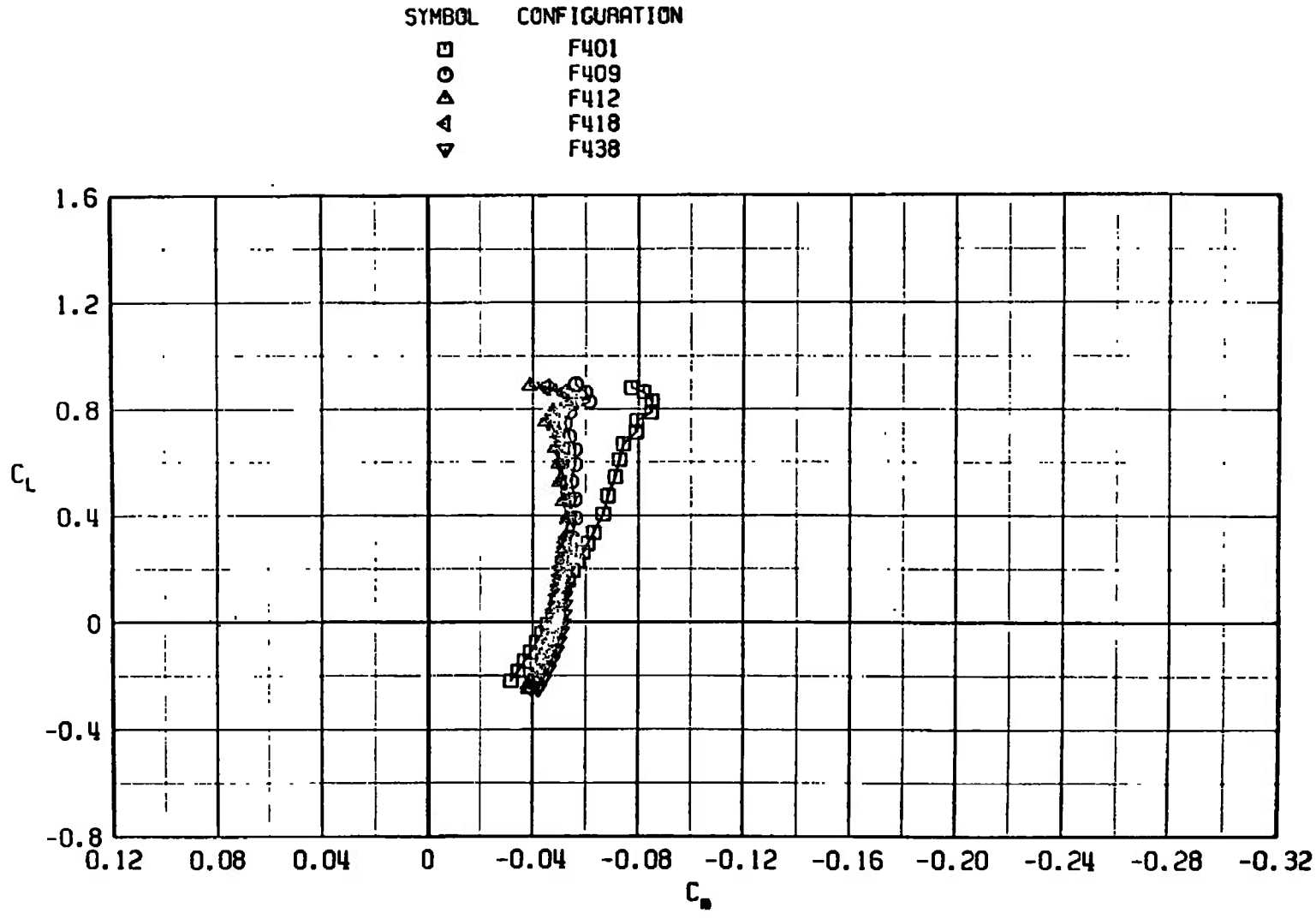

a. $M_\infty = 0.75$

Fig. 34 Pitching-Moment Coefficient Variation with Lift Coefficient for Configurations F401, F409, F412, F418, and F438

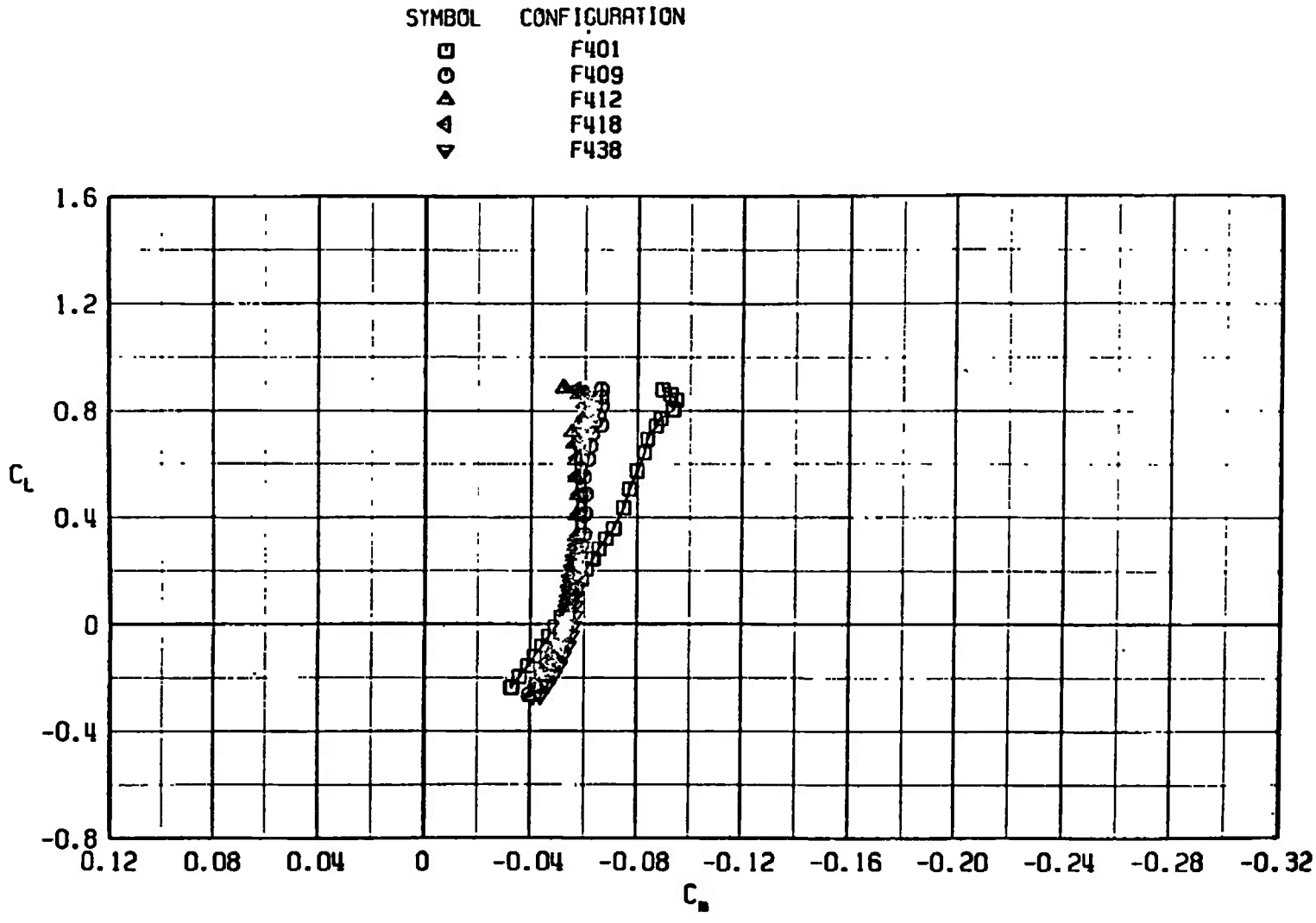

b. $M_\infty = 0.85$

Fig. 34 Continued

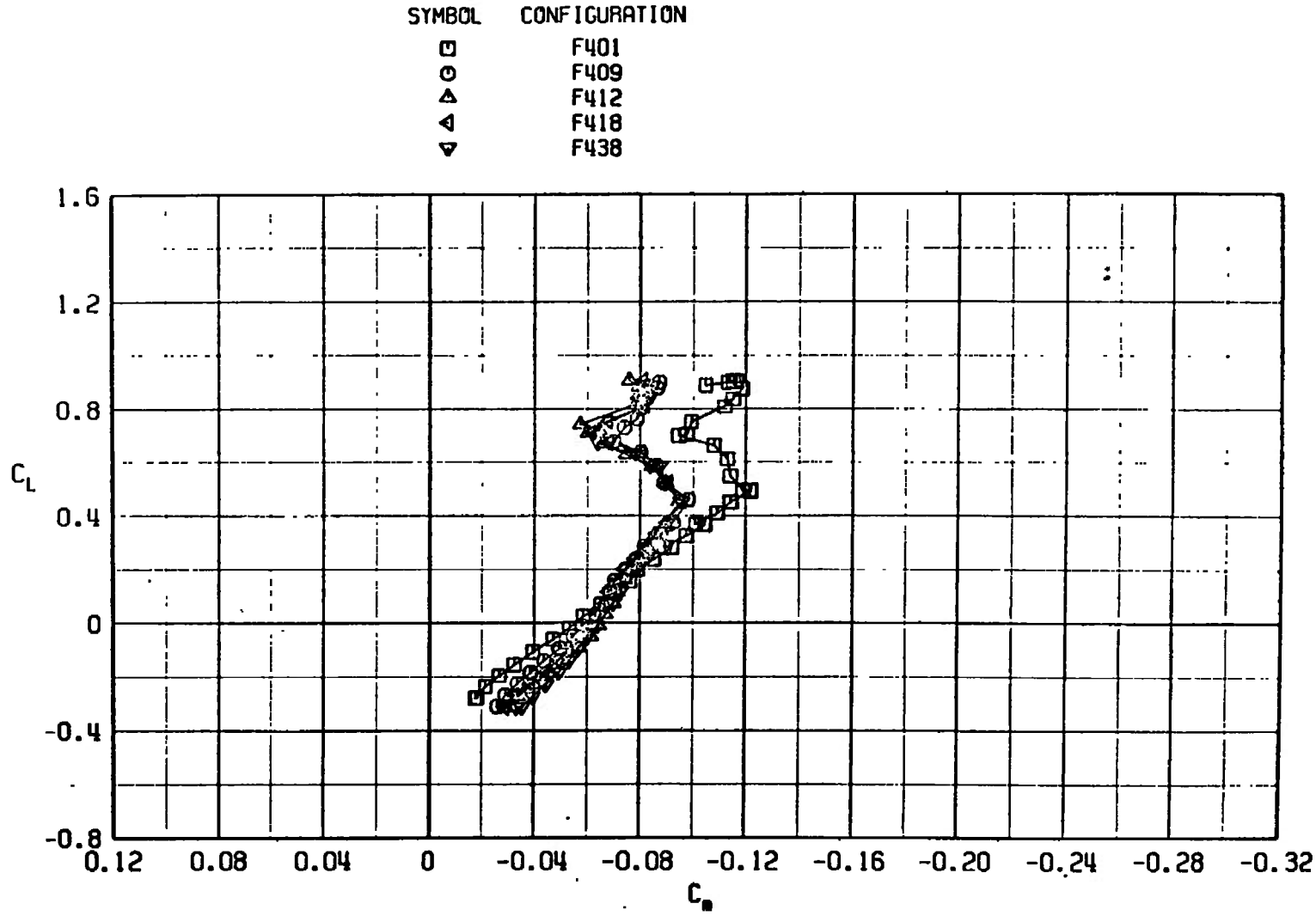

c. $M_\infty = 0.95$

Fig. 34 Continued

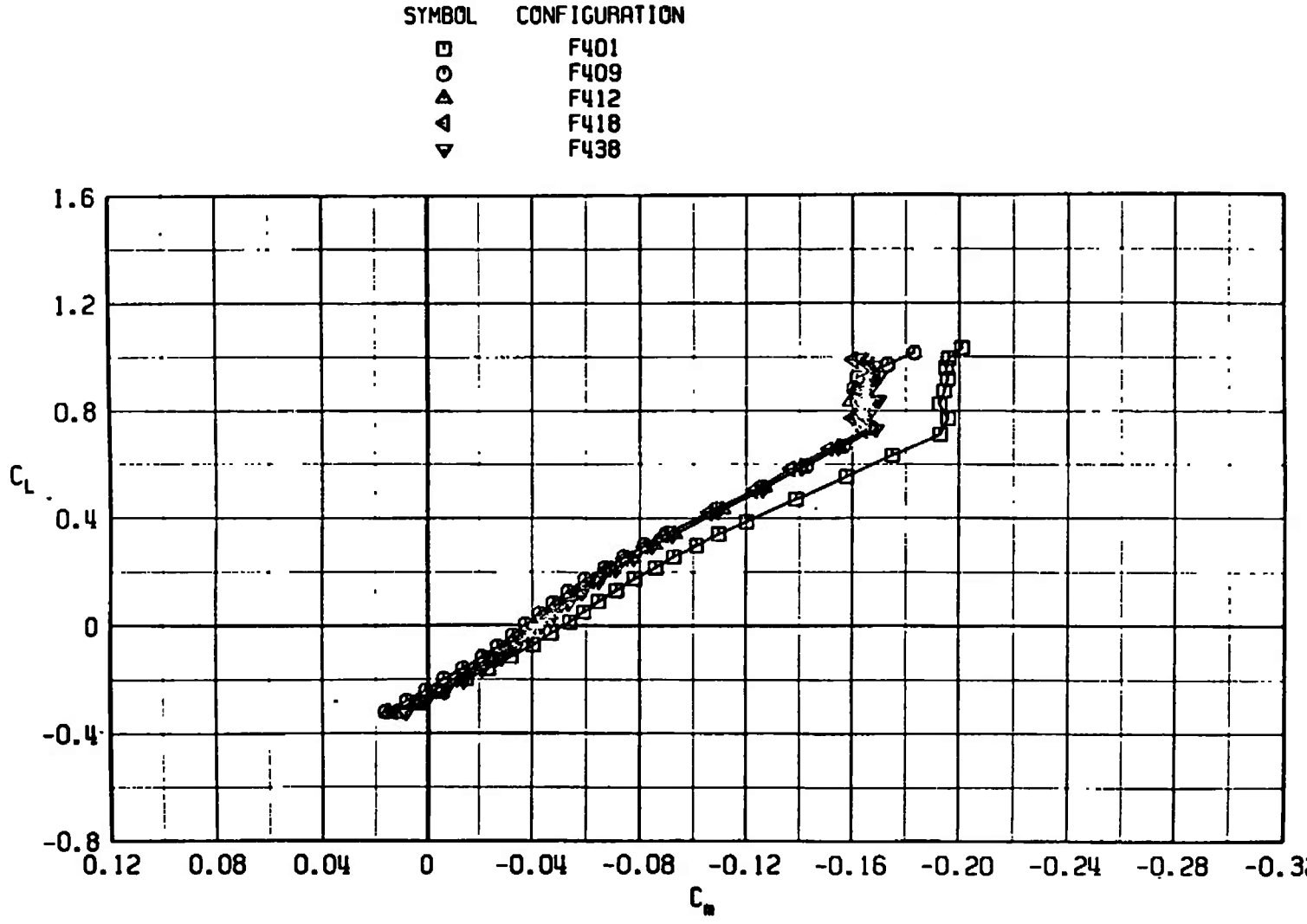

d. $M_\infty = 1.10$

Fig. 34 Continued

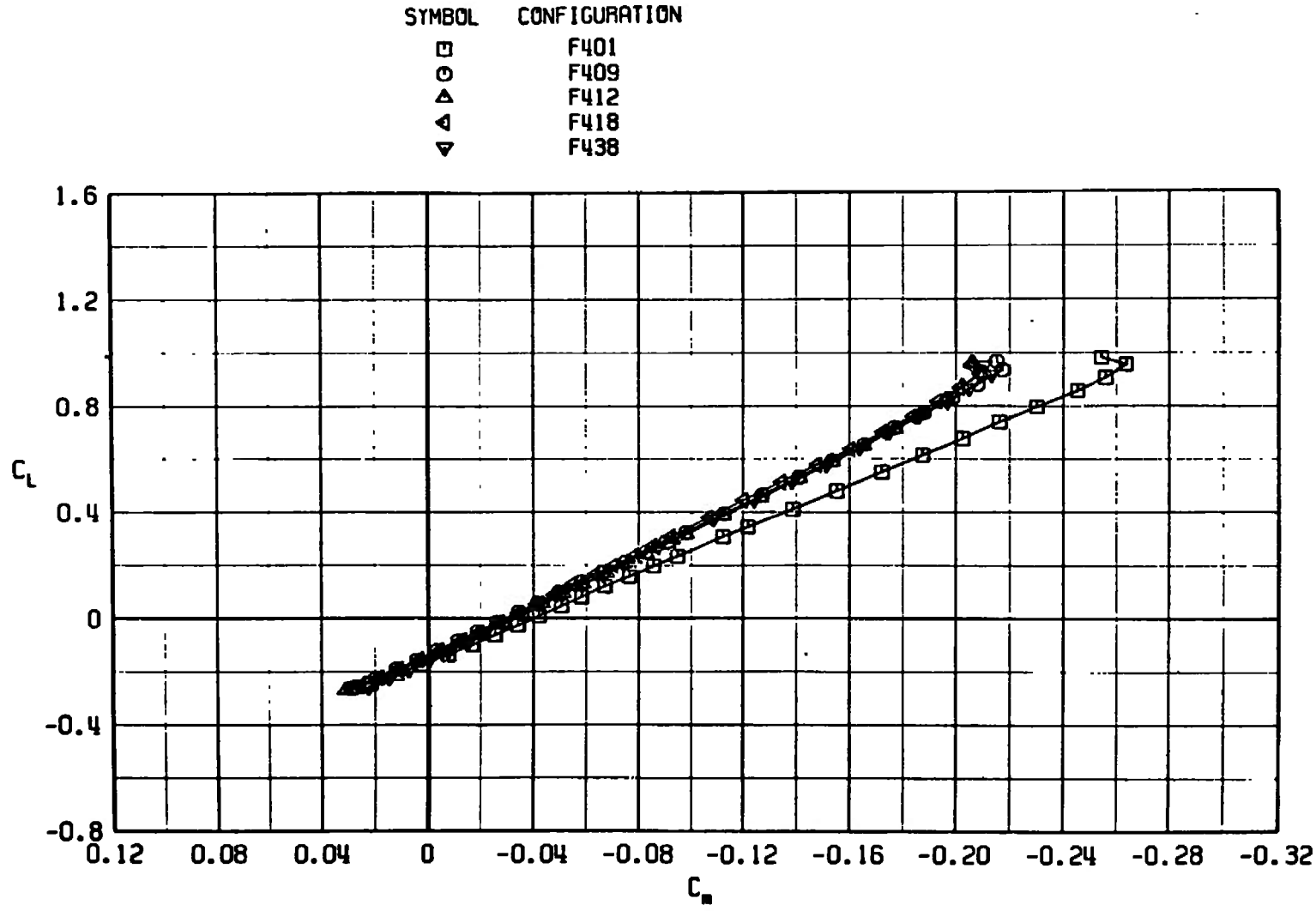

e. $M_\infty = 1.30$

Fig. 34 Concluded

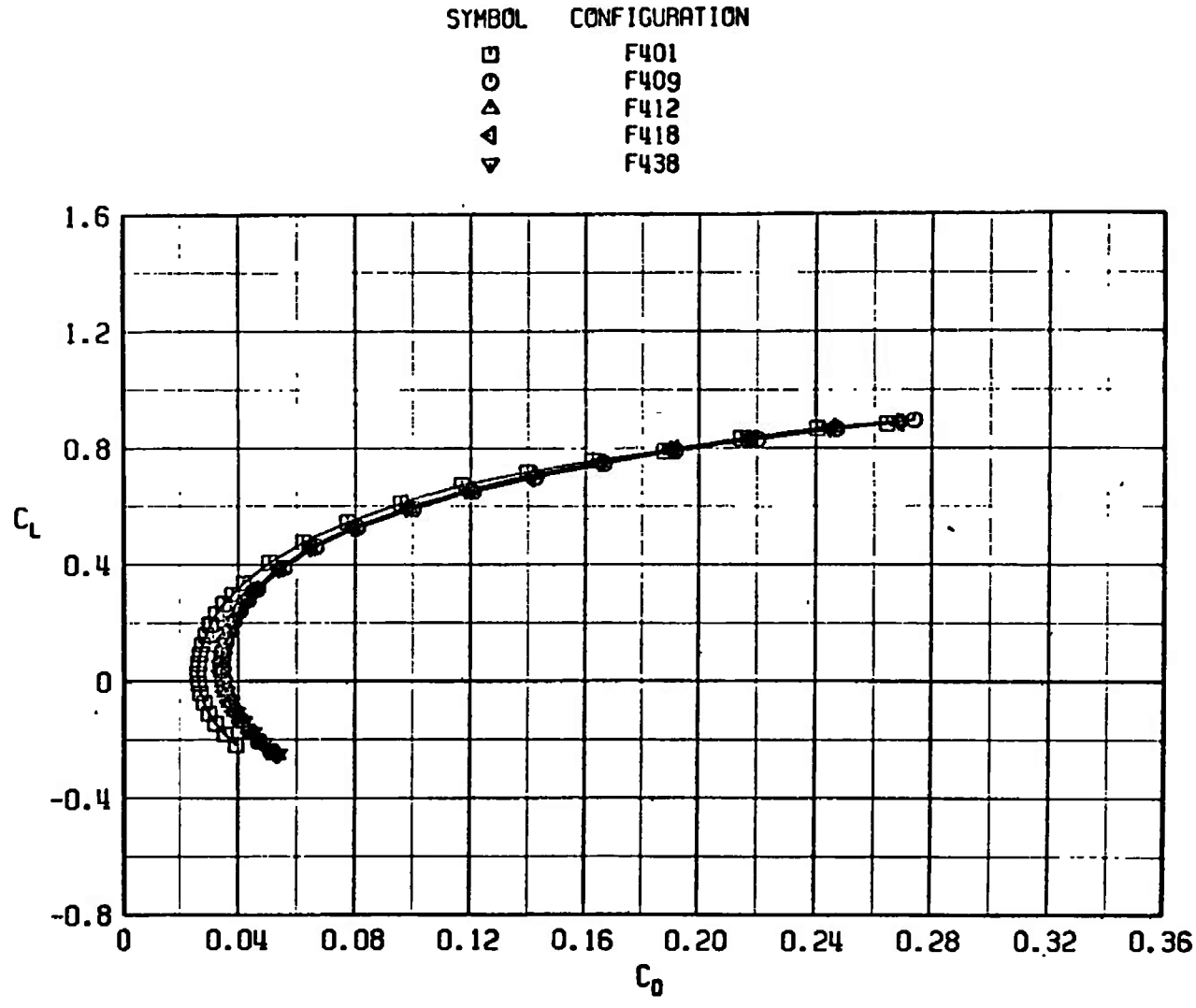

a. $M_\infty = 0.75$

Fig. 35 Drag Coefficient Variation with Lift Coefficient for Configurations F401, F409, F412, F418, and F438

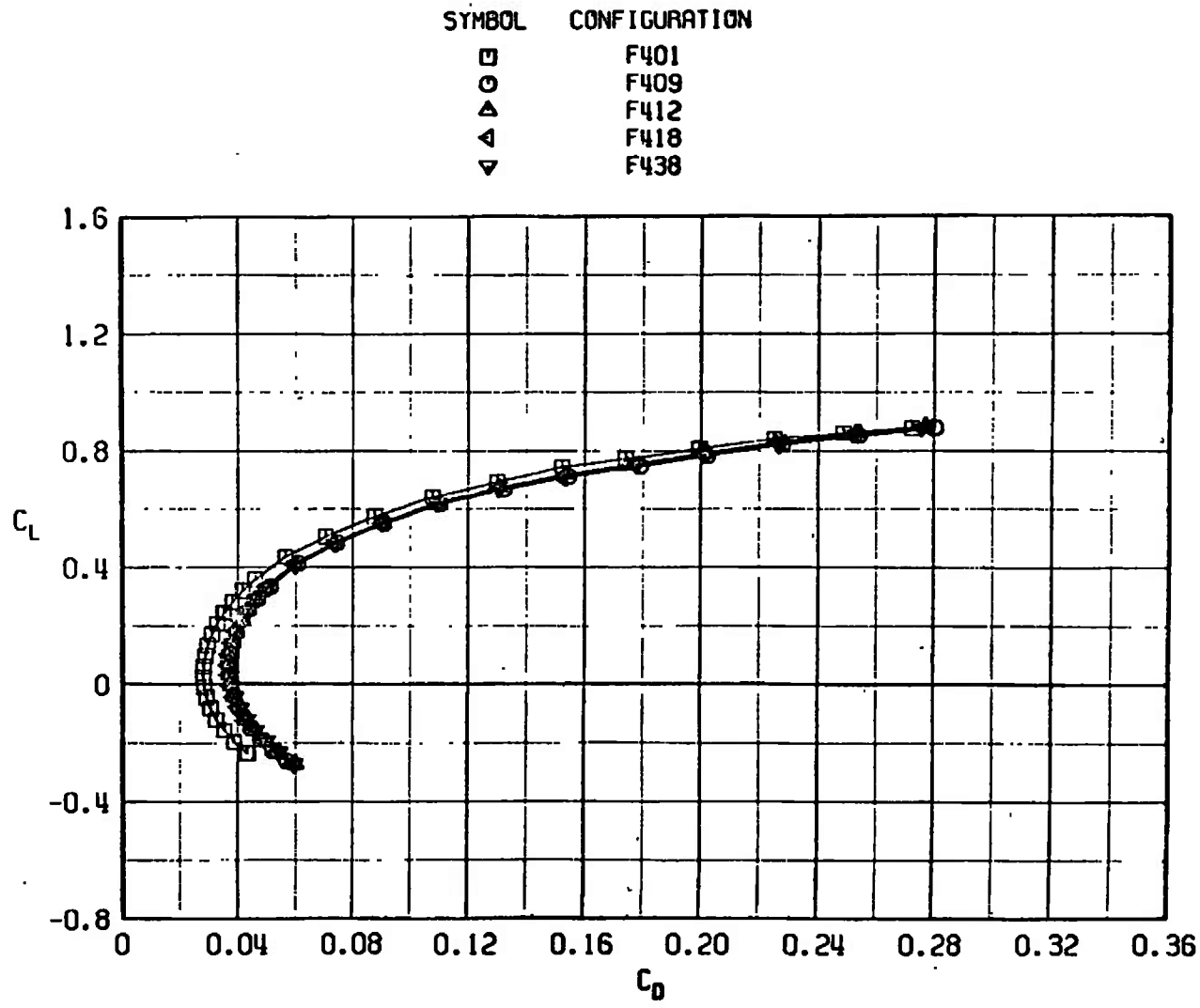

b. $M_\infty = 0.85$

Fig. 35 Continued

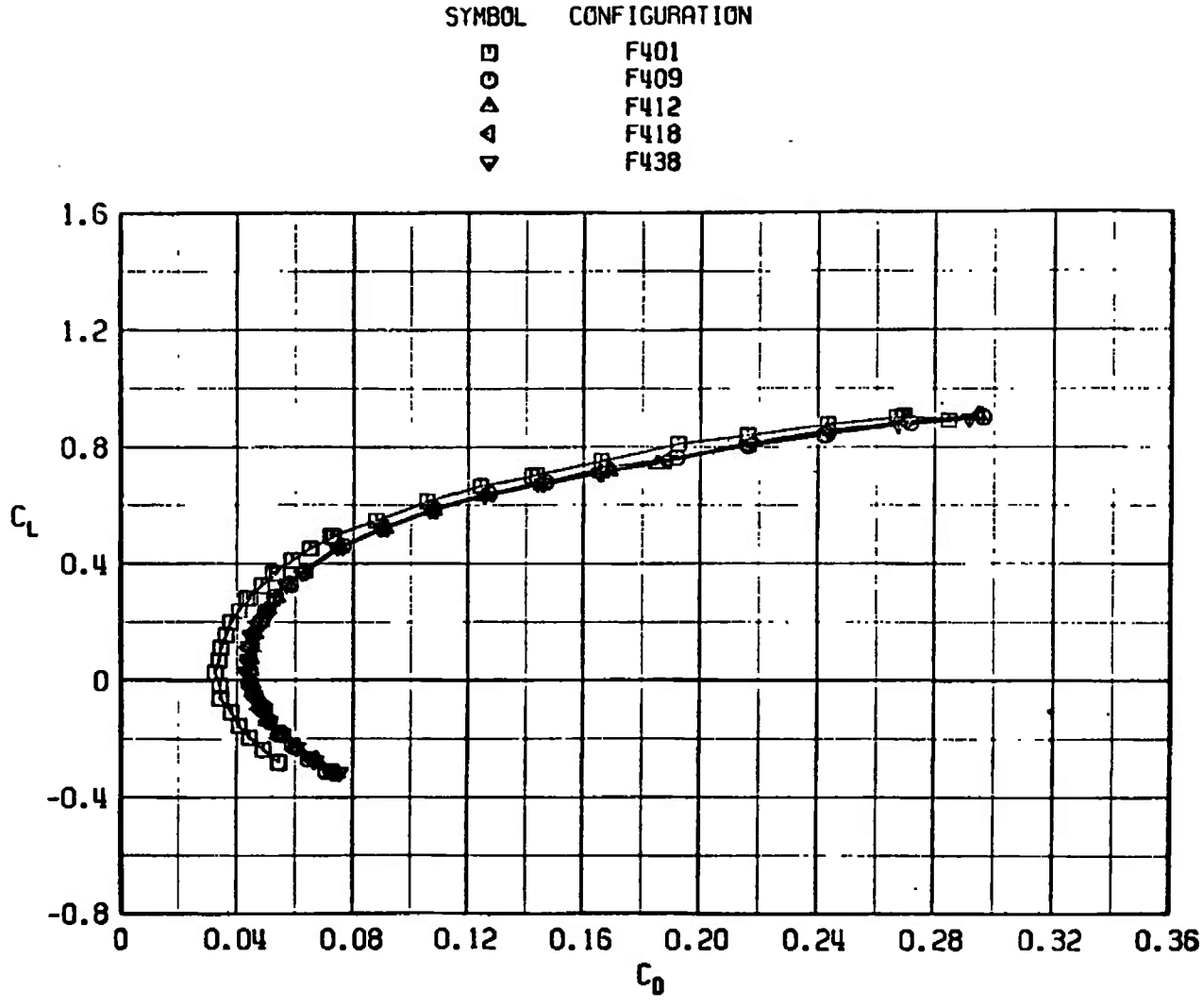

c. $M_\infty = 0.95$

Fig. 35 Continued

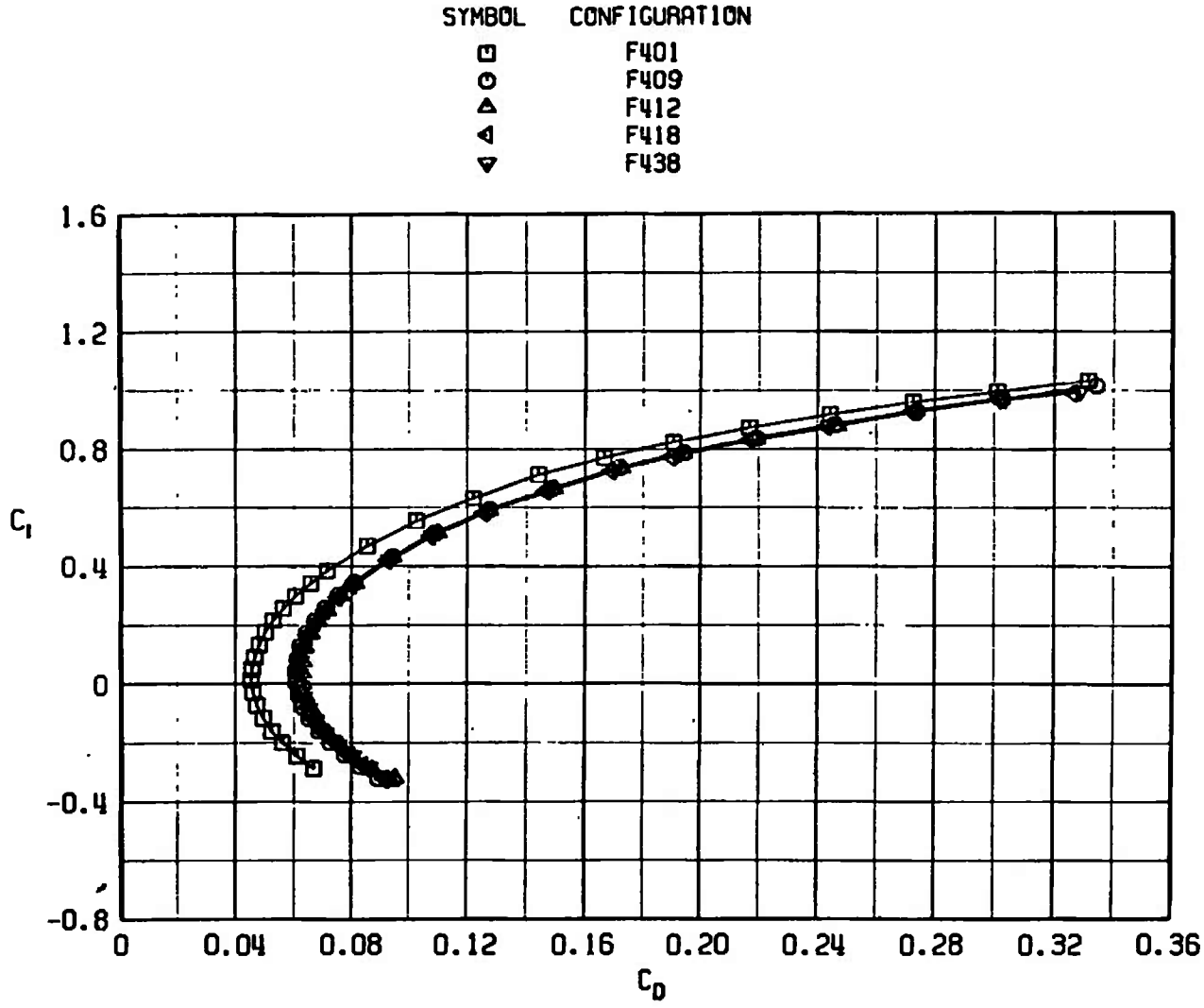

d. $M_\infty = 1.10$

Fig. 35 Continued

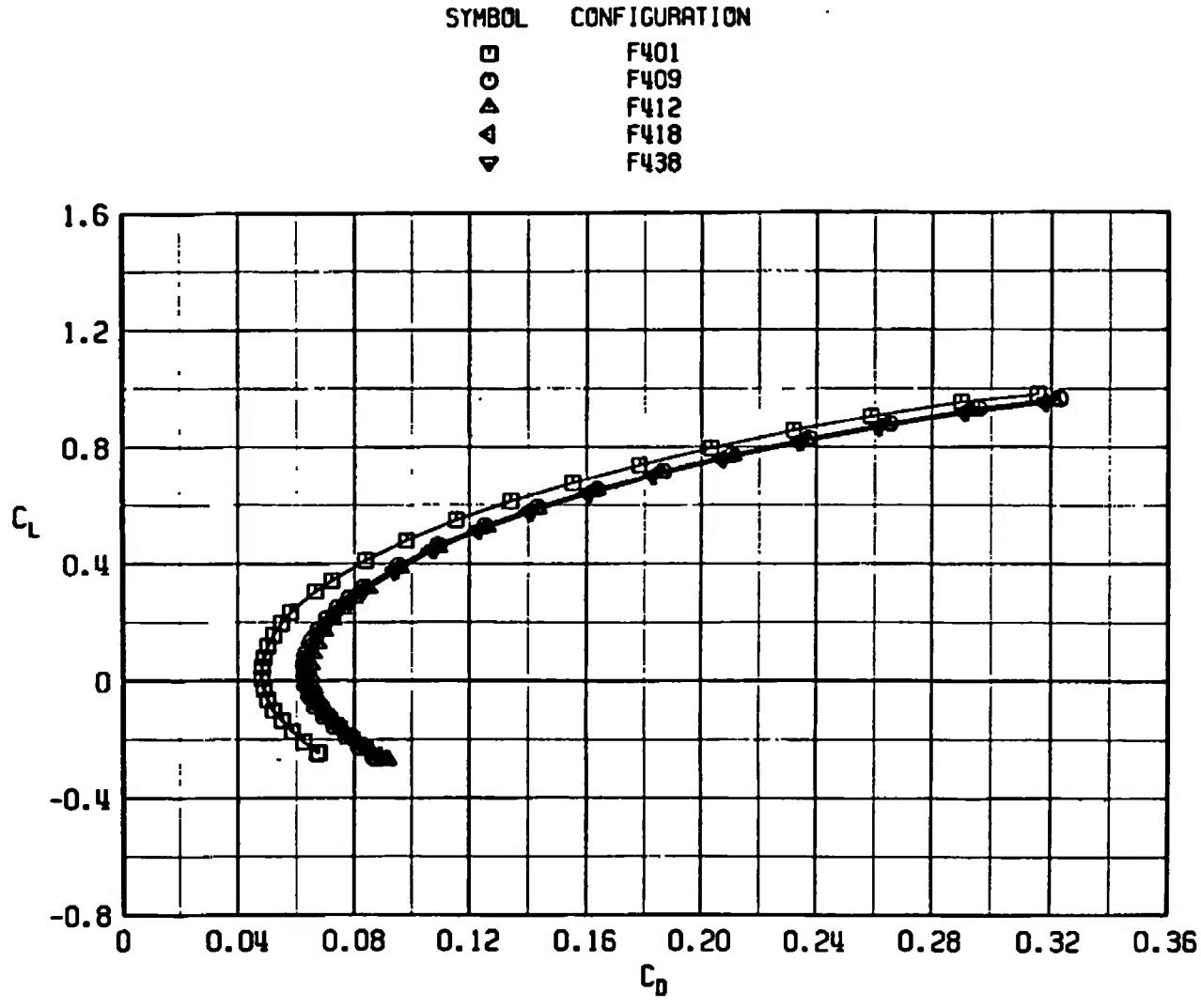

e. $M_\infty = 1.30$

Fig. 35 Concluded

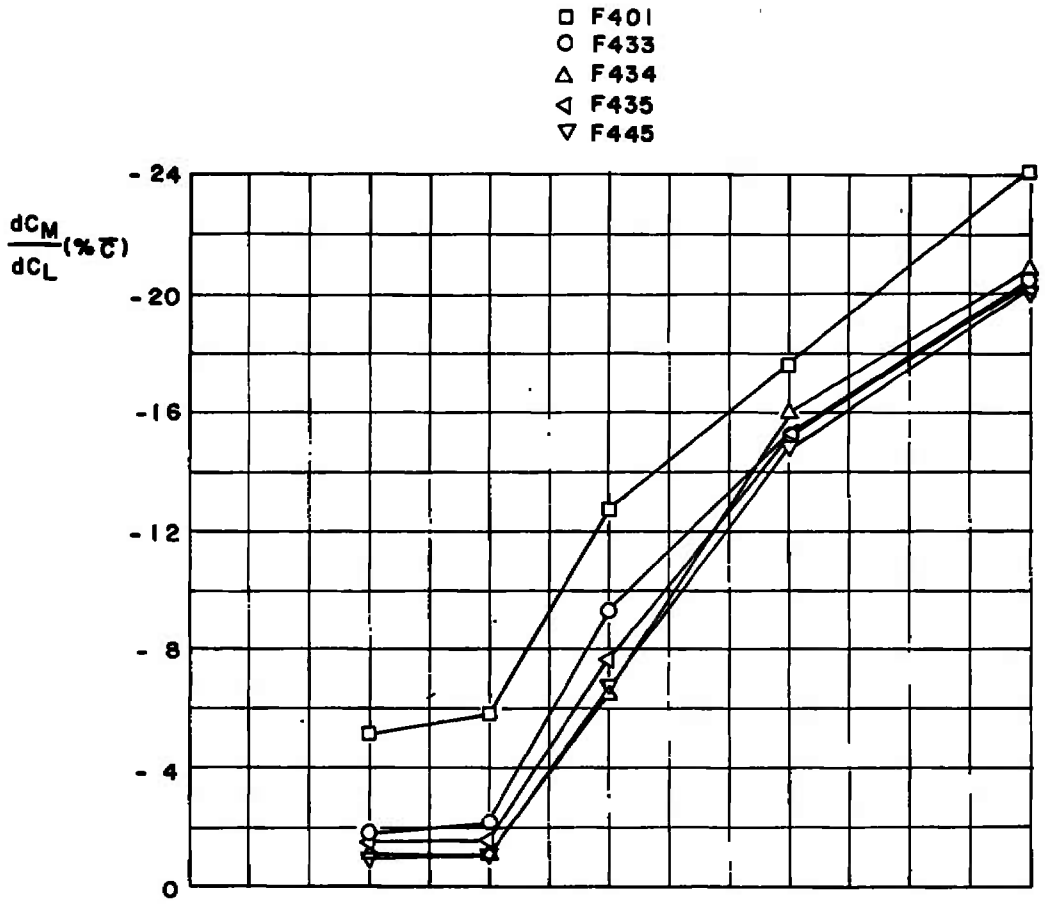

a. $\partial C_m/\partial C_L$ versus M_∞ at C_L = 0.20 in percentage of $\bar{c}$

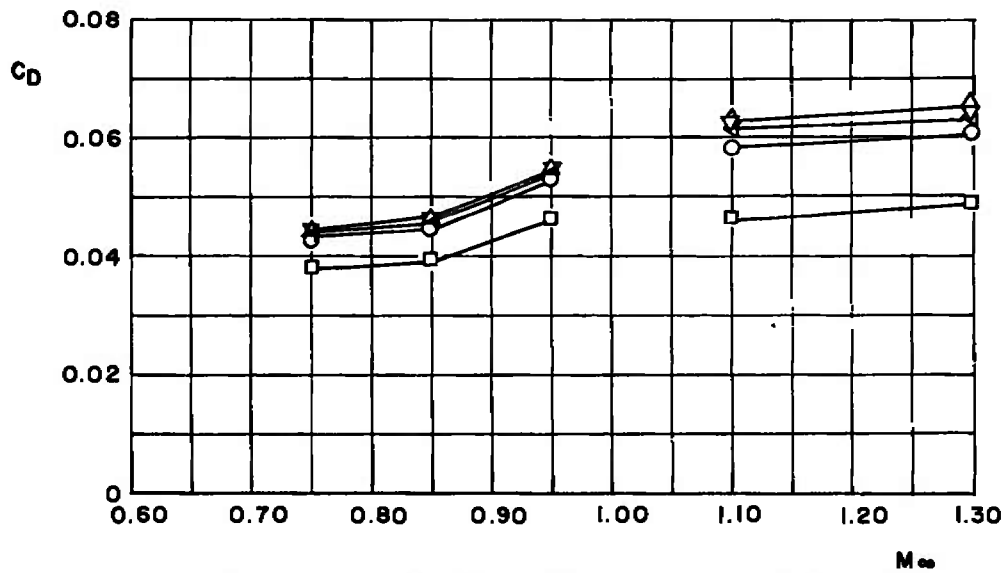

b. C_D versus M_∞ at C_L = 0.30, $M_\infty < 1.0$, and C_L = 0.10, $M_\infty > 1.0$

Fig. 36 Drag Coefficient and $\partial C_m/\partial C_L$ Variation with Mach Number for Configurations F401, F409, F412, F418, and F438

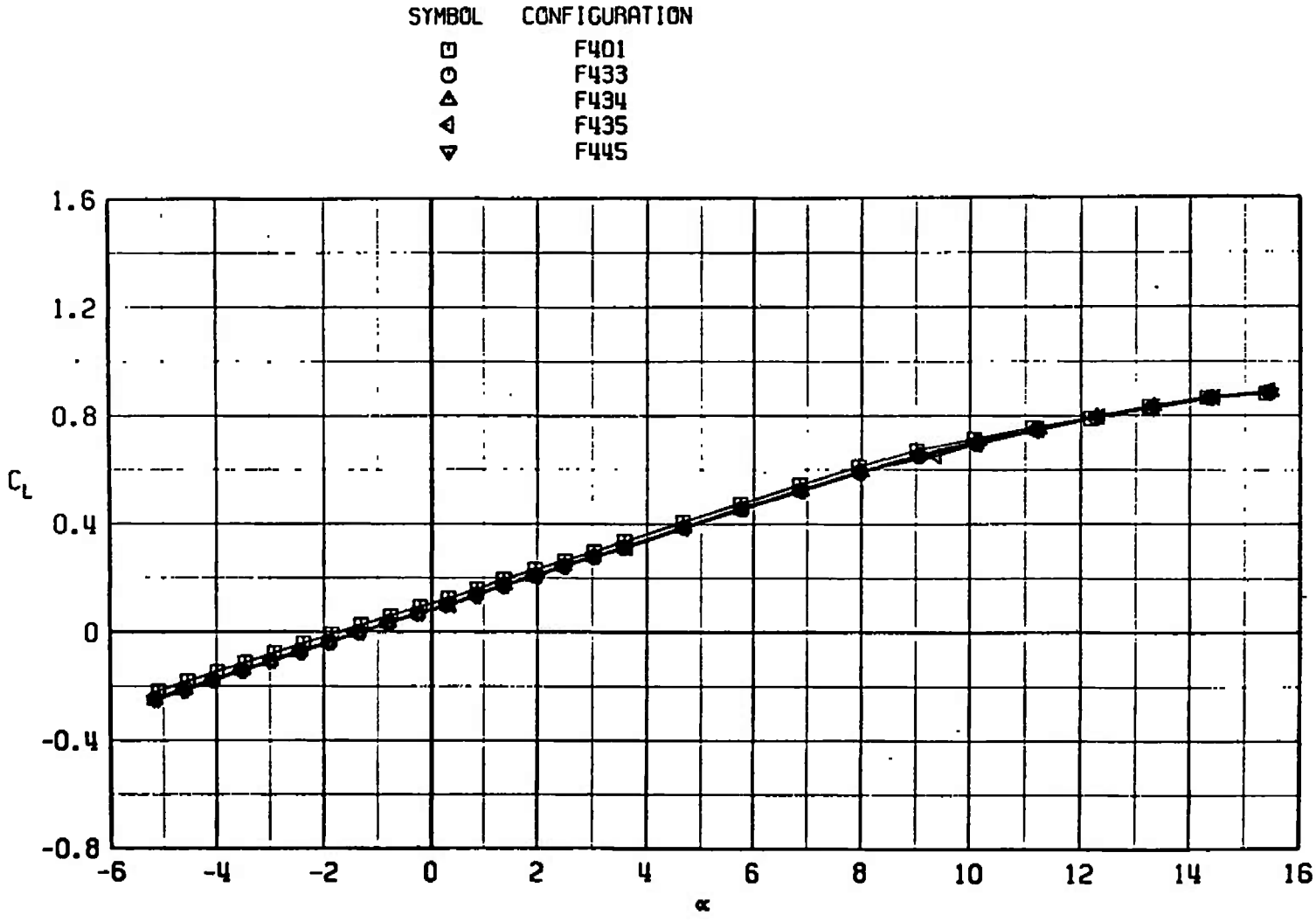

a. $M_\infty = 0.75$

Fig. 37 Lift Coefficient Variation with Angle of Attack for Configurations F401, F433, F434, F435, and F445

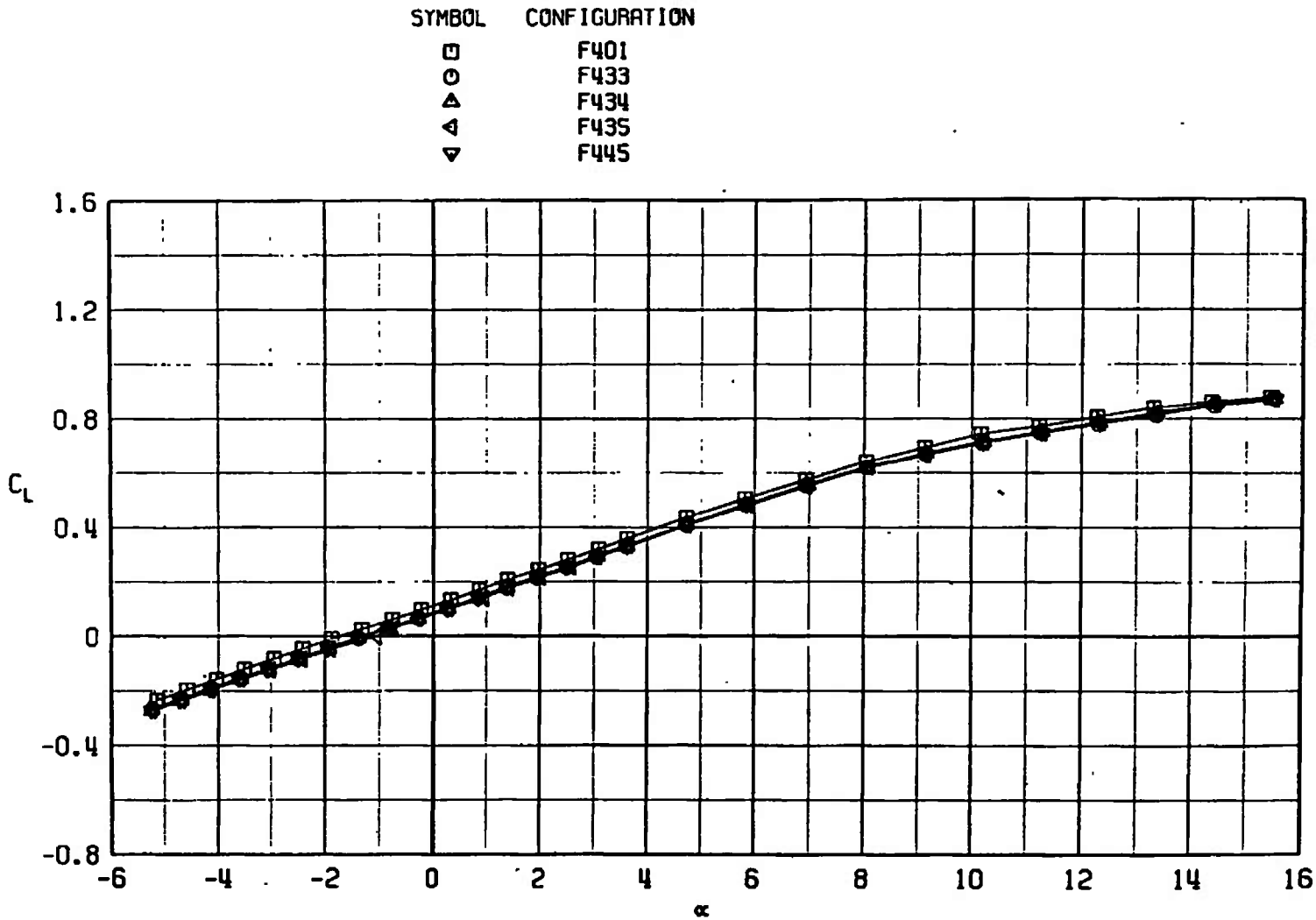

b. $M_\infty = 0.85$

Fig. 37 Continued

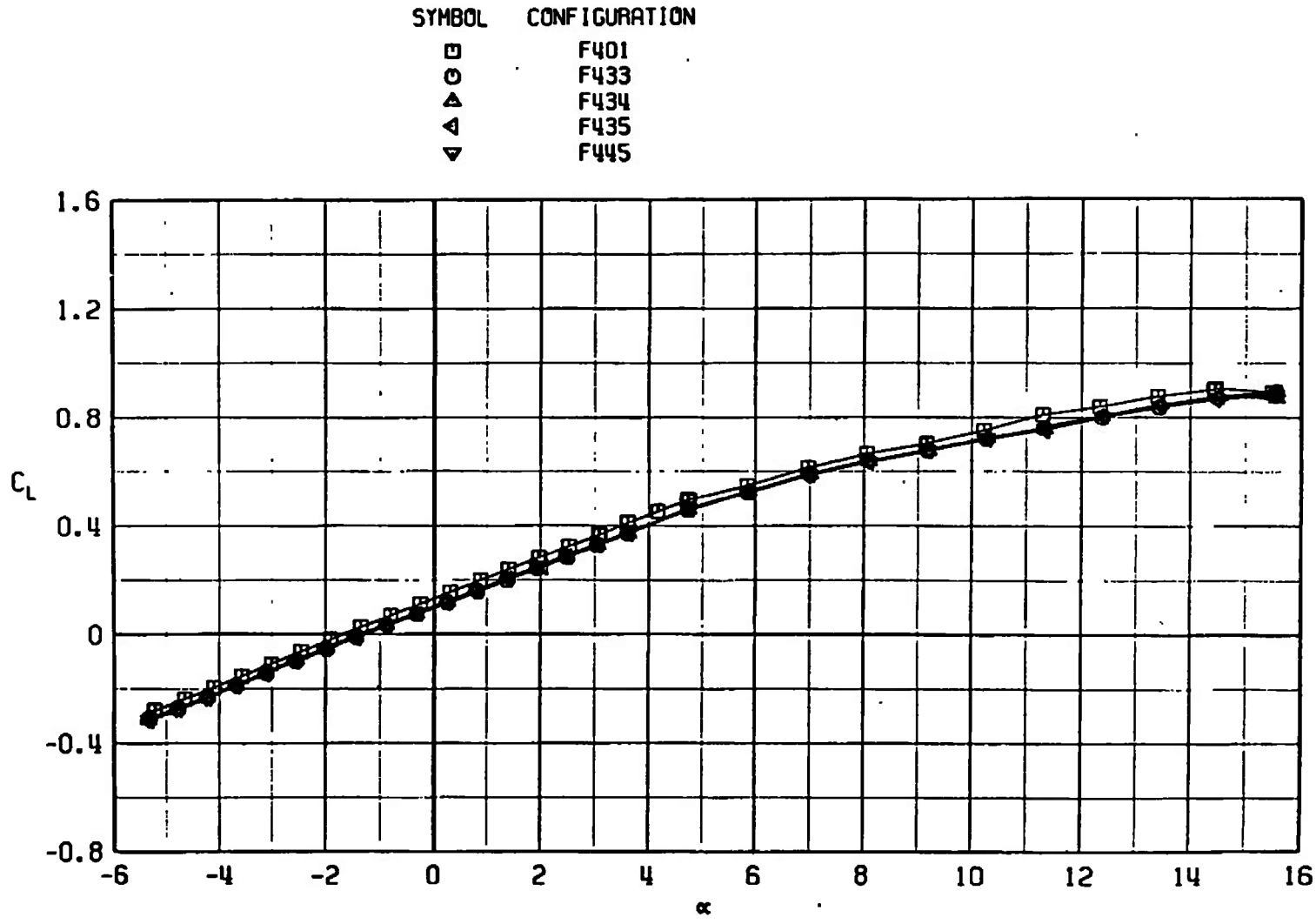

c. $M_\infty = 0.95$

Fig. 37 Continued

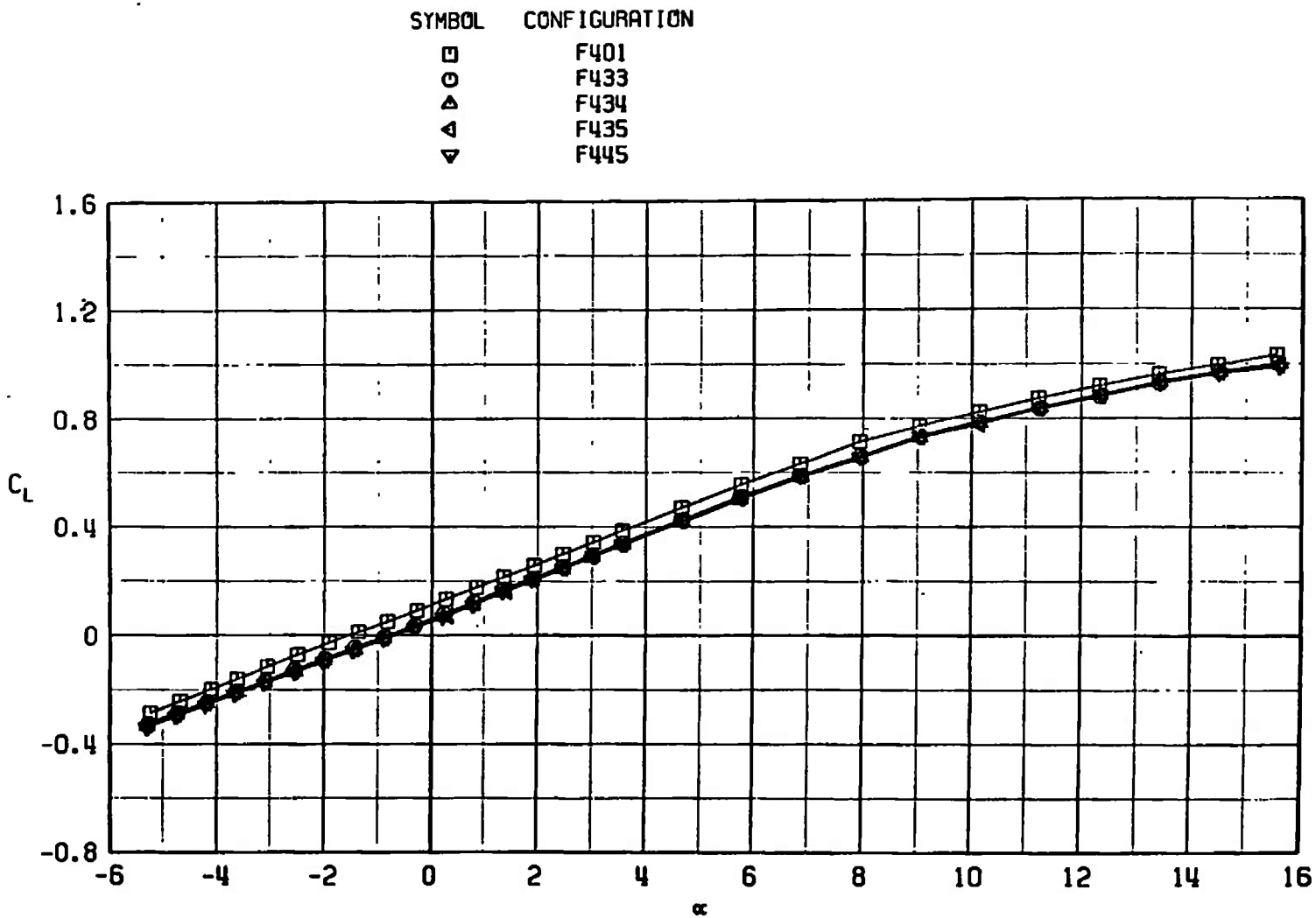

d. $M_\infty = 1.10$

Fig. 37 Continued

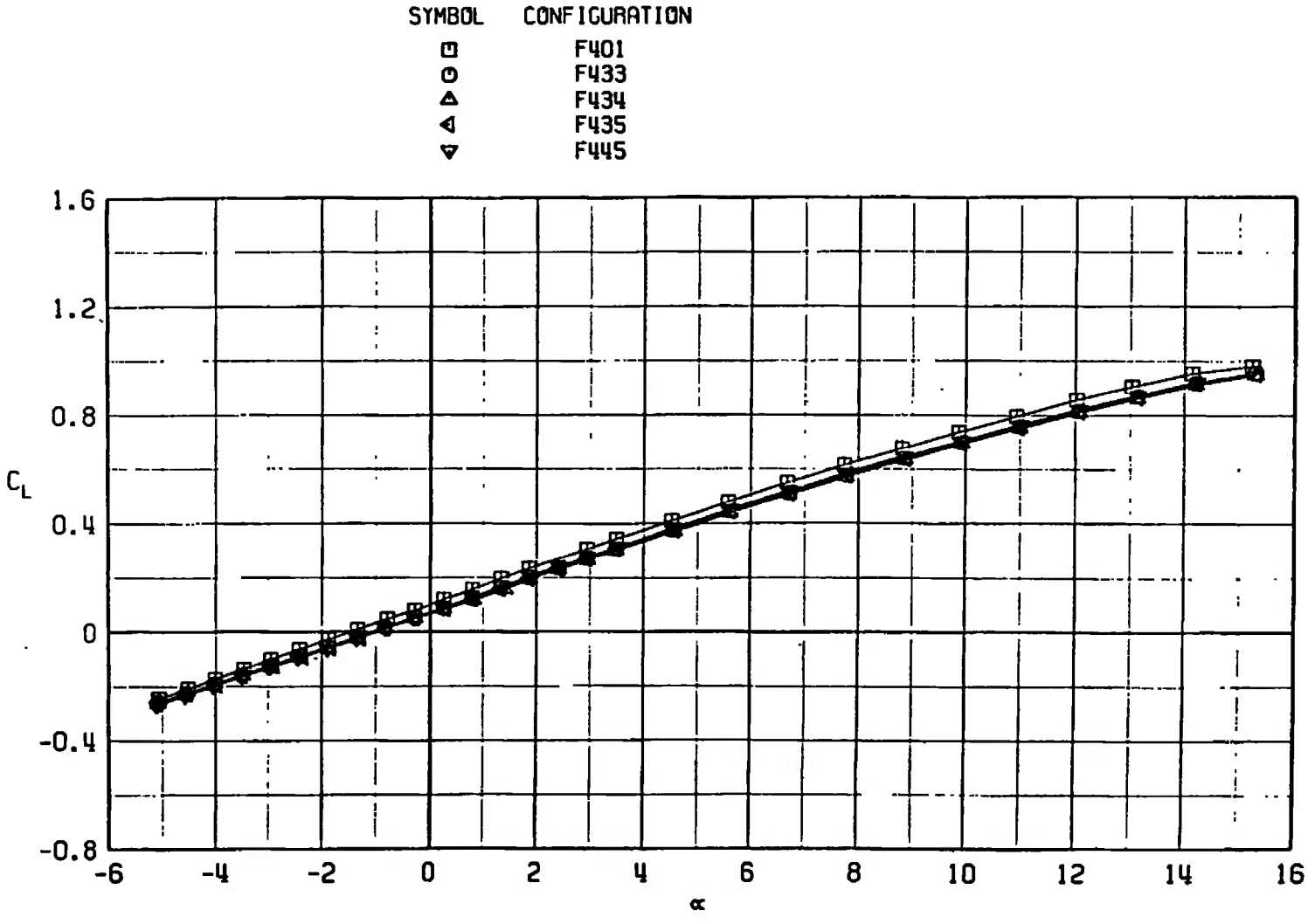

e. $M_\infty = 1.30$

Fig. 37 Concluded

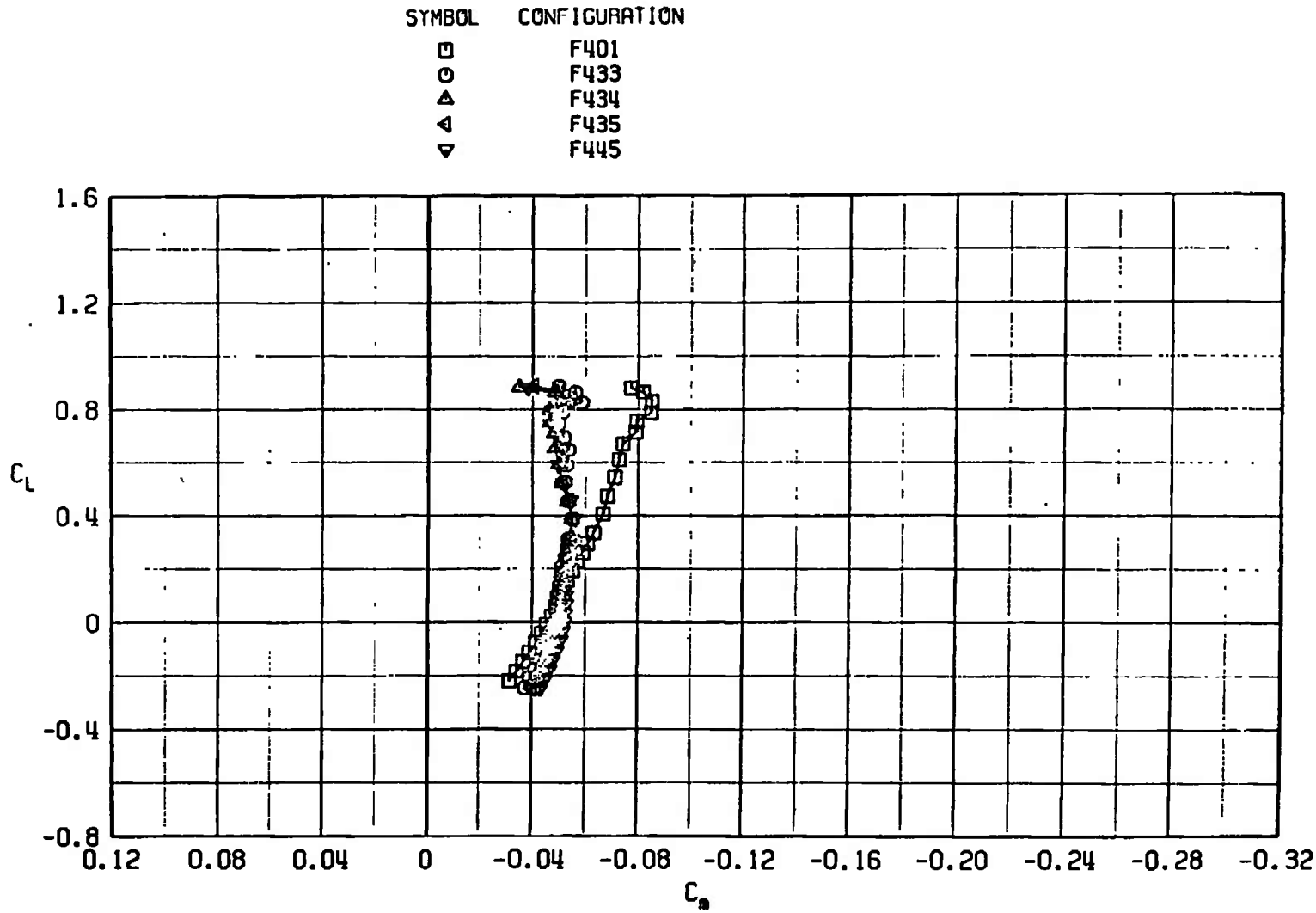

a. $M_\infty = 0.75$

Fig. 38 Pitching-Moment Coefficient Variation with Lift Coefficient for Configurations F401, F433, F434, F435, and F445

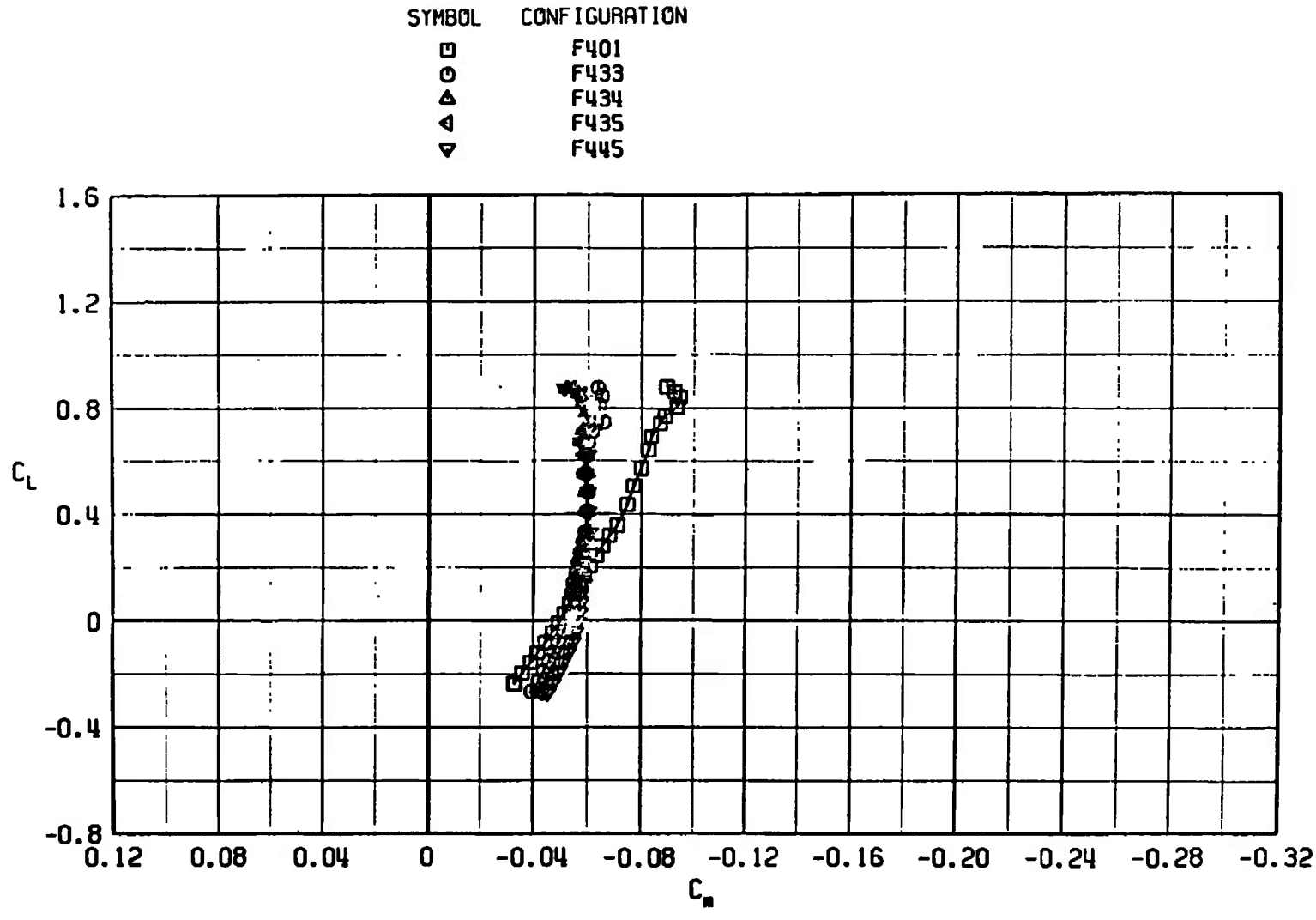

b. $M_\infty = 0.85$

Fig. 38 Continued

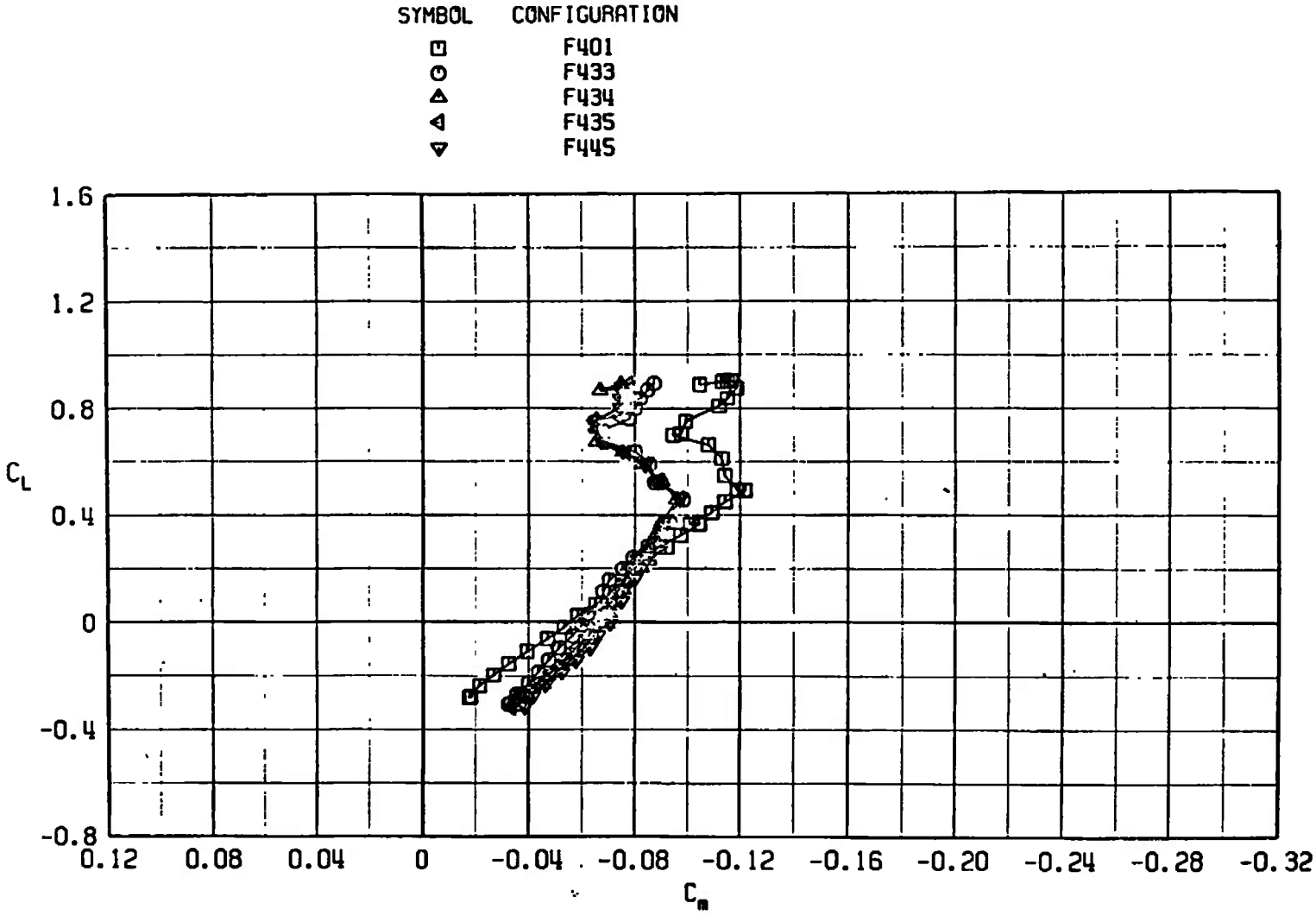

c. $M_\infty = 0.95$

Fig. 38 Continued

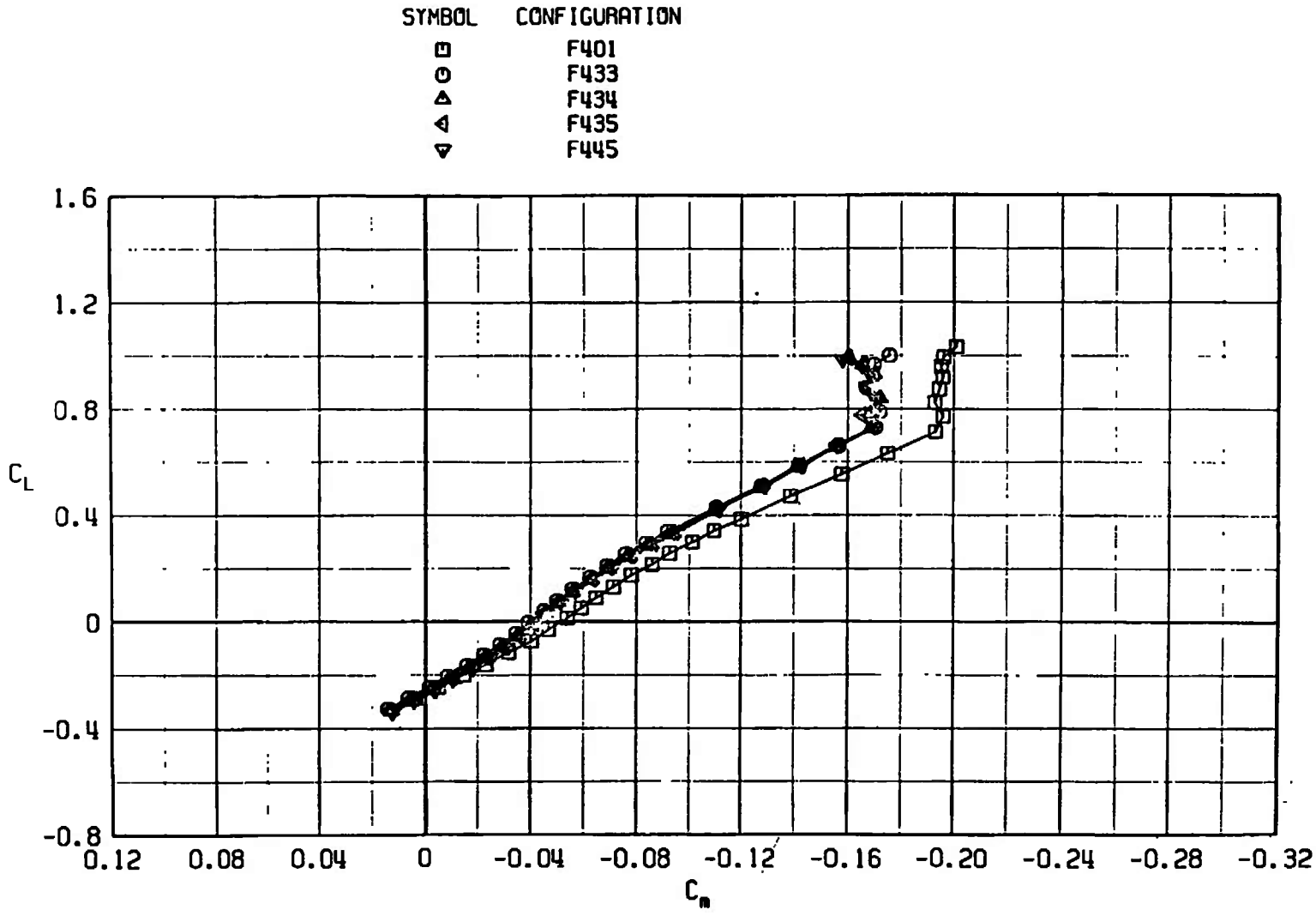

d. $M_\infty = 1.10$

Fig. 38 Continued

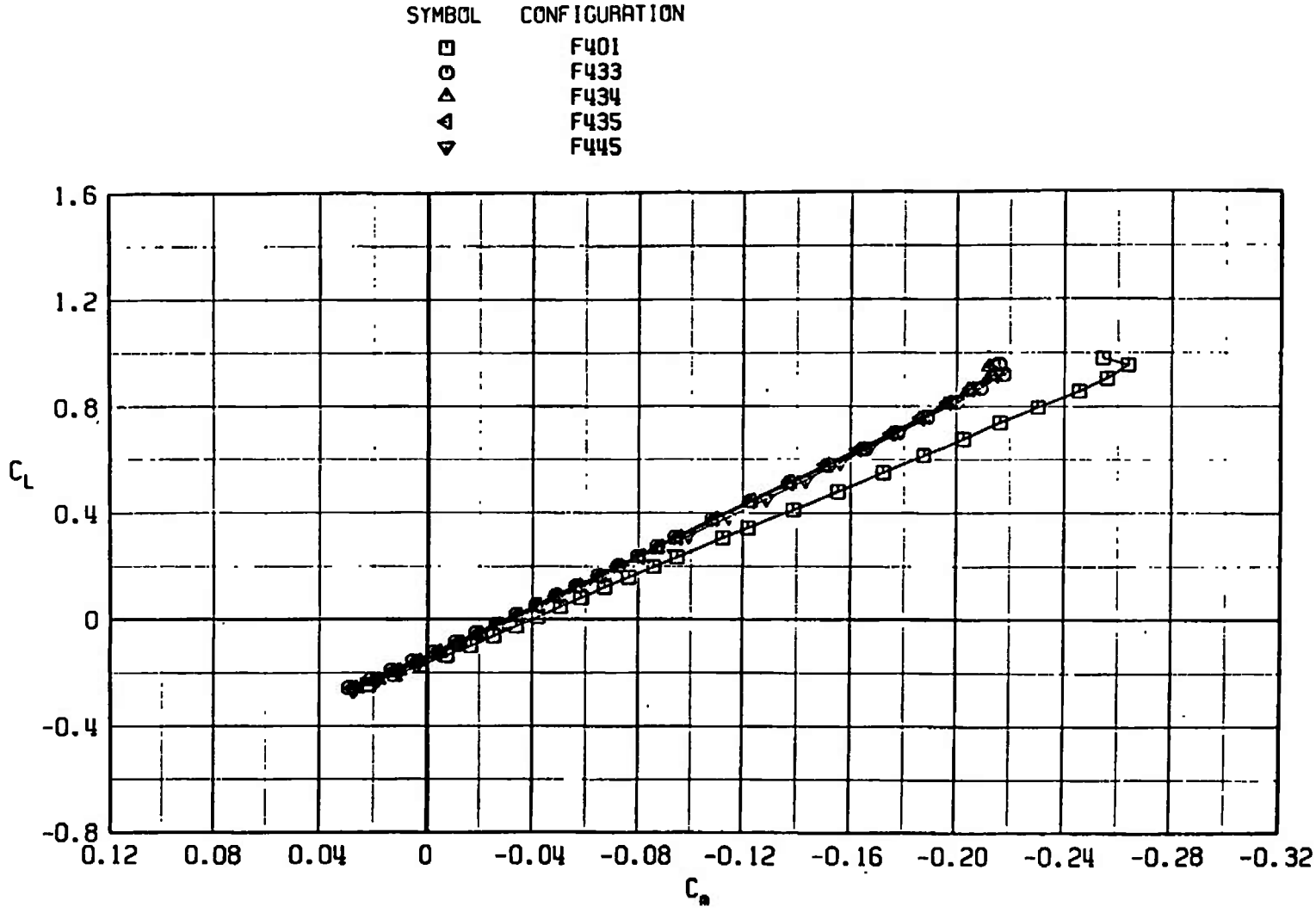

e. $M_\infty = 1.30$

Fig. 38 Concluded

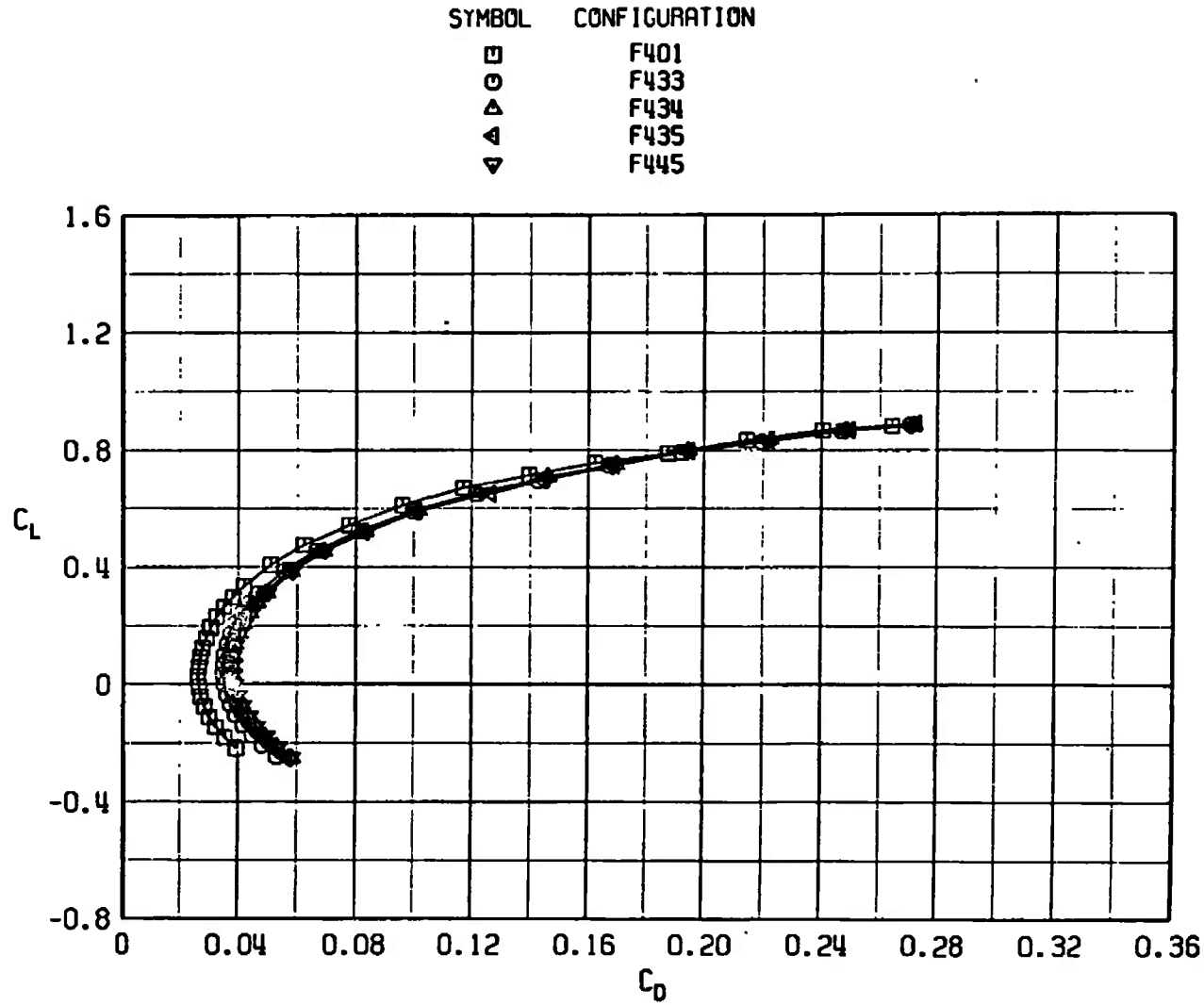

a. $M_\infty = 0.75$

Fig. 39 Drag Coefficient Variation with Lift Coefficient for Configurations F401, F433, F434, F435, and F445

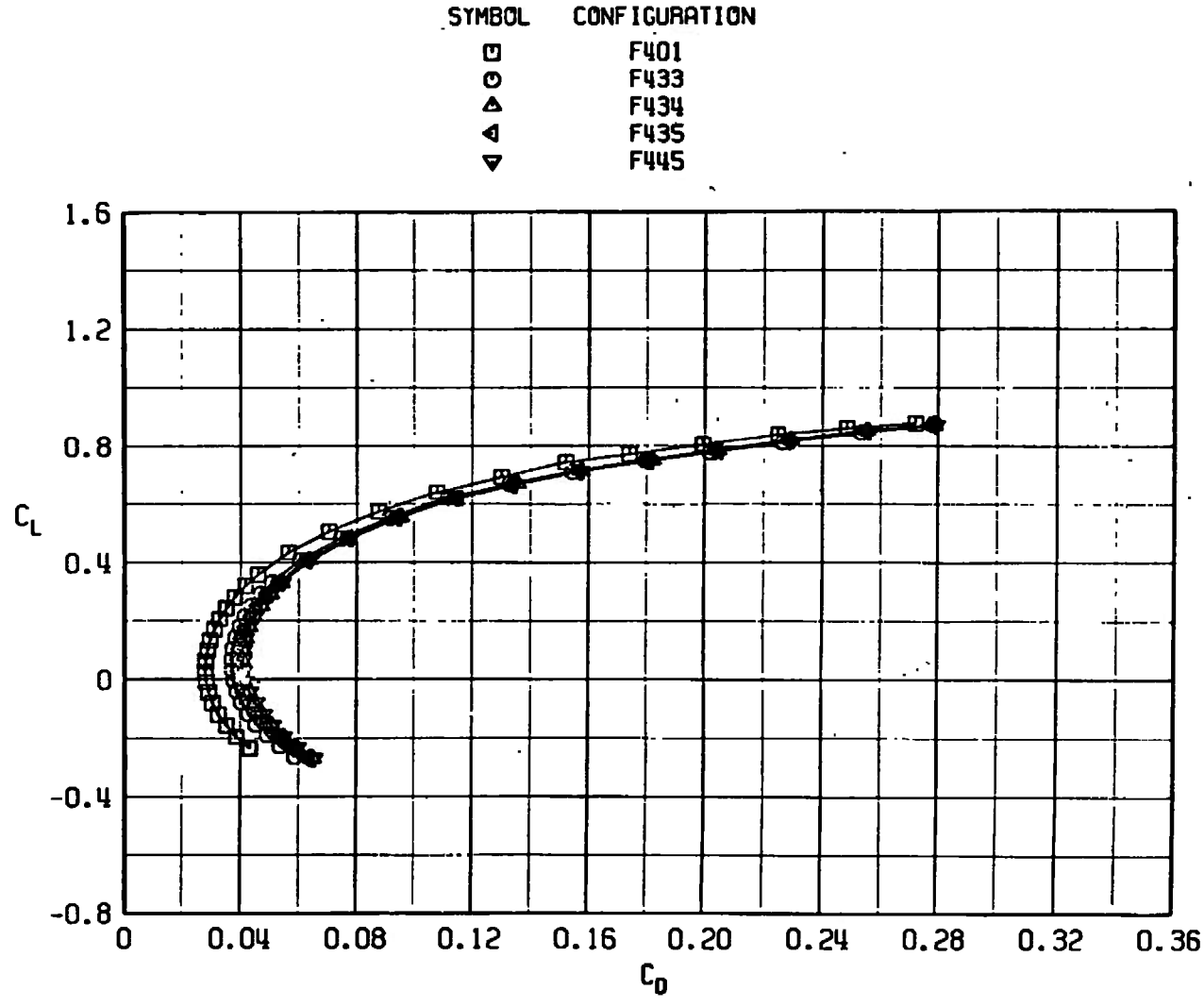

b. $M_\infty = 0.85$

Fig. 39 Continued

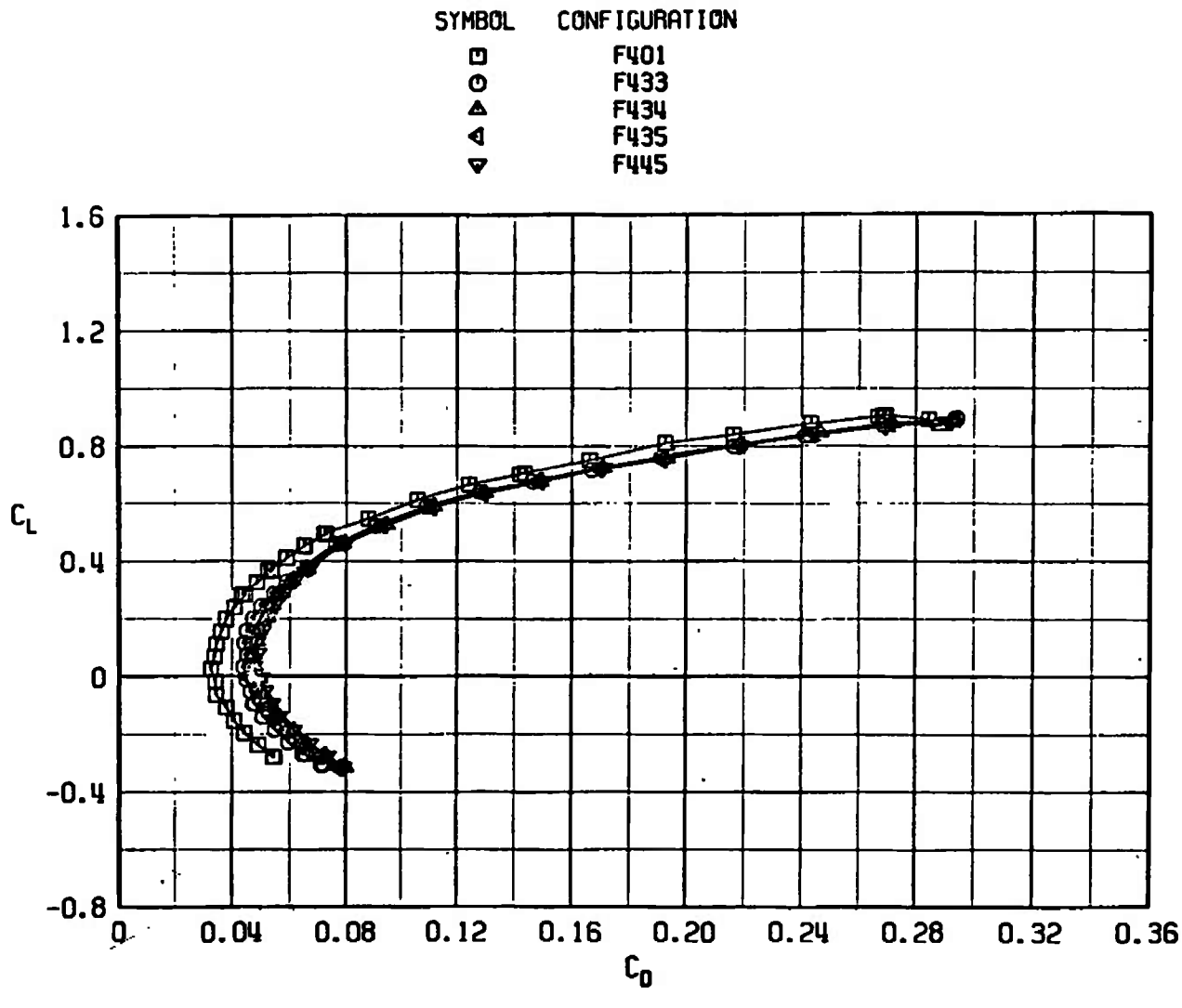

c. $M_\infty = 0.95$

Fig. 39 Continued

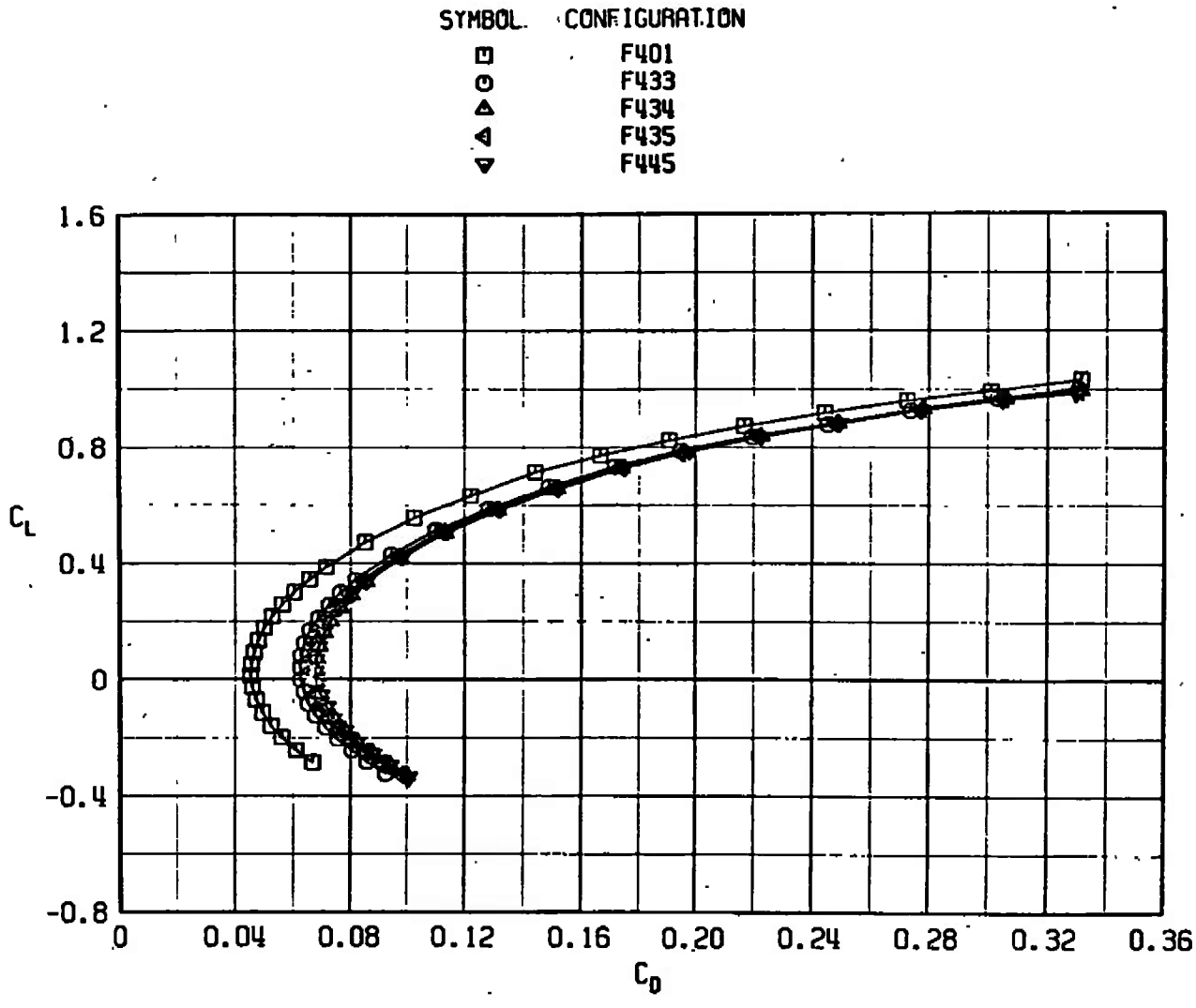

d. $M_\infty = 1.10$

Fig. 39 Continued

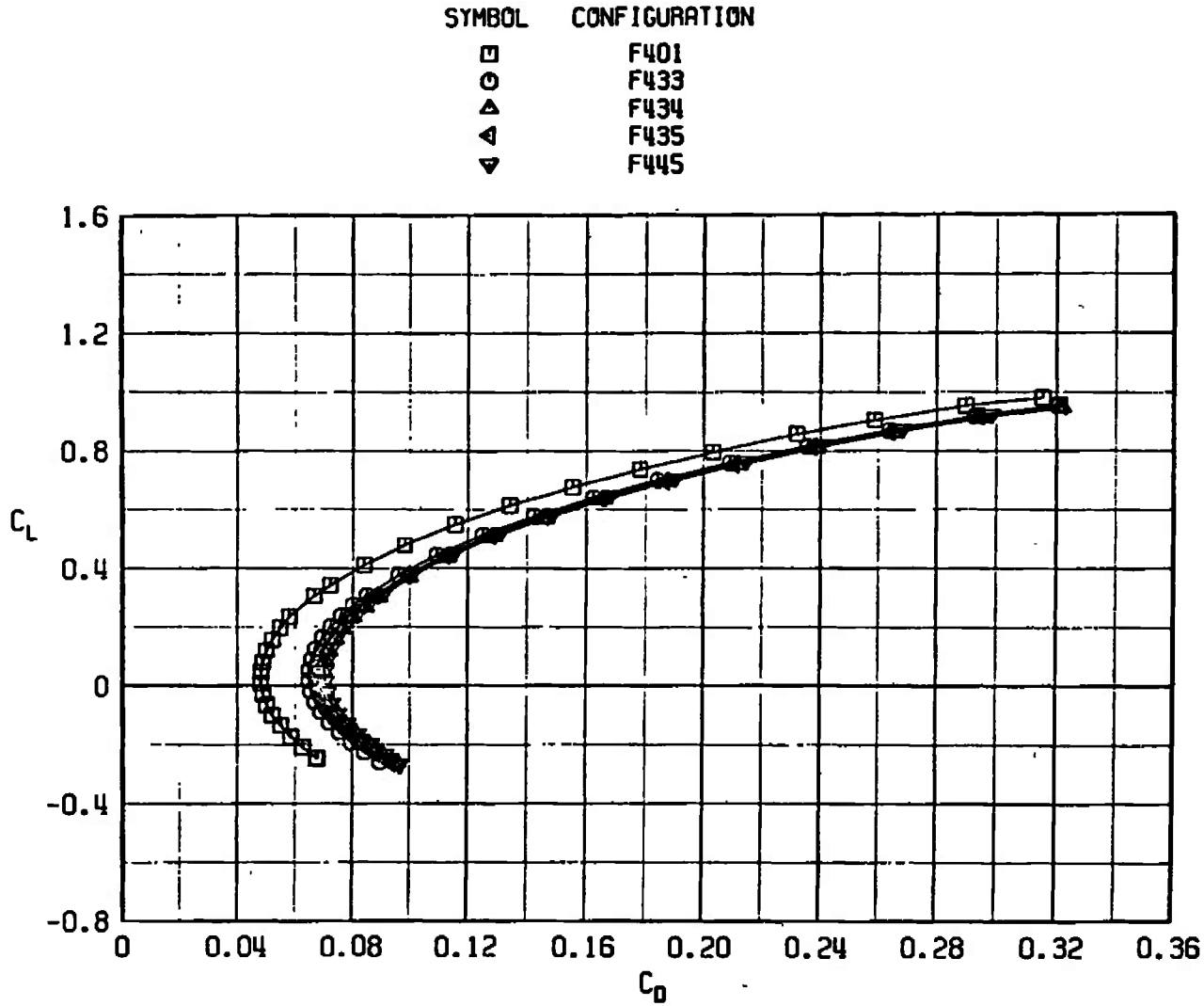

e. $M_\infty = 1.30$

Fig. 39 Concluded

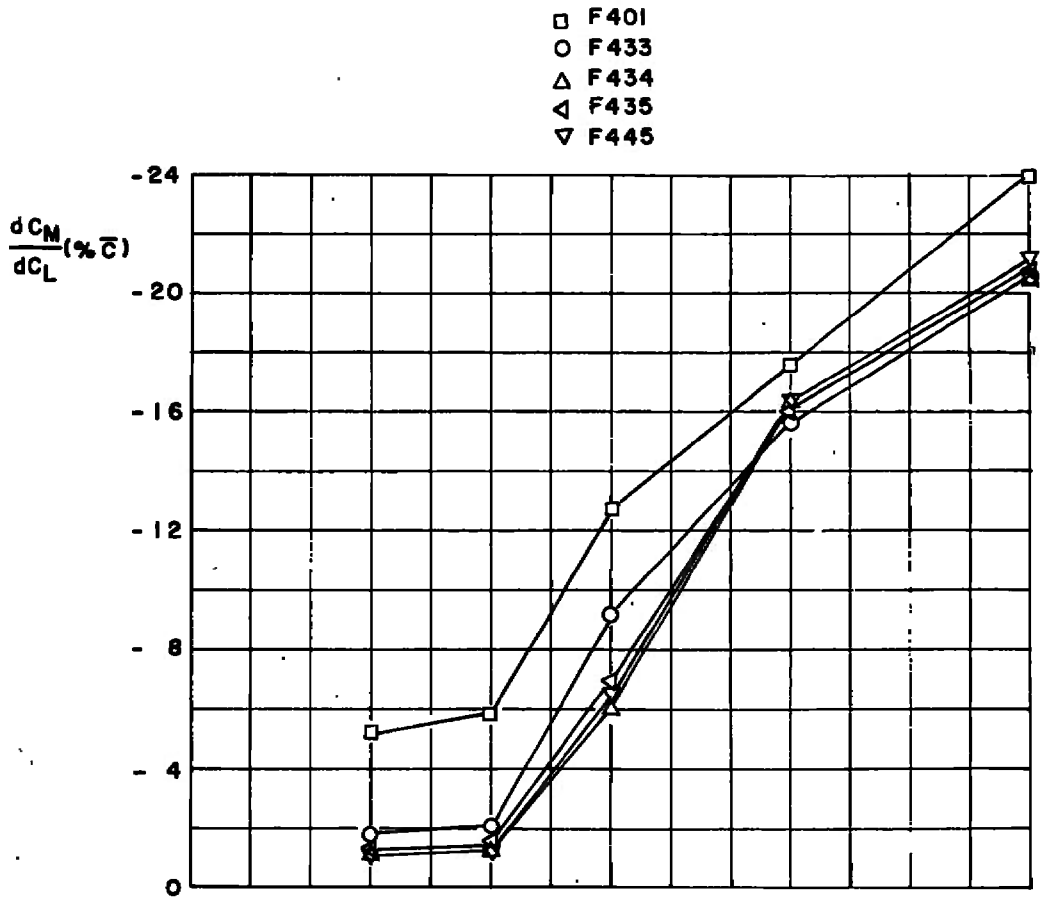

a. dC_m/dC_L versus M_∞ at $C_L = 0.2$ in percentage $\bar{c}$

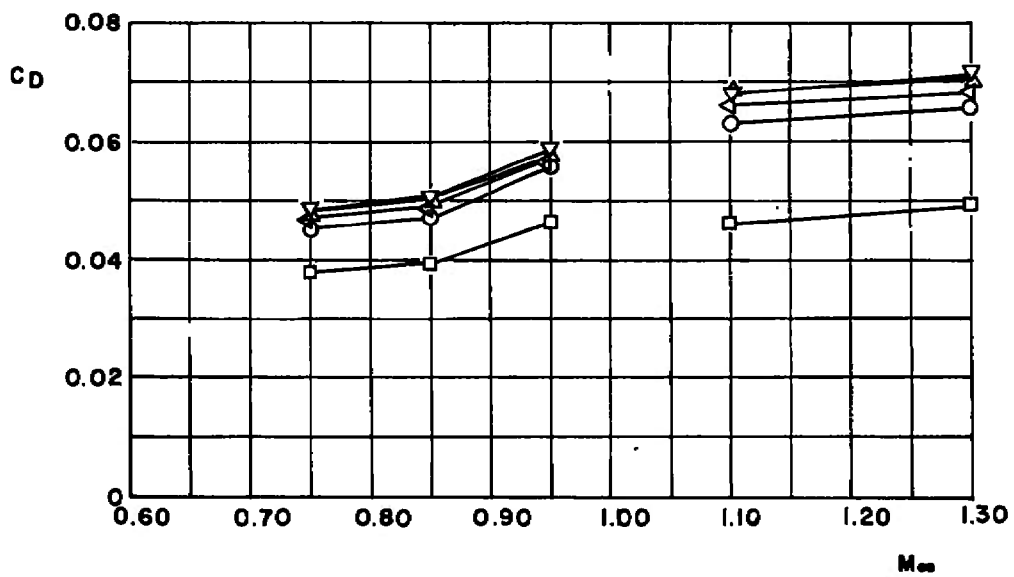

b. C_D versus M_∞ at $C_L = 0.30$, $M_\infty < 1.0$, and $C_L = 0.10$, $M_\infty > 1.0$

Fig. 40 Drag Coefficient and dC_m/dC_L Variation with Mach Number for Configurations F401, F433, F434, F435, and F445

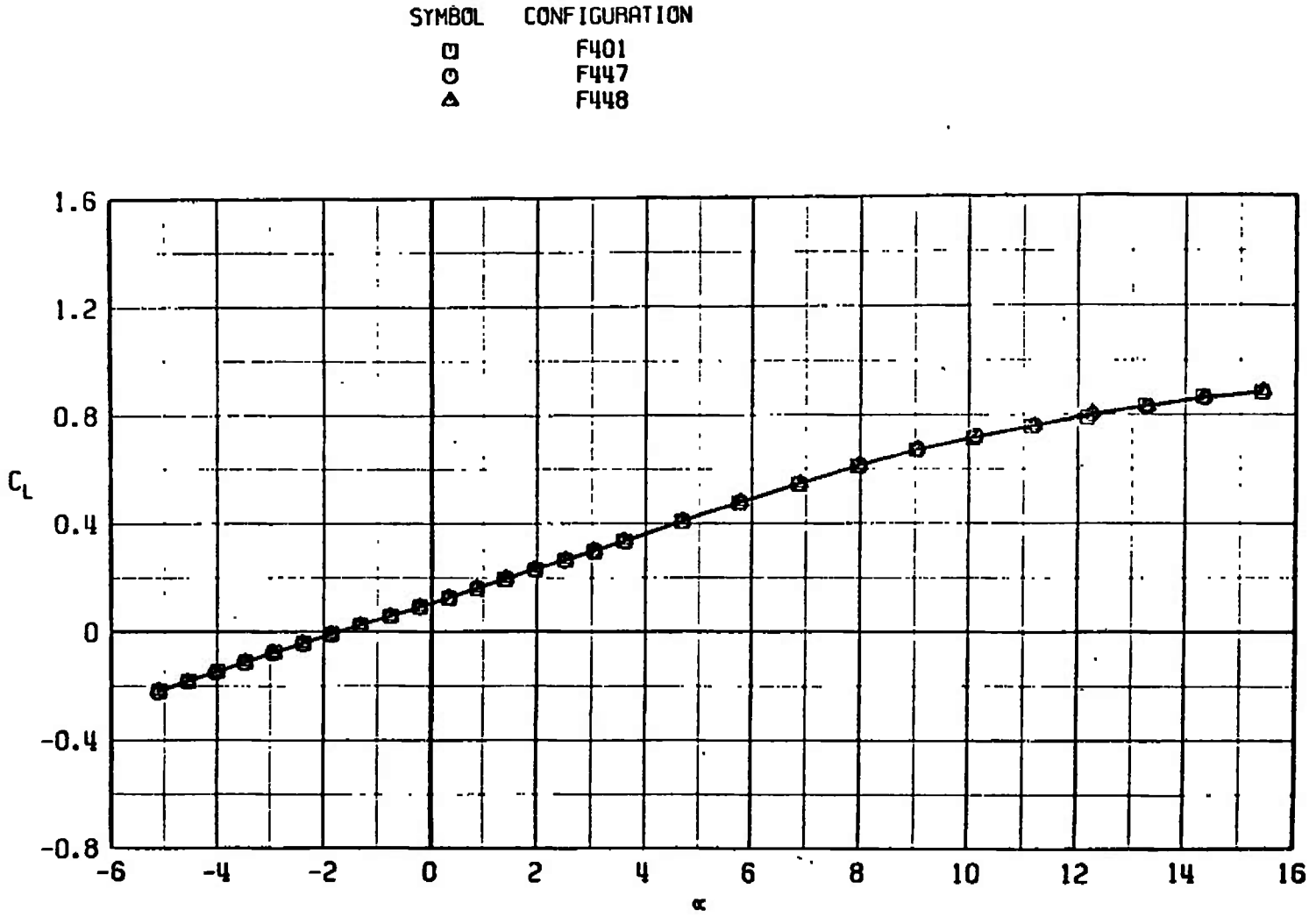

a. $M_\infty = 0.75$

Fig. 41 Lift Coefficient Variation with Angle of Attack for Configurations F401, F447, and F448

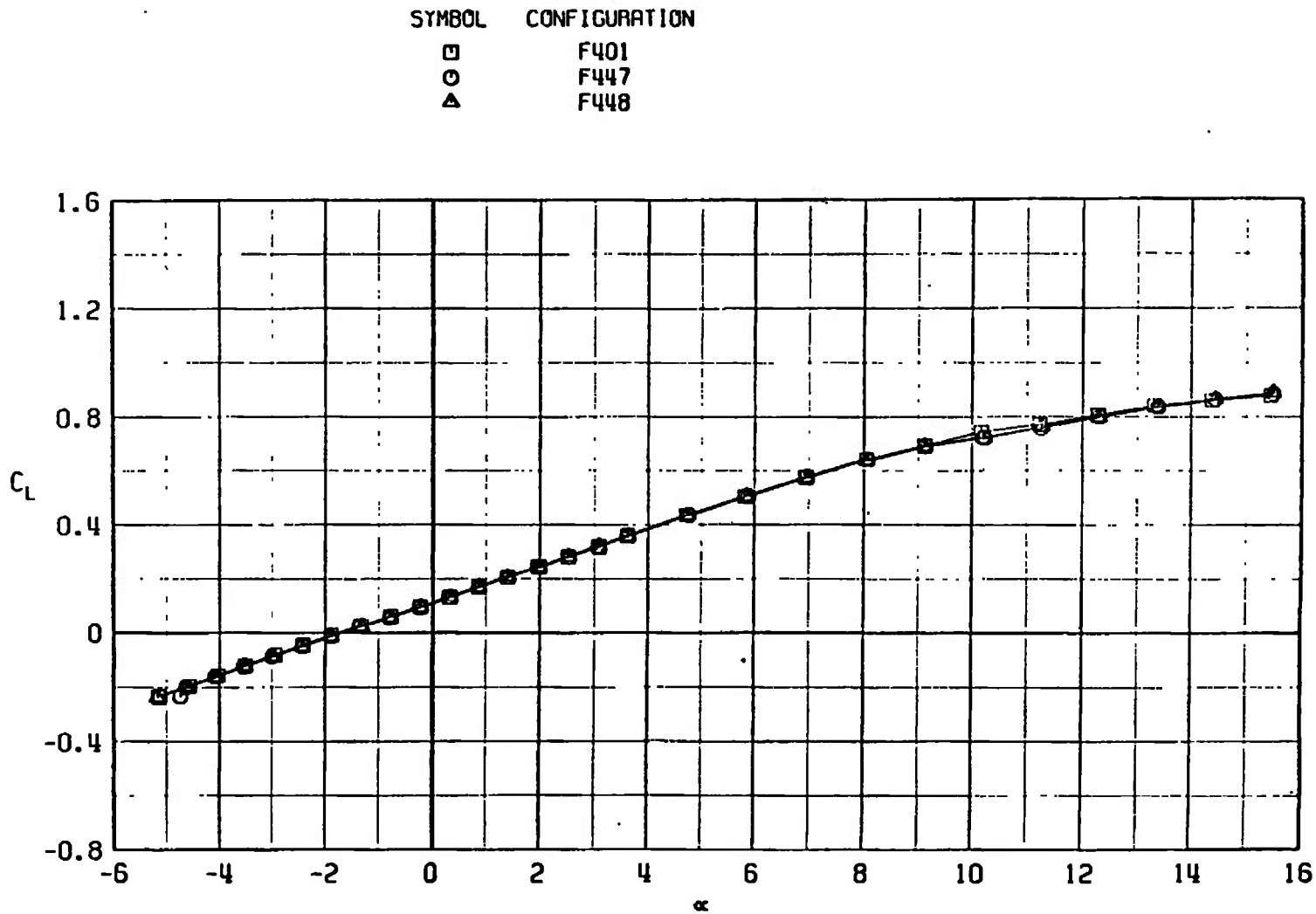

b. $M_\infty = 0.85$
Fig. 41 Continued

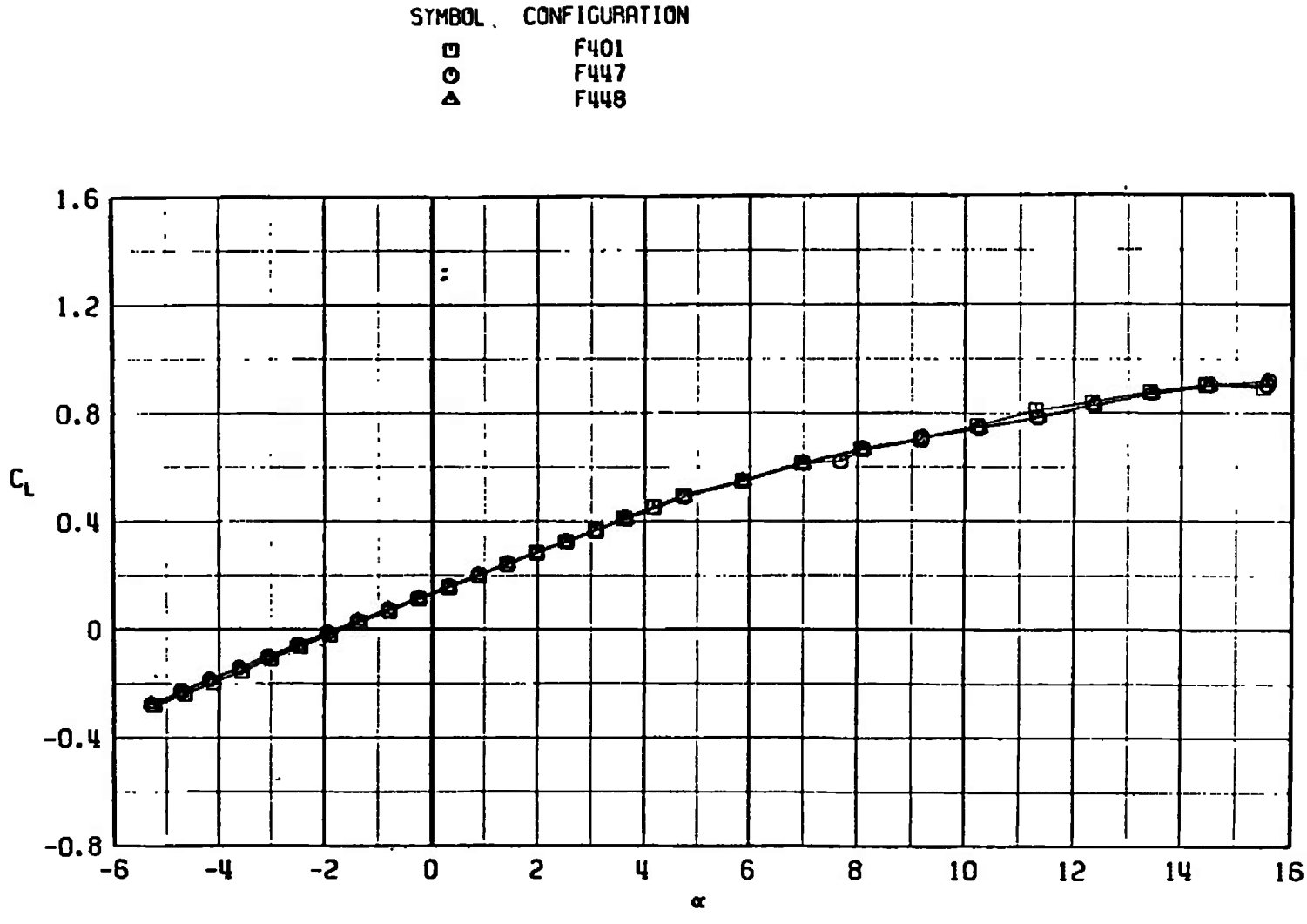

c. $M_\infty = 0.95$

Fig. 41 Continued

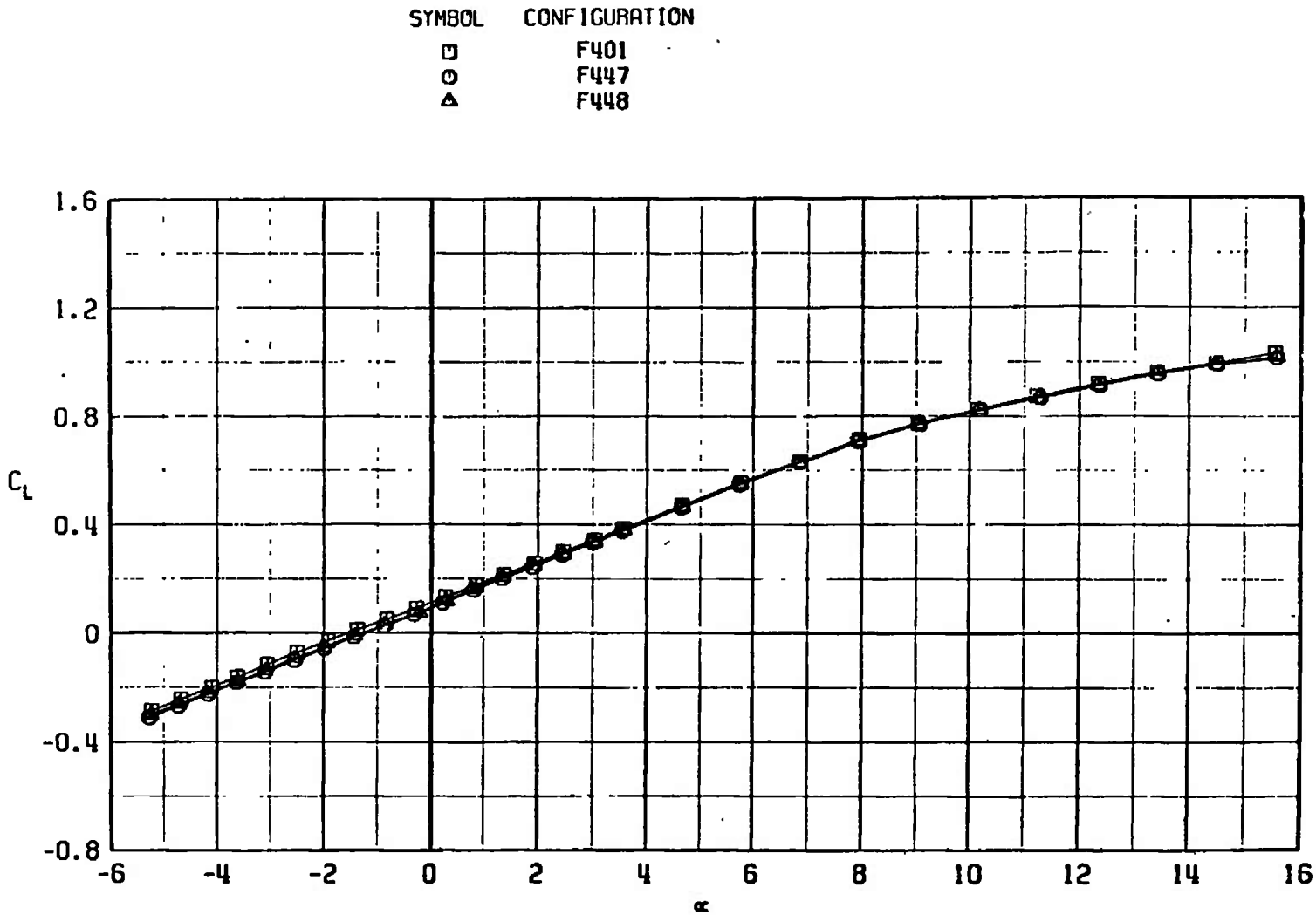

d. $M_\infty = 1.10$

Fig. 41 Continued

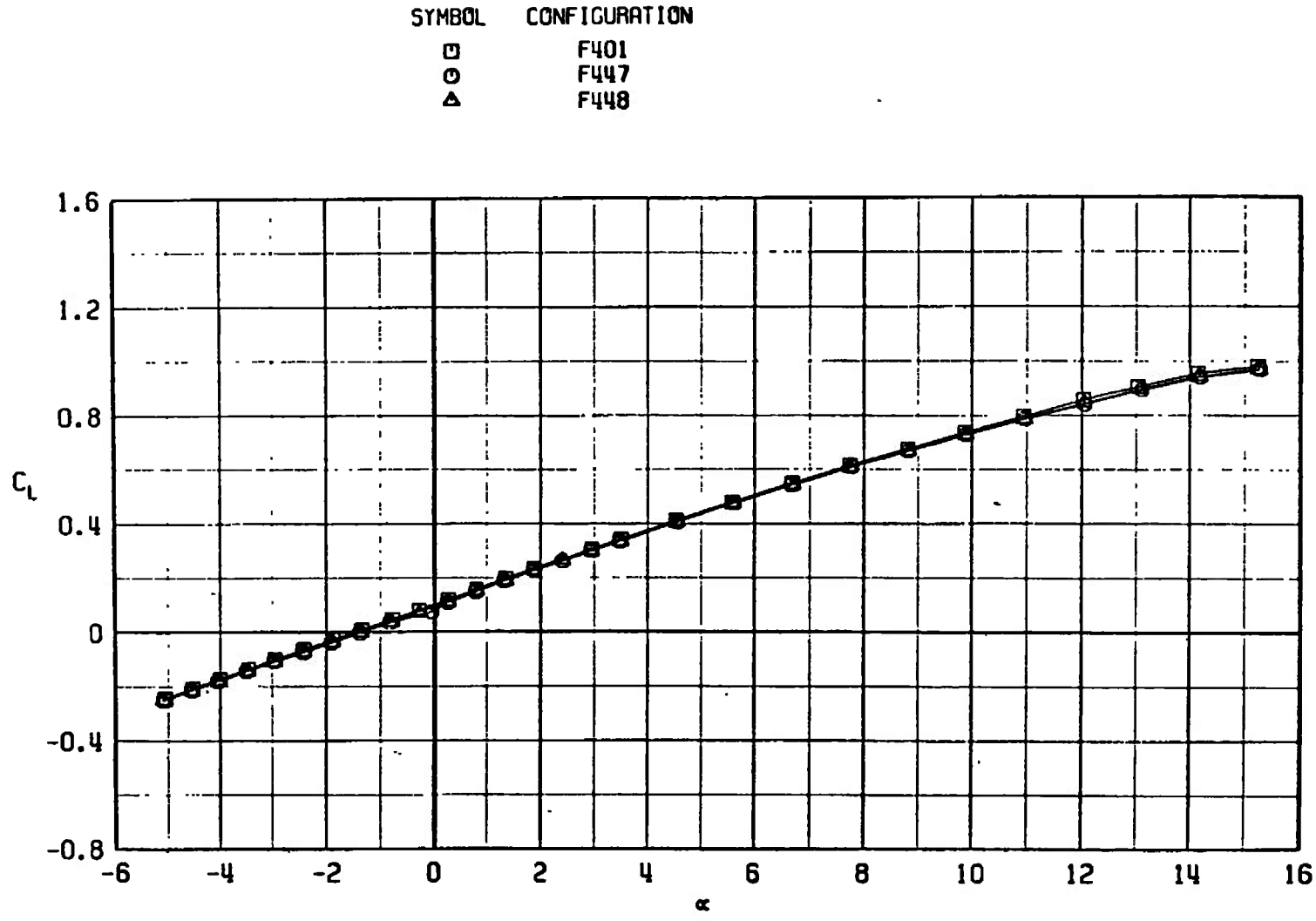

e. $M_\infty = 1.30$

Fig. 41 Concluded

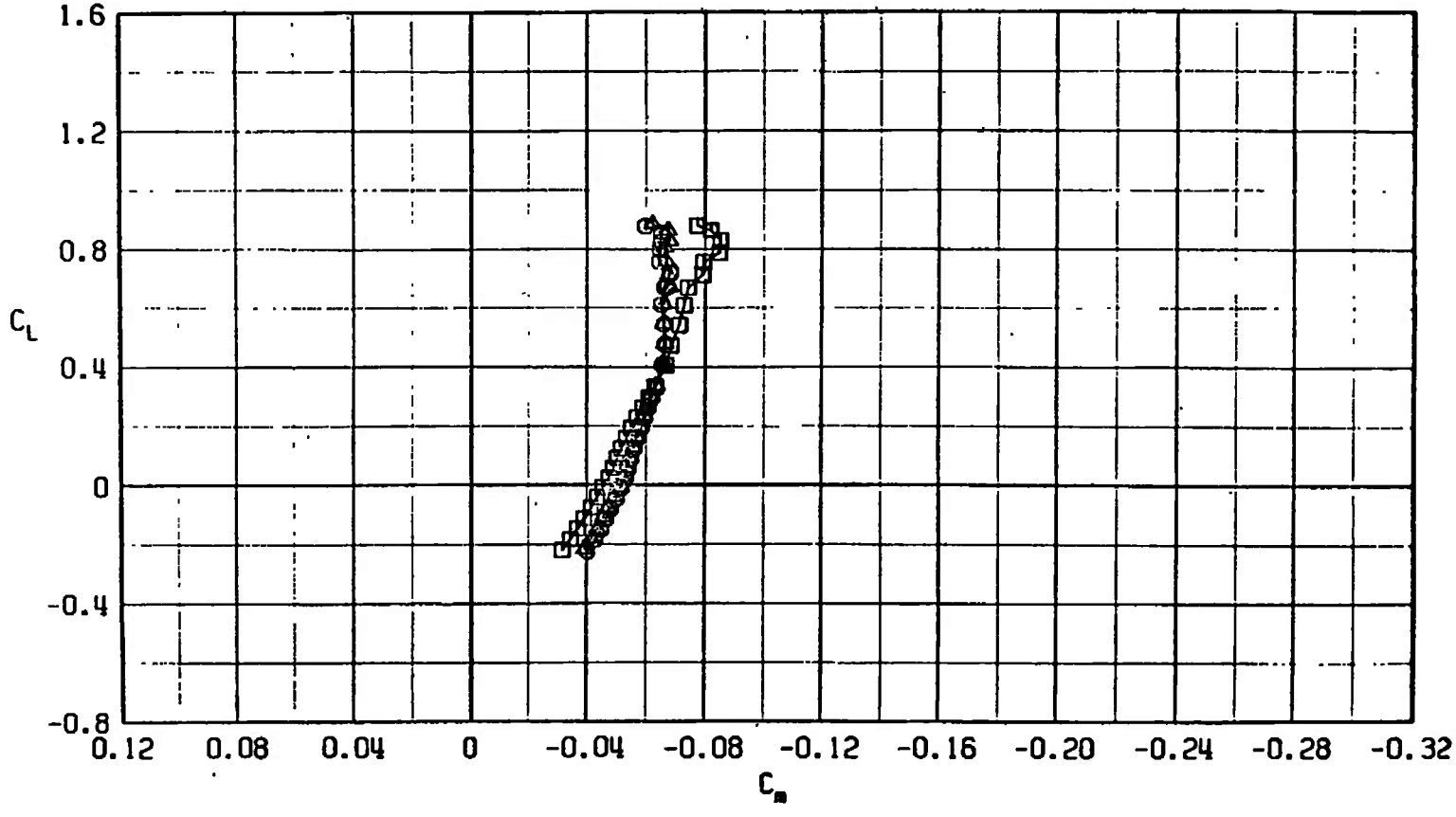

a. $M_\infty = 0.75$

Fig. 42 Pitching-Moment Coefficient Variation with Lift Coefficient for Configurations F401, F447, and F448

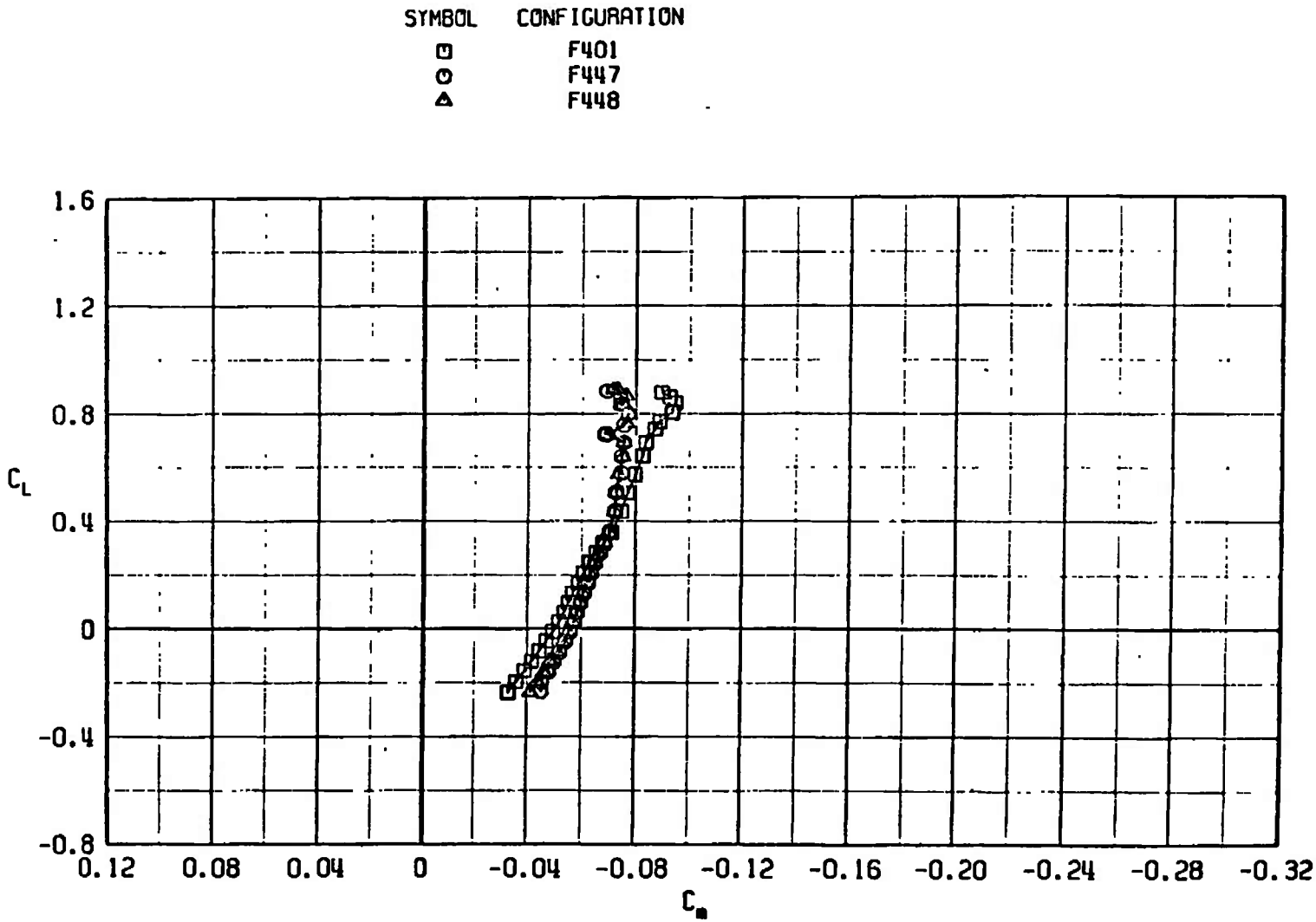

b. $M_\infty = 0.85$

Fig. 42 Continued

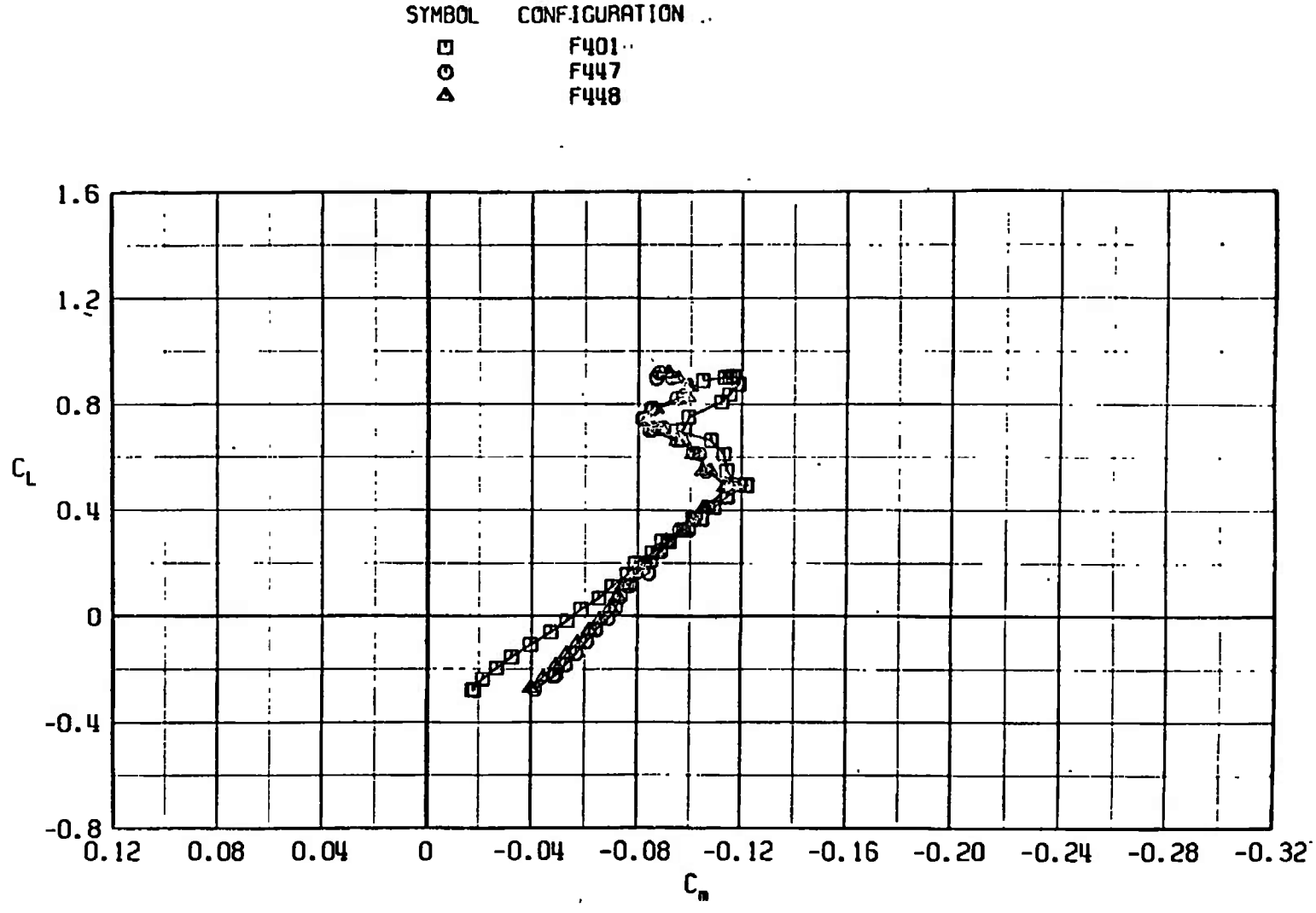

c. $M_\infty = 0.95$

Fig. 42 Continued

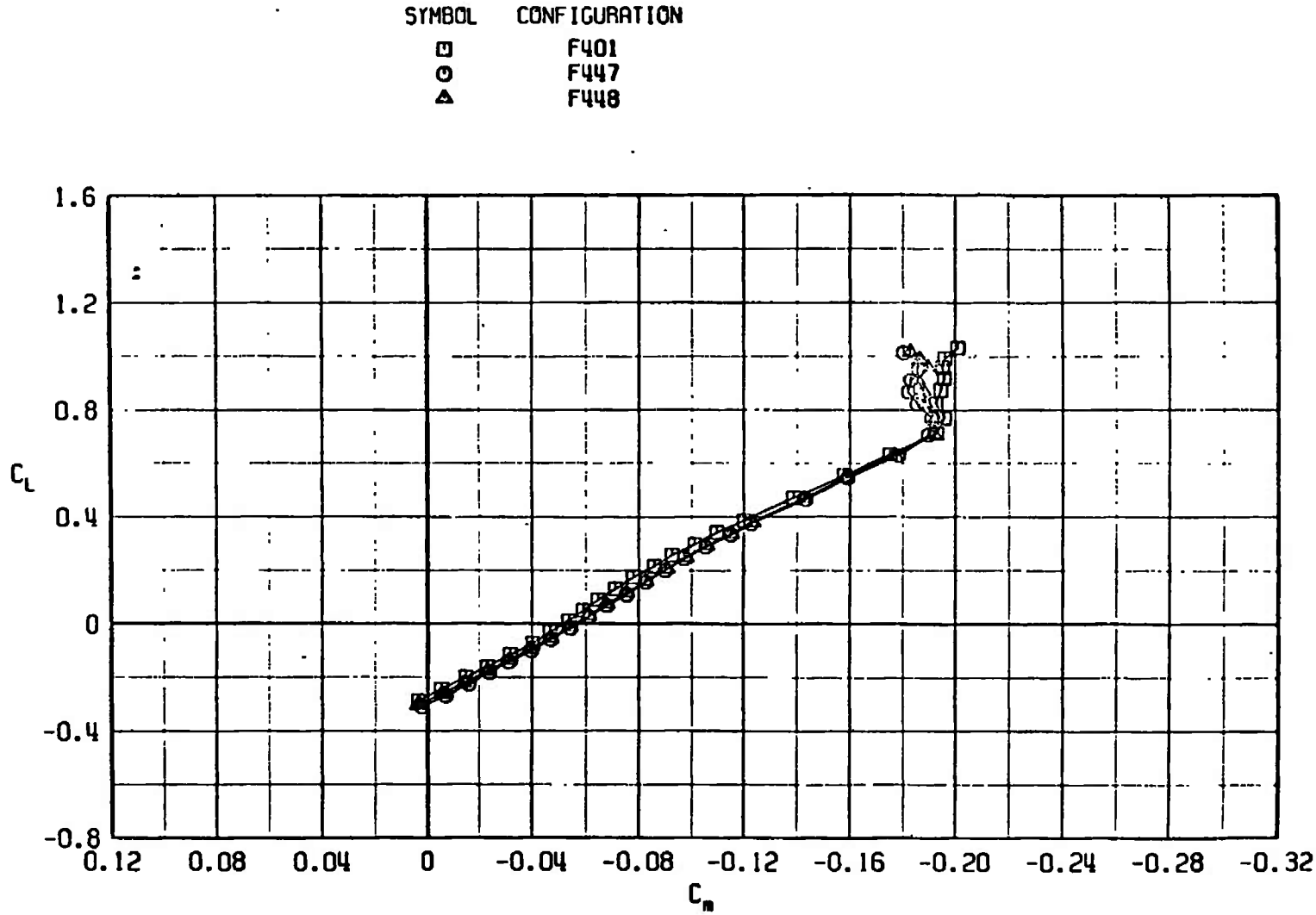

d. $M_\infty = 1.10$

Fig. 42 Continued

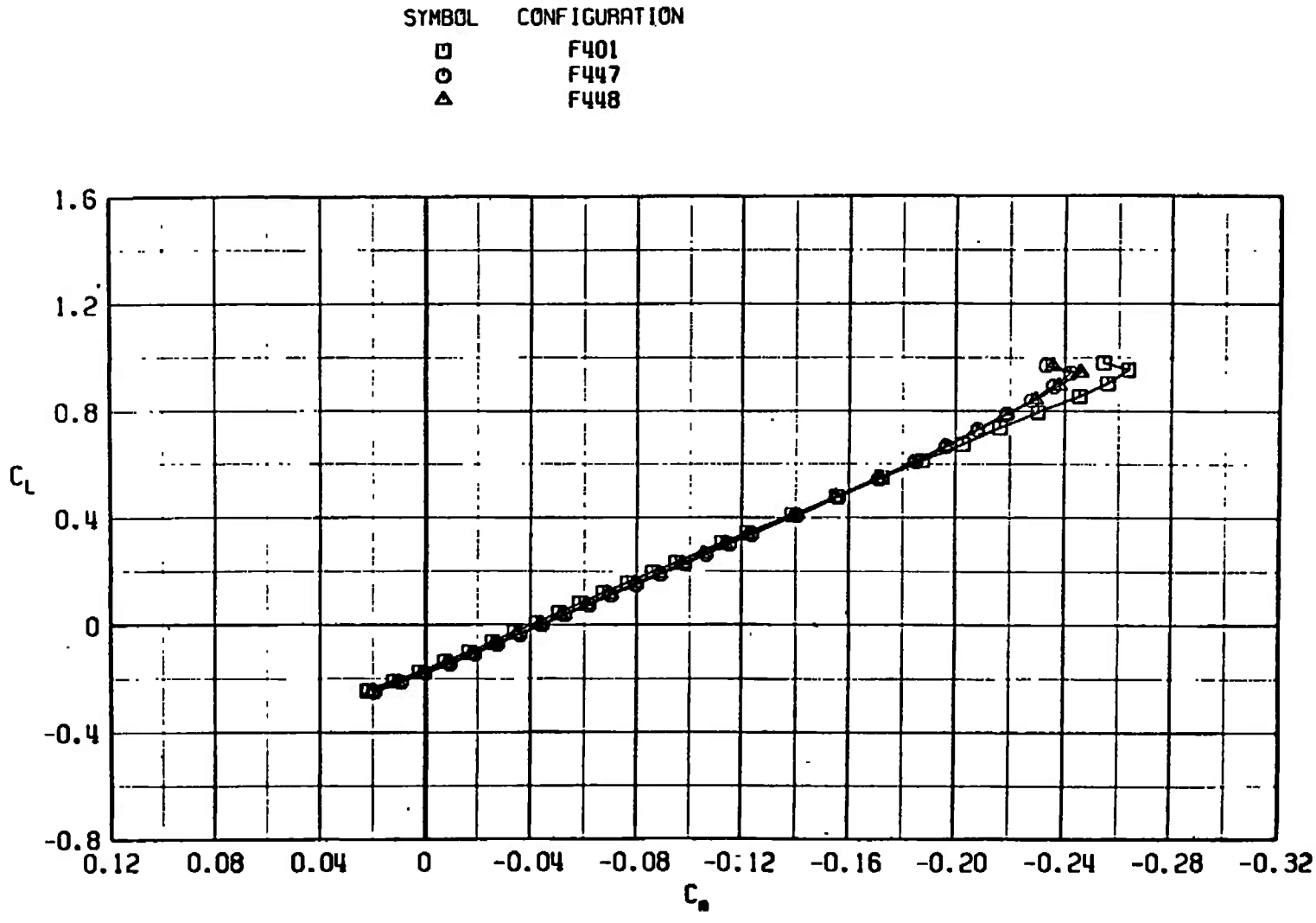

e. $M_\infty = 1.30$

Fig. 42 Concluded

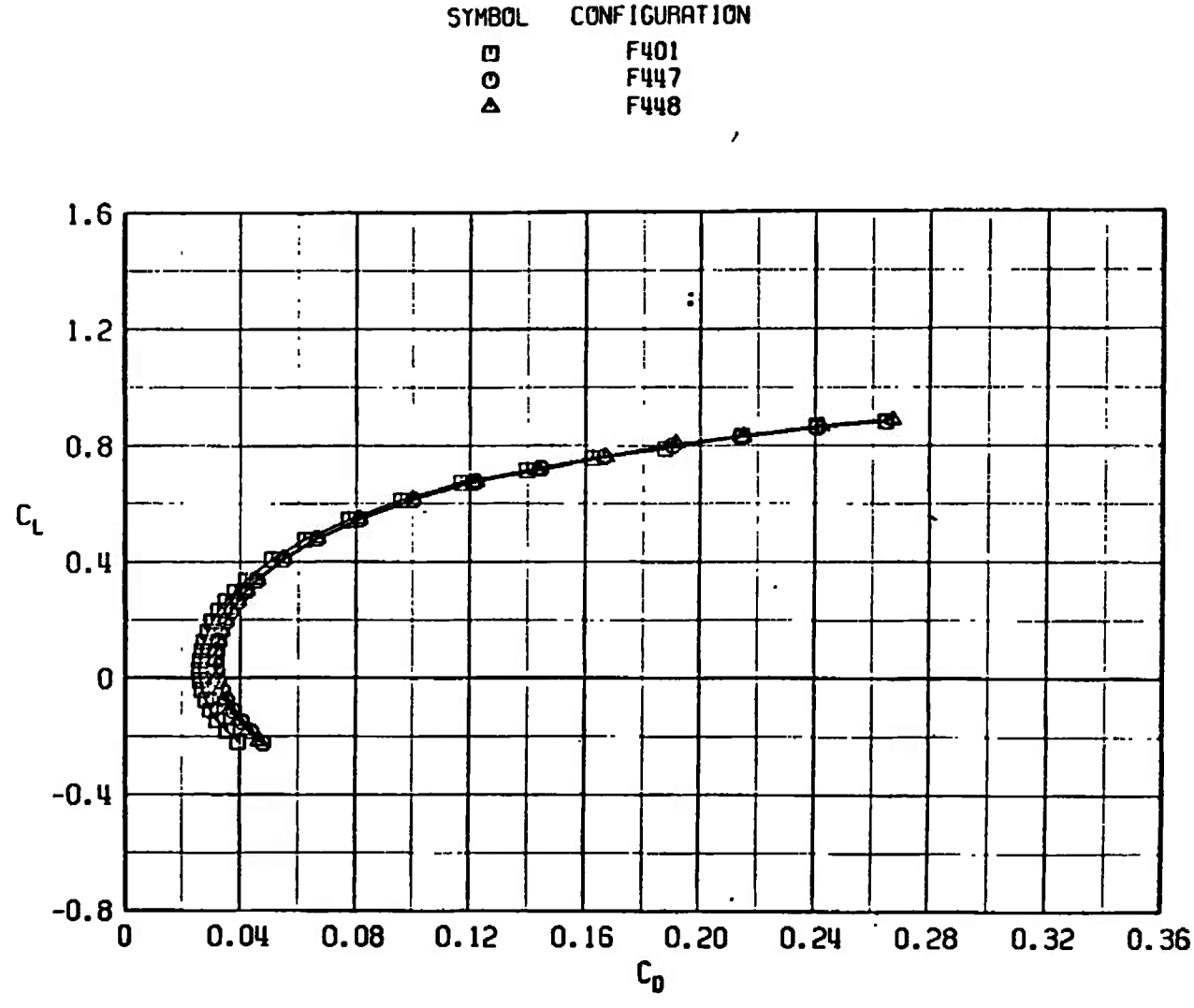

a. $M_\infty = 0.75$

Fig. 43 Drag Coefficient Variation with Lift Coefficient for Configurations F401, F447, and F448

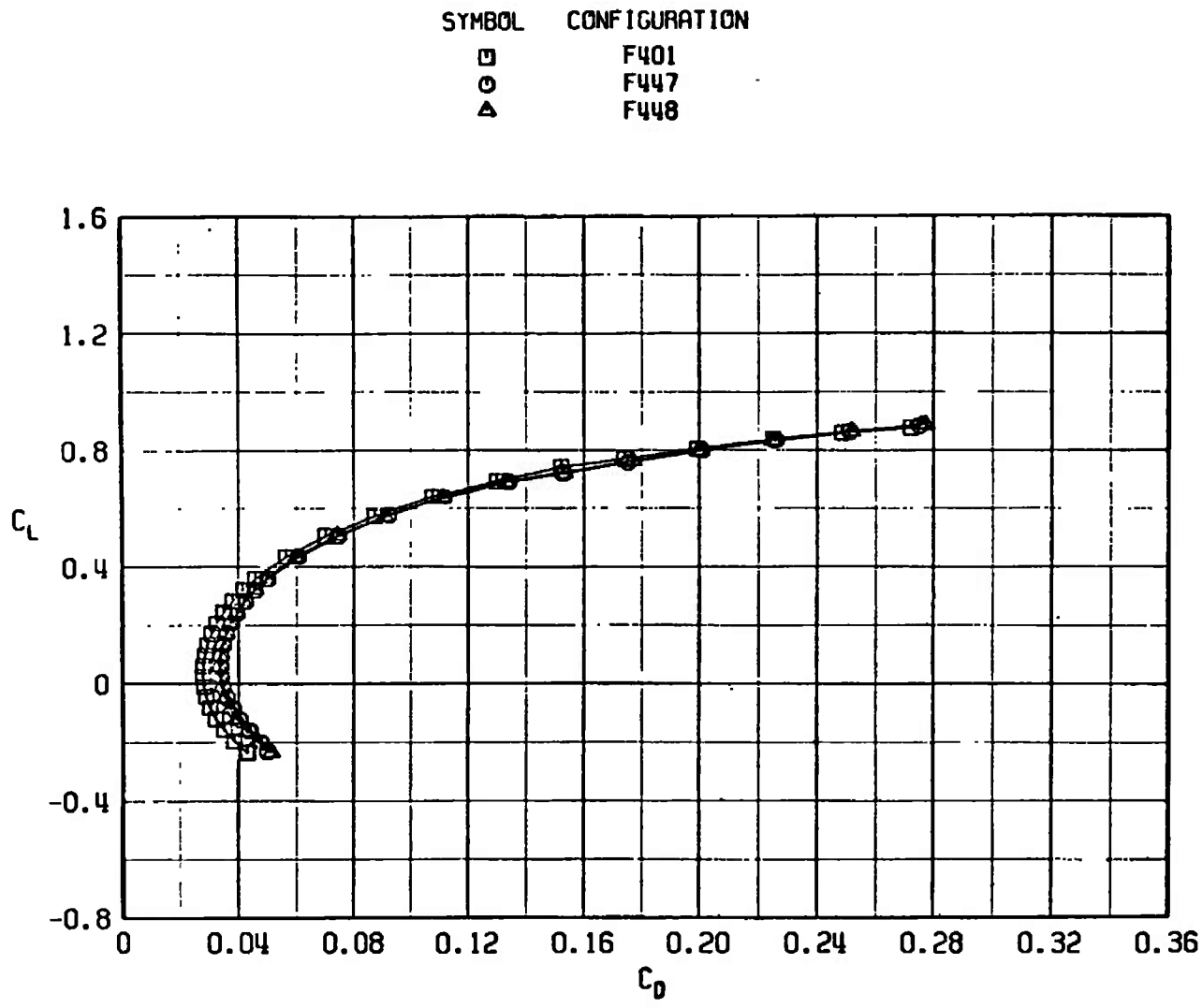

b. $M_\infty = 0.85$

Fig. 43 Continued

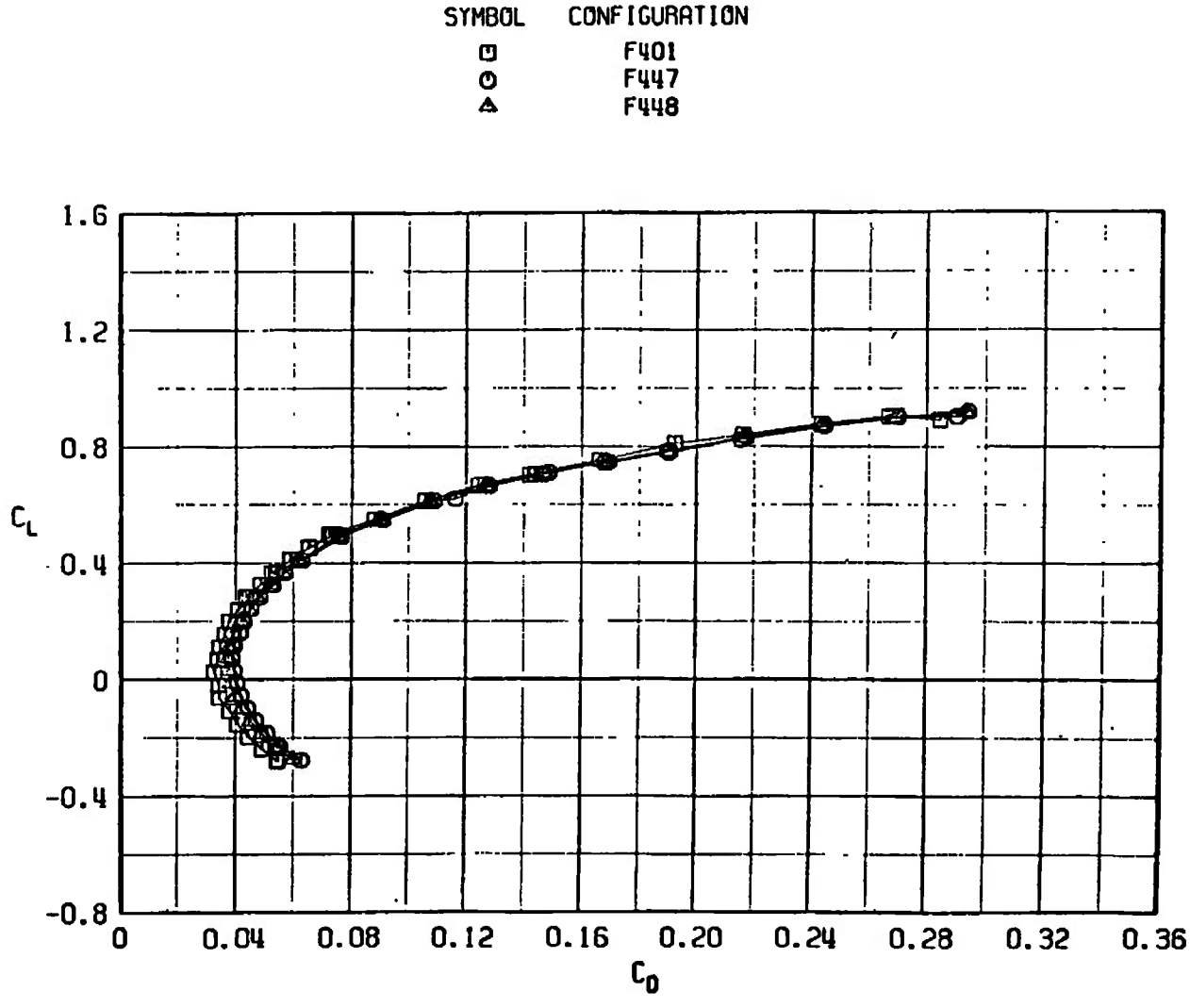

c. $M_\infty = 0.95$

Fig. 43 Continued

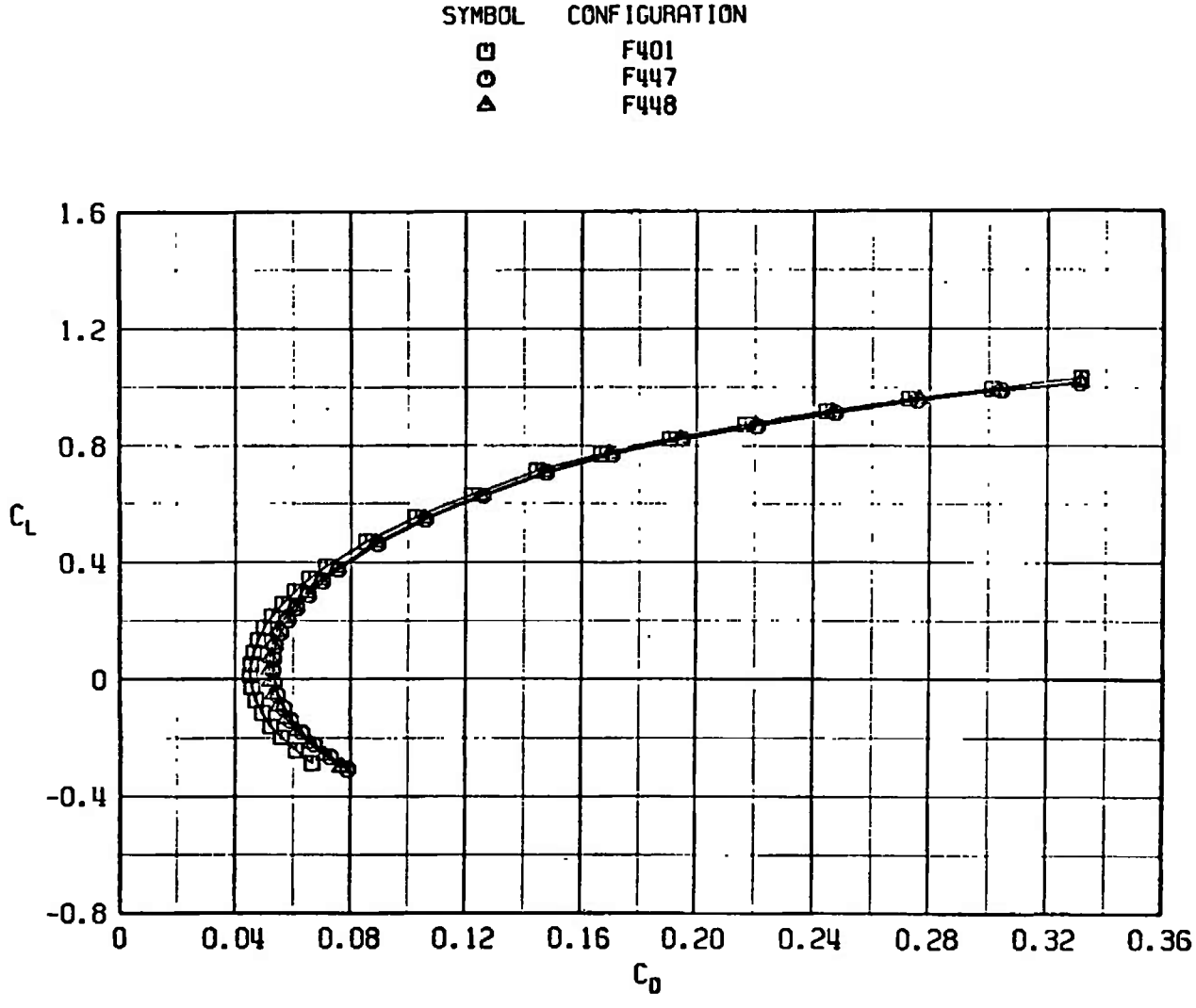

d. $M_\infty = 1.10$

Fig. 43 Continued

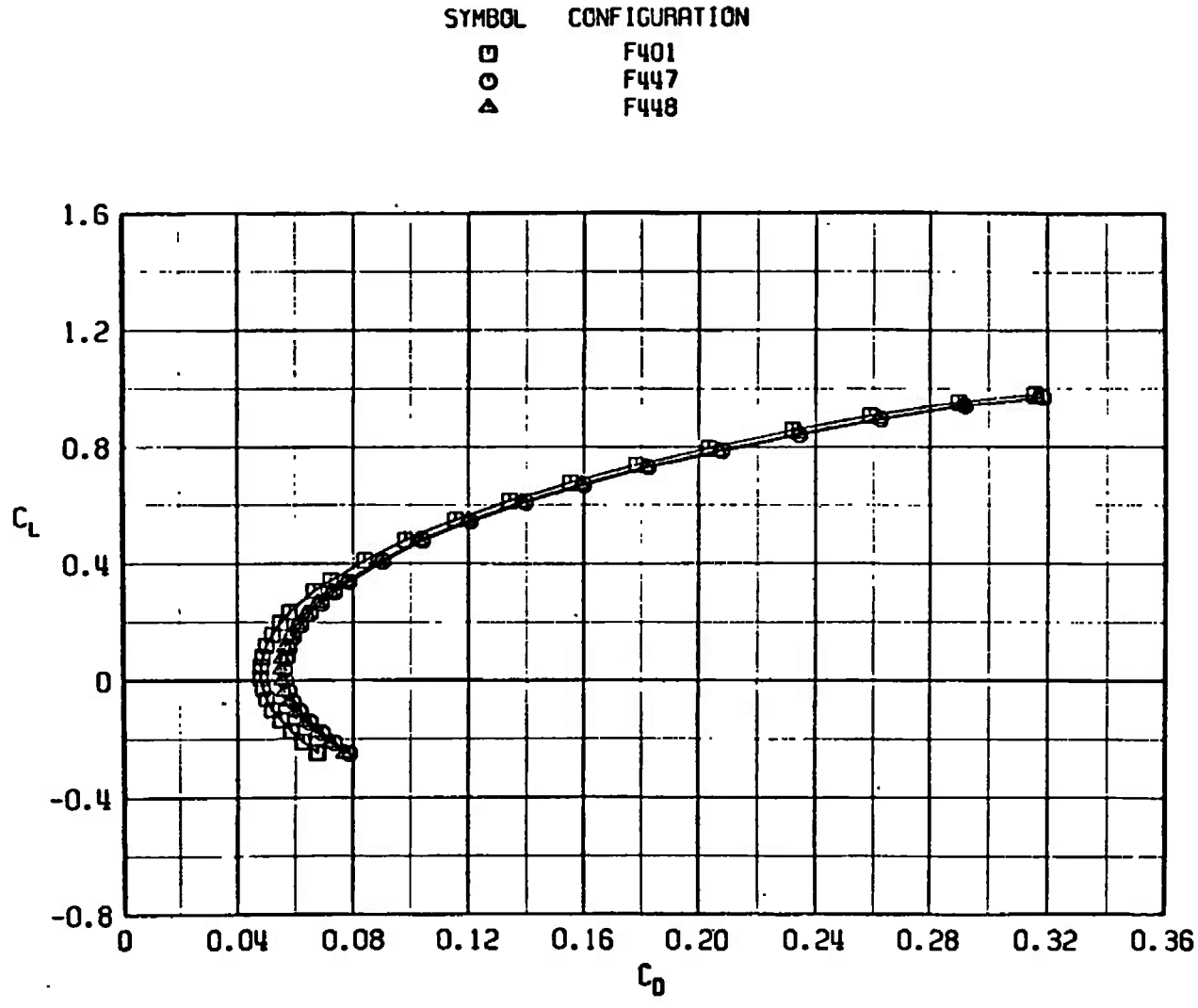

e. $M_\infty = 1.30$

Fig. 43 Concluded

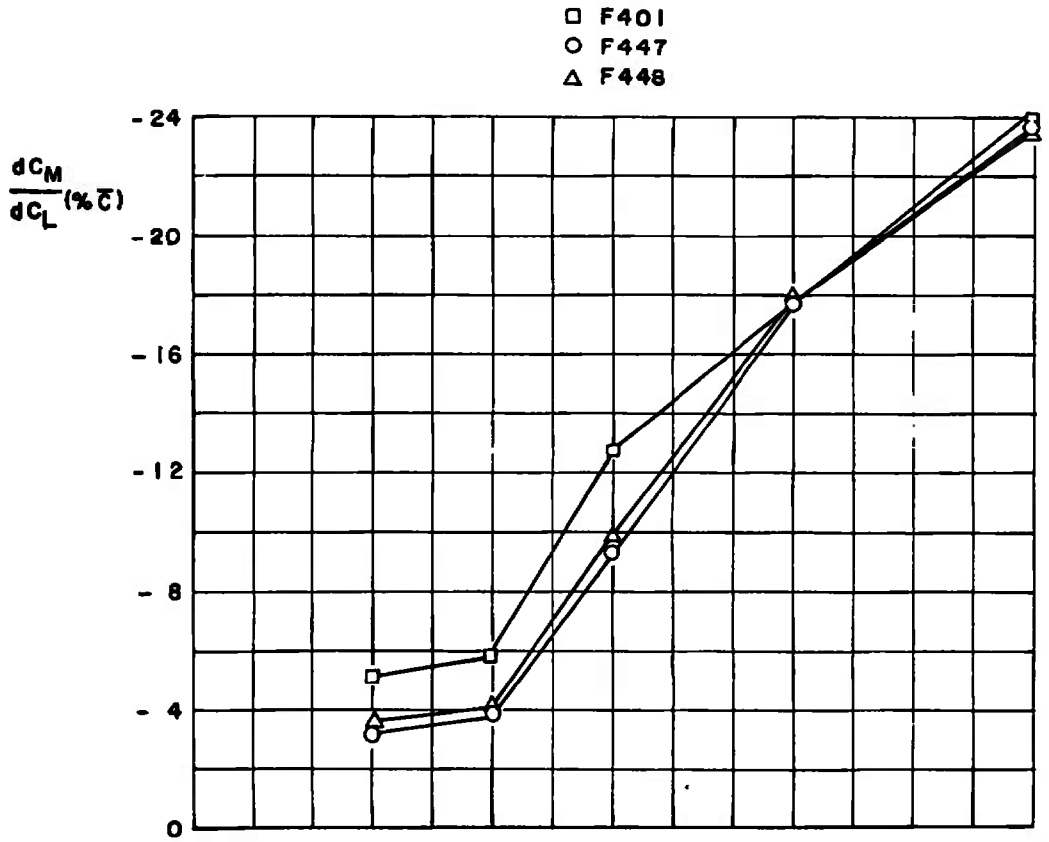

a. dC_m/dC_L versus M_∞ at $C_L = 0.20$ in percentage of $\bar{c}$

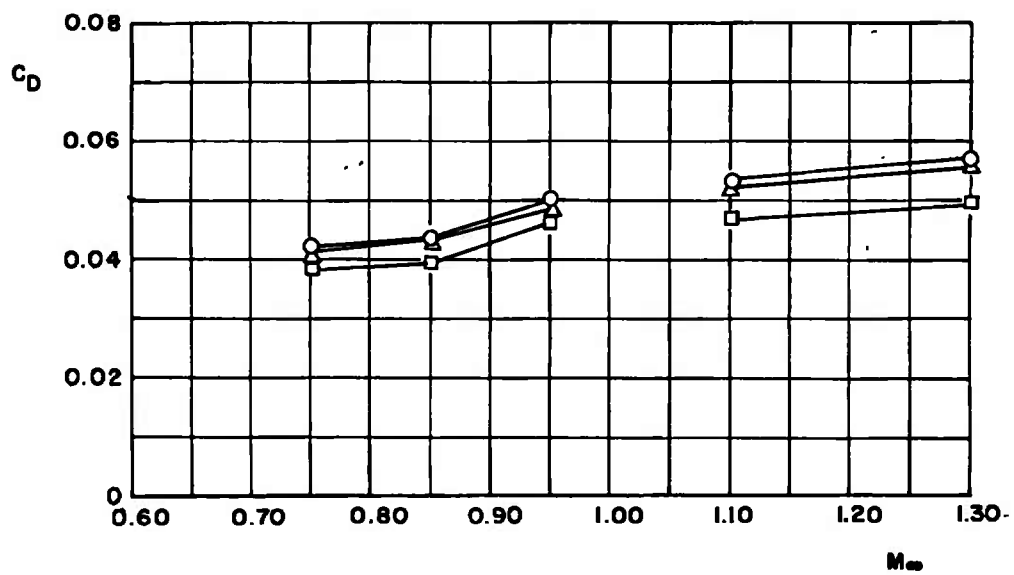

b. C_D versus M_∞ at $C_L = 0.30$, $M_\infty < 1.0$, and $C_L = 0.10$, $M_\infty > 1.0$

Fig. 44 Drag Coefficient and dC_m/dC_L Variation with Mach Number for Configurations F401, F447, and F448

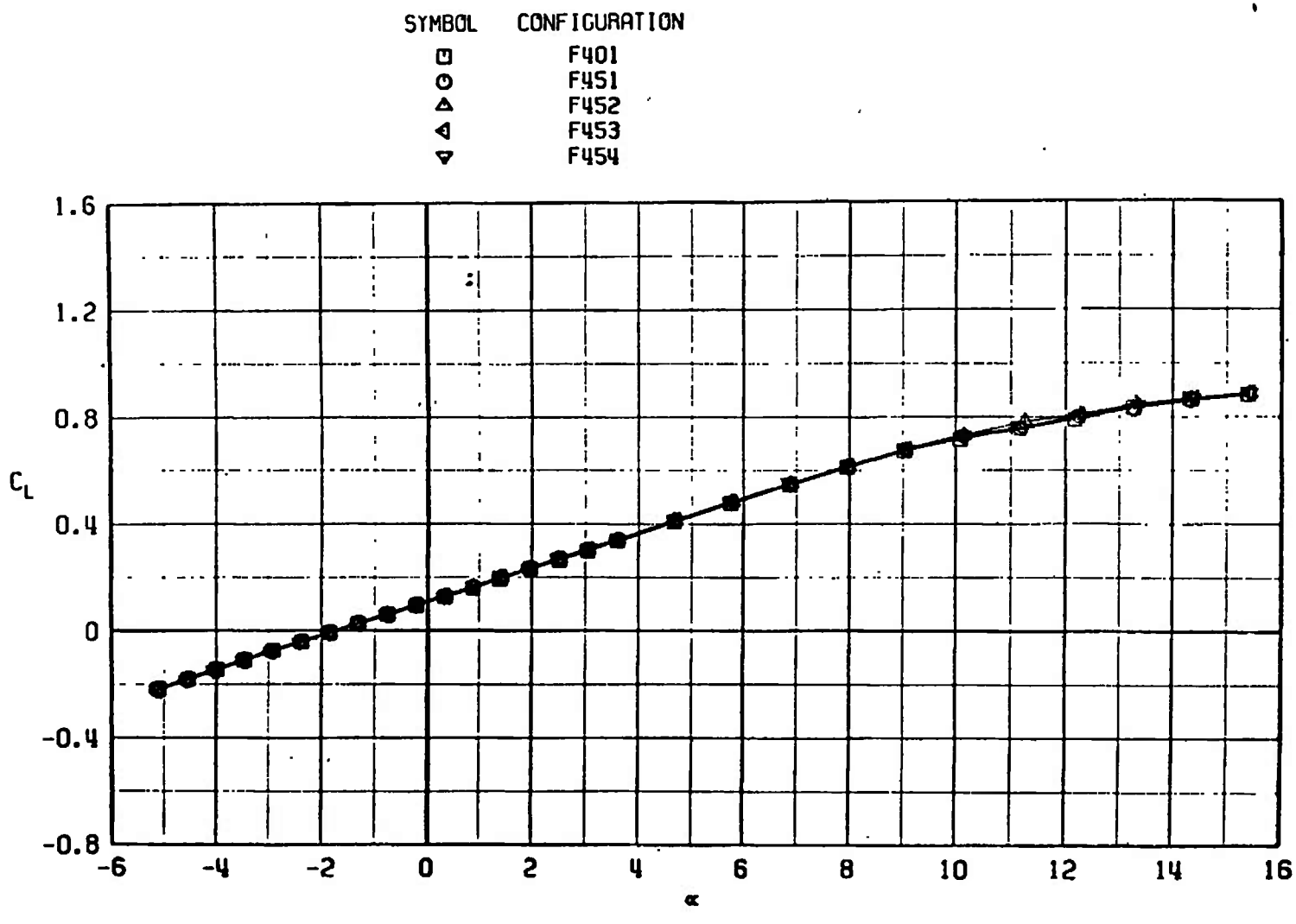

a. $M_\infty = 0.75$

Fig. 45 Lift Coefficient Variation with Angle of Attack for Configurations F401, F451, F452, F453, and F454

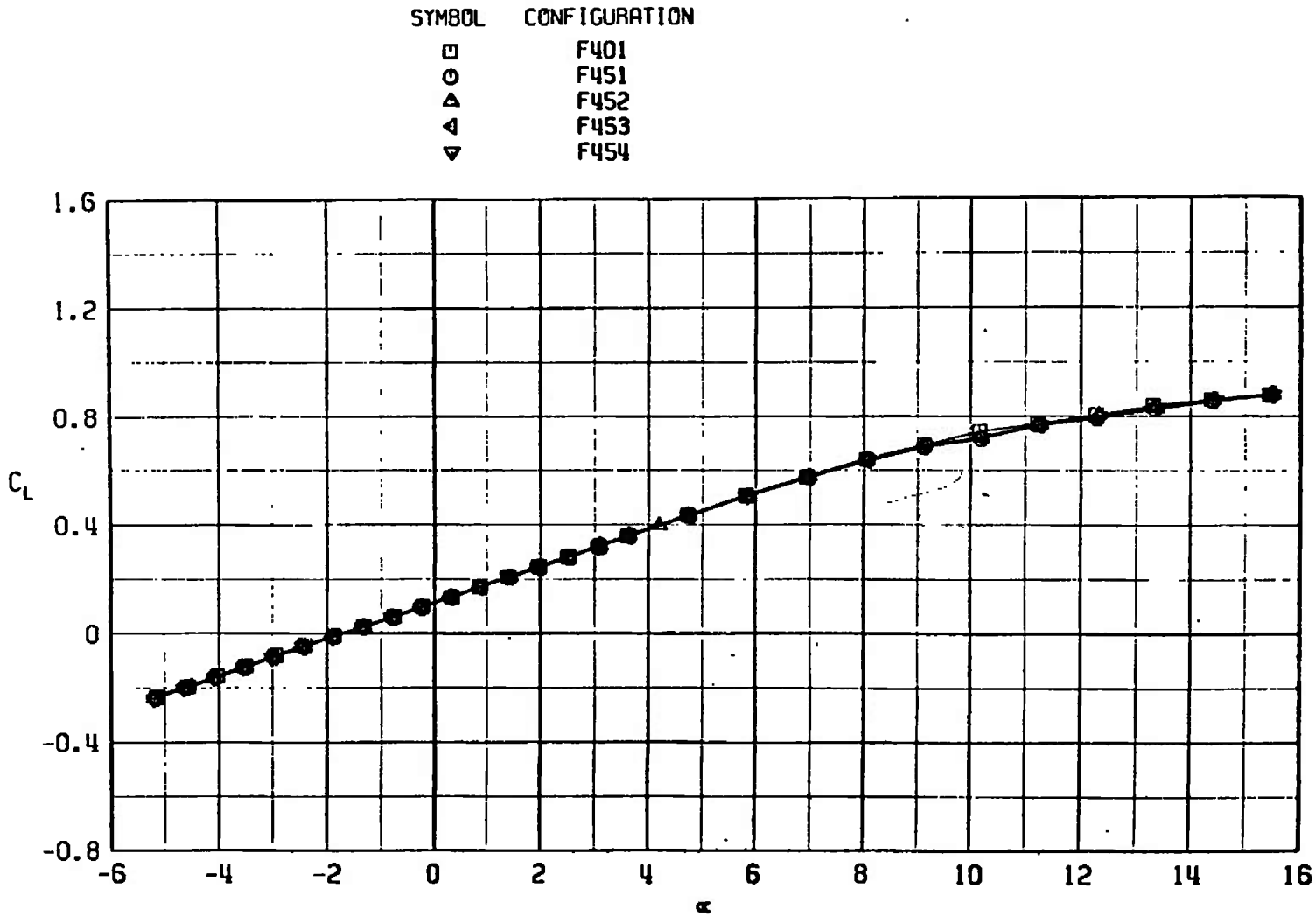

b. $M_\infty = 0.85$

Fig. 45 Continued

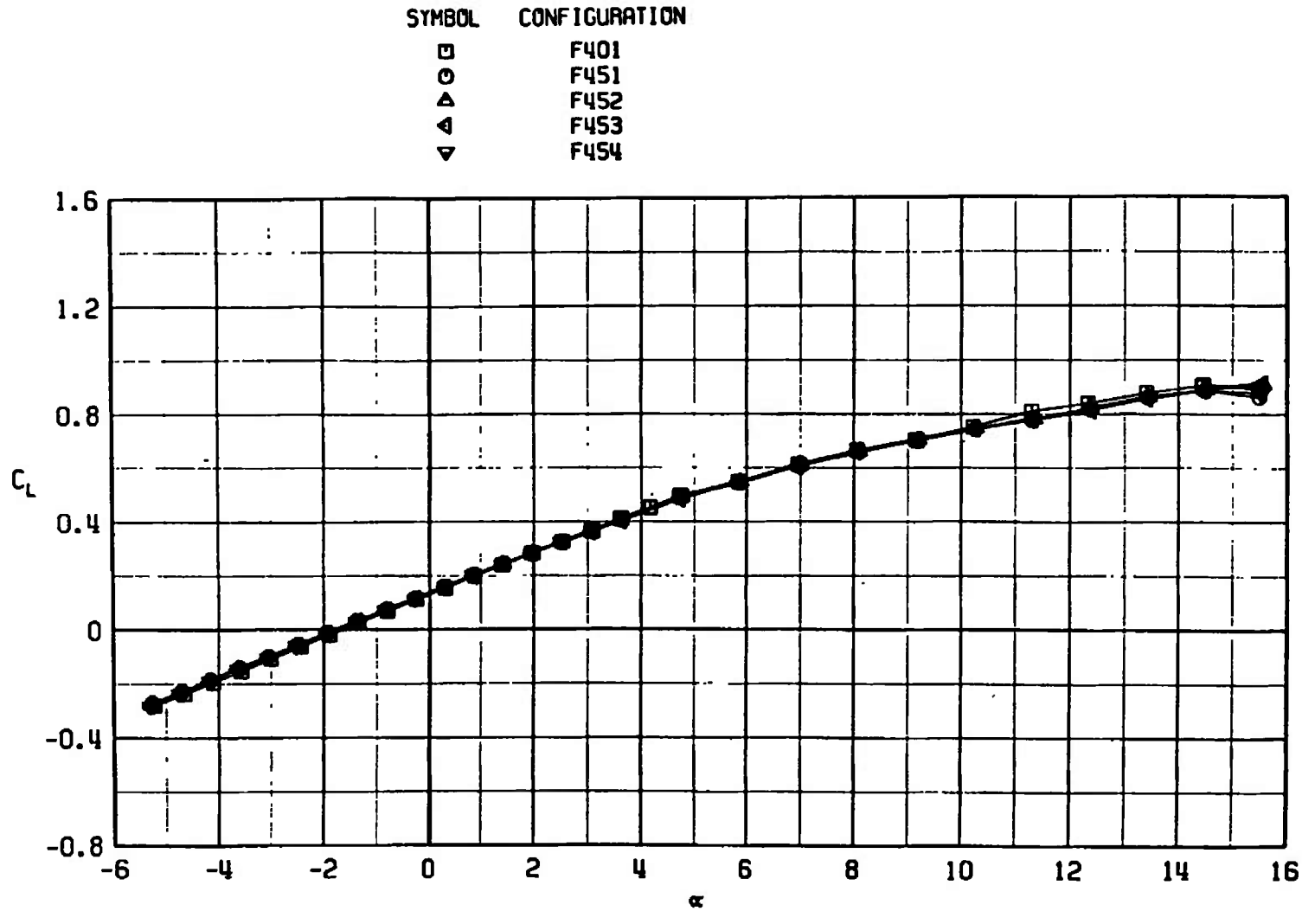

c. $M_\infty = 0.95$

Fig. 45 Continued

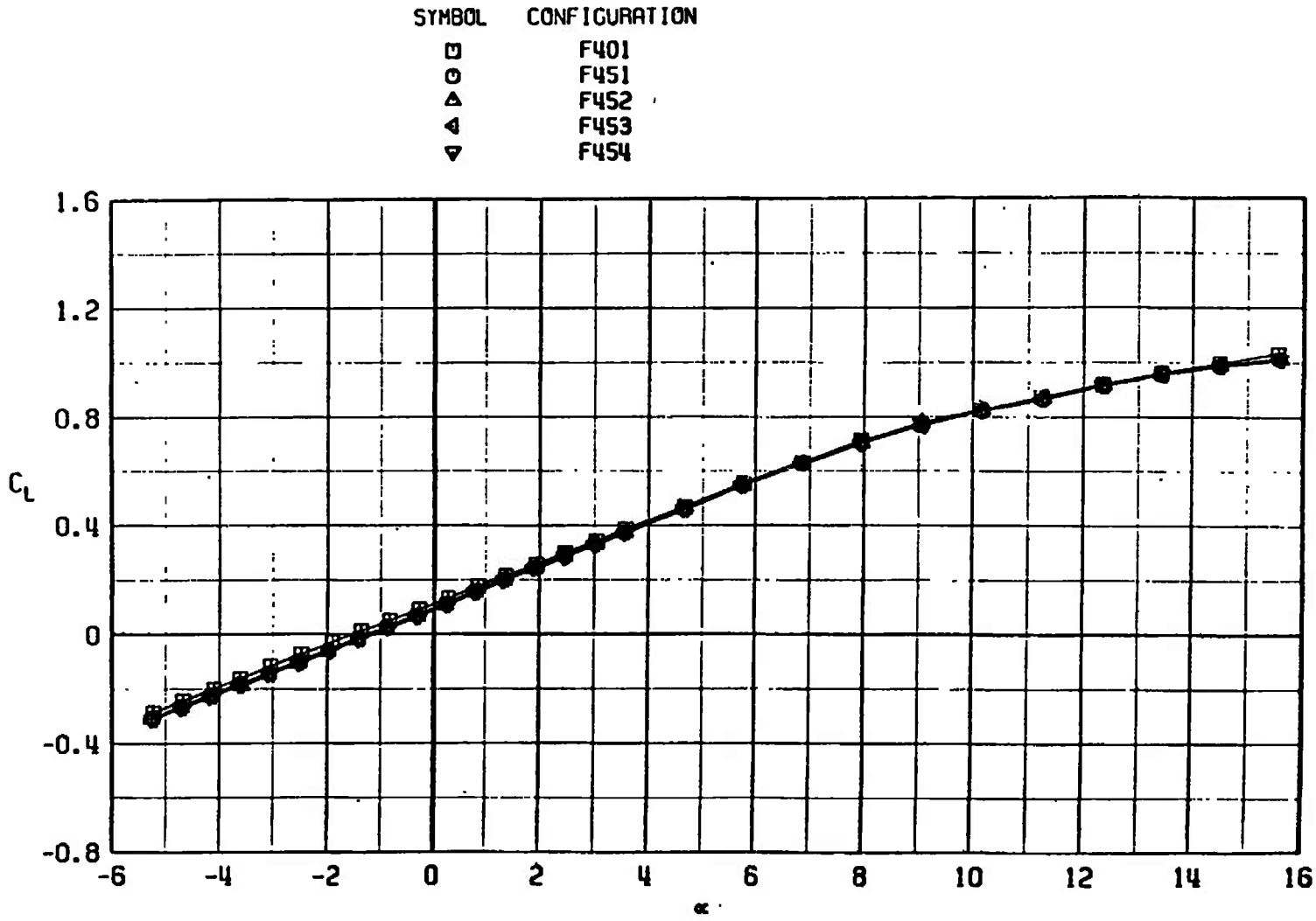

d. $M_\infty = 1.10$
Fig. 45 Continued

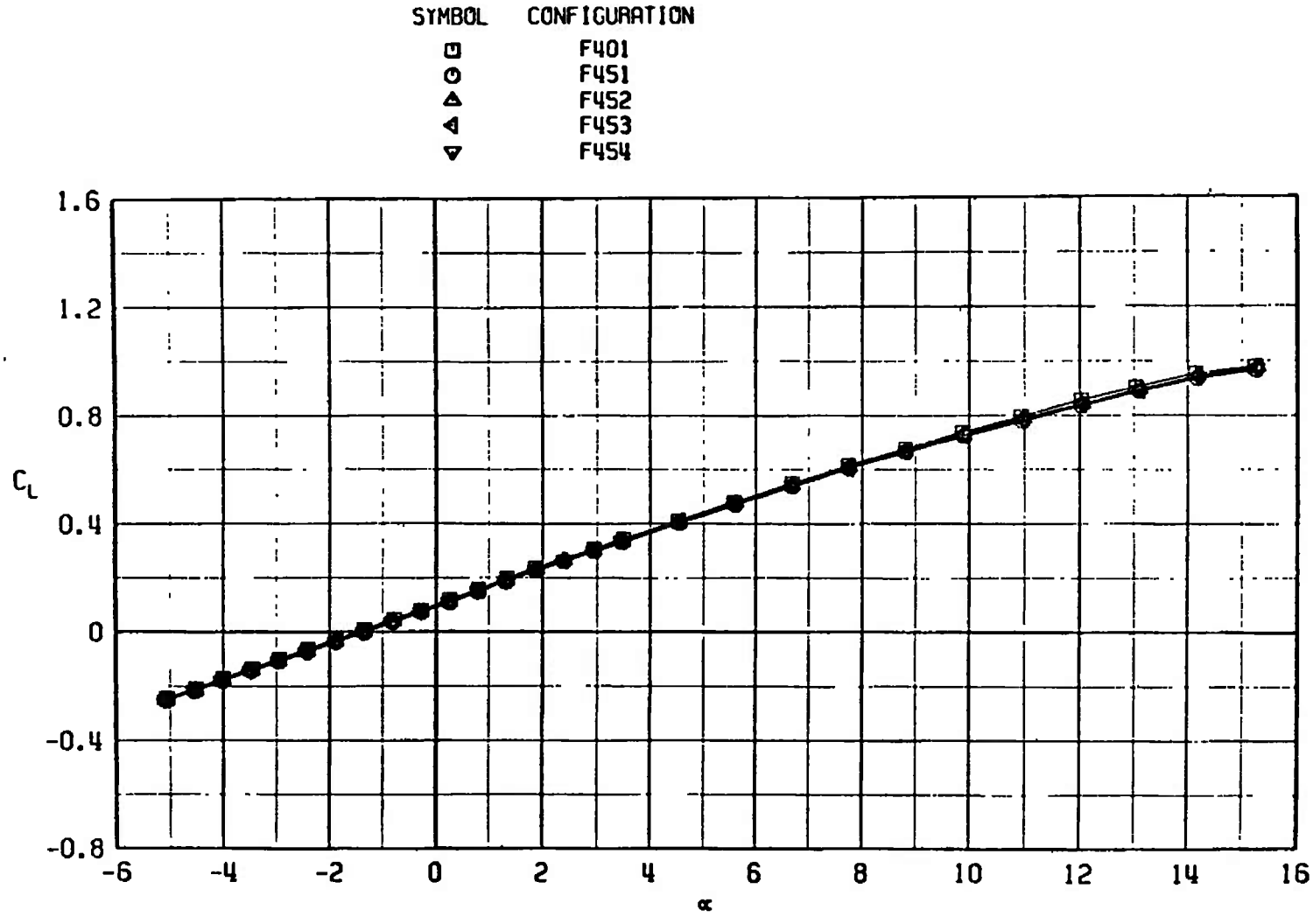

e. $M_\infty = 1.30$

Fig. 45 Concluded

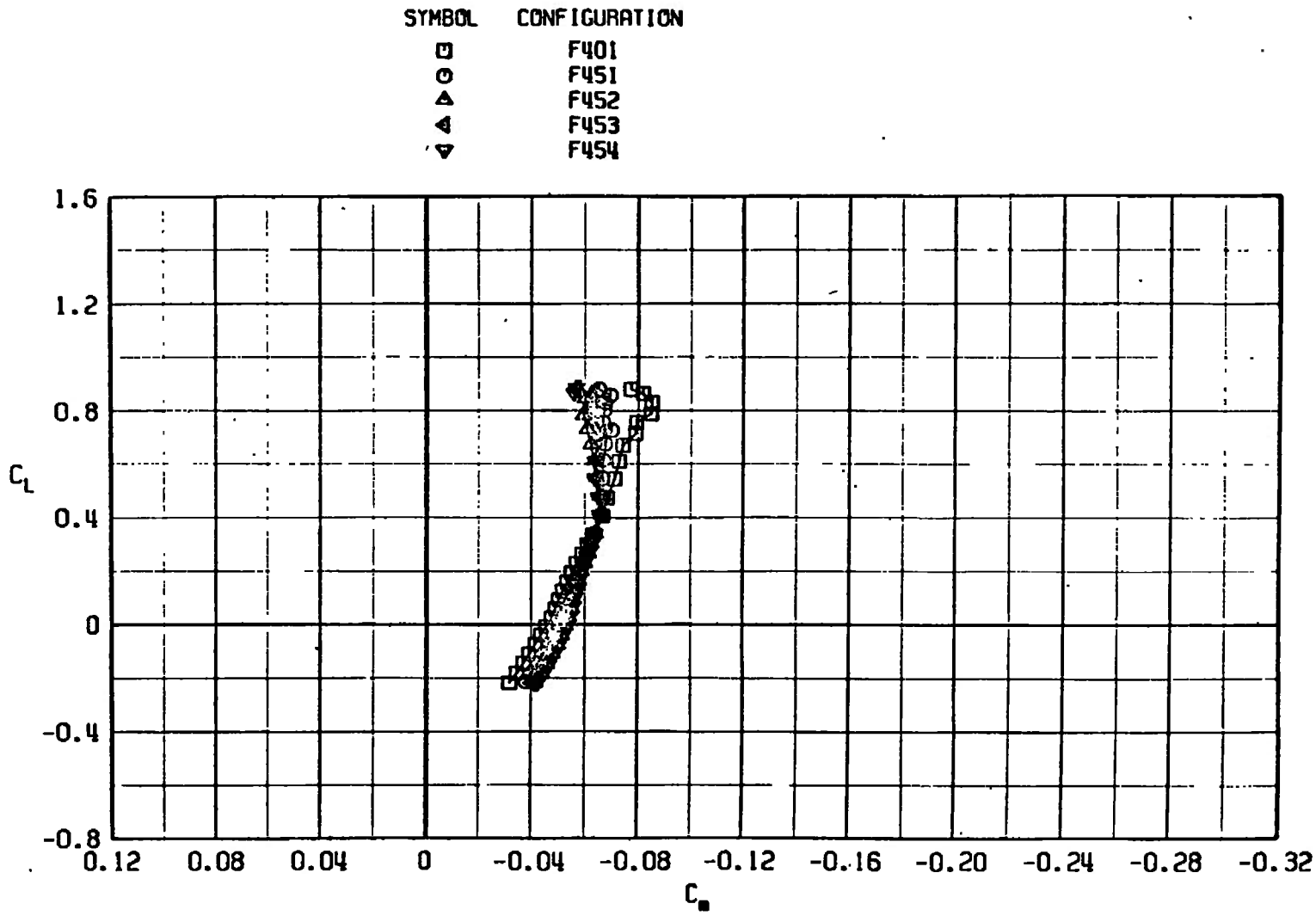

a. $M_\infty = 0.75$

Fig. 46 Pitching-Moment Coefficient Variation with Lift Coefficient for Configurations F401, F451, F452, F453, and F454

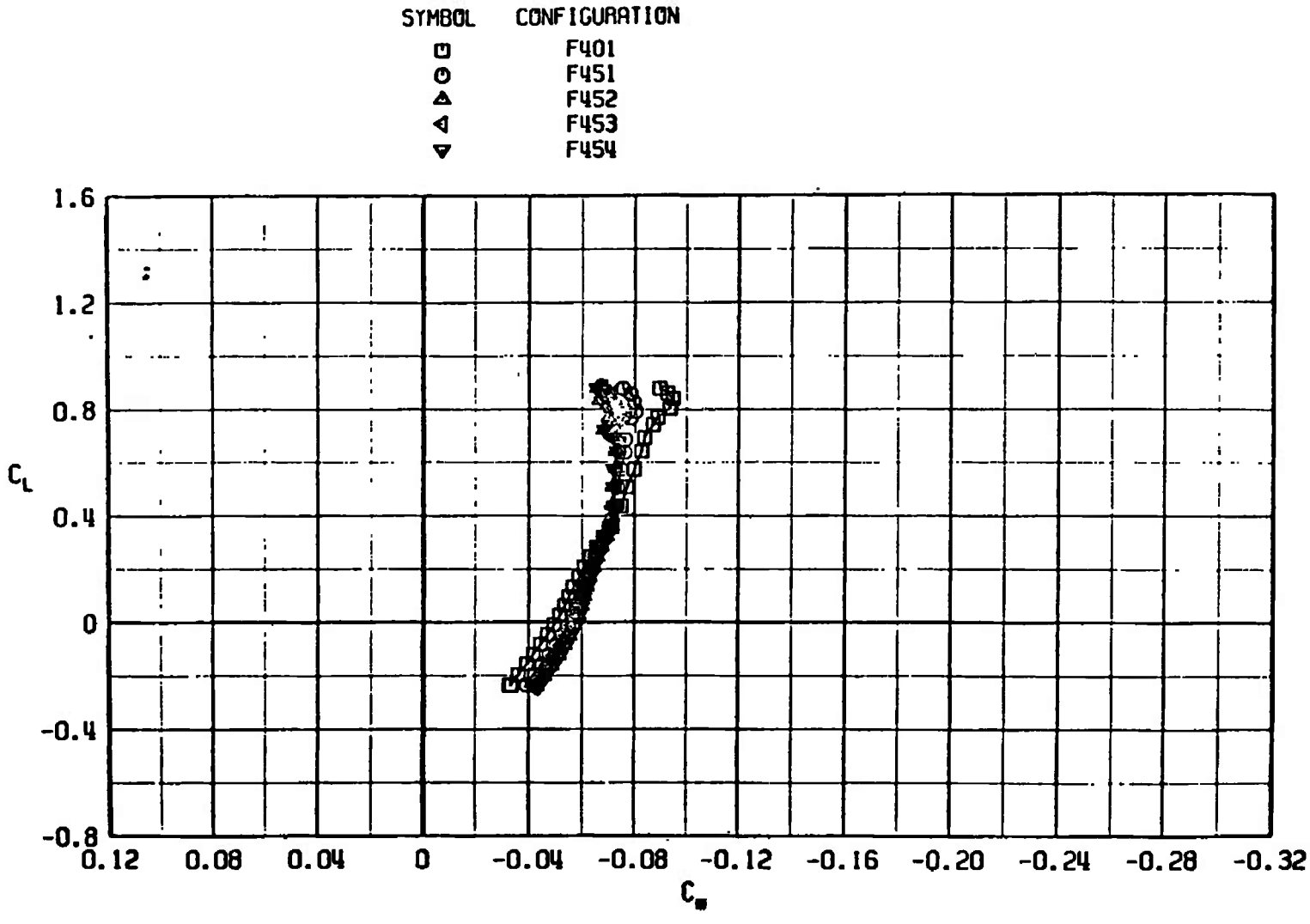

b. $M_\infty = 0.85$

Fig. 46 Continued

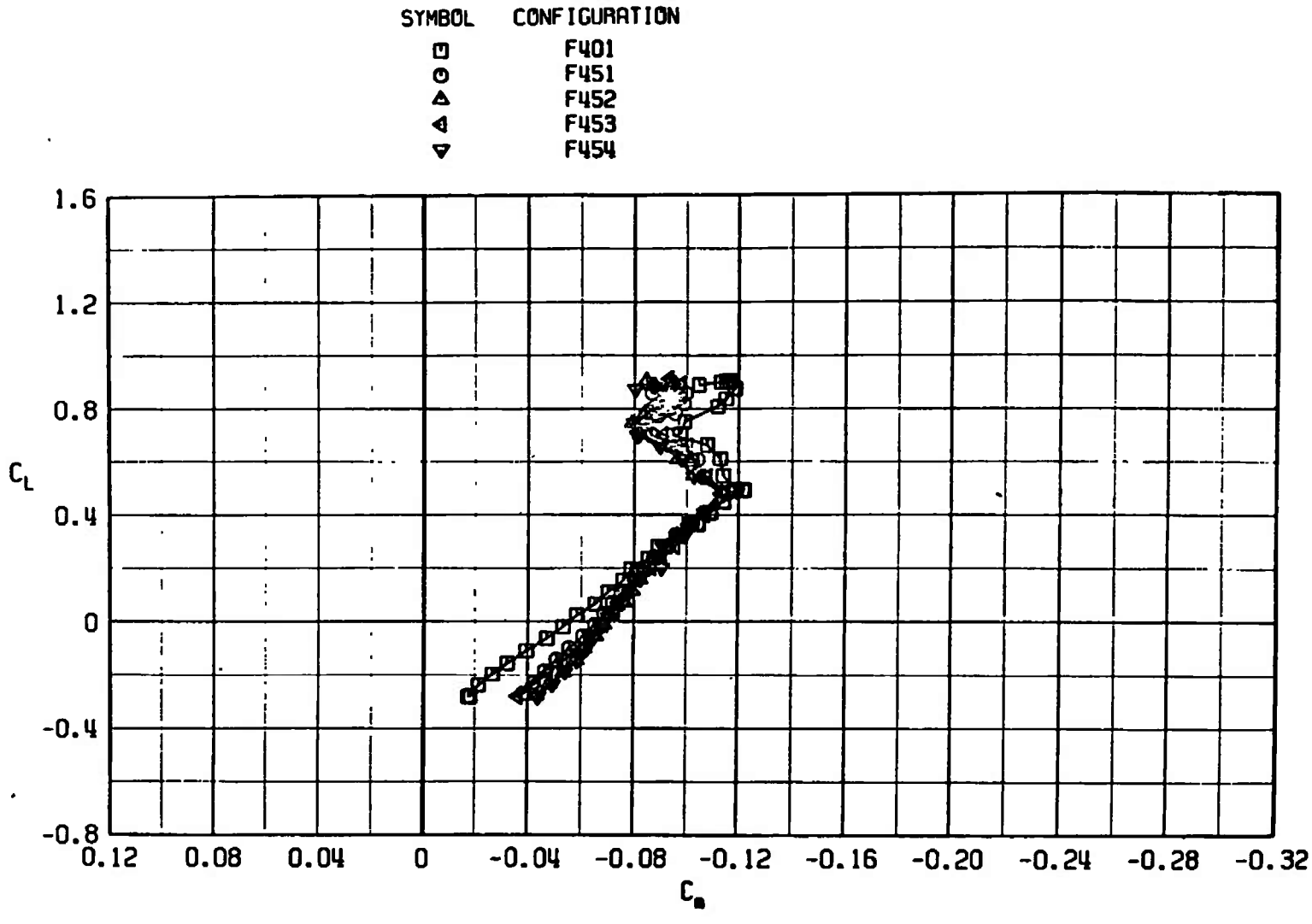

c. $M_\infty = 0.95$

Fig. 46 Continued

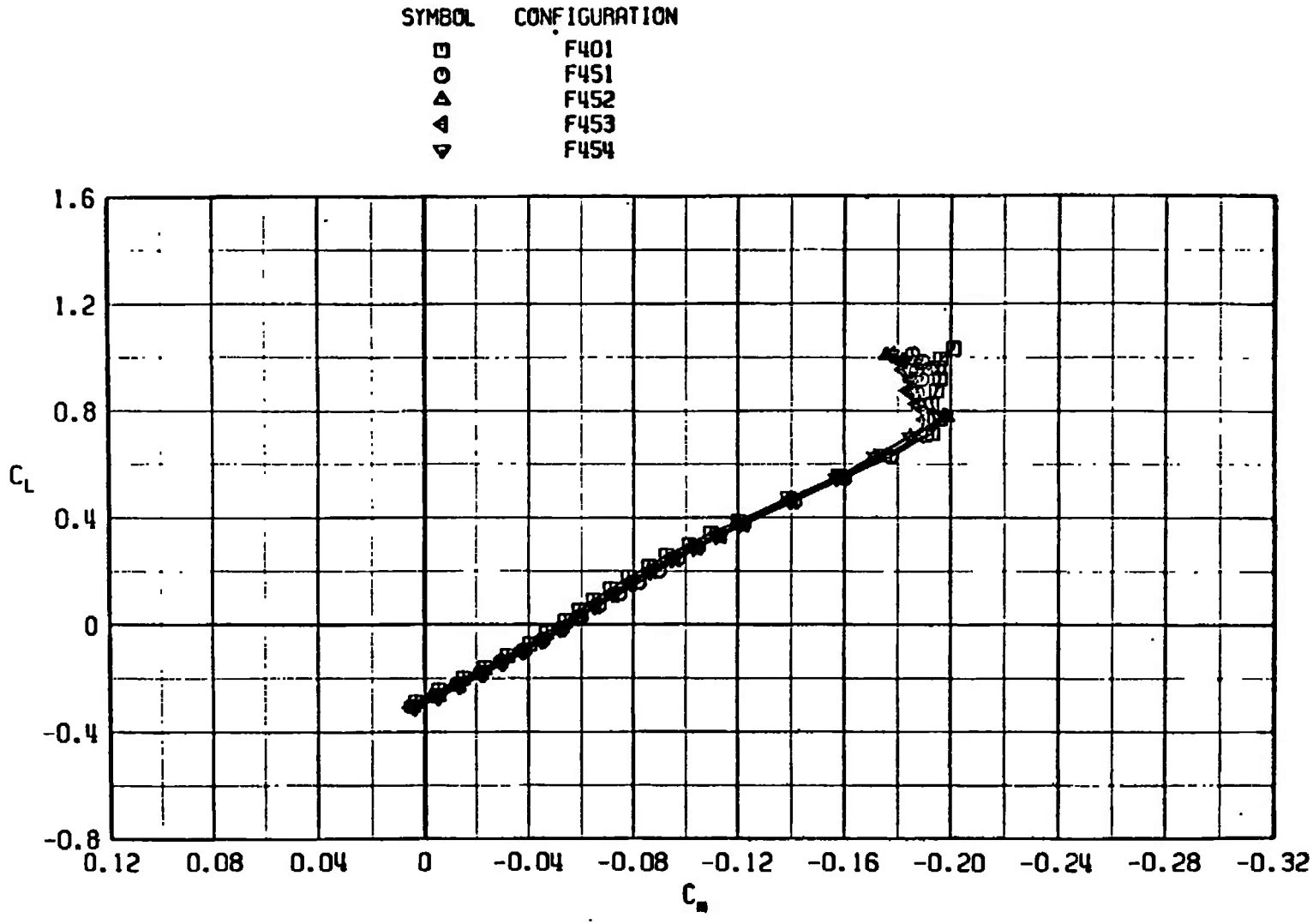

d. $M_\infty = 1.10$

Fig. 46 Continued

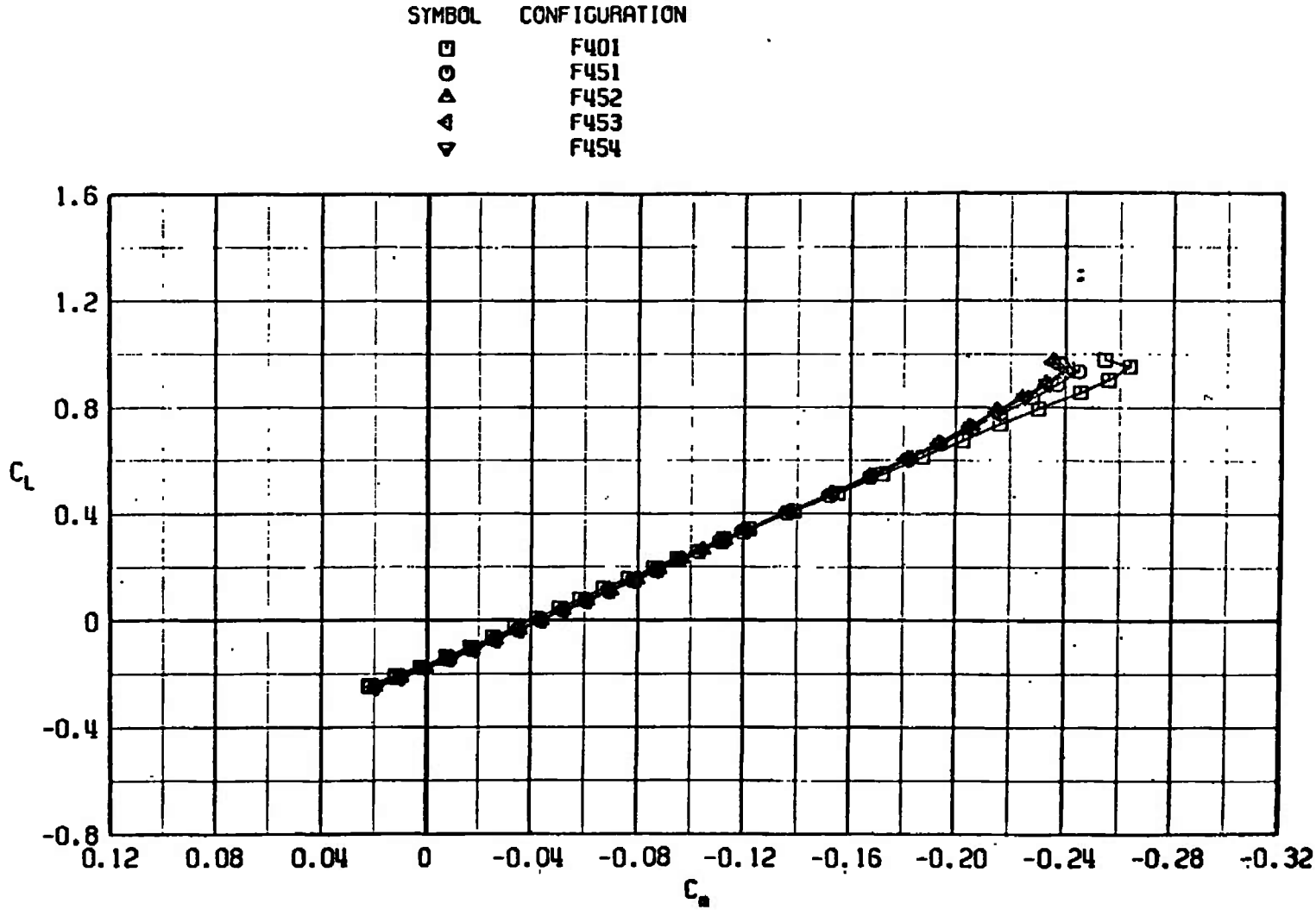

e. $M_\infty = 1.30$

Fig. 46 Concluded

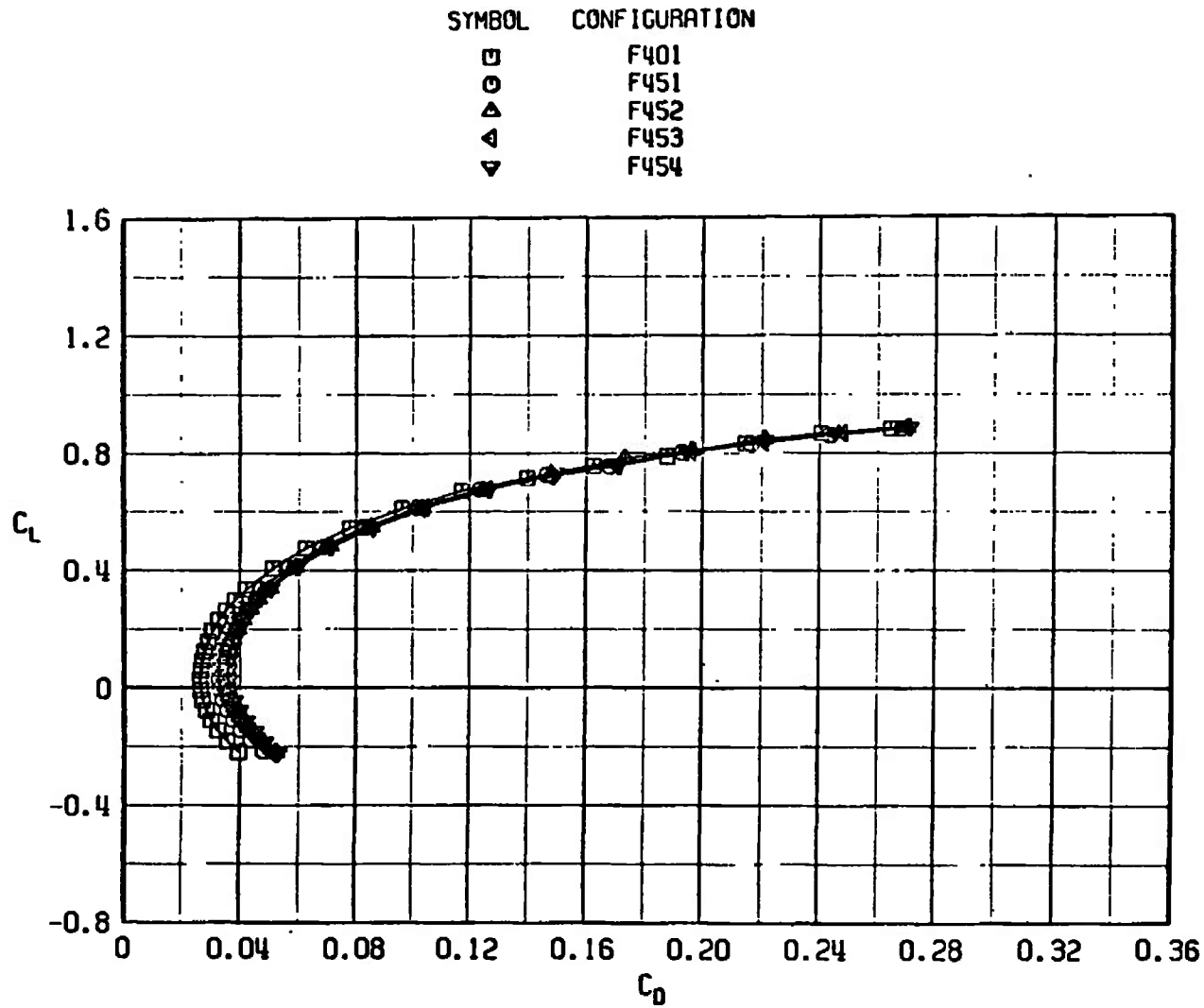

a. $M_\infty = 0.75$

Fig. 47 Drag Coefficient Variation with Lift Coefficient for Configurations F401, F451, F452, and F454

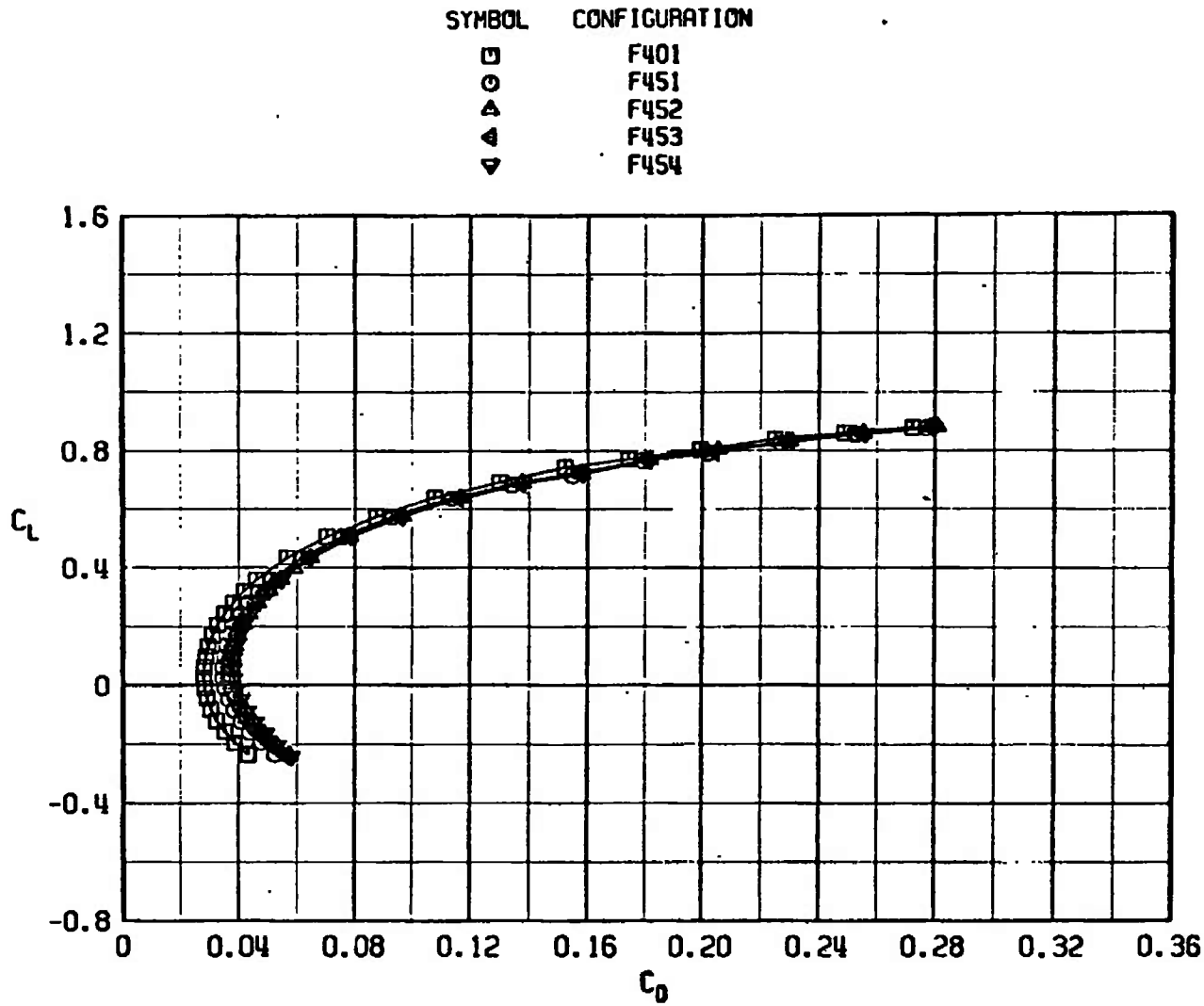

b. $M_\infty = 0.85$

Fig. 47 Continued

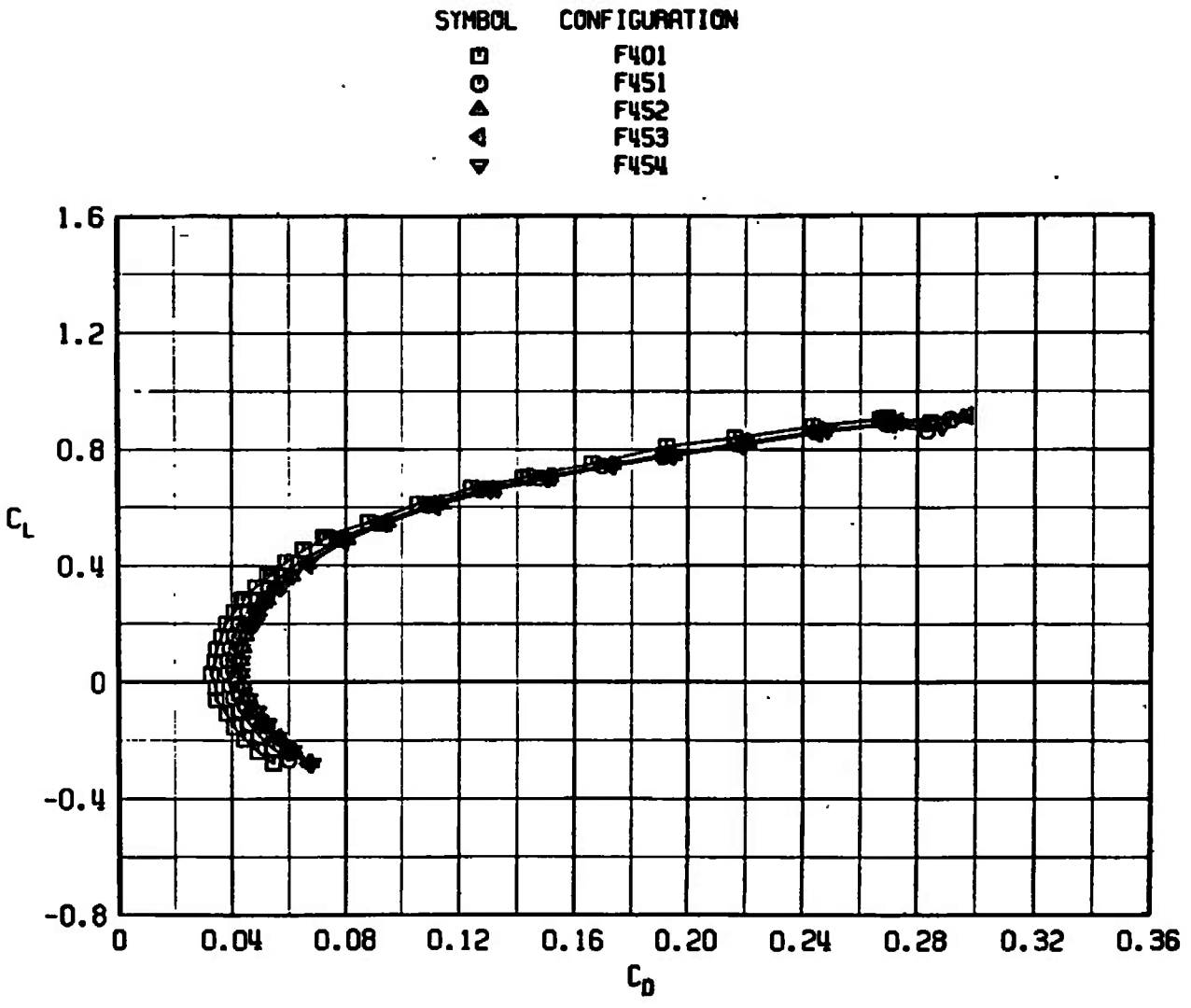

c. $M_\infty = 0.95$.

Fig. 47 Continued

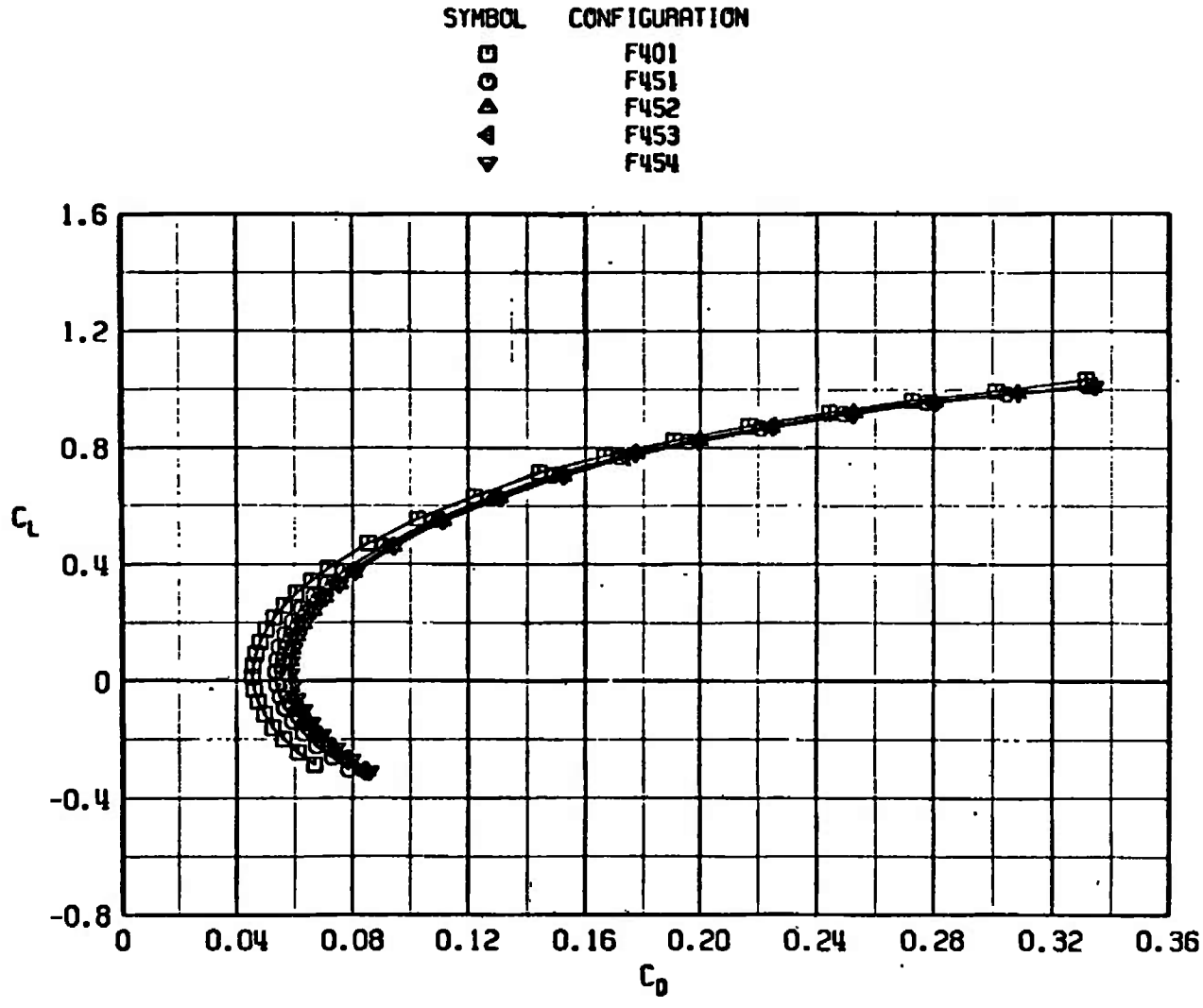

d. $M_\infty = 1.10$

Fig. 47 Continued

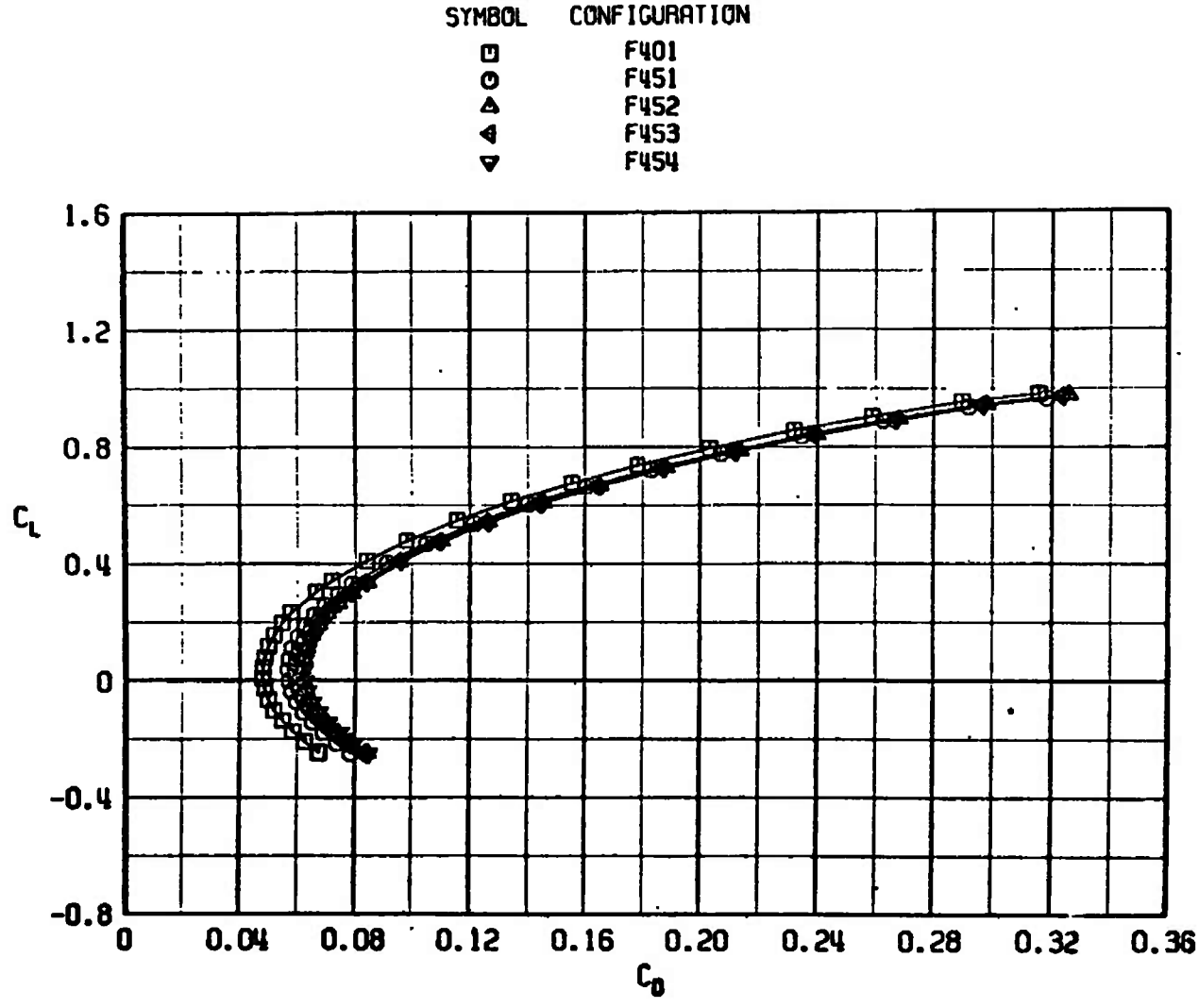

e. $M_\infty = 1.30$

Fig. 47 Concluded

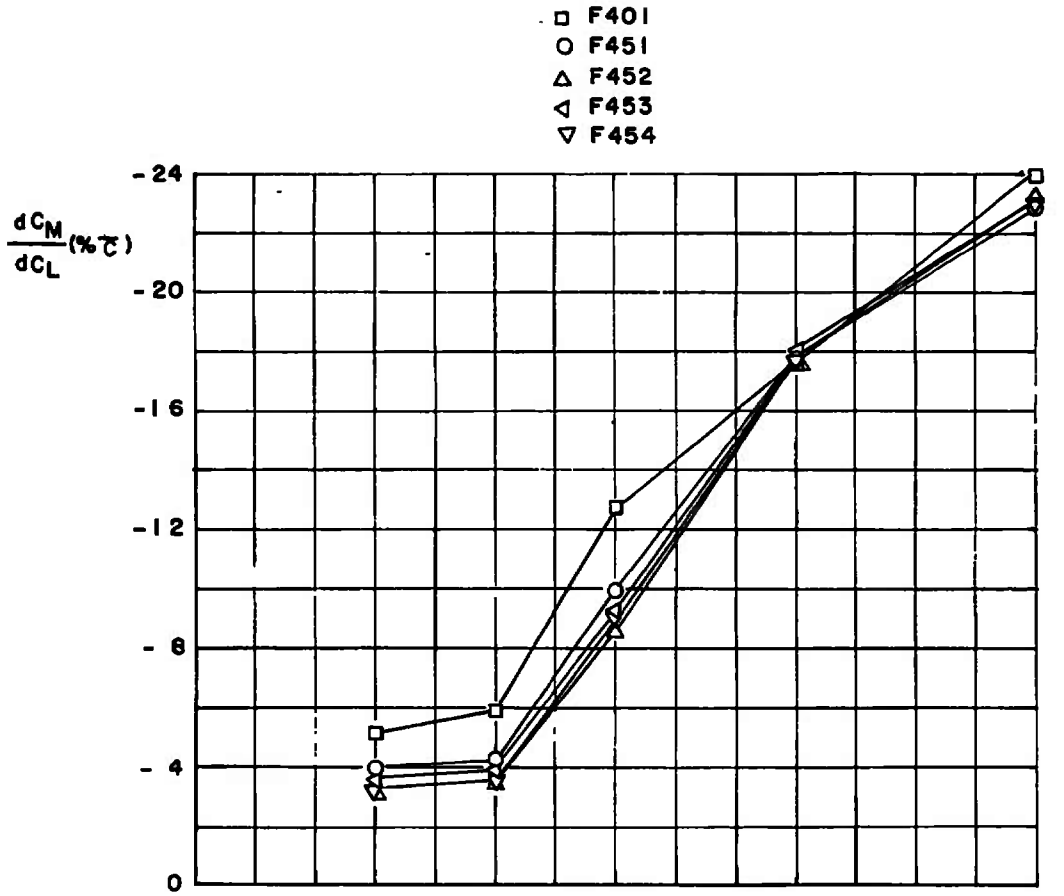

a. dC_m/dC_L versus M_∞ at $C_L = 0.20$ in percentage of $\bar{c}$

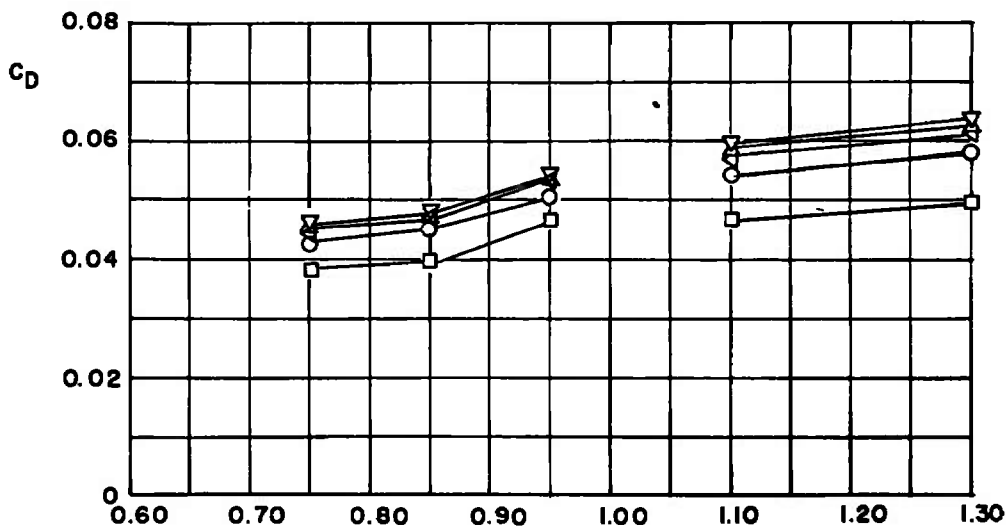

b. C_D versus M_∞ at $C_L = 0.30$, $M_\infty < 1.0$, and $C_L = 0.10$, $M_\infty > 1.0$

Fig. 48 Drag Coefficient and dC_m/dC_L Variation with Mach Number for Configurations F401, F451, F452, F453, and F454

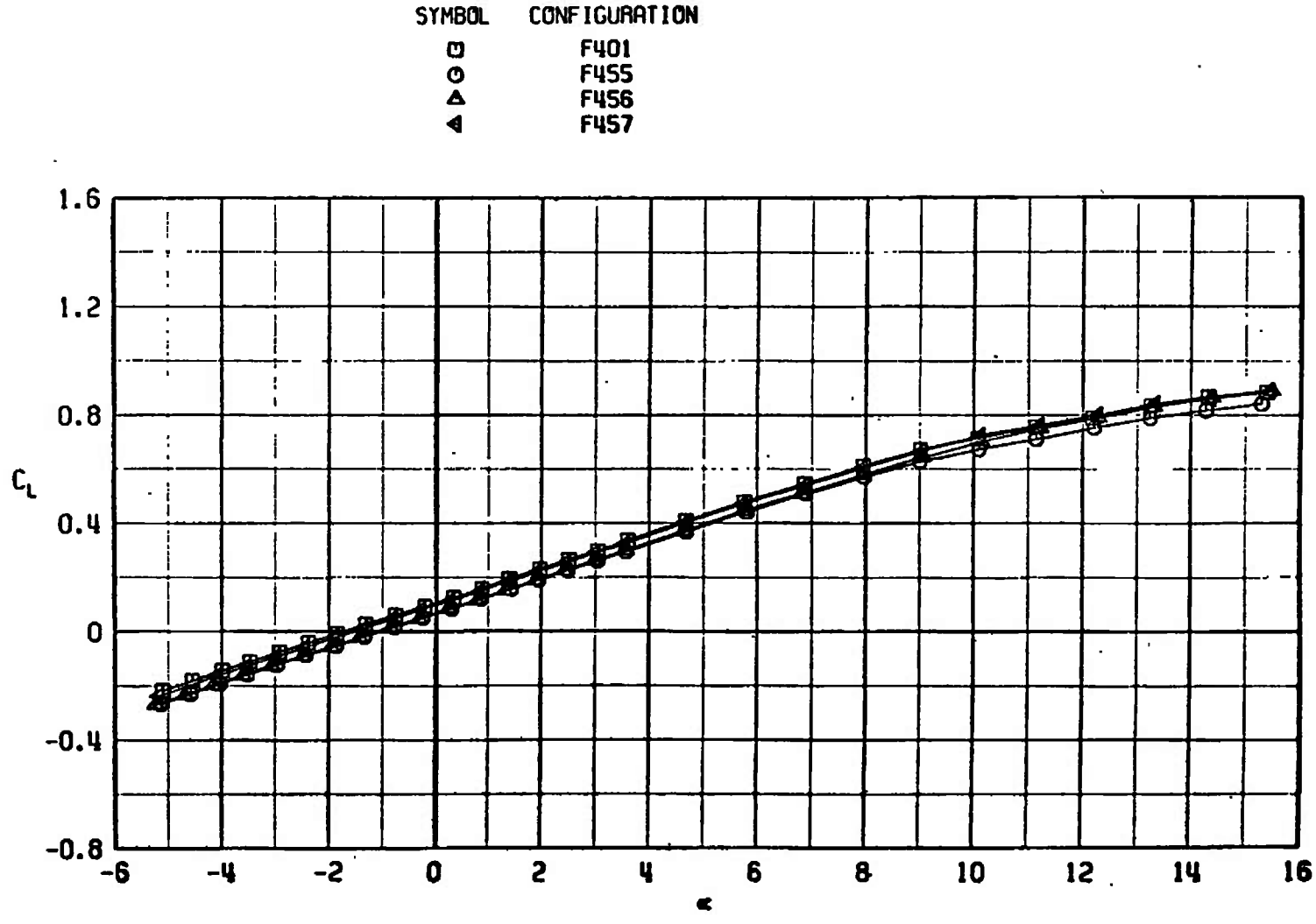

a. $M_\infty = 0.75$

Fig. 49 Lift Coefficient Variation with Angle of Attack for Configurations F401, F455, F456, and F457

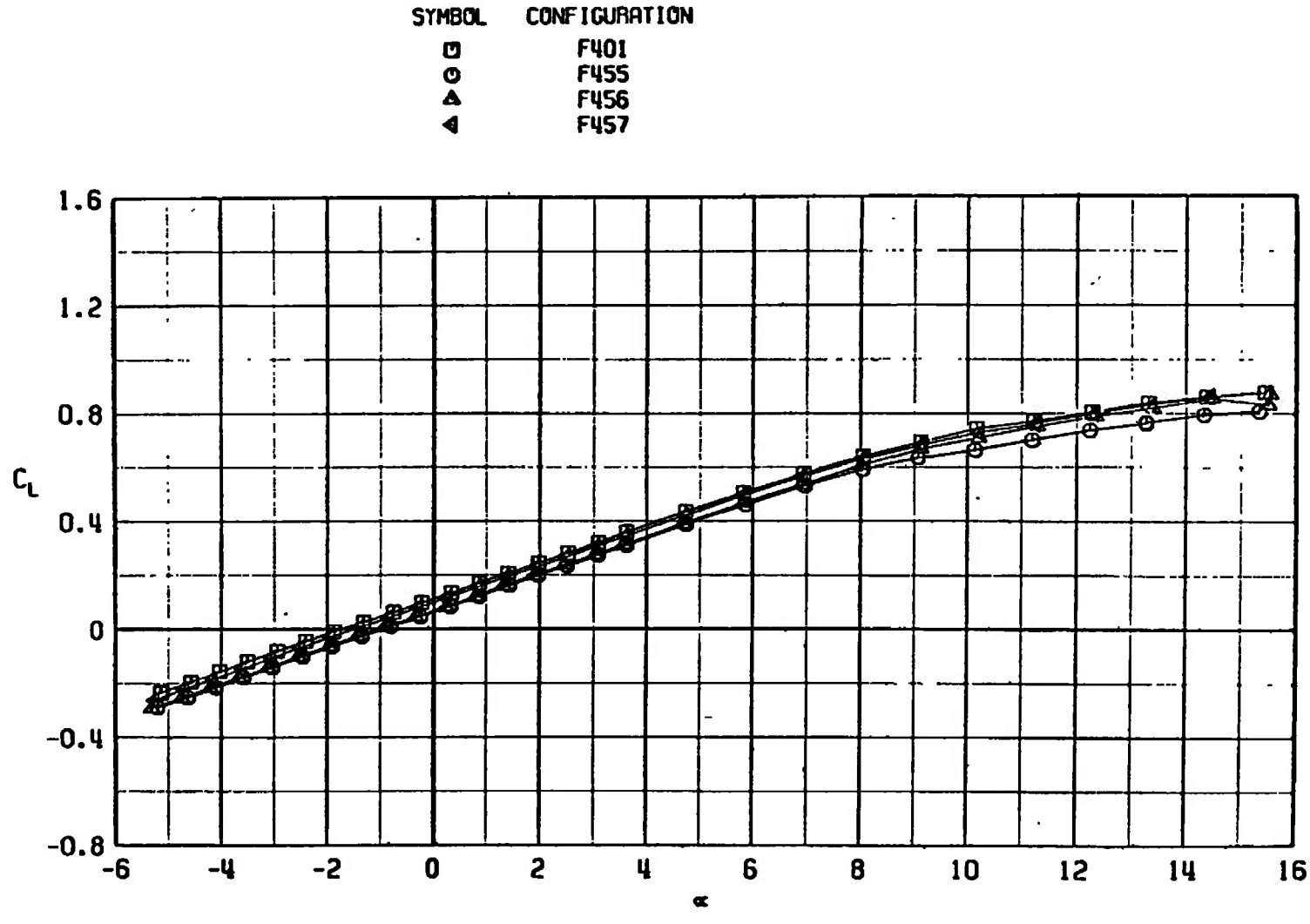

b. $M_\infty = 0.85$
Fig. 49 Continued

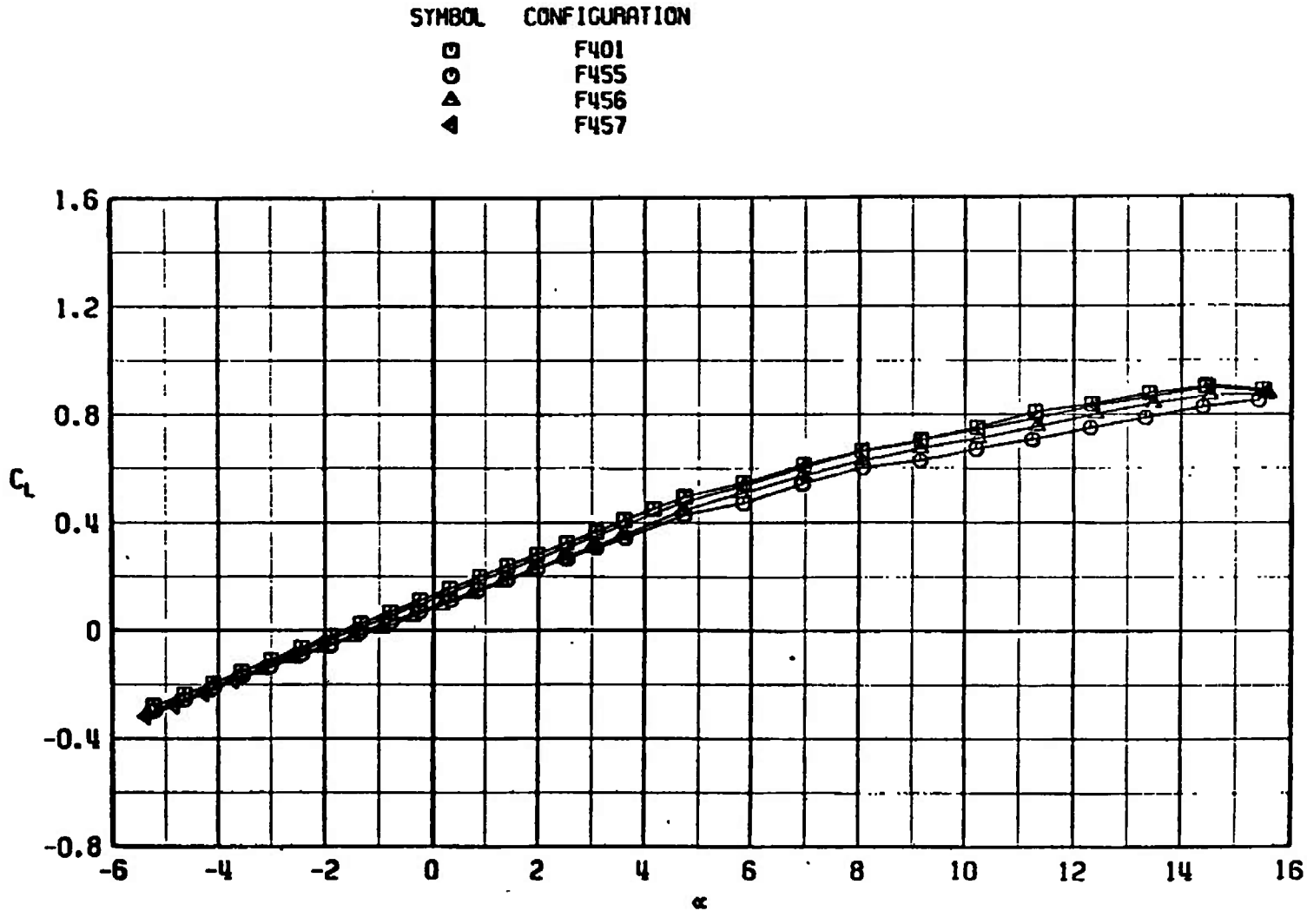

c. $M_\infty = 0.95$

Fig. 49 Continued

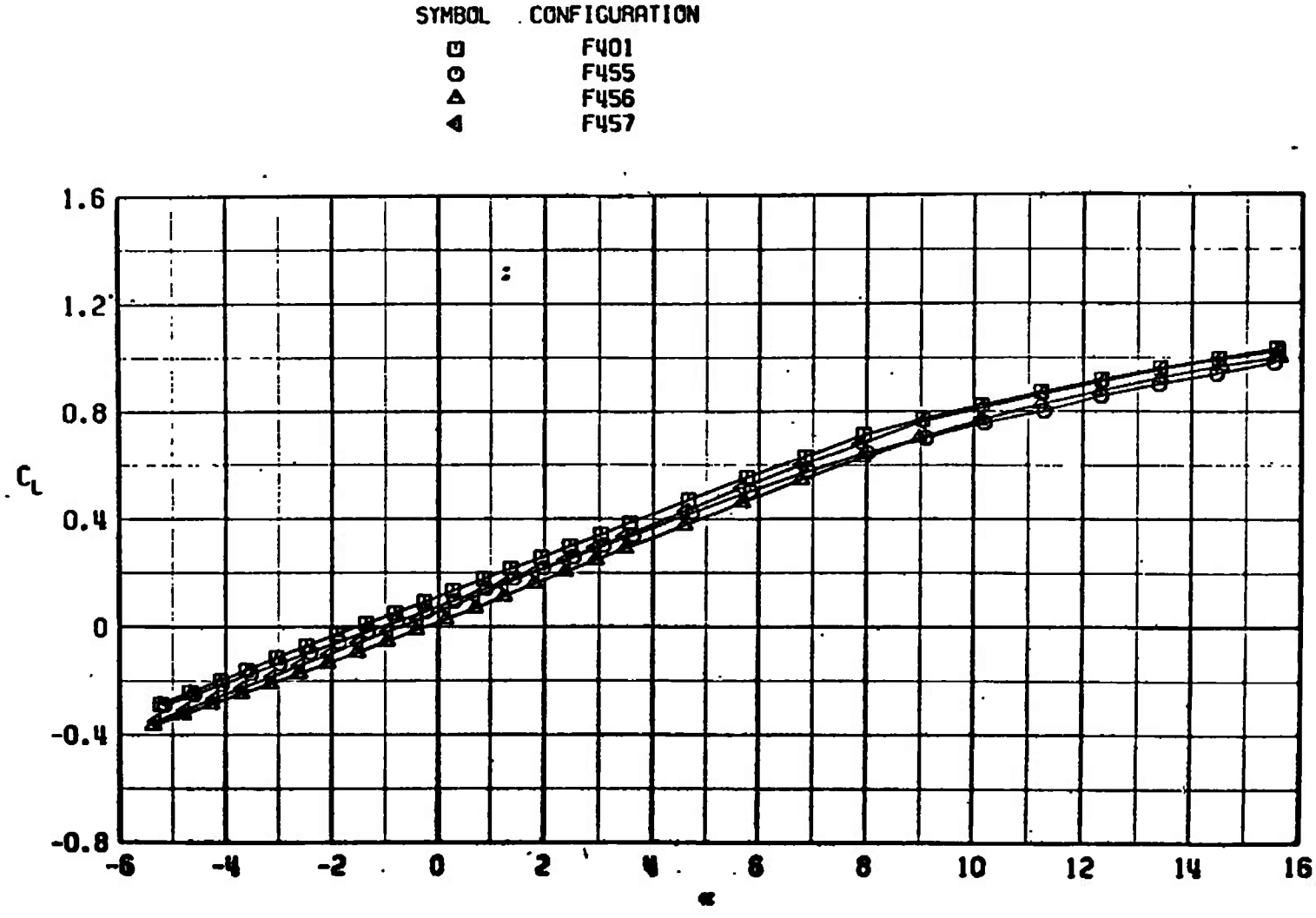

d. $M_\infty = 1.10$
Fig. 49 Continued

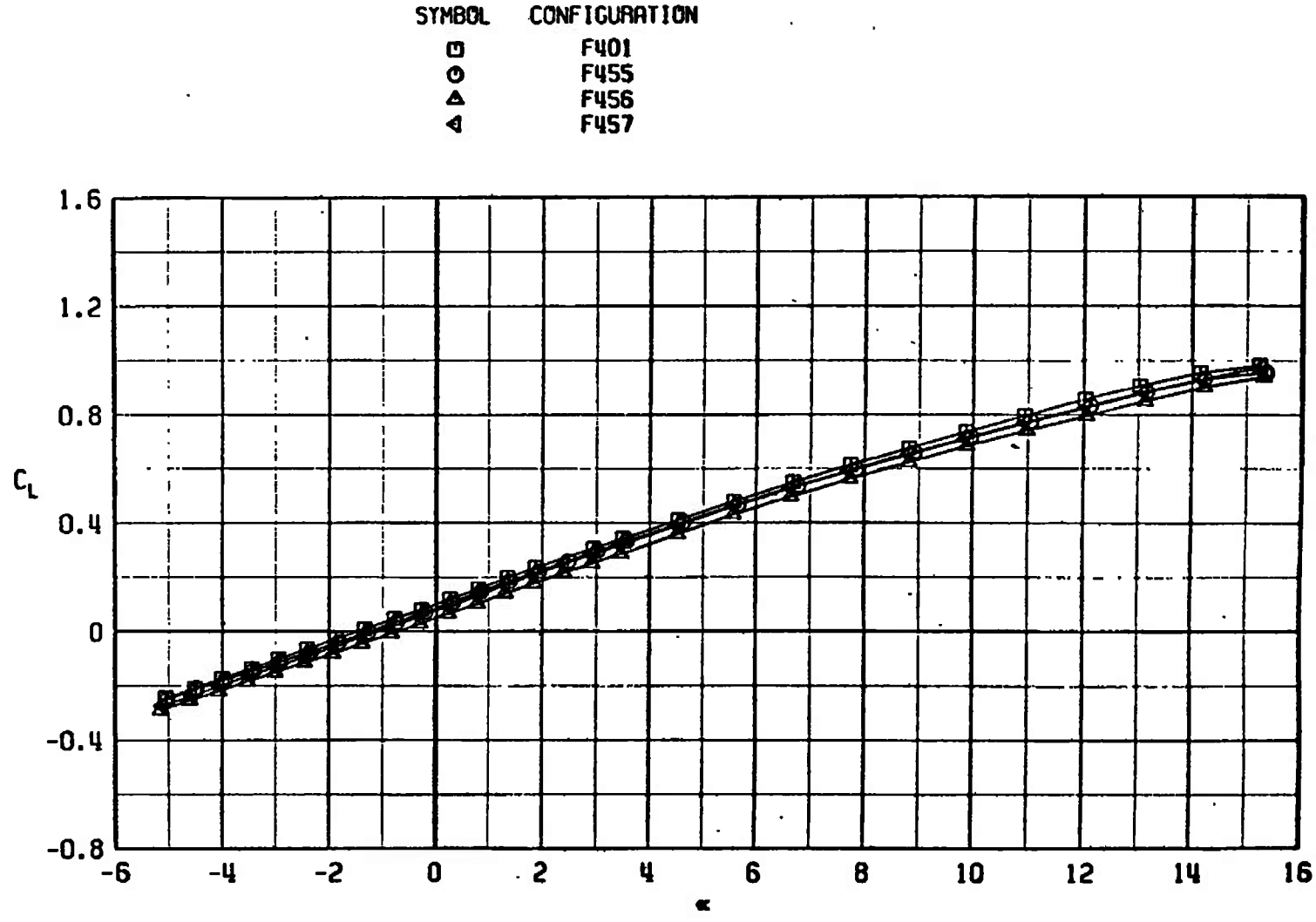

e. $M_\infty = 1.30$

Fig. 49 Concluded

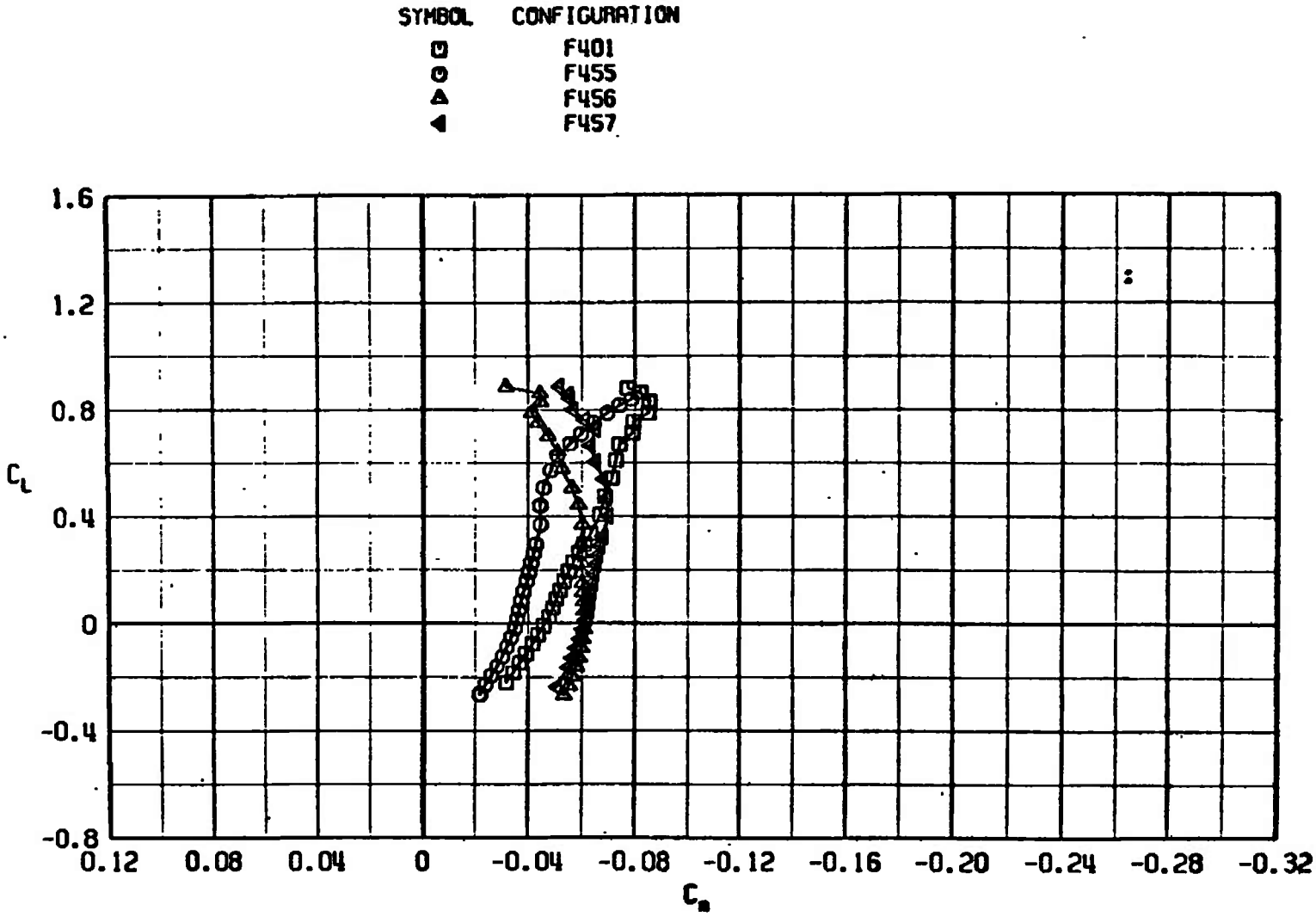

a. $M_\infty = 0.75$

Fig. 50 Pitching-Moment Coefficient Variation with Lift Coefficient for Configurations F401, F455, F456, and F457

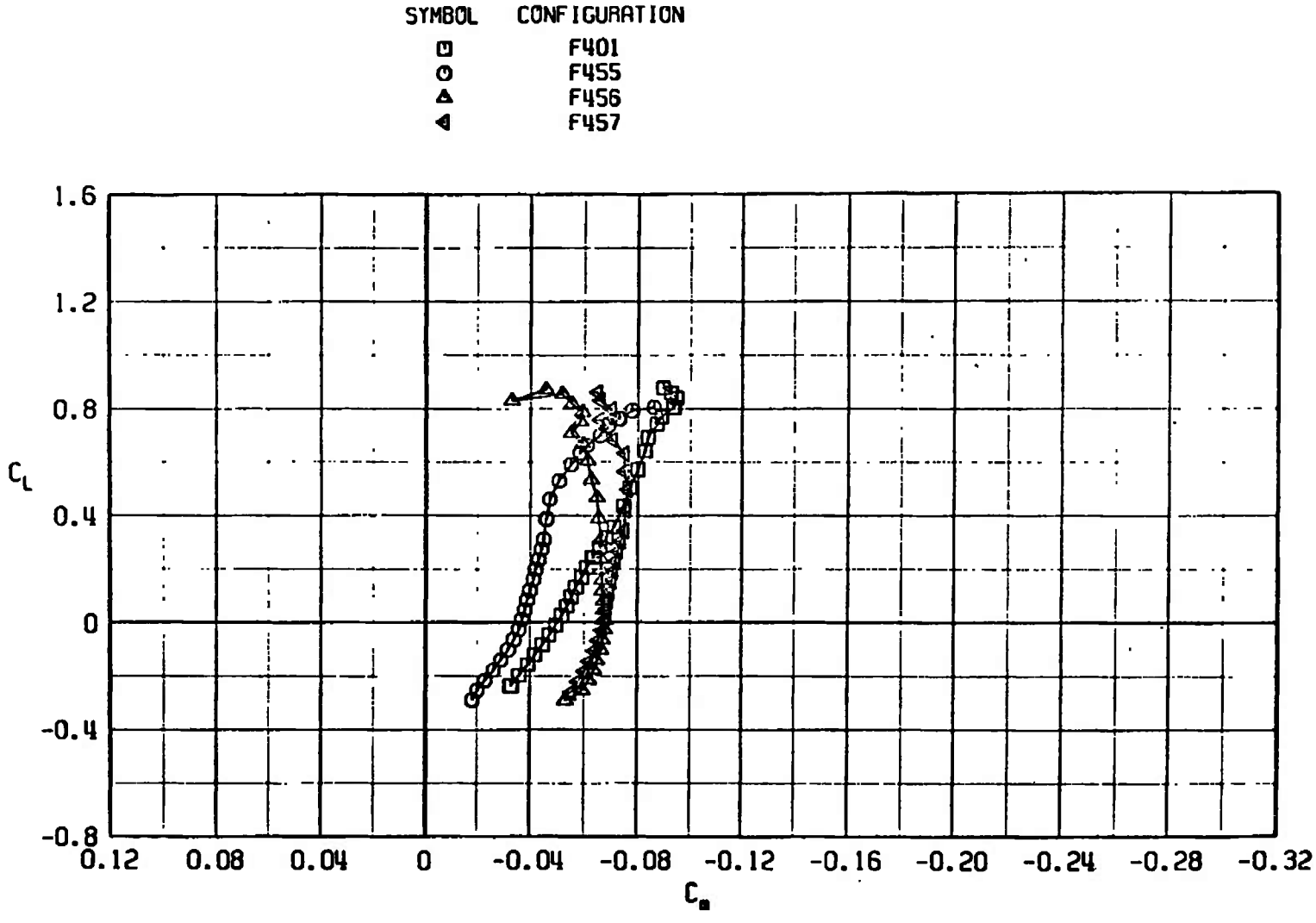

b. $M_\infty = 0.85$

Fig. 50 Continued

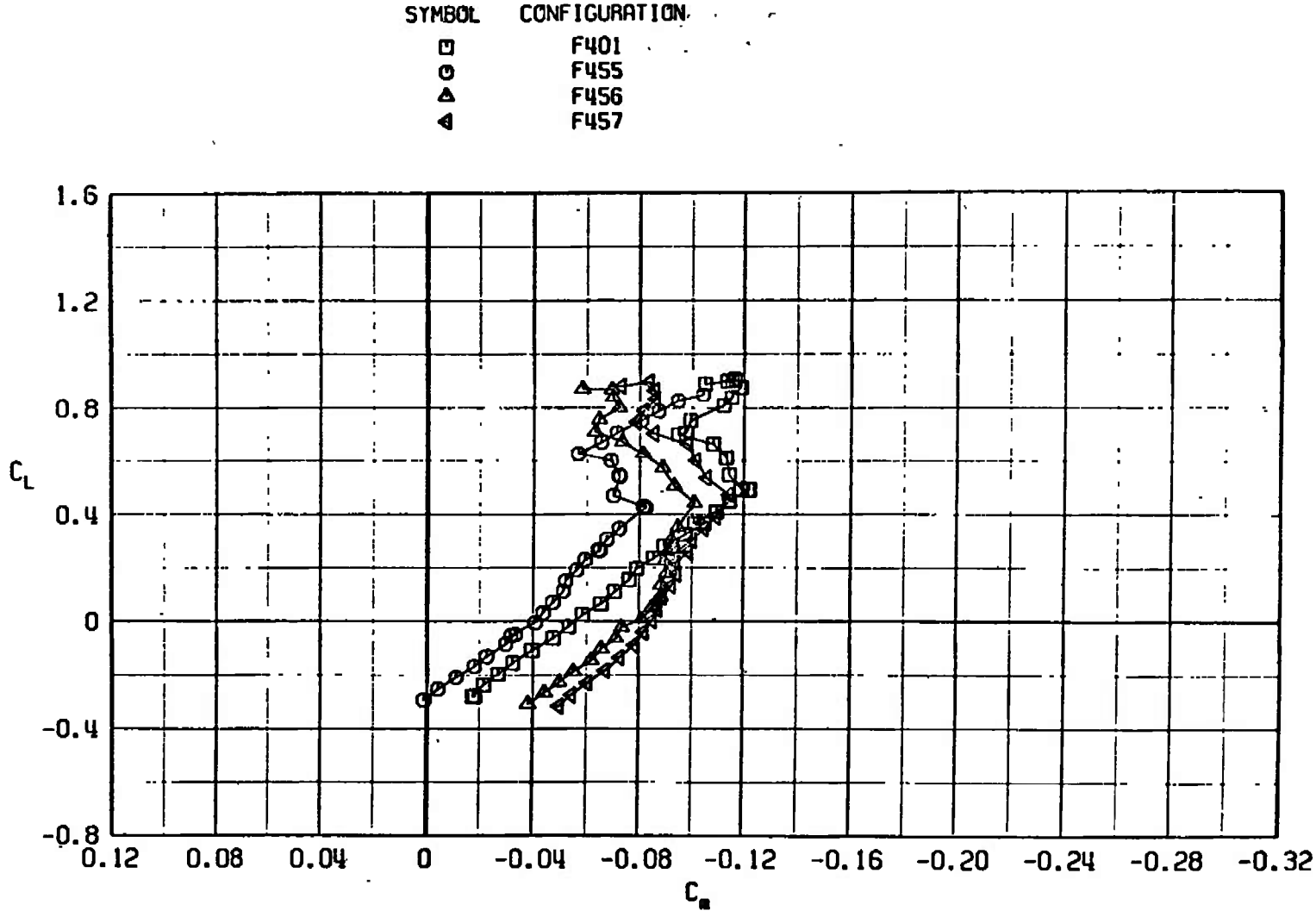

c. $M_\infty = 0.95$

Fig. 50 Continued

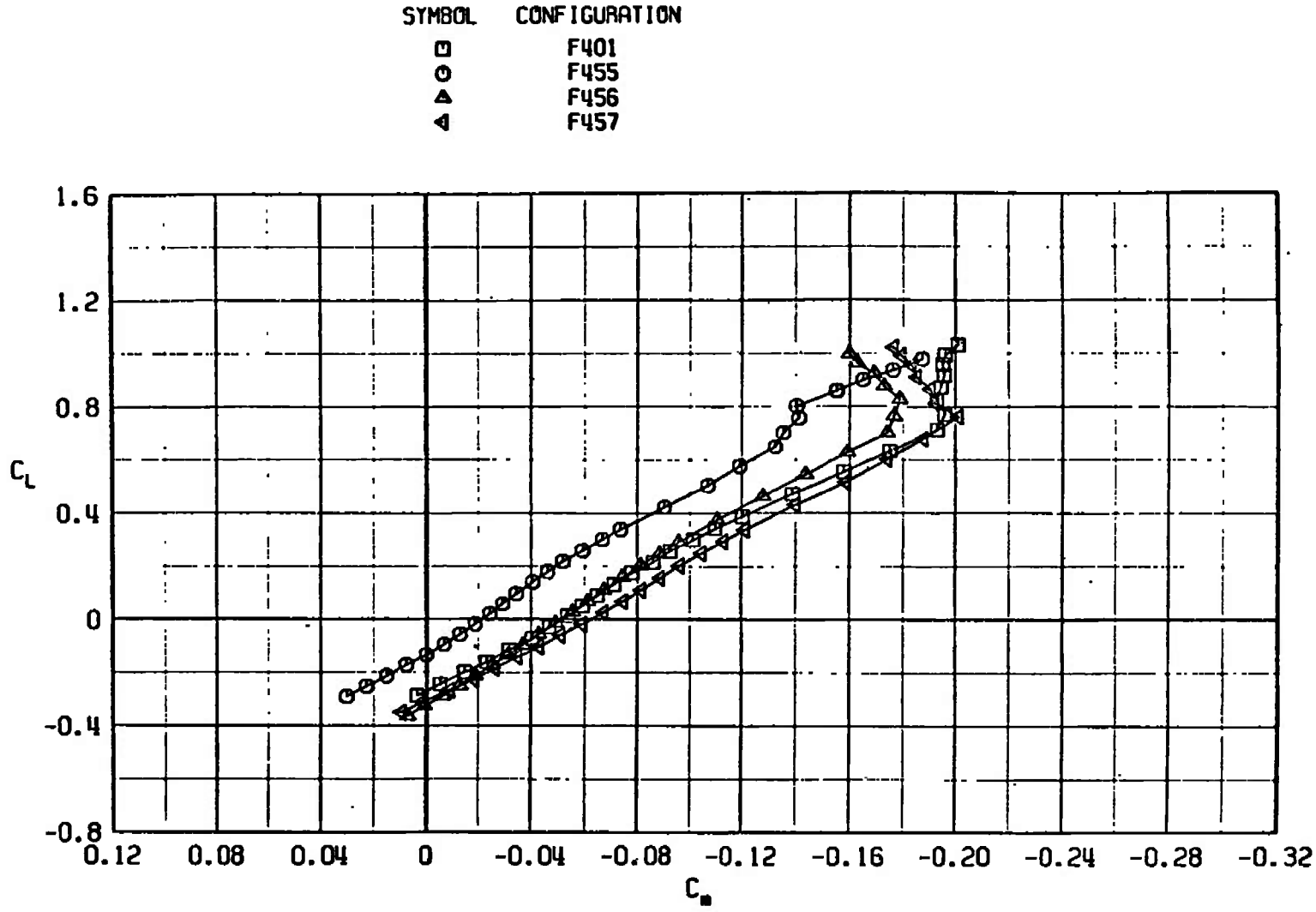

d. $M_\infty = 1.10$

Fig. 50 Continued

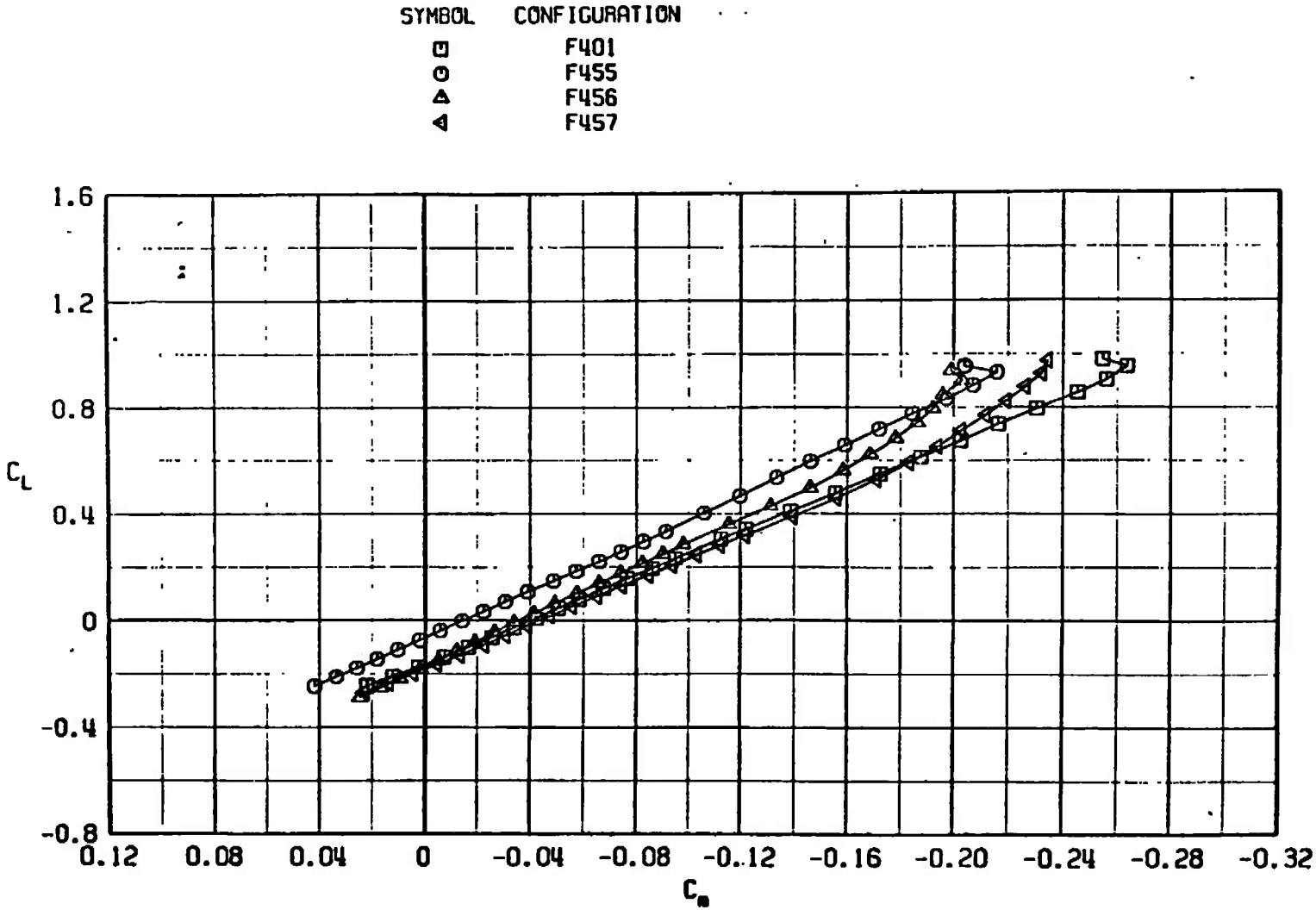

e. $M_\infty = 1.30$

Fig. 50 Concluded

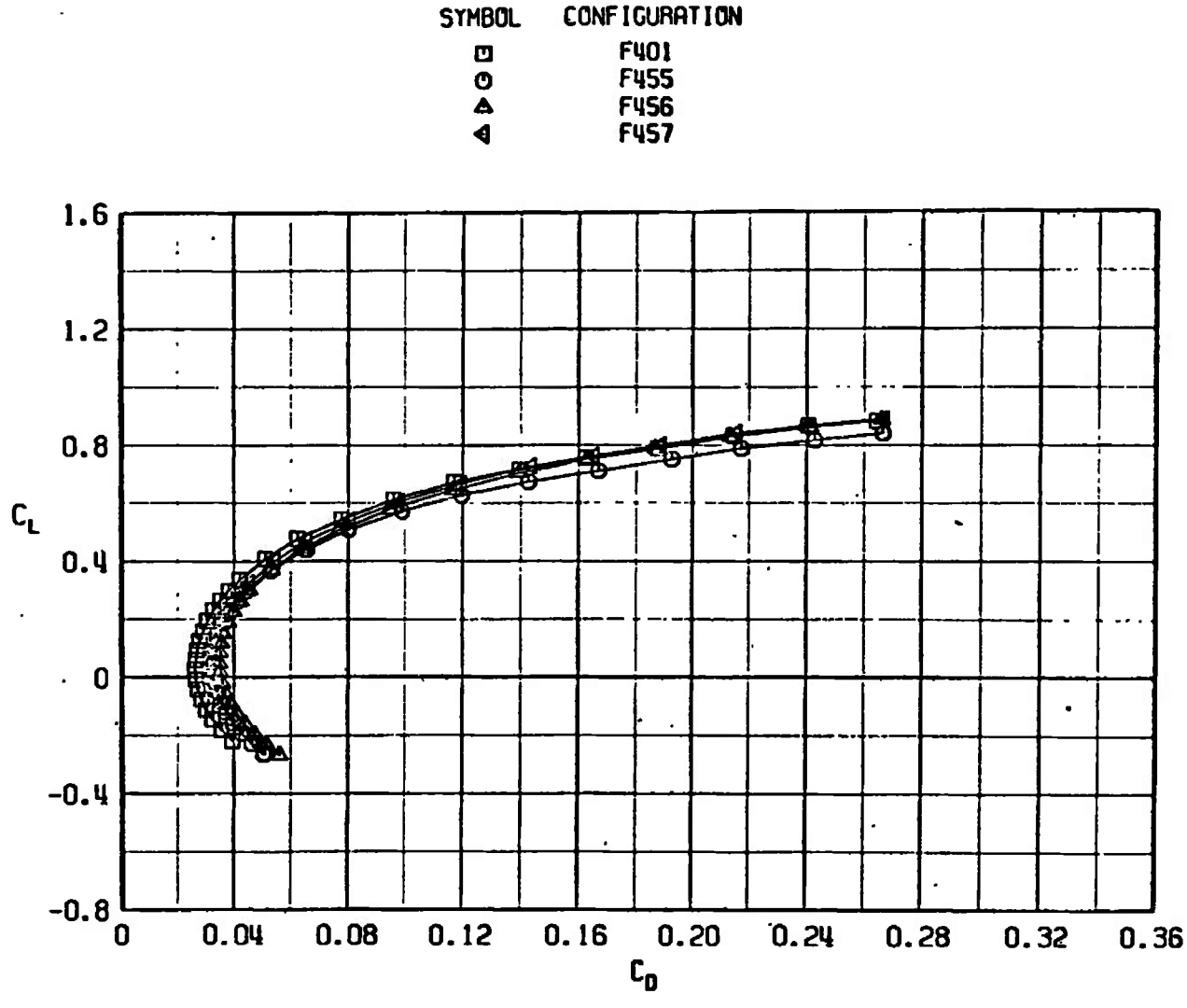

a. $M_\infty = 0.75$

Fig. 51 Drag Coefficient Variation with Lift Coefficient for Configurations F401, F455, F456, and F457

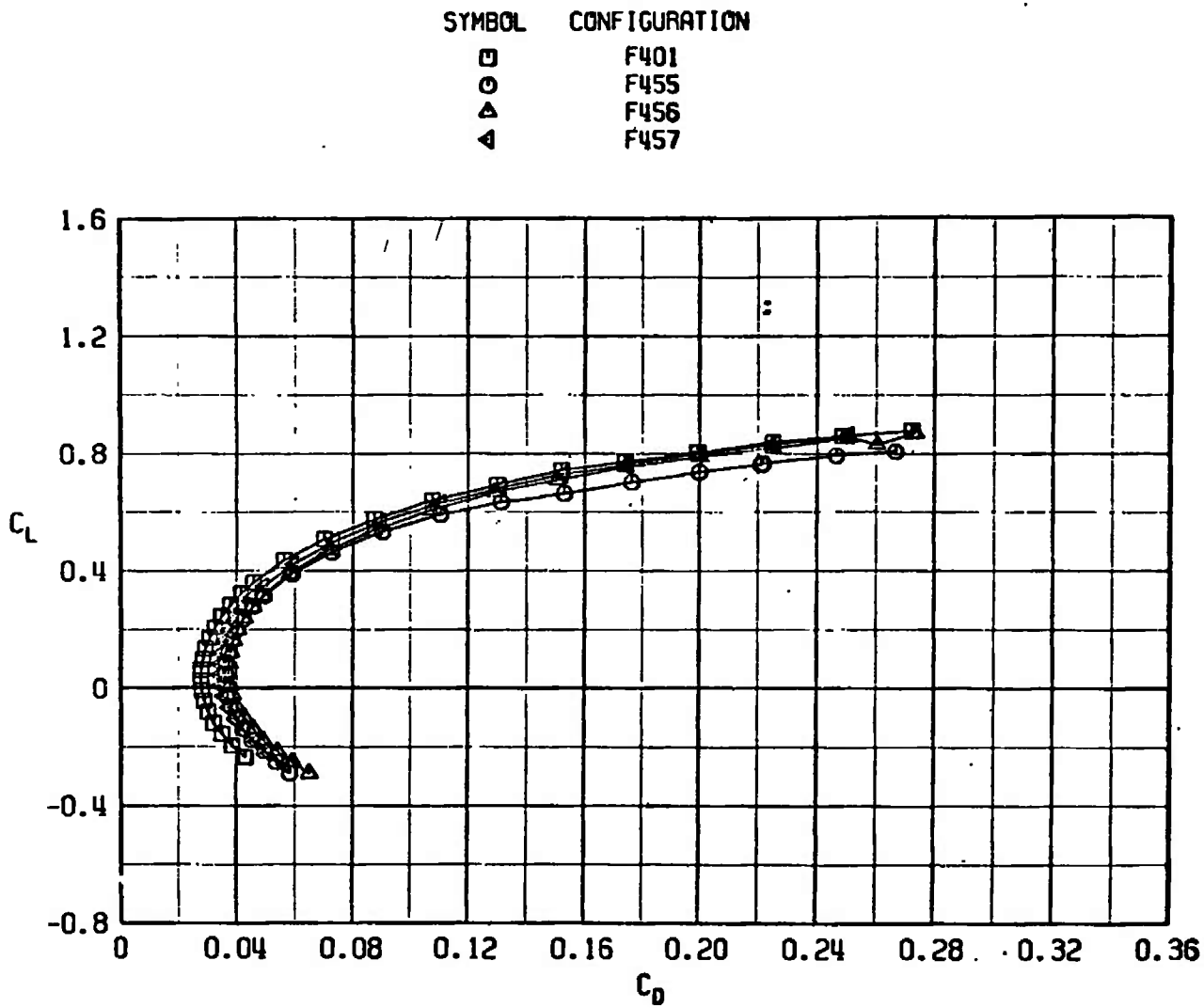

b. $M_\infty = 0.85$

Fig. 51 Continued

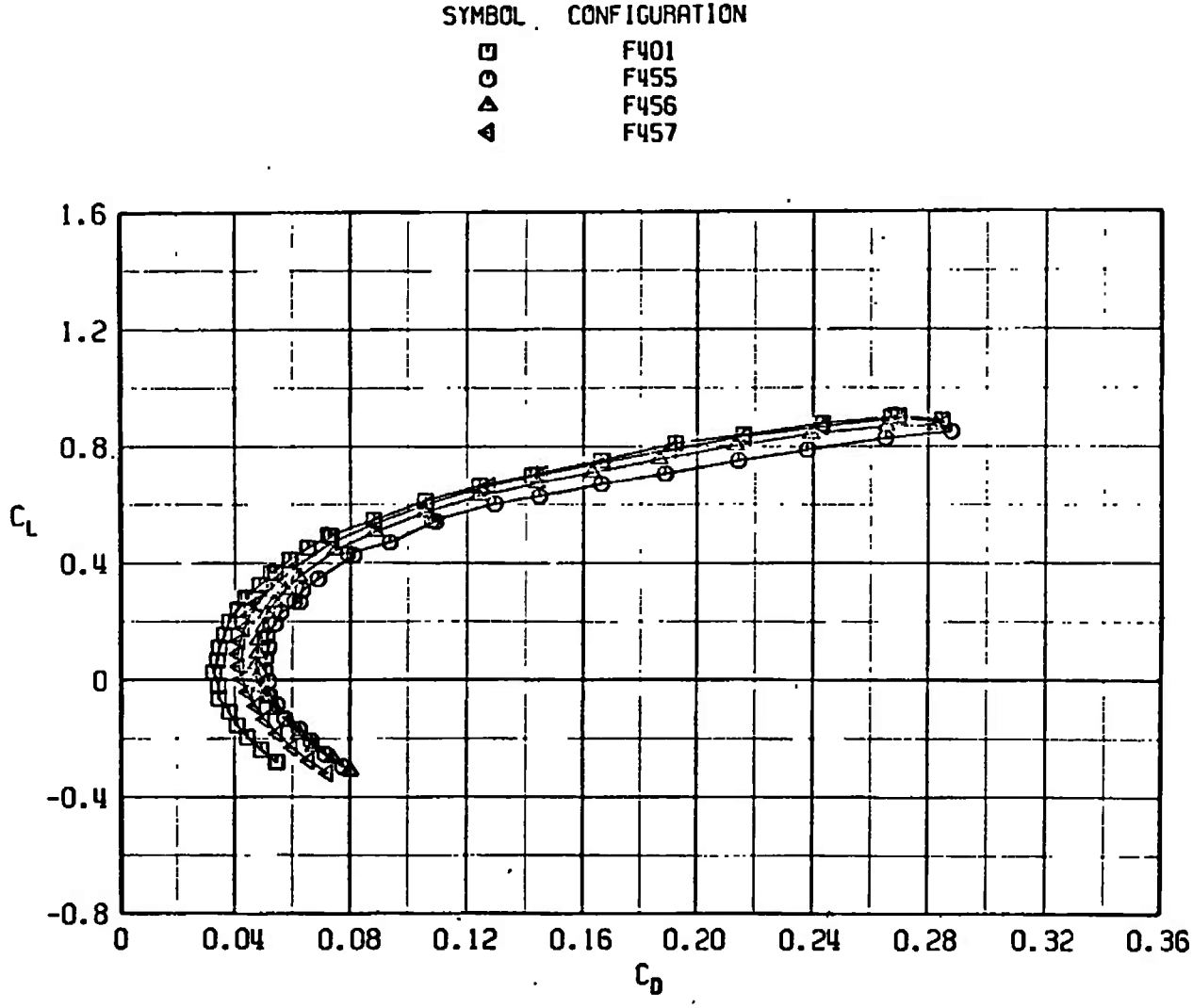

c. $M_\infty = 0.95$

Fig. 51 Continued

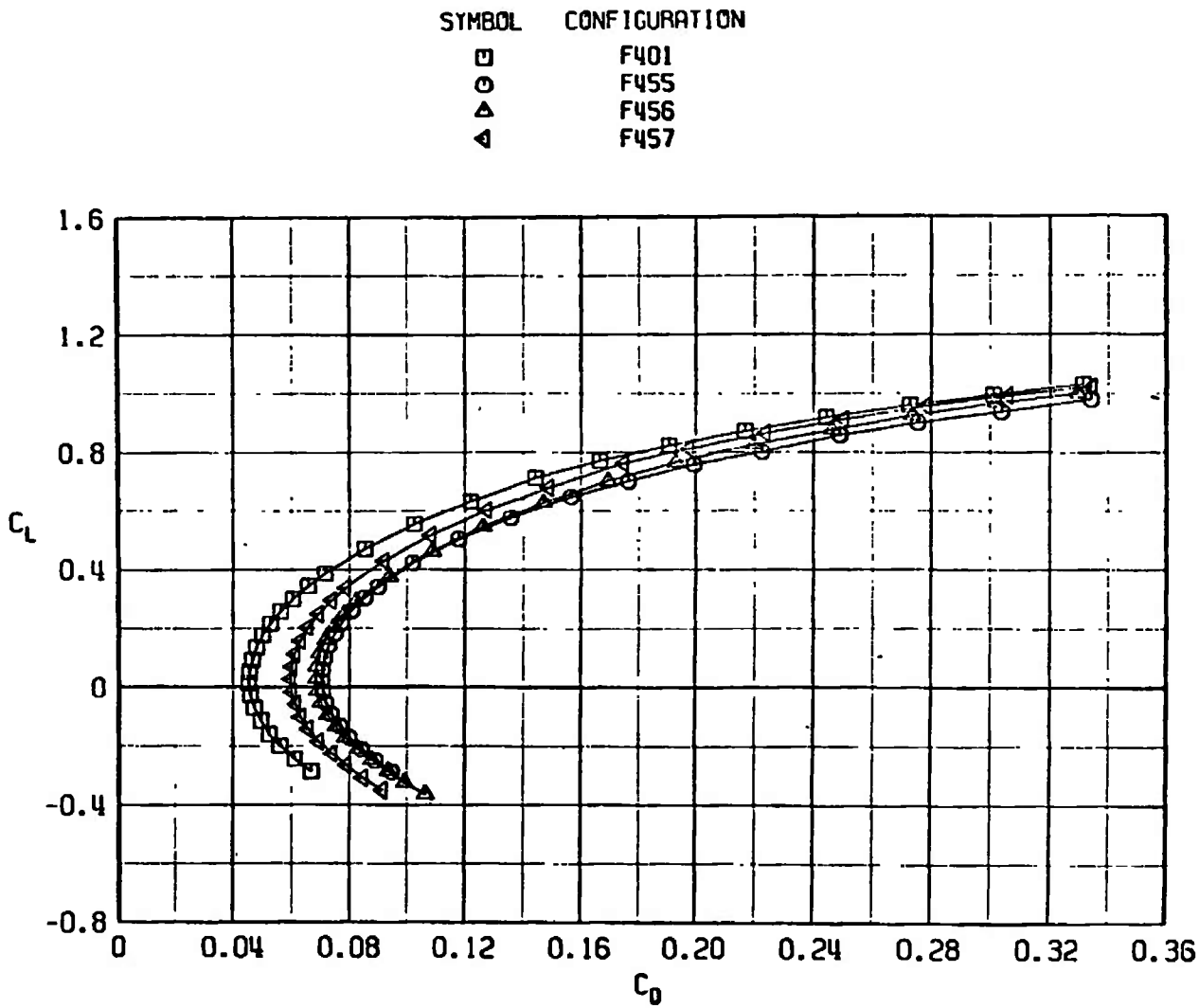

d. $M_\infty = 1.10$
Fig. 51 Continued

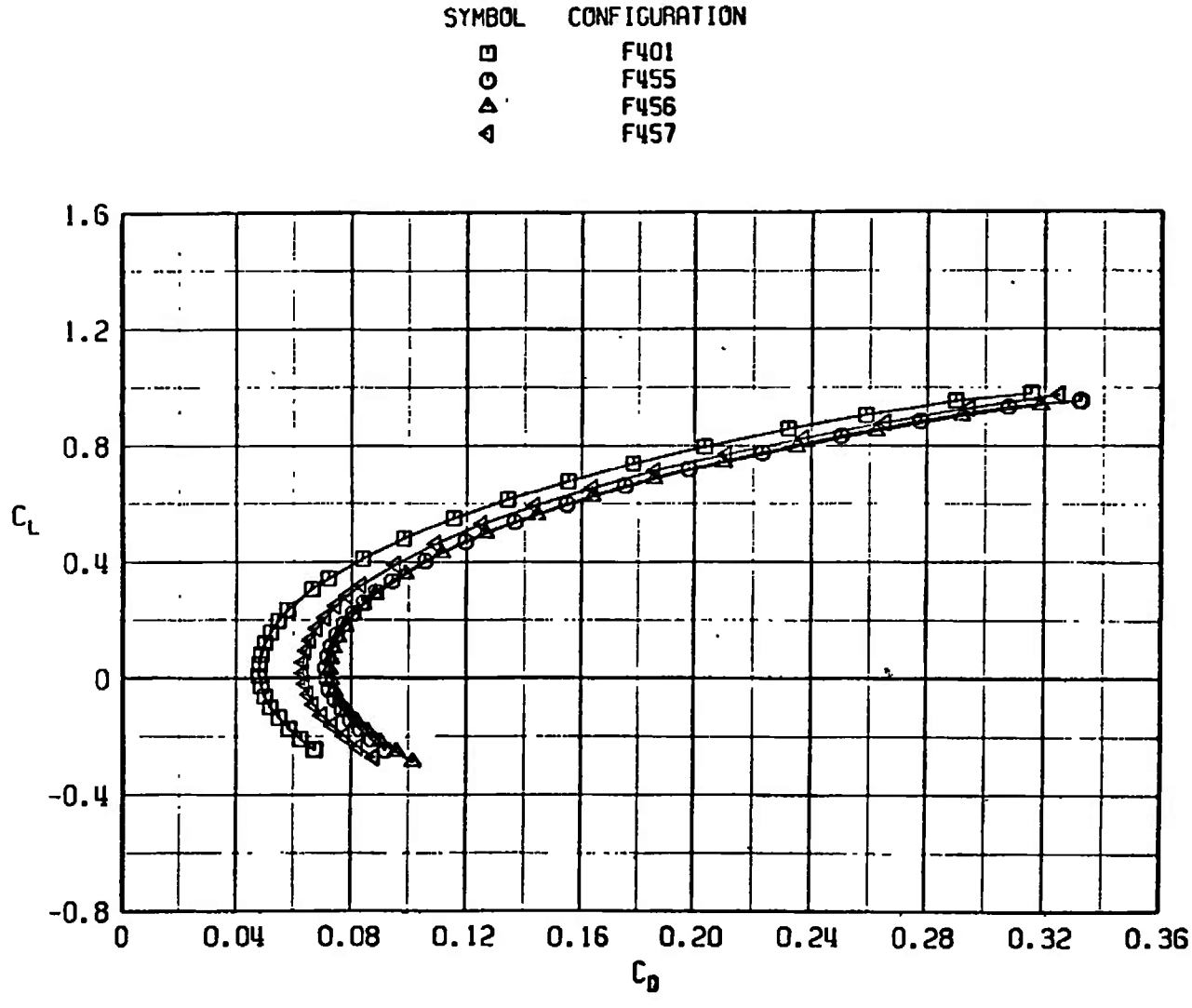

e. $M_\infty = 1.30$

Fig. 51 Concluded

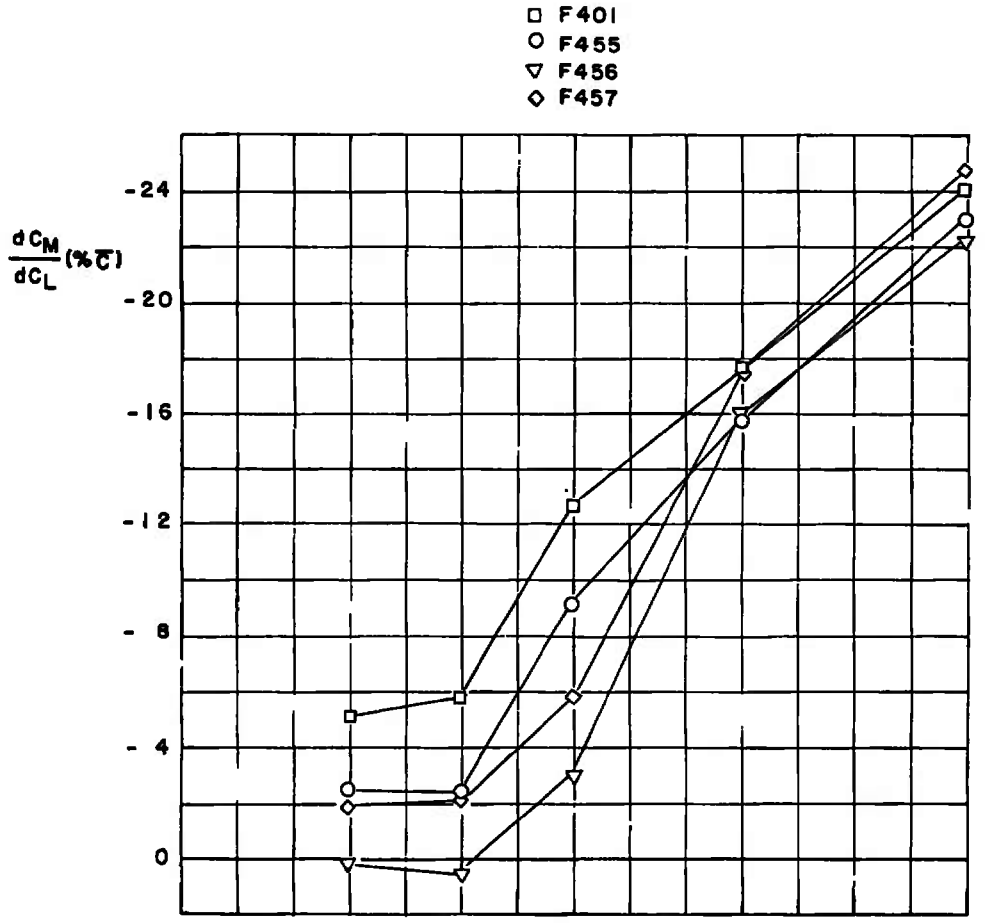

a. dC_m/dC_L versus M_∞ at $C_L = 0.2$ in percentage of $\bar{c}$

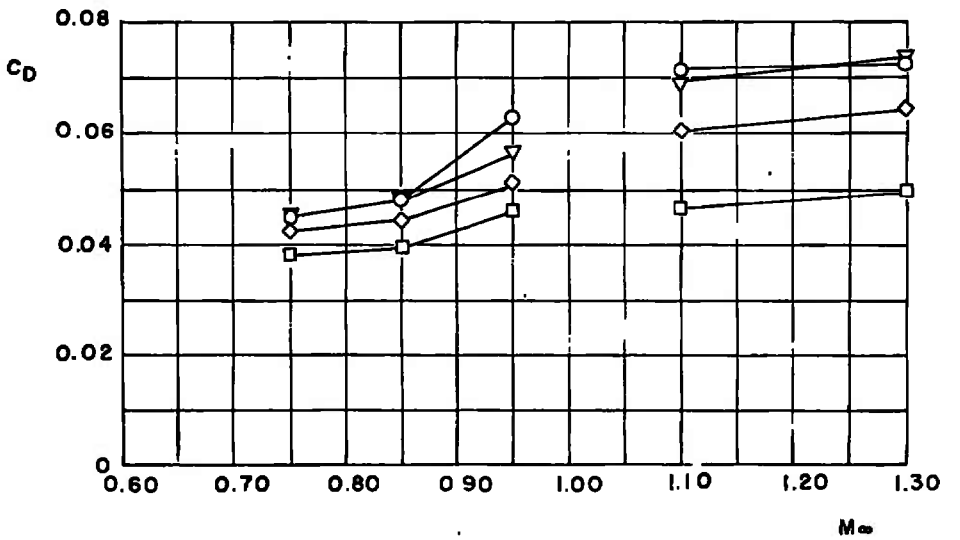

b. C_D versus M_∞ at $C_L = 0.3$, $M_\infty < 1.0$, and $C_L = 0.1$, $M_\infty > 1.0$

Fig. 52 Drag Coefficient and dC_m/dC_L Variation with Mach Number for Configurations F401, F455, F456, and F457

TABLE I
AIRCRAFT LOAD CONFIGURATIONS

	Inboard	Outboard
F401	Clean	Clean
F402	Clean	370-gal fuel tank
F403	Pylon	Clean
F404	Pylon	370-gal fuel tank
F405	Pylon plus TRL1	
F406	Pylon plus TRL1 plus M1, sta 2	
F407	Pylon plus TRL1 plus M1, sta 1, 2	
F408	Pylon plus TRL1 plus M1, sta 1,2,3	
F409	Pylon plus TRL2	
F410	Pylon plus TRL2 plus M2; sta 2	
F411	Pylon plus TRL2 plus M2; sta 1,2	
F412	Pylon plus TRL2 plus M2; sta 1,2,3	
F413	Pylon plus TRL2 plus M2, sta 2,3	
F414	Pylon plus TRL2 plus M2, sta 3	
F415	Pylon plus TRL2 plus M2, sta 1,3	
F416	Pylon plus TRL2 plus M4; sta 2	
F417	Pylon plus TRL2 plus M4; sta 1,2	
F418	Pylon plus TRL2 plus M4. sta 1,2,3	
F419	Pylon plus TRL3	
F420	Pylon plus TRL3 plus M2, sta 2	
F421	Pylon plus TRL3 plus M2; sta 1,2	
F422	Pylon plus TRL3 plus M2; sta 1,2,3	
F423	Pylon plus TRL3 plus M2; sta 2,3	
F424	Pylon plus TRL3 plus M2; sta 3	
F425	Pylon plus TRL3 plus M2; sta 1,3	
F426	Pylon plus TRL4	
F427	Pylon plus TRL4 plus M2; sta 2	
F428	Pylon plus TRL4 plus M2; sta 1,2	
F429	Pylon plus TRL4 plus M2, sta 1,2,3	
F430	Pylon plus TRL4 plus M2, sta 2,3	
F431	Pylon plus TRL4 plus M2, sta 1,3	
F432	Pylon plus TRL4 plus M2; sta 3	

TABLE I (Concluded)

	Inboard	Outboard
F433	Pylon plus QRL1	370-gal fuel tank
F434	Pylon plus QRL1 plus M2; sta 1,2,3,4	
F435	Pylon plus QRL1 plus M4; sta 1,2,3,4	
F436	Pylon plus TRL2 plus M3; sta 2	
F437	Pylon plus TRL2 plus M3; sta 1,2	
F438	Pylon plus TRL2 plus M3, sta 1 2,3	
F439	Pylon plus TRL3 plus M3; sta 2	
F440	Pylon plus TRL3 plus M3, sta 1,2	
F441	Pylon plus TRL3 plus M3; sta 1,2,3	
F442	Pylon plus TRL4 plus M3; sta 2	
F443	Pylon plus TRL4 plus M3; sta 1,2	
F444	Pylon plus TRL4 plus M3; sta 1,2,3	
F445	Pylon plus QRL1 plus M3; sta 1,2,3,4	
F446	Pylon plus TRL1 plus M1; sta 1,2,3	Clean
F447	Pylon plus TRL2 plus M2; sta 1,2,3	
F448	Pylon plus TRL2 plus M4; sta 1,2,3	
F449	Pylon plus TRL3 plus M2; sta 1,2,3	
F450	Pylon plus TRL4 plus M2; sta 1,2,3	
F451	Pylon plus QRL1	
F452	Pylon plus QRL1 plus M2; sta 1,2,3,4	
F453	Pylon plus QRL1 plus M4; sta 1,2,3,4	
F454	Pylon plus QRL1 plus M3; sta 1,2,3,4	
F455	Clean	Pylon plus ATRA 30 x 30
F456	Pylon plus ATRL 30 x 30	370-gal fuel tank
F457	Pylon plus ATRL 30 x 30	Clean

UNCLASSIFIED

Security Classification

DOCUMENT CONTROL DATA - R & D

(Security classification of title, body of abstract and indexing annotation must be entered when the overall report is classified)

1 ORIGINATING ACTIVITY (Corporate author)	2a. REPORT SECURITY CLASSIFICATION
Arnold Engineering Development Center ARO, Inc., Operating Contractor Arnold Air Force Station, Tennessee 37389	UNCLASSIFIED
	2b. GROUP N/A

3 REPORT TITLE

LONGITUDINAL STATIC STABILITY AND DRAG CHARACTERISTICS OF F-4D AIRCRAFT WITH VARIOUS EXTERNAL STORE CONFIGURATIONS AT TRANSONIC SPEEDS

4 DESCRIPTIVE NOTES *(Type of report and inclusive dates)*

Final Report, April 22 to 27, 1971

5 AUTHOR(S) *(First name, middle initial, last name)*

D. K. Smith, ARO, Inc.

6 REPORT DATE	7a. TOTAL NO. OF PAGES	7b. NO OF REFS
August 1971	211	3

8a. CONTRACT OR GRANT NO.	9a. ORIGINATOR'S REPORT NUMBER(S)
F40600-72-C-0003 b. PROJECT NO. 2567 c. Program Element 62602F d.	AEDC-TR-71-162 AFATL-TR-71-99 9b. OTHER REPORT NO(S) *(Any other numbers that may be assigned this report)* ARO-PWT-TR-71-117

10. DISTRIBUTION STATEMENT Distribution limited to U.S. Government agencies only; this report contains information on test and evaluation of military hardware; August 1971; other requests for this document must be referred to Armament Development and Test Center (DLII), Eglin AFB, FL 32542.

11 SUPPLEMENTARY NOTES	12 SPONSORING MILITARY ACTIVITY
Available in DDC.	Armament Development and Test Center (DLII), Eglin AFB, FL 32542

13 ABSTRACT

Force and moment data were obtained with a 0.05-scale model of the F-4D aircraft at Mach numbers from 0.75 to 1.30 to determine the effects of different store and rack configurations on the static stability and drag of the aircraft. Six proposed rack launchers and four proposed store shapes were tested for a total of 57 external loading configurations.

DD FORM 1 NOV 68 1473

UNCLASSIFIED

Security Classification

14 KEY WORDS	LINK A ROLE	LINK A WT	LINK B ROLE	LINK B WT	LINK C ROLE	LINK C WT
F-4D						
jet fighters						
aircraft external stores						
longitudinal stability						
drag						
transonic wind tunnels						

1. Airplane -- F-4D.
2 " -- Stability
3 " -- Drag
4 " -- Store effects
5 Store -- Effects